

University of Southampton Research Repository

Copyright © and Moral Rights for this thesis and, where applicable, any accompanying data are retained by the author and/or other copyright owners. A copy can be downloaded for personal non-commercial research or study, without prior permission or charge. This thesis and the accompanying data cannot be reproduced or quoted extensively from without first obtaining permission in writing from the copyright holder/s. The content of the thesis and accompanying research data (where applicable) must not be changed in any way or sold commercially in any format or medium without the formal permission of the copyright holder/s.

When referring to this thesis and any accompanying data, full bibliographic details must be given, e.g.

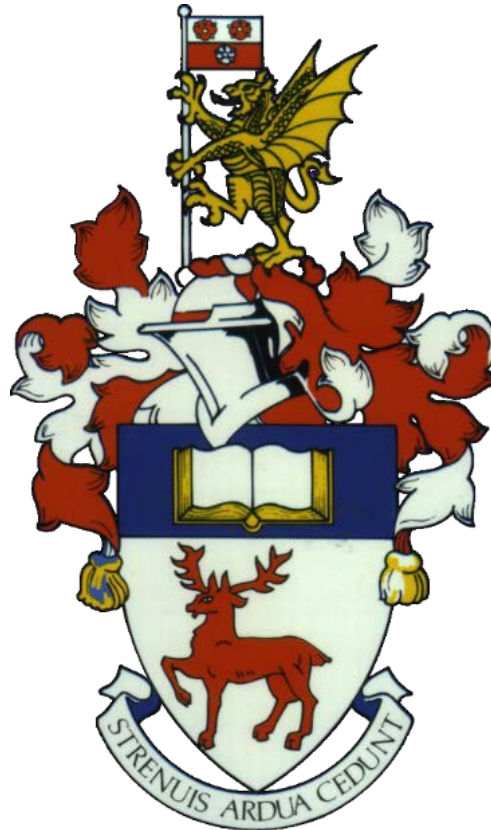
Thesis: Author (Year of Submission) "Full thesis title", University of Southampton, name of the University Faculty or School or Department, PhD Thesis, pagination.

Data: Author (Year) Title. URI [dataset]

[University of Southampton](#)

FACULTY OF ENVIRONMENTAL AND LIFE SCIENCES

School of Biological Sciences



**Developing a *Drosophila*-based model in which to study
aspects of pathological Tau transfer and seeding**

by

Ben Batchelor
ORCID ID 0009-0009-6722-9874

Thesis for the degree of Doctor of Philosophy

September 2023

University of Southampton

Abstract

FACULTY OF ENVIRONMENTAL AND LIFE SCIENCES

School of Biological Sciences

Thesis for the degree of Doctor of Philosophy (2023)

DEVELOPING A *DROSOPHILA*-BASED MODEL IN WHICH TO STUDY ASPECTS OF PATHOLOGICAL TAU TRANSFER AND SEEDING

Ben Batchelor

Prion-like propagation through neuronal circuitry is believed to be the mechanism by which Tau pathology spreads throughout the brain in tauopathies such as Alzheimer's disease (AD). This is reflected in the neuropathological Braak-staging of disease and manifests in the progressive cognitive decline evident clinically. Though various synaptic proteins are implicated, the precise players and mechanism(s) mediating the trans-cellular spread of pathological Tau species remains unclear. Furthermore, although the trans-cellular spread of pathological Tau species has been demonstrated in many experimental models, the neurobiological consequences in recipient neurons are largely unknown. Moreover, in almost all such studies, the Tau species that propagates is invariably mutated or isolated from pathological fractions of brains of Tauopathy patients. However, in the majority of AD cases it is wild-type Tau that spontaneously becomes pathological and spreads in AD, with this process accompanied by neurodegeneration. Therefore, there is a need to further understand the mechanisms of Tau spread and how wild-type Tau becomes pathological with time.

Drosophila's genetic tractability, combined with detailed mapping of connections and physiological readouts, offer an ideal organism in which to study aspects of Tau spread and seeding. Using the Gal4.UAS system a mCherry tagged Tau^{ON4R} construct was expressed in both large and small olfactory circuitry, creating two potential models of Tau spread. A third model type was also investigated, using the injection of an exogenously-characterised Tau species into a human Tau background to investigate the relationship between Tau seeding potential and spread. Immunohistochemistry was used on the *Drosophila* brains to amplify Tau signal and provide further information on conformation. Tau spread and misfolding in these brains was followed by confocal microscopy at select time points.

In all potential models the spontaneous aggregation of Tau^{ON4R} was observed and evidence of spread beyond expressed or injected regions was seen. Expression in the small circuit lends itself to the study of Tau spread between interneurons due to the physiology of the olfactory bulb. The large circuit offers opportunities to study a system in which Tau spread has functional consequences for the organism, and spread itself can be modulated by neuronal activity mutants. Finally, injected Tau seeds were seen to rapidly spread beyond the recipient neuronal populations and showed the ability to convert naïve human Tau to a disease-relevant conformation in the fly brain.

Further development of all three model types will allow for investigation into the key synaptic players and mechanism(s) underlying prion like spread. Deeper understanding of this will provide better diagnosis, treatments and prognosis to those affected by this disease.

Table of Contents

Table of Contents	i
Table of Tables	vii
Table of Figures	viii
Research Thesis: Declaration of Authorship	ix
Acknowledgements	x
Definitions and Abbreviations	xvii
Chapter 1 Introduction	20
1.1 Neurodegenerative disease	20
1.2 Alzheimer’s disease	21
1.3 Amyloidosis.....	22
1.4 Amyloid hypothesis.....	23
1.5 Moving away from the Amyloid hypothesis	26
1.6 Tauopathies	26
1.7 Tau structure.....	27
1.8 Tau function.....	28
1.9 Tau’s Pathological changes	29
1.10 Tau propagation.....	35
1.11 Current models of Tau propagation.....	41
1.12 Drosophila Tau and other homologues.....	49
1.13 Proposed model.....	50
Chapter 2 Aims	54
2.1 Thesis Summary.....	54
2.2 Thesis Aims	55
Chapter 3 Materials & methods	56
3.1 Fly stocks.....	56
3.2 Recombinant fly generation.....	60
3.3 Experimental Crosses.....	61

3.4	Longevity Assays	65
3.5	Injections	65
3.6	Dissections	66
3.7	Immunohistochemistry (IHC)	67
3.8	Confocal imaging	69
3.9	Analysis	69
3.10	Statistics	70
3.11	Figures and Diagrams.....	70
3.12	Reagents	70
Chapter 4 Simulating Tau spread in a small number of olfactory neurons by expressing mCherryTau^{ON4R} in Or88a olfactory circuitry		72
4.1	Introduction	73
4.2	Summary of Aims and Objectives:	77
4.3	Results	78
4.4	Discussion	92
Chapter 5 Modelling Tau spread in all <i>Drosophila</i> olfactory neurons		103
5.1	Introduction	104
5.2	Aims and hypothesis	106
5.3	Results	107
5.4	Discussion	123
Chapter 6 Injections of externally characterised Tau species into the <i>Drosophila</i> brain		131
6.1	Introduction	132
6.2	Aims and hypothesis	134
6.3	Results	135
6.4	Discussion	117
6.5	Conclusion and future directions	122
Chapter 7 Overall conclusions and future directions		124
7.1	Summary	124
7.2	Modelling Tau spread in a small number of olfactory neurons using <i>Drosophila's</i> olfactory system.....	124
7.3	Modelling and modulating Tau spread in a large number of neurons using <i>Drosophila's</i> olfactory system	125
7.4	Injecting externally characterised Tau species into the <i>Drosophila</i>	126

7.5 Future directions for Drosophila models.....	126
7.6 Presentations of this work.....	128
Appendix	129
Bibliography	141

Table of Tables

Table 1: Table summarizing the advantages and disadvantages of three different types of mouse models of Tau pathology	23
Table 2: Table demonstrating the relative advantages and disadvantages of <i>Drosophila melanogaster</i> as a model organism for studying Tau propagation and seeding	25
Table 3. Fly lines used in this thesis, (BL = Bloomington <i>Drosophila</i> stock centre and Allen lab (University of British Columbia).....	33
Table 4: Table of fly crosses, parents and offspring genotype in the results of this thesis	38
Table 5: Description of all antibodies and their dilutions used in experiments within this thesis	44
Table 6: A table outlining the fluorescent tags used in this thesis and the corresponding excitation and collection parameters used to image them on a Leica SP8 Inverted scanning confocal microscope.....	46
Table 7: Reagents, their ingredients and suppliers used in experiments this thesis.....	47

Table of Figures

Figure 1: Braak staging.....	22
Figure 2: Diagram showing the processing of the Amyloid precursor protein into A β ₄₂ and A β ₄₀ peptides.....	23
Figure 3: Diagram of the Amyloid cascade and its interaction with Tau.....	25
Figure 4: Tau isoforms and their corresponding molecular weight (actual and apparent).	28
Figure 5: Diagram of the proposed mechanisms of Tau's transynaptic spread.	39
Figure 6: Diagram of the olfactory receptor neurons in the antennae.....	51
Figure 7: Diagram of olfactory circuitry in the <i>Drosophila melanogaster</i> brain.....	52
Figure 8: Schematic outlining the time taken to carry out an experimental time course from the setting of genetic crosses to final confocal imaging.	60
Figure 9: Schematic of injections into the 2 nd or 3 rd antennal segment.	66
Figure 10: Schematic of wells created atop slides using cover slips into which stained <i>Drosophila</i> brains are mounted	68
Figure 11: Graphical abstract of Chapter 4; Simulating Tau spread in a small number of olfactory neurons by expressing mCherryTau ^{ON4R} in Or88a olfactory circuitry	72
Figure 12: The proposed model in which to simulate Tau spread	76
Figure 13: UAS.cd8.GFP expression driven in different olfactory subunit and projection neuron- targeted GAL4 drivers.	80
Figure 14: mCherryTau ^{ON4R} does not spread from Or88a olfactory receptor neurons at 23°C.....	82
Figure 15: Characterising mCherryTau ^{ON4R} expression in Or88a olfactory receptor neurons at 29°C.....	86
Figure 16 Investigating the conformation of mCherryTau ^{ON4R} in the Or88a olfactory receptor neurons	88
Figure 17 Staining of the UAS.mCherryTau ^{ON4R} construct alone at 29°C	91
Figure 18: Schematic of the results found in this chapter.....	99
Figure 19: Schematic outlining future directions from this chapter	102
Figure 20 Graphical abstract of Chapter 5.....	103
Figure 21 Diagram of the proposed model in which to simulate Tau spread in a large number of neurons.	105
Figure 22: Longevity assay of the Orco.Gal4-driven UAS.mCherryTau ^{ON4R} offspring and its parent.....	107
Figure 23 Orco.Gal4 driving expression of both UAS.mCherryTau ^{ON4R} and UAS.cd8::GFP at 25°C over a two-week time course.	110
Figure 24 Analysis of signal in the medulla in the brains from Figure 23	112
Figure 25 Orco.Gal4 driving mCherryTau ^{ON4R} and the hyperactivity mutant Kir2.1 in Orco- expressing neurons at 25°C, stained with anti-mCherry and AT8.....	114
Figure 26 Orco.Gal4 driving mCherryTau ^{ON4R} and the hypo-activity mutant Nav1.1 in Orco expressing neurons at 25°C, stained with anti-mCherry and AT8.....	116
Figure 27: Quantification of AT8 and mCherry coverage in Orco.Gal4UAS.mCherryTau ^{ON4R} recombinant flies with either a neuronal hyper- or hypoactive mutation compared with the recombinant line without any neuronal modulation at 25°C.....	119
Figure 28: Quantification of AT8 and mCherry coverage in the medulla of Orco.Gal4 UAS.mCherryTau ^{ON4R} recombinant flies crossed with either a neuronal hyper or hypoactive mutant compared with the recombinant line crossed with an unmodulated fly at 25°C (n=3)	122
Figure 29 Diagram of the results found in this chapter.....	128
Figure 30: Diagram of the future directions offered in this chapter	130
Figure 31 Graphical abstract of Chapter 6 Injecting externally characterised Tau species into the <i>Drosophila</i> brain	131
Figure 32 Graphical abstract of the methodology used in Chapter 6; Injecting externally characterised Tau species into the <i>Drosophila</i> brain	133
Figure 33 The injection sites used, located in the 2 nd and 3 rd antennal segments	136
Figure 34: 1hr after injection of the dextran conjugate and Tau fibrils	139
Figure 35: Injection of Tau Fibrils vs a control injected brains expressing nSyb:EGFP:Tau ^{ON4R} after 24 hours (n=3)	116
Figure 36 Graphical abstract of Chapter 6's Future work, injecting externally-characterised Tau species into the <i>Drosophila</i> brain.....	123
Figure 37 Graphical abstract of Chapter 6's Future work, injecting externally-characterised Tau species into the <i>Drosophila</i> brain.....	123

Research Thesis: Declaration of Authorship

Print name: Ben Batchelor

Title of thesis: Developing a *Drosophila* – based model in which to study aspects of pathological Tau transfer and seeding

I declare that this thesis and the work presented in it are my own and has been generated by me as the result of my own original research.

I confirm that:

1. This work was done wholly or mainly while in candidature for a research degree at this University;
2. Where any part of this thesis has previously been submitted for a degree or any other qualification at this University or any other institution, this has been clearly stated;
3. Where I have consulted the published work of others, this is always clearly attributed;
4. Where I have quoted from the work of others, the source is always given. With the exception of such quotations, this thesis is entirely my own work;
5. I have acknowledged all main sources of help;
6. Where the thesis is based on work done by myself jointly with others, I have made clear exactly what was done by others and what I have contributed myself;
7. None of this work has been published before submission

Signature:..... Date: 27/09/2023

Acknowledgements

I would like to thank Professor Amritpal Mudher and Professor Douglas Allan for giving me the opportunity, tools and support to carry out this project. Many thanks also to the Gerald Kerkut Charitable Trust for their financial support and for providing many opportunities to present my work to a wide-ranging and knowledgeable audience. I would also like to thank Dr Mark Willet and Dr David Johnston for the countless hours of help and support they have both given with confocal microscopy techniques.

To the Mudher and Wijnen lab groups, both past and present for the insights, help and advice, both within the lab and across our lab meetings. In particular, I'd like to thank Dr George Devitt, Brad Richardson and Amber Cooper, who have become great friends over the years, offering coffee, guidance and laughter.

To the Lunch Beacon; Michael, Katie, Dan and Rachel - a greater group of friends could not be asked for, always ready to down tools and keep each other sane over a sandwich. Thank you for always being there both in and out of work and filling the PhD with fun.

To my family - Mum, Dad, Scott and Lidi, along with Nan and Grandad, who always supported their son/brother/grandson. Providing love, encouragement and frequent reminders to not look too much like a mad scientist!

Finally, to my wonderful fiancée Rosie Hopkins, who without her endless patience, kindness, support, understanding and humour, none of this would be possible

Definitions and Abbreviations

A β	Amyloid Beta; a short protein cleaved from the Amyloid precursor protein, either 40 or 42 amino acids long.
AD	Alzheimer's disease; a neurodegenerative disease that causes progressive memory loss. Its' hallmarks are Amyloid plaques and neurofibrillary tangles.
AFM	atomic force microscopy; a microscopy technique using a cantilever which is bent by a sharp tip passing over a samples surface. A laser light detects the bending of this cantilever providing a measurement of the height of the surface.
APP	amyloid precursor protein; a single pass transmembrane protein that is processed into amyloid beta 40 and 42
AMMC	Antennal Mechanosensory and Motor Center
CyO	Curly of Oster; a homozygous lethal mutation in <i>Drosophila</i> with a heterozygous curled wing phenotype, used to balanced insertions on chromosome two
CSF	cerebrospinal fluid
DNA	deoxyribonucleic acid; two polynucleotide chains that encode the genetic sequence of all known organisms
EM	Electron microscopy
FAD	Familial Alzheimer's disease; an inherited form of neurodegenerative disease that causes progressive memory loss, Hallmarks are Amyloid plaques and neurofibrillary tangles.
FDA	The United States Food and Drug Administration
FISH.....	fluorescence in-situ hybridization
GSK3 β	Glycogen synthase kinase-3 beta, proline directed serine-threonine kinase
GFP	green florescent protein
HSPGs	heparan sulfate proteoglycans; a linear polysaccharide found on cell surface and extracellular matrix which interacts with protein ligands

Ivlp.....	inferior ventrolateral protocerebrum
LC neurons.....	lobula columnar neurons, a class of <i>Drosophila</i> neurons that project to the optic glomeruli
LH	Area of the <i>Drosophila</i> brain that is key for learned and innate olfactory behaviors. Receives input from the olfactory bulb.
LHONs.....	lateral horn output neurons
LHLNs.....	lateral horn local neurons
LRP1.....	low-density lipoprotein receptor-related protein 1; a plasma membrane protein that facilitates endocytosis
MAP	microtubule-associated protein; interacts with microtubules that make up the cytoskeleton
Mmus.....	<i>M. musculus</i> , common house mouse
MTBD.....	microtubule binding domain; a region of the Tau protein, allowing for interaction with microtubules
NMDAR	N-methyl-D-aspartate receptor; a glutamate and ion channel receptor playing a role in neuronal excitation and plasticity
NGS.....	normal goat serum; used for blocking non-specific protein interactions in Immunofluorescence
PBST.....	Phospho Buffered Saline with Triton X-100; a buffer solution with detergent
PRD	proline-rich domain; a region of Tau protein with a high Proline content
PHF	paired helical filaments, the main conformation of intraneuronal neurofibrillary tangles
PFA.....	paraformaldehyde (a fixative solution)
PSP.....	progressive supranuclear palsy; a late-onset brain disorder that causes problems with balance, walking and eye movement
SF	straight filaments; a minority conformation of intraneuronal neurofibrillary tangles
ts.....	temperature-sensitive
WT	wild-type
Vlp	ventrolateral protocerebrum

UAS.....upstream-activating sequence; a yeast promotor binding region

UBC.....University of British Columbia

UoSUniversity of Southampton

Chapter 1 Introduction

1.1 Neurodegenerative disease

Neurodegenerative disease is an umbrella term encompassing a wide range of disorders that affect the nervous system, causing degeneration, often as a result of the inclusion of protein abnormalities. These are commonly grouped into amyloidosis, tauopathies, α -synucleinopathies, and transactivation response DNA-binding protein 43 (TDP-43) proteinopathies (Dugger and Dickson 2017). The individual disorders within these groups are classified relating to their clinical presentation (such as Alzheimer's disease (AD)) or for their pattern and distribution of degeneration (for example, frontal temporal dementia) (Dugger and Dickson 2017). Though classed as individual disorders, these diseases can contain multiple abnormalities. This includes AD, which exhibits amyloidosis through $A\beta$ plaques and tauopathies through neurofibrillary tangles. These abnormalities can occur and accumulate before symptoms become apparent (Dugger and Dickson 2017) and can cause progressive neuronal dysfunction and death, resulting in memory loss, cognitive dysfunction and loss of coordination (Dugger and Dickson 2017).

The impact of these symptoms is not only felt by the patient suffering from AD but also by family members and loved ones caring for the patient. In 2020 in the US alone, an estimated eleven million family members and other unpaid caregivers provided approximately 15.3 billion hours of care to people with Alzheimer's or other dementias. This care has been valued at nearly \$271.6 billion when factoring in the increased risk for emotional distress and adverse mental and physical health effect, further heightened during the recent pandemic (The Alzheimer's Association 2022). The global number of persons aged over 65 is predicted to double from an estimated 727 million to 1.5 billion between 2020 and 2050. As ageing is a primary risk factor in these diseases, with one in ten individuals over 65 years having AD, the cost and impact of neurodegenerative diseases are only predicted to grow (Hou, Dan et al. 2019, United Nations Department of Economic and Social Affairs 2020).

1.2 Alzheimer's disease

The most common neurodegenerative disease is Alzheimer's disease, accounting for 60-80% of cases. However, half of these also contain another brain change related to other dementias such as Lewy body disease (known as "mixed dementia") (The Alzheimer's Association 2022). The cognitive decline in those with AD manifests in early disease stages, with patients struggling to recall recent conversations, names and events, along with potential apathy and depression (The Alzheimer's Association 2022). This is classed as "mild Alzheimer's disease" when the individual can carry out basic tasks and exhibits a high degree of independence, only requiring assistance with select tasks (The Alzheimer's Association 2022). However, with time these symptoms develop further into impaired communication, disorientation and confusion until the late stages of the disease when the individual has difficulty speaking, swallowing and walking, becoming bedridden and requiring around-the-clock care (The Alzheimer's Association 2022). This pathological process can begin up to 20 years before the first symptoms are detected (The Alzheimer's Association 2022). Currently, no cure exists for AD, but five drugs for the treatment of symptoms are currently FDA-approved, with a 6th drug, Aducanumab, designed and available in recent years through an accelerated approval pathway to target amyloid plaques, one of two key pathological hallmarks. However, this drug does not work in every case but seems effective at the early stages of AD (The Alzheimer's Association 2022). A 7th drug, Lecanumab, has very recently completed its 3rd stage of clinical trials and is also found to be most effective at the early stages of AD, further reinforcing the idea that therapeutic intervention should occur as early as possible in the disease (van Dyck, Swanson et al. 2022).

The progression from mild to severe AD symptoms can be tracked in the brain through the deposition of two key pathological hallmarks with time. These hallmarks are Tau and Amyloid-Beta (A β), which form neurofibrillary tangles and amyloid plaques respectively. In 1991, Braak and Braak established a series of stages by tracking AD symptom progression, where the appearance of these tangles and plaques in particular areas of the brain correlated with disease progression (Figure 1). With time, the presence of these 'pathological hallmarks' also correlated with neuronal loss and reduced size of the hippocampus and cortex (Braak and Braak 1991). This pathological spread of Tau and A β through the brain and the subsequent degradation of neurones in the affected areas leads to the progression of AD symptoms. These two proteins represent two forms of abnormalities – tauopathies and amyloidosis.

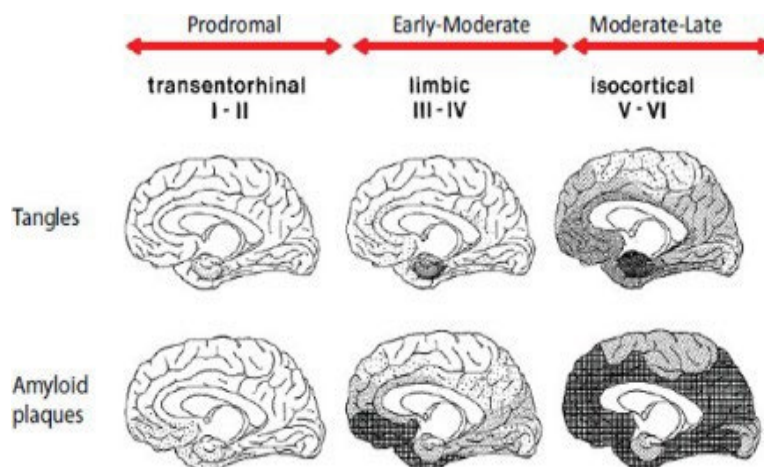


Figure 1: Braak staging

Both amyloid and tangle pathology spread between connected brain regions as Alzheimer's disease progresses. This is indicated by the shading in each brain; the darker the shading, the higher the burden. However, the pattern of spread differs, with tangle pathology spreading between connected brain regions from the entorhinal cortex to the limbic areas and finally the neocortex as AD progresses, as shown in the top row. $A\beta$, on the other hand, develops in distinct neocortical regions followed by allocortical brain regions and the forebrain. Figure modified from Braak and Braak (1991).

1.3 Amyloidosis

Amyloidosis is a group of hereditary or acquired disorders caused by insoluble extracellular amyloid deposits in the body resulting from the processing of a precursor protein (Westermarck, Benson et al. 2007). In AD, $A\beta_{42}$ comprise the main component of the key pathological hallmarks, amyloid plaques, and is formed from the cleavage of the Amyloid Precursor Protein (APP) by β and γ secretase alongside another fragment $A\beta_{40}$, the ratio of which is changed in favor of $A\beta_{42}$ in early-onset familial AD (Devkota, Williams et al. 2021). The physiological role of APP and $A\beta$ in the body remains unclear. Suggestions, however, cover a wide range of areas, from antimicrobials and tumour suppression (Tharp and Sarkar 2013) to plugging holes in the blood-brain barrier and synaptic modulation in the hippocampus (Brothers, Gosztyla et al. 2018). Monomeric $A\beta_{42}$ is soluble; however, if synthesis outweighs clearance, these monomers can misfold, gaining the characteristic secondary structure and aggregating into the external amyloid plaques seen in AD in what is known as the Amyloid hypothesis.

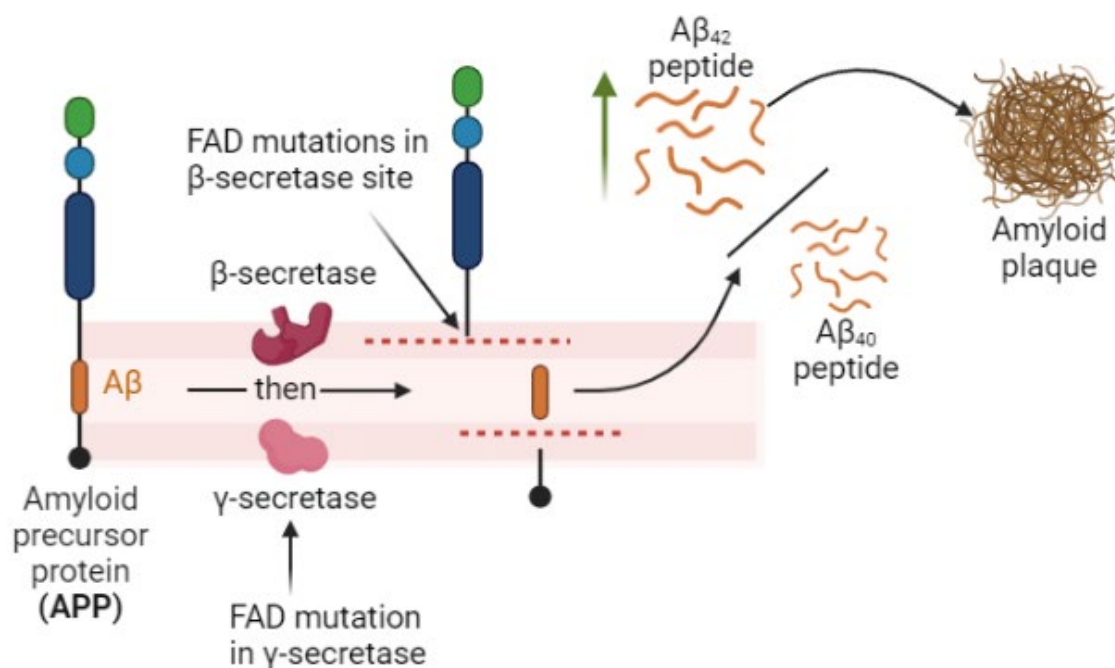


Figure 2: Diagram showing the processing of the Amyloid precursor protein into $A\beta_{42}$ and $A\beta_{40}$ peptides

APP is processed first by β -secretase, then by γ -secretase to produce the peptides $A\beta_{42}$ and $A\beta_{40}$. Mutations affecting the β -secretase cleavage site and γ -secretase are inherited in the familial form of Alzheimer's disease. These mutations lead to a greater ratio of $A\beta_{42}$ to $A\beta_{40}$ production and subsequent increase in amyloid plaque burden in those patients.

1.4 Amyloid hypothesis

For nearly 30 years, Amyloid- β has been believed to be the leading cause of AD in what was known as the Amyloid hypothesis (Selkoe and Hardy 2016). This hypothesis originated from multiple observations in which enhancement of $A\beta$ production led to a corresponding increase in resulting pathology. For example, in Trisomy 21, otherwise known as Down's syndrome, AD-like pathology by the age of 40 is observed due to an extra copy of the APP gene (located on chromosome 21) leading to greater $A\beta$ production (Kolata 1985). A more telling example occurs in Familial Alzheimer's Disease (FAD), an inherited but rarer form of AD where mutations occur within the presenilin 1 or 2 subunits of γ secretase (Walker, Martinez et al. 2005, Shen and Kelleher 2007). These mutations decrease the function of γ secretase, leading to a decrease in the overall amount of $A\beta$ ($A\beta_{40}$ and $A\beta_{42}$) but a relative increase in the ratio of $A\beta_{42}:A\beta_{40}$. This increase leads to an earlier onset of AD due to the larger amount of this toxic species being present in the body.

Mutations also occur in the APP gene, which also contributes to AD. The Swedish mutation, a double mutation KM670/671NL in APP, alters the site adjacent to β -secretase's action. This leads

to greater levels of A β production and an increased chance of early-onset AD (Mullan, Crawford et al. 1992). Counter to this, the Icelandic mutation A673T, also close to the β -secretase site, provides a neuroprotective effect (Jonsson, Atwal et al. 2012). This effect results from A673T making APP a weaker substrate for β -secretase and lowering the overall levels of A β . Taken together, these two mutations suggest a strong role for A β in the progression of AD. The precise mechanism of A β 42 pathology in AD, however, remains unknown. The formation of oligomers and plaques through the hydrophobic interactions of the A β monomers was previously thought to lead to toxicity. However, it has been found that oligomers, not plaques, are toxic species, for example, studies of the E693 deletion mutation (also known as the Osaka familial mutant) show that whilst individuals have severe cognitive impairments, their plaque burden remains low, but cerebral spinal fluid testing shows a high level of A β oligomers (Tomiya, Nagata et al. 2008, Shimada, Ataka et al. 2011, Kutoku, Ohsawa et al. 2015, Shimada, Minatani et al. 2020). This neuropathology of high A β oligomers and low plaque burden has been recapitulated in transgenic mouse models carrying the Osaka mutation where it was found to be associated with memory impairment, Tau phosphorylation and microglial activation (Tomiya, Matsuyama et al. 2010). The toxicity of the oligomeric species is thought to occur due to a reduction of hippocampal long-term potentiation (LTP) in early AD in response to excitotoxicity and neuronal death as time progresses (Cullen, Suh et al. 1997, Mucke and Selkoe 2012). These effects may be a pathological form of APP/A β 's potential physiological function, as A β release has been observed in healthy individuals and has been linked with modulation in neuronal excitability (Kamenetz, Tomita et al. 2003).

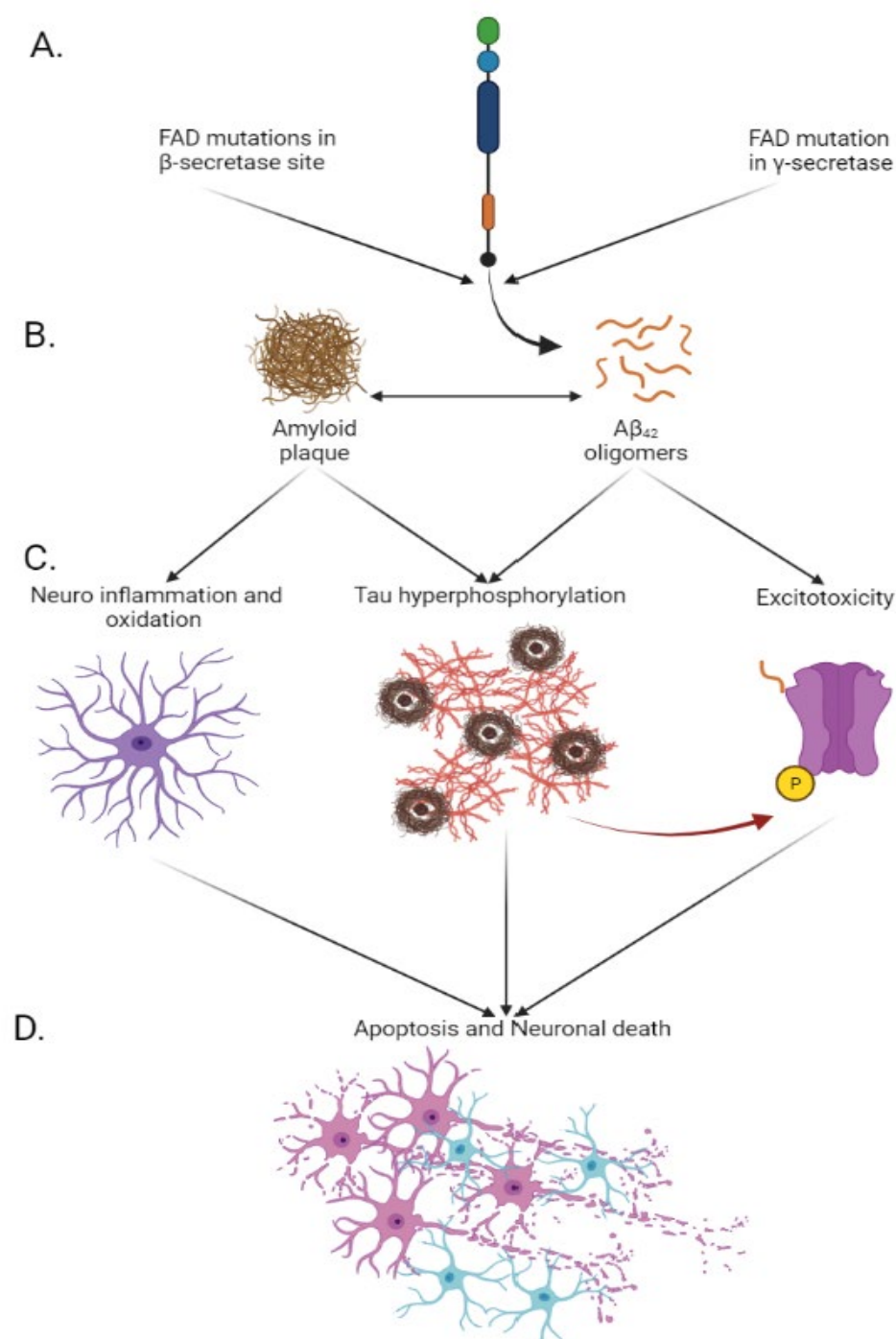


Figure 3: Diagram of the Amyloid cascade and its interaction with Tau

A) APP is processed by β -secretase, then γ -secretase to produce the peptides $A\beta_{42}$ and $A\beta_{40}$. Mutations in the β -secretase cleavage site and in γ -secretase itself lead to a greater ratio of $A\beta_{42}$ to $A\beta_{40}$ production in familial cases. B) $A\beta_{42}$ oligomers and then amyloid plaques are formed by the prior process. C) $A\beta$ species cause neuroinflammation, Tau hyperphosphorylation and excitotoxicity in neurons leading to apoptosis and neuronal death D) Hyperphosphorylation of Tau also results in a reduction of $A\beta_{42}$ induced excitotoxicity (red arrow), suggesting that there are varied interactions between these two key proteins in AD.

1.5 Moving away from the Amyloid hypothesis

Despite evidence that A β plays a crucial role in AD, its role has been challenged. The first evidence contradicting the Amyloid hypothesis began with rodent models, which have found that an increase in A β_{42} expression will induce plaque formation but does not result in neuronal death (Kim, Chakrabarty et al. 2013). This implies that A β by itself does not represent a toxic species. Furthermore, clinical studies have identified patients who exhibit AD symptoms but lack A β pathology (Ch  telat 2013), showing that this is not a phenomenon only found in mice. Whilst the experiments in the previous section clearly show that genetic mutations in APP and A β play a role in inherited AD, the more common, sporadic form of AD occurs much later in life and may not assume the same triggers.

Interestingly, despite years of study, it is only very recently that an A β -targeting drug has been successfully trialed, Aducanumab, a monoclonal antibody that targets the A β protein (Cummings, Aisen et al. 2021). This therapy has shown a dose-dependent response in initial trials, reducing the amyloid plaque and phosphorylated Tau levels and has recently been granted priority review by the FDA (Cummings, Aisen et al. 2021). It has also been approved for patients with mild cognitive impairment and early AD (Tampi, Forester et al. 2021). Another A β targeting therapy, Lecanemab, which targets A β protofibrils rather than the larger aggregates, has recently finished Phase III clinical trials and is also in fast-track status (van Dyck, Swanson et al. 2022).

The failure of most A β -targeting drugs to improve cognition in AD patients has caused some to question their role in AD, with drugs targeting A β production, aggregation and clearance failing to have a therapeutic effect until recently (Panza, F et al 2019). However, there is a possibility that these drugs are provided to patients too late, effectively once the damage has already been done (Cummings, Aisen et al. 2021). Therefore, despite challenges in therapeutic design, A β may still play a role in AD (Fan and Wang 2019). This mainly concerns its interaction with Tau tangles, the other major hallmark in Alzheimer's disease whose pathology relates more closely to the decline of cognitive function (Arriagada, Growdon et al. 1992, Van Rossum, Visser et al. 2012, Rolstad, Berg et al. 2013).

1.6 Tauopathies

The deposition of abnormal Tau protein in the brain characterises a range of heterogeneous diseases known as Tauopathies. Whether Tau is the primary cause of disease or acts as a secondary factor differentiates Tauopathies into primary or secondary Tauopathies (Williams 2006). The location of these deposits and their isoforms result in the disease phenotype with the 3R isoform aggregating and causing Pick's disease, the 4R isoform causing progressive supranuclear palsy (PSP)






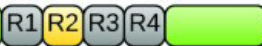


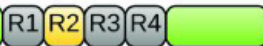
and 3R/4R mixed isoforms associated with AD (Fitzpatrick, Falcon et al. 2017, Falcon, Zhang et al. 2018, Alyenbaawi, Allison et al. 2020).

1.7 Tau structure

Tau is a microtubule-associated protein (MAP) that can become misfolded into a disease-causing confirmation after it becomes hyperphosphorylated (Brion, Couck et al. 1985, Grundke-Iqbal, Iqbal et al. 1986). Tau is encoded by the MAPT gene on chromosome 17 (human), producing six different isoforms (37-46kDa) in the adult CNS via alternative splicing of exons 2, 3 and 10 and diagrammatized in Figure 4 (Guo, Noble et al. 2017). In foetal brains, only the shortest isoform of Tau is expressed, which is highly phosphorylated (Goedert, Spillantini et al. 1989). In the adult peripheral nervous system, and in both neurones that project into or are within the CNS, a unique isoform of Tau known as “big Tau” is produced which has a large addition known as exon 4a (not shown in Figure 4) (Fischer and Baas 2020). The adult isoforms differ in the number of N terminal domains (0, 1 or 2) and the number of binding repeat regions (3 or 4), giving a range of 441 amino acids (2N4R) to 352 amino acids (0N3R) in length.

The Tau protein is highly soluble and unstructured, meaning it is a natively unfolded protein (Schweers, Schonbrunn-Hanebeck et al. 1994). The Tau protein has four functional regions, shown in Figure 4. The N-terminal (N) acts as a spacer between microtubules, dictating their separation distance and interactions with other cell components as well as facilitating interaction with the plasma membrane (Chen, Kanai et al. 1992, Gauthier-Kemper, Weissmann et al. 2011). The proline-rich domain (PRD) is the main site of Tau phosphorylation and modulates the N region and the micro tubule binding domain (MTBD) by acting as a signaling hub via kinases and phosphatases (Brandt and Lee 1993). The microtubule-binding domain (MTBD) contains three or four repeat regions, which work together in a multi-valent manner to bind the microtubule (Figure 4). Whilst the MTBD region alone is sufficient to bind Tau, experiments using Tau fragments expressed in *Escherichia coli* showed full-length Tau to have greater binding efficiency to microtubules (Brandt and Lee 1993). The C-terminal region (C), which has been shown, using cell-based assays and phospho-mimicking mutations, to play a role in both modulating the binding of the MTBD and in interactions with the neuronal membrane by phosphorylation of sites within the C terminal region (Eidenmüller, Fath et al. 2001).

Four-repeat (4R) tau isoforms

	N	PRD	MTBD	C	Actual MW	App. MW
2N4R					45,850	67,000
1N4R					42,967	59,000
0N4R					40,007	52,000

Three-repeat (3R) tau isoforms






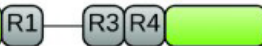


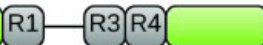
	N	PRD	MTBD	C	Actual MW	App. MW
2N3R					42,603	62,000
1N3R					39,720	54,000
0N3R					36,760	48,000

Figure 4: Tau isoforms and their corresponding molecular weight (actual and apparent).

The N-terminal (N), proline-rich domain (PRD), microtubule binding domain (MTBD) with each repeat region (R1-4) and C-terminal (C) are shown above each isoform. These key domains define Tau's ability to interact with other molecules and in the case of the repeat regions in the MTBD to aggregate with other Tau proteins. The inclusion or otherwise of these regions arises from alternative splicing of the MAPT gene to generate the 6 Tau isoforms. Also shown is the actual molecular weight (MW) in kDa and apparent molecular weight on a SDS page gel, indicated on the right for each isoform. Figure modified from Guo, Noble *et al* (2017).

1.8 Tau function

Expression of Tau is primarily confined to neurons in the human brain, with physiological levels of Tau being around $2\mu\text{M}$ (Butner and Kirschner 1991, Khatoon, Grundke-Iqbal *et al.* 1992). However, Tau can also be found in oligodendrocytes and astrocytes in small amounts and in other organs/tissues, though its function beyond the nervous system is unclear, as reviewed by Kent, Spires-Jones *et al.* (2020). The majority of Tau is found in the axon within the neuron itself, however a somatodendritic population of Tau is also present. Tau's primary physiological role is in the axon, where it binds to and stabilizes microtubules via a rapid binding and unbinding, termed "kiss and hop" (Janning, Igaev *et al.* 2014). This stabilisation role is supported by findings that the microtubule stabilising drug NAP (davunetide) and an analogous protein SAL is capable of rescuing microtubule breakdown and axonal transport deficits in *Drosophila melanogaster* (hereafter referred to as just *Drosophila*) models of Tauopathies (Quraishe, Sealey *et al.* 2016). However, a recent study by Qiang, Sun *et al.* (2018) observed that the knockdown of Tau expression in a rodent

brain causes microtubule loss to come specifically from the labile domain rather than the stable domain of the microtubules (Qiang, Sun et al. 2018). This is significant as rescue experiments using GFP-tagged Tau find Tau localised to these labile domains. These labile domains are more dynamic than stable domains due to being less acetylated and detyrosinated (Qiang, Sun et al. 2018). Therefore, the authors propose that Tau is not a true microtubule stabilising protein. Its role is to instead preserve the labile domain of microtubules by preventing the binding of true microtubule stabilisers such as MAP6, which is counter to current doctrine.

Tau's role in stabilising microtubules in the axon is well documented, but its function in the dendrites is still not fully understood. A reduction in Tau expression causes synaptic loss in hippocampal neurons in rats (Chen, Zhou et al. 2012), which suggests a key role for Tau at the synapse. The mechanisms of this are thought to result from the interaction of Tau with Fyn kinase and the PSD-95-NMDA receptor complex (Mondragón-Rodríguez, Trillaud-Doppia et al. 2012). Tau is capable of binding to Fyn via the Pro-X-X-Pro motifs in its' proline-rich region, which interact with SH2 and SH3 domains in Fyn (Usardi, Pooler et al. 2011). This interaction localises the Tau-bound Fyn to the postsynaptic density where Fyn phosphorylates the NMDA receptor, increasing NMDA receptor-mediated transmission (Salter and Kalia 2004). In this way, Tau plays a role in LTP and LDP and is regulated by phosphorylation of these domains when NMDA is activated, potentially to avoid hyperexcitation (Mondragón-Rodríguez, Trillaud-Doppia et al. 2012, Regan, Piers et al. 2015). However, the necessity of Tau-Fyn binding for this process is not completely clear (Miyamoto, Stein et al. 2017). NMDA receptor activation results in the reversible phosphorylation of Tau at disease-relevant sites AT8 and AT180 (Mondragón-Rodríguez, Trillaud-Doppia et al. 2012). It is possible that the hyper-phosphorylation of Tau, a key event in Tau pathology described in section 1.9.1, is a physiological process that goes wrong, producing a pathological state That is potentially mediated through the NMDA receptor where A β can perhaps induce Tau pathology (Ittner, Ke et al. 2010, Mondragón-Rodríguez, Trillaud-Doppia et al. 2012, Kobayashi, Tanaka et al. 2017).

1.9 Tau's Pathological changes

1.9.1 Post-translational modifications

Post-translational modifications, such as phosphorylation and acetlation, are key to Tau's pathology in AD. Tau can undergo several post-translational modifications (PTM), including ubiquitination, acetylation, methylation, truncation, sumoylation, nitration, oxidation, glycation, glycosylation and phosphorylation (Guo, Noble et al. 2017). In AD, phosphorylation is the most disease-relevant PTM as in AD Tau becomes hyper-phosphorylated. During this process, Tau proteins gain around eight phosphate groups, as compared to the two in normal healthy human adults (Kopke, Tung et al. 1993). There are 85 potential phosphorylation sites in Tau (Serine (53%),

Threonine (41%) and Tyrosine (6%)) (Guo, Noble et al. 2017). Of these, four key sites for Tau phosphorylation have been identified within the microtubule-binding repeat sites (Ser262, Ser293, Ser324 and Ser356) and phosphorylation of these sites prevents binding to the microtubule (Guo, Noble et al. 2017). Another key site for phosphorylation is in the proline-rich domain adjacent to the microtubule-binding sites. Serine-Proline (SP) and Threonine-Proline (TP) pairs in this region are known to be “disease-associated sites” that together, when phosphorylated, make Tau pathological (Steinhilb, Dias-Santagata et al. 2007).

Several other sites have been identified as being phosphorylated in AD (identified in PHFs, NFTs or NTs) but not in healthy adult brains. These are Ser202/Thr205, Tyr18, Ser 396, Thr231, Ser 262, Ser396 and Ser422. Phosphorylation at Ser202/Thr205 is well-characterised and is recognised by the phosphodependent antibody AT8. This site and antibody are used for Braak staging of AD brains (Braak and Braak 1991, Goedert, Jakes et al. 1993). Interestingly, this disease-associated site, along with Tyr18 and Ser 396, are found to be transiently phosphorylated in foetal Tau, suggesting that Tau phosphorylation has a role in embryonic brain development (Bramblett, Goedert et al. 1993, Goedert, Jakes et al. 1993, Lee, Thangavel et al. 2004). However, other sites such as Thr231, Ser 262, Ser396 and Ser422 are phosphorylated in the AD brain and are highly disruptive to MT binding (Lauckner, Frey et al. 2003, Cho and Johnson 2004, Green, Steffan et al. 2008, Lund, Cowburn et al. 2013). Being said, this phosphorylation of Ser262 and Ser356 has been shown in cell models to be required for neuronal process formation, with the authors also postulating that very brief and local phosphorylation of Tau may be required to clear the microtubule for vesicle transport (Biernat and Mandelkow 1999). However, such processes require tight control by kinases and phosphatases.

Many kinases and phosphatases work in concert to regulate Tau in a physiological context and disease. Kinases acting on Tau have been broadly classed into three categories (Guo, Noble et al. 2017):

1. Proline-directed serine/threonine-protein kinases (GSK3 β , Cdk5 and MAK)
2. Non-proline directed serine/threonine-protein kinases (TTBK1/2, CK1 and PKA/pkC)
3. Protein kinases specific for tyrosine residues (Src, Fyn, Abl and Syk)

The most disease-relevant kinase is believed to be GSK3 β , whose activity itself is regulated by phosphorylation of Tyr 216 and Ser 9.29 of its' 40 phosphorylation sites are found to be phosphorylated in AD. This includes Thr231, a phosphorylation site known to have a role in the Tau aggregation process (Cho and Johnson 2004). GSK3 β is also part of the downstream signaling cascade of the NMDAR's and plays a role in synaptic plasticity (Peineau, Taghibiglou et al. 2007, Kimura, Whitcomb et al. 2014). Furthermore, both the total protein and activity levels of GSK3 β increase with the disease alongside localisation of Tau tangles. In addition, mouse models of AD have found that the inhibition of GSK3 β by the thiadiazolidinone compound NP12 rescues memory

loss. This competitive inhibitor rescues a disease phenotype of neuronal loss and Tau pathology in a mouse expressing both APP with the Swedish mutation and a triple human Tau mutation associated with Parkinson's and frontotemporal dementia (G272V, P301L and R406W) (Serenó, Coma et al. 2009). Such evidence has made GSK3 β a favoured target for treating AD, though multiple clinical trials of potential drugs targeting it have failed (Guo, Noble et al. 2017). GSK3 β is not the only proline-directed serine/threonine-protein kinase against Tau; Cdk5 has also been associated with Tau phosphorylation and neurofibrillary degeneration and is present in neurofibrillary tangles along with GSK3 β (Guo, Noble et al. 2017, Brunello, Merezko et al. 2019). Other kinases have also been associated with Tau pathology such as CK1 δ , DYRK1A and TAOs, suggesting that the inhibition of one kinase is not enough to reduce Tau pathology. In addition, not all kinases targeting Tau work upon serine/threonine; a group of five tyrosine residues can also be phosphorylated by Src family kinases and this phosphorylation has been associated with Tau aggregation. Of interest in these Src family kinases is Fyn which targets Tyr18 and plays a role in synaptic plasticity, as well as potentially mediating A β 's toxic effect (Haass and Mandelkow 2010, Guo, Noble et al. 2017).

The removal of phosphates added by Fyn is largely carried out by protein phosphatase 2A (PP2A). PP2A's activity is roughly halved in patients with AD, offering a potential pathway for Tau to become hyperphosphorylated (Guo, Noble et al. 2017). It has been found that GSK3 β and PP2A can interact with each other in a regulatory loop involving the Akt/mTOR pathway. Therefore, an unbalance in the proportion of these two enzymes may have grave results for pathological Tau hyperphosphorylation (Guo, Noble et al. 2017).

The hyperphosphorylation of Tau precedes the self-aggregation of Tau (Alonso, Zaidi et al. 2001), with the extra phosphate groups and their distribution on Tau promoting microtubule uncoupling and aggregate formation. This implies that not only does the phosphorylated Tau destabilise microtubule formation, but it also drives its aggregation into mostly paired helical, or a small number of straight filaments, that then make up the tangles seen in AD patients (Grundke-Iqbal, Iqbal et al. 1986, Grundke-Iqbal, Iqbal et al. 1986, Goedert, Spillantini et al. 1992).

1.9.2 Tau-mediated toxicity

The consequences of the presence of these tangles for the neuron and the precise mechanisms of Tau toxicity are undefined. Toxicity is present when one considers the large amount of neuronal atrophy in a late-stage Alzheimer's brain. However, it is unclear which product of the aggregation process is most toxic: individual Tau monomers, small molecular weight oligomers or fragments of the tangles (Naseri, Wang et al. 2019). It is also not currently known how these products or resulting changes in Tau activity cause the toxicity observed.

1.9.2.1 Loss of function

Toxicity from loss of function occurs due to the unbinding of pathological Tau from the microtubules. As discussed previously, Tau's primary physiological role is in the stabilisation of the microtubules. When hyperphosphorylated, Tau's ability to bind to the microtubule is compromised, leading to its disassociation from the microtubule. This, in turn, leads to a breakdown in microtubule structure and axonal transportation, as seen in transgenic AD mouse models with hyperphosphorylated Tau inclusions and in Tau knockout mice (Cash, Aliev et al. 2003, Dawson, Cantillana et al. 2010). Breakdown of microtubule transport can lead to organelle missorting with subsequent damaging consequences for the neuron (Ozcelik, Sprenger et al. 2016).

As previously alluded to, Tau may play a role in the dendritic compartment, where its loss of function may result in pathological effects. In transgenic Tau mouse models of AD, overexpressing Tau mutants cause synaptic dysfunction and loss which is observed even before neuronal loss (Jaworski, Lechat et al. 2011, Hoffmann, Dorostkar et al. 2013, Dejanovic, Huntley et al. 2018). However, whether this represents a loss of physiological function or a gain of toxic function remains unclear.

1.9.2.2 Gain of toxic function

The events described in previous sections represent toxicity through a loss of function. However, hyperphosphorylated Tau may also undergo a gain of function. Once the native Tau, bound to microtubules, has been converted to a pathological conformation, it gains the ability to convert other Tau monomers to its pathological state. In doing so, this pathological Tau causes further loss of Tau from the microtubules and, so, a loss of function. Furthermore, pathological Tau unbound from the microtubule mislocalizes in the neuron, potentially gaining a toxic function (Mudher, Colin et al. 2017). It has been shown that the mislocalisation of FTD Tau mutants into the cell body causes invaginations of the nuclear membrane in human stem cell models, disrupting nucleocytoplasmic transport (Paonessa, Evans et al. 2019).

In mouse models, hyperphosphorylated Tau expression has led to the mislocalisation of Tau to dendritic spines and subsequent decrease in synaptic function, but without any overt neuronal degeneration (Hoover, Reed et al. 2010). Of note in this study is the decrease in AMPA receptors observed. A β is excitotoxic, and this excitotoxicity is facilitated through AMPA and NMDA receptors. Therefore, Tau hyperphosphorylation may offer a protective mechanism through which, with time, becomes dysregulated, causing pathology. It has been observed in mouse brains that A β -induced neuronal hyperactivity can be silenced by soluble P301L Tau expression (Busche, Wegmann et al. 2019). Such silencing can occur as dendritic Tau is thought to mediate A β 's hyperexcitability by

forming postsynaptic excitotoxic signalling complexes that are engaged by A β (Ittner, Chua et al. 2016). Indeed pseudophosphorylation of Tau at Thr205 (T205E) has been seen to reduce binding to PSD-95, disrupting the NR/PSD-95/tau/Fyn complex and leading to less neuronal death compared to controls. Furthermore, increasing phosphorylation of Thr205, by the kinase p38 γ via AAV-mediated p38 γ expression in a mouse model (APP23 mice) rescues memory defects. Memory defects occur through the expression of human K670N/M671L mutant APP in neurons. . However, other classes of P38 MAPKs, such as P38 α and P38 β , have the opposite effect and are implicated in A β 's excitotoxicity (Ittner, Chua et al. 2016).

Monomeric Tau has also been found to be associated with the inner and outer membrane of mitochondria in small amounts (Cieri, Vicario et al. 2018). Activation of caspase 3, due to A β -induced neuronal apoptosis (Gamblin, Chen et al. 2003) and a downstream event of Tau hyperphosphorylation, directly cleaves Tau at Asp421 generating a truncated protein lacking the last 20 C-terminal residues (Cieri, Vicario et al. 2018). This cleavage leads to a truncated protein that aggregates more readily than full-length Tau but also increases the association between the endoplasmic reticulum and mitochondria and so interferes with communication between the two (Cieri, Vicario et al. 2018).. It has been observed that the ER's calcium levels decrease in the presence of truncated Tau, disrupting cellular calcium homeostasis (Cieri, Vicario et al. 2018). . Such a strengthening of interactions between the ER and mitochondria is also observed in Parkinson's disease, another Tauopathy (Cieri, Vicario et al. 2018).

These gains of toxic functions as described above could also be the result of Tau aggregating into larger molecular weight species such as oligomers, perhaps leading to exposure of certain regions of the protein that represent a gain of toxicity function, which further interferes with axonal trafficking beyond that is caused by the breakdown of microtubules (Morfini, Burns et al. 2009). The growth of these oligomers into the lesions seen in AD may also represent a mechanism of toxicity. This is because the lesions occupy large amounts of space within a cell due to their insoluble aggregates on top of the prior insults described. However, NFTs can be present in the brain for between 20-30 years and neuronal function can be restored despite their presence, suggesting that the smaller molecular weight Tau species are the overtly toxic types (Morsch, Simon et al. 1999, Santacruz, Lewis et al. 2005).

1.9.3 Structural basis of Tau aggregation

The basis for Tau aggregation is encoded in Tau within 6 residues (VQIVYK) of the microtubule-binding domain (MTBD), presenting an interaction motif for Tau monomers to come together (Brunello, Merezko et al. 2019). A second interaction motif (VQIINK) is found in exon 10 of Tau and so is only included in Tau^{ON4R} isoforms, suggesting that this is why they are more

aggregation-prone than Tau^{ON3R} isoforms (Brunello, Merezhko et al. 2019). A cysteine residue in MTBD 2 and 3 stabilise the aggregation of Tau monomers by forming a salt bridge (Brunello, Merezhko et al. 2019). These regions have a high propensity to form β -sheets and allow for Tau dimerization and eventual elongation from this nucleation core (Guo, Noble et al. 2017). However, these β -sheets form the core of paired helical filaments but only make up a small proportion of the aggregated Tau fibres. The next subunit can bind upon this core whilst the rest of the Tau molecule remains disordered and forms a 'fuzzy coat' around this central core (Mandelkow and Mandelkow 2012).

Whilst the presence of VQIVYK and VQIINK motifs allows for Tau aggregation in AD, they alone are not enough for spontaneous aggregation to occur. The fact Tau forms well-defined aggregates, depending upon their structure, is rather odd given that Tau is highly soluble and unstructured and a natively unfolded protein (Schweers, Schonbrunn-Hanebeck et al. 1994). A cofactor is required to allow Tau to overcome the nucleation barrier, either by reducing long-range electrostatic charge interactions or by creating a localised increase in Tau concentration (Goedert, Jakes et al. 1996, Kampers, Friedhoff et al. 1996, Jeganathan, Von Bergen et al. 2008, Ramachandran and Udgaonkar 2011). *In vitro*, these cofactors are often heparin sulphate or other sulphated glycosaminoglycans but Tau aggregation can also be stimulated by RNA (Kampers, Friedhoff et al. 1996) and aradonic acid (Mitra, Gupta et al. 2015). *In vivo*, however, this nucleation cofactor is unknown (Mandelkow and Mandelkow 2012, Scheres, Zhang et al. 2020) and it is also unknown whether cofactors are required for Tau aggregation or whether the inclusion of these potential co-factors is just a result of this (Fichou, Al-Hilaly et al. 2019).

It is crucial to understand further the role cofactors play in Tau aggregation as the packing of the central core results in either paired helical or straight filaments in AD (Fitzpatrick, Falcon et al. 2017). However, different folds of Tau are reported in other Tauopathies such as Pick's disease (Falcon, Zhang et al. 2018), chronic traumatic encephalopathy (Falcon, Zivanov et al. 2019) and corticobasal degeneration (Zhang, Tarutani et al. 2020). The conformation or strain of Tau is disease-dependent, but can also vary within the disease in question, as best exemplified by the two filament types in AD; straight or paired helical filaments. However, the *in vitro* cofactors present can also affect the fibril formation within a disease type, with recent work finding that heparin-induced Tau filaments differ from those seen in AD (Zhang, Falcon et al. 2019). However, *in-vivo* it has been suggested that multiple Tau species are present in 'typical' AD, leading to patient-patient heterogeneity based on the PTM's and Tau's ability to seed aggregation in naïve populations (Dujardin, Commins et al. 2020).

This ability to seed aggregation in naïve populations is a key theory in AD. Once instigated, Tau aggregation can be induced by a misfolded "seed" in a prion-like manner. Once a seed-competent Tau species is formed, it can rapidly induce aggregation in the surrounding Tau monomers. Evidence

for this has been found in numerous studies involving the injection of seed-competent conformers from AD patients into mouse models (Clavaguera, Akatsu et al. 2013). In such models, the presence of an aggregated Tau “seed” can induce aggregation in the wild-type Tau population. This seed is also capable of inducing aggregation through multiple individuals via intracranial injections. One study has demonstrated this by injecting human AD brain homogenate into a previously uninfected mouse, converting the mouse’s wild-type Tau into a diseased conformation. This change was identified through MC1 staining of the disease conformer in the brain. The brain homogenate from this mouse was then injected into a new individual and, again, conversion of the wild-type Tau to a diseased conformation occurred as shown by AT8 staining (Sanders, Kaufman et al. 2014). This seeding ability is dependent on the previously outlined VQIVKY and VQIINK motifs (Falcon, Cavallini et al. 2015). However, for the spread of Tau pathology, via seeding and toxic functions to occur, the Tau seed must first propagate to a naïve neuron.

1.10 Tau propagation

The spread of Tau pathology through the brain can be described as prion-like (Mudher et al 2017). Similar to prions (seen in Creutzfeldt-Jakob Disease or kuru), misfolded protein seeds can spread between synaptically-connected neurons and inducing their misfolded disease conformation in the local naïve protein population. Braak and Braak's staging is suggestive of trans-synaptic propagation of Tau, with synaptically-connected regions demonstrating the appearance of pathogenic Tau with time (Braak and Braak 1991). However, the first evidence of the ability of Tau to propagate through a system was reported by Duyckaerts *et al* in 1997 (Duyckaerts, Uchihara et al. 1997). They described a female patient who had undergone an operation to remove a meningioma 27 years prior to their death, and who had also had their front cortex disconnected in the process. Later in life, the patient contracted AD and tangle pathology was discovered throughout her brain, including limbic and isocortical regions. However, there was a complete absence of Tau pathology in her frontal cortex (Duyckaerts, Uchihara et al. 1997). Given the consensus that Tau spreads throughout the brain in set stages, the absence of pathology in the brain's frontal cortex suggests that spread is mediated by the propagation of a pathological conformer of Tau along connected neurons. Spread between connected regions has been demonstrated in mouse models with injected or expressed disease-relevant Tau species in defined areas, leading to the spread of Tau pathology into connected regions (Clavaguera, Bolmont et al. 2009, Lasagna-Reeves, Castillo-Carranza et al. 2012, Liu, Drouet et al. 2012, Wegmann, Bennett et al. 2019). More recent studies in the human brain, using Tau positron emission tomography and mathematical predictions, have highlighted the importance of neuronal connectivity in relation to Tau spread (Vogel, Iturria-Medina et al. 2020, Franzmeier, Brendel et al. 2022).

The Tau propagation hypothesis rests on the idea that Tau seeds are released by diseased neurones and taken up by recipient healthy neurones which are then converted to a diseased state. This is demonstrated clearly by Hallinan *et al* (2019) in their hippocampal monoculture model. The use of a microfluidic device to isolate neurons in chambers, with channels that only allow the neuron's axons to project through, shows that synaptic contacts are crucial to modelling wild-type Tau and pathological Tau's spread, not close proximity (Dujardin, Lécolle *et al.* 2014, Calafate, Buist *et al.* 2015, Hallinan, Vargas-Caballero *et al.* 2019). The spread of Tau is described as 'prion-like' as, whilst having many of the hallmarks of other prion proteins (for instance, the formation of ordered assemblies and intercellular propagation), Tau seeds lack the ability to naturally transfer between individual organisms and so are only prion-like, rather than actual prions (Mudher, Colin *et al.* 2017). This is an important distinction when considering scientific reporting in the media. However, the precise mechanism of Tau's prion-like spread remains an open field.

1.10.1 Pre-synaptic mechanisms

The mechanisms mediating the release of Tau seeds are unclear, as the Tau protein does not contain a signalling peptide for conventional secretory release (Chai, Dage *et al.* 2012). As a result, different non-conventional mechanisms for its release have been proposed, ranging from exosomes (Saman, Kim *et al.* 2012, Simón, García-García *et al.* 2012, Asai, Ikezu *et al.* 2015, Wang, Balaji *et al.* 2017, Yan and Zheng 2021), ectosomes (Dujardin, Bégard *et al.* 2014) and even as free Tau (Dujardin, Bégard *et al.* 2014, Wang, Balaji *et al.* 2017) (Figure 5). The spread of Tau across the synapse is potentially facilitated and influenced by a number of mechanisms Figure 5. These range from vesicle-mediated release and uptake through to direct translocation across the synaptic membranes. Whilst evidence exists for the role of many of these mechanisms in spread it remains unknown which plays significant roles in physiology or pathology. The synaptic environment and synaptic activity may also influence mechanisms and glia could also play a role. This adds further complexity to the system, but also potential therapeutic avenues, by offering new therapeutic targets if pathological changes are identified in these other factors. Of these forms, it has been reported that extracellular wt-Tau in rat cortical cells was distributed as 90% free Tau and 10% as vesicular Tau (7% in ectosomes and 3% exosomal) (Dujardin, Bégard *et al.* 2014). This suggests that no single path for Tau spread exists, however the challenge is to identify what pathways are physiologically relevant and which are disease-relevant in AD.

1.10.1.1 Free Tau

Clinically found in human CSF and observed in the supernatant of cell models and the ISF of mouse brains, free Tau is found in both monomeric and oligomeric forms (Chai, Dage *et al.* 2012, Matsumoto, Motoi *et al.* 2015, Cicognola, Brinkmalm *et al.* 2019). Precisely how this free Tau

escapes the neuron is still poorly understood. However, studies suggest that it could be translocated directly across the plasma membrane by becoming hyperphosphorylated and binding to key lipids such as phosphatidyl inositol _{4,5} phosphate (PI_(4,5)P₂) on the inner leaflet and then to heparin sulfate proteoglycans on the outer leaflet (Katsinelos, Zeitler et al. 2018, Merezhko, Brunello et al. 2018). Heparin sulfate proteoglycans are known cofactors involved in Tau aggregation, as discussed above, and also may play a role in Tau uptake.

1.10.1.2 Vesicular Tau

Whilst 90% of Tau released from cells is in a free form, the remaining 10% is bound in extracellular vesicles and may still contribute to pathology. 7% of this is in ectosomes which bud directly from the plasma membrane (Meldolesi 2018). This method of Tau release has been suggested to be a physiological phenomenon, whilst exosomal Tau may be pathological (Dujardin, Bégard et al. 2014, Spitzer, Mulzer et al. 2019). Studies on exosomes isolated from the CSF of an AD patient have been found to contain seed-competent Tau species (Saman, Kim et al. 2012, Wang, Balaji et al. 2017, Leroux, Perbet et al. 2022). Recent work has shown that this vesicle-mediated Tau accumulates in GABAergic interneurons (Ruan, Pathak et al. 2021). Exosomes have been identified in the spread of other pathological proteins such as α -synuclein, prion protein and A β , as reviewed by Howitt and Hill (2016). The release of these exosomes depends on synaptic activity (Lachenal, Pernet-Gallay et al. 2011) and can be facilitated by microglia (Asai, Ikezu et al. 2015), suggesting consequences for the synaptic environment on Tau spread mechanisms. Interestingly however, Tau binding to synaptic vesicles via its N-terminal domain has been shown to restrict vesicle mobilization, reducing synaptic vesicle release rate and thereby neurotransmission (Zhou, L. *et al* 2017)

1.10.2 Post-synaptic mechanisms

Whilst uptake mechanisms are equally unclear on the other side of the synapse evidence broadly points to endocytosis, mediated by heparan sulfate proteoglycans (HSPGs) (Hallinan, Pitera et al. 2019). Tau trimers are the minimum-sized aggregates required to initiate this mechanism (Mirbaha, Holmes et al. 2015) but a second route exists for monomeric Tau which can enter neurons via actin-dependent micropinocytosis (Evans, Wassmer et al. 2018). The rapid and efficient uptake of Tau into neurons, especially of monomeric species, is again an indication that the spread of Tau between neurons may have a physiological role (Evans, Wassmer et al. 2018).

Recently, the focus has turned to uptake mechanisms associated with HSPGs due to the identification of a role for low-density lipoprotein receptor-related protein 1 (LRP1) via cell and mouse models. LRP1 is known to associate with HSPGs and has been identified as a key mediator of Tau endocytosis (Rauch, Luna et al. 2020). The importance of LRP1 in Tau uptake was previously demonstrated in a series of genetic knockout experiments, highlighting the importance

of a series of lysine residues in the Tau microtubule-binding domain for LRP binding and internalization (Rauch, Luna et al. 2020). LRP1 is also known to play a role in ApoE internalization (the ApoE4 gene is a significant risk factor in AD) and impacts A β degradation and production. This is theorized to be due to competitive interactions between the ApoE and Tau (Rauch, Luna et al. 2020).

Another mechanism of Tau spread remains possible with tunnelling nanotubes (TNTs), which transfer α -synuclein seeds between cells and have been shown to contain Tau, adding more complexity to the picture (Hallinan, Pitera et al. 2019). The various uptake and release mechanisms are shown diagrammatically in Figure 5.

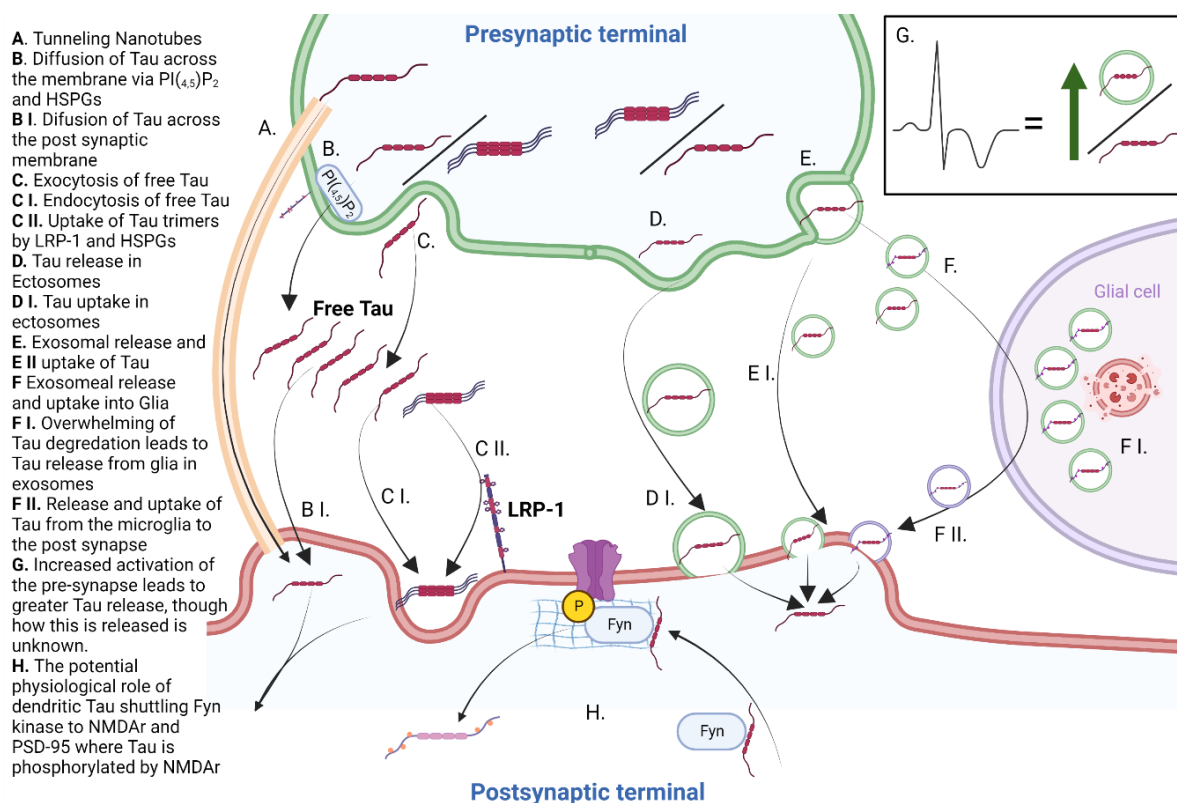


Figure 5: Diagram of the proposed mechanisms of Tau's transynaptic spread.

The spread of Tau across the synapse is potentially facilitated and influenced by a number of mechanisms as outlined in the key. This ranges from vesicle-mediated release and uptake through to direct translocation across the synaptic membranes. Whilst evidence exists for the role of many of these mechanisms it remains unknown which play significant roles in physiology or pathology. These mechanisms may also be influenced by the synaptic environment, with synaptic activity and glia playing a role adding further complexity, but also potential therapeutic avenues.

1.10.3 Impact of events and actors at the synapse on Tau spread

1.10.3.1 Hyperactivity

Reports of hyperactivity of the hippocampal neurons, prior to degeneration and hypoactivity, are reported through fMRI scans in patients early on in AD or in individuals diagnosed with MCI (Bassett, Yousem et al. 2006, Celone, Calhoun et al. 2006). This hyperactivation can manifest in epilepsy in young-onset cases or early in sporadic AD (Amatniek, Hauser et al. 2006).

Despite the precise mechanism of Tau release being unknown, it has been shown that potentially-physiological Tau release is linked to synaptic activity (Pooler, Phillips et al. 2013, Yamada, Holth et al. 2014). Pooler *et al* (2013) used ELISA assays to determine the concentration of Tau released by the primary culture of cortical neurons upon glutamate stimulation. Significant increases in Tau release at 10 μ M and 100 μ M glutamate were observed, although even untreated neurons were

found to release Tau. This suggests a low baseline leakage of Tau from the neurons into their surroundings that are increased upon stimulation. Tau from untreated neurons was not pathogenic but represented a physiological release of Tau for an unknown function. The authors attributed this physiological release to either direct signalling to the target neuron, by Tau's activation of muscarinic acetylcholine receptors, or by modulating the post-synapse's response once endocytosed (Pooler, Phillips et al. 2013). Physiological modulation of the post-synapse by wt-Tau propagation can become pathological when Tau seeds are present. This process could, theoretically, allow for the transfer of the diseased conformation. Prior analysis of released physiological Tau showed that it was dephosphorylated and intact (Hanger, Anderton et al. 2009). A physiological role of Tau is in the dendrites, where it shuttles Fyn kinase to the post-synaptic density. This may be part of the LTP pathway as, by extruding Tau to be taken up in the dendrite of the post-synapse, the neuron strengthens its connection by providing more dendritic Tau for shuttling. In AD, Tau is often hyperphosphorylated and cleaved, in contrast to the theorized physiologically-released Tau, to which Pooler *et al* claim that one or both of these modifications modulate Tau's release from neurons (Pooler, Phillips et al. 2013). Other studies, however, have shown that hyperphosphorylated Tau, particularly phosphorylation in the PRD and C-terminus, results in a preferential release of these phosphorylated species (Ismael S et al 2021). This shows that the precise role of hyperphosphorylation in Tau spread is still poorly understood. The mechanism for Tau release from the neuron under stimulation is also poorly understood, but depolarization of neurons has been shown to promote the release of exosomes that contain Tau (Wang, Balaji et al. 2017). Nonetheless, Pooler *et al* postulate that whilst the mechanism is dependent on synaptic vesicles, activity stimulates a non-exosomal secretion of Tau (Pooler, Phillips et al. 2013). Stimulation of the neuron is not only linked to increasing spread of Tau protein but also has been shown to accelerate Tau seed pathology, resulting in greater cell atrophy in an optogenetically driven mouse model (Wu, Hussaini et al. 2016).

1.10.3.2 The role of glia

Another factor at the synapse is the action of microglia, which usually function to maintain neuronal health by clearing debris, aggregates and dying cells, but can also play a role in neurodegenerative diseases (Colonna and Butovsky 2017). Microglia can internalize and degrade Tau, however their ability to do so is limited. Once they can no longer degrade the internalised Tau, the aggregate formation can occur and potentially secrete these Tau aggregates into the extracellular space via exosomes (Asai, Ikezu et al. 2015, Hopp, Lin et al. 2018, Romero-Molina, Navarro et al. 2018). Depletion of microglia and their signalling pathways, or inhibition of exosome synthesis, has been used in mouse models to suppress Tau propagation (Asai, Ikezu et al. 2015, Wang, Fan et al. 2022).

Together, neuronal activity and microglia add another layer of complexity in investigating Tau spread and must be taken into account when studying this.

1.10.4 Effect of A β on Tau spread and pathology

The Pooler et al (2013) study suggests that hyperactive neurons are clustered around plaques in APP/presenilin mutated mice. This suggests that A β plaques have some role in Tau propagation by stimulating the nearby neurons. A β_{42} can induce hyperactivation in a neuron by the overstimulation of the NMDA receptor, driving the propagation of Tau seeds and increasing release, suggesting another link between A β_{42} and Tau. However, this was not directly tested in the experiment. A β 's effect on Tau propagation may also extend to kinases such as c-Jun N-terminal kinase (JNK). JNK is activated by A β and phosphorylates Tau, potentially increasing its seeding potential (Ma, Yang et al. 2009). Phosphorylation could also potentially have a role in Tau's transmissibility. In this way, not only could A β increase Tau release, but it could also increase the potency of the Tau seed, further accelerating pathological spread. Indeed, a mixed-modelling approach based on human PET scans has shown that regions with A β burden have an increased Tau content than predicted, based on neuronal connections. This suggests that A β accelerates Tau spread (Vogel, Iturria-Medina et al. 2020).

The experiments described demonstrate that physiological Tau propagation may be hijacked for pathological Tau to spread to naïve neurons, potentially piggybacking on normal Tau release upon excitation. Differentiating between pathological and physiological Tau secretion and uptake will be challenging to achieve and is influenced by other pathological proteins in AD.

The findings discussed so far have been discovered using a range of models developed to study the wide-ranging aspects of Tau propagation. These models have allowed for the study of either a highly defined connection or broadly-defined regions of spread and are discussed in Section 1.11.

1.11 Current models of Tau propagation

1.11.1 Cell models

Current models of Tau propagation are based on two main types: cellular and mouse. Cell models have used a variety of cells, including non-neuronal and neuronal types, stem cell-derived neurons and primary neurons (Hallinan, Pitera et al. 2019). Molecular models often either use the extracellular application of recombinant Tau or cells which are transfected with plasmids encoding Tau. Recombinant Tau is purified from *Escherichia coli* and, as outlined earlier, Tau misfolding and aggregation require a cofactor. For recombinant Tau, these cofactors are often arachidonic acid, free fatty acids or heparin (Hallinan, Pitera et al. 2019). Alternatively, a truncated Tau fragment (known as K18) centred on the microtubule-binding domain is often used due to its propensity to aggregate (Hallinan, Pitera et al. 2019). Whilst these methods are able to cause aggregation in Tau,

the precise conformers they form may not be representative of those found in *in vivo*.

Transfection by plasmids offers a more controlled way to express Tau in a cellular system and allows for modulation of the system itself. This method often involves expressing a full-length mutant form of Tau, P301L. This form of human Tau is a common mutation that readily aggregates and is found in those with frontotemporal dementia (Hallinan, Pitera et al. 2019). Using these approaches, cell models have uncovered several key insights into Tau propagation surrounding the uptake of extracellular Tau into cells (Frost, Jacks et al. 2009, Wu, Herman et al. 2013, Takeda, Wegmann et al. 2015, Rauch, Chen et al. 2018), Tau secretion and its mechanisms (Chai, Dage et al. 2012, Karch, Jeng et al. 2012, Saman, Kim et al. 2012, Pooler, Phillips et al. 2013, Wu, Hussaini et al. 2016) and attributes of the Tau seed and its spread (Dujardin, Lécolle et al. 2014, Michel, Kumar et al. 2014, Calafate, Buist et al. 2015).

Cellular models are now becoming more advanced with the adoption of microfluidic devices. A microfluidic device often contains two or more independent horizontal channels within which neuronal cells are cultured. These channels are linked by fine vertical passages that can be shaped to ensure the uniform direction of the axons that pass into them. Such a system allows for the compartmentalisation of the pre- and postsynaptic neurons, introducing defined connections more akin to those found *in vivo*. These cell models can observe Tau spread between individual hippocampal mouse neurons and isolate distinct regions within the neuron, including within axonal and somatodendritic regions. This offers an incredibly precise tool, as Hallinan et al (2019) discussed in their comprehensive review. However, such models are often a monoculture that cannot recapitulate the complexity of the brain, overlooking key physiological processes and cell types such as glia and astrocytes that may play a key role in Tau transmission (Asai, Ikezu et al. 2015, Chiarini, Armato et al. 2017). This has been further developed using 3D microfluidic devices to include multiple cell types such as neurons, astrocytes, and microglia (Park, Wetzel et al. 2018). However, by only focusing on the cell itself, downstream effects of Tau propagation on the circuitry or organism as a whole may not be evident. This is supported by findings that Tau propagation have little overt effect on the recipient neuron, leaving it viable and electrically competent (Hallinan, Vargas-Caballero et al. 2019).

1.11.2 Mouse models

Mouse models of Tau propagation can be grouped into regional promoters, inoculation and viral models based upon how Tau is introduced into the system. The advantages and disadvantages are discussed below and summarized in Table 1.

Regional Promotors

Regional promoters express Tau within specific neurons in defined brain regions such as the entorhinal cortex in rTgTauEC mice (P301L Tau) (de Calignon, Polydoro et al. 2012). Whilst predominantly expressed in these specific regions, some 'leakage' of the transgene can sporadically be observed in the hippocampal neurons of the dentate gyrus, CA1 regions and CA3 regions, though such leakage is characterizable (Yetman, Lillehaug et al. 2016). One study using regional promoter models found that initially, Tau displayed diffuse staining, associated with a normal wild-type distribution but at three months there was evidence of misfolding in the axon terminal zone, as shown by Alz50 staining. This Tau spread to connected areas in layer II of the dentate gyrus within 18 months, as shown by histological analysis using Alz50 and PHF1 monoclonal antibodies to identify misfolded Tau aggregates. Alz50 recognises a misfolded conformation of Tau, one of the earliest detectable points in Tau aggregation, by binding to the amino acids at 2-10 and 312-342, which are brought into close proximity by misfolding (Hyman, Van Hoesen et al. 1988). PHF1 recognises phosphorylation at serine-396 and serine-404 (Otvos Jr., Feiner et al. 1994). Crucially, when the Tau spread was further investigated using FISH (fluorescence in situ hybridization), only a third of the Alz50 aggregates contained human Tau mRNA (in other words, Tau from the medial entorhinal cortex (MEC)). This showed that human Tau aggregates could turn mouse Tau into an aggregate-forming species that could propagate the misfolded conformation throughout the neurons. However, aggregation only occurred in areas connected to the dentate gyrus, particularly in the CA1 and CA2/3, by 21 months of age (de Calignon, Polydoro et al. 2012). This reinforces the idea of Tau spread between neuroanatomically connected regions and potentially across synapses. Caveats to these types of mouse models revolve around the use of frontal-temporal dementia mutant P301L. This mutant, whilst related to AD, better recapitulates familial forms rather than the more common spontaneous forms. Furthermore, such transgenic mice are expensive and time-consuming to create and maintain and whilst useful and genetically relevant to humans, they do not lend themselves to a rapid investigation of novel constructs.

Inoculation-Based Models

These rely on the injection of Tau aggregates or seeds into a mouse brain. Whilst lacking the specificity of regional promoters, injection offers a chance to study seeding and conformer properties. For example, the injection of Alzheimer patient-derived, high molecular weight paired helical filaments (PHFs) into the dentate gyrus of wild-type and mutant mice showed that the high molecular weight PHFs are inefficient as seeds (Audouard, Houben et al. 2016). Such a model was also used to show that Tau seeding is templated, stable and produces conformationally-distinct strains. This study inoculated three successive generations of mice with brain homogenate from

the previous generation. Three different strains were tested, each producing a unique pathological phenotype (Sanders, Kaufman et al. 2014). Again, Tau spread was seen to occur to neuroanatomically-connected regions (Sanders, Kaufman et al. 2014). Caveats centre on the injection site of the mouse, which may cause unintended damage, along with the random nature of neuron uptake of the injected material. Both of these have the potential to affect the experimental outcome. However, such a system allows for the easy characterisation of the Tau species *in vitro* before injecting them *in vivo*.

Viral Models

Viral models offer a faster and more versatile way to induce Tau expression in mice compared to traditional transgenics (Dassie, Andrews et al. 2013). These models often use adeno-associated virus (AAV) or lentivirus as the viral vector, delivering Tau or Tau mutants into specific brain regions and leading to long-term and local expression (Cubinková, Valachová et al. 2017). AAVs are replication- defective, non-pathogenic single-stranded DNA viruses requiring a helper virus particle (adenovirus) for infection and replication. This makes AAV infectious but it lacks virulence, allowing for sustainable transgene expression in receiving cells (Cubinková, Valachová et al. 2017). Such models have demonstrated the ability to produce Tau aggregates and spread between neuroanatomically- connected regions and have also shown that Tau expression is critical for A β 's toxic role (Cubinková, Valachová et al. 2017). Another interesting finding which has utilised such models is that the depletion of microglia can suppress Tau propagation, suggesting microglia play a role in propagation through exosome secretion (Asai, Ikezu et al. 2015). Caveats with these models include mosaicism as not all cells are transduced by the injected AAV, creating a variation between the start points between repeats. This is somewhat mitigated by the co-expression of GFP markers in expressing cells to delineate them from Tau in neurons as an uptake of spread (Wegmann, Bennett et al. 2019). Furthermore, unintended injury from the injection may lead to the activation of inflammatory pathways which can interfere with Tau propagation (Laurent, Buée et al. 2018). Finally, viral vectors are small, offering a limited packaging size and so, the size of potential constructs. However, such a system allows for relatively rapid creation of constructs, which can be injected into previous transgenic lines to alter backgrounds.

Table 1: Table summarizing the advantages and disadvantages of three different types of mouse models of Tau pathology.

Model of Tauopathies	Advantages	Disadvantages
Regional Promotors	Able to express Tau constructs within a subset of neurons in the mouse brain	Leakage of genetic material can occur Low resolution as it targets brain regions, not specific neurons
Inoculation-Based	Addition of pre-characterised or patient-derived seeds to a brain region	Chance of damage and potential inflammation and death around the injection site Random uptake of injected Tau seeds into neurons occurs
Viral	Faster and more versatile than regional promotors Can influence neuronal environment e.g. glial knockdown	Mosaicism in infected tissue The small size of the vector limits the size of the construct Injury and inflammation at the injection site can occur

1.11.3 Why a new model is needed

Several overall problems persist with the use of all types of cell and mouse models. For example, a key issue with cell models is that they cannot effectively replicate the degree of complexity present in the brain. Whilst well-suited for asking questions about specific neurons and connections, they cannot imitate the complexity of an organism in terms of both connections and cell types present (structural and glial cells are key examples), nor can they replicate the downstream effects of Tau propagation upon an organism such as altered behaviour or decreased lifespan. Conversely, mouse models have shown that Tau aggregates can aggregate and spread in an age-dependent manner in the complex environment of the mouse brain. However, unlike with cell models, it is difficult to study individual neuronal connections and these mouse models can take up to 2 years to age effectively, limiting their use for high throughput screens. Furthermore, the Tau mutant commonly used in both model types, P301L, is a representative form for frontal temporal dementia and hereditary AD (Terwel, Lasrado et al. 2005) but not for the more common, sporadic form of AD. Indeed, due to the many different potential conformations and post-translational modifications of Tau, it is still unknown which conformer(s) are responsible for Tau propagation and toxicity. Rapid

testing of multiple conformers and their effects on multiple aspects of a system will be key to understanding Tau propagation and another model type is required to achieve this.

1.12 Suitability of *Drosophila melanogaster*

For over a century, *Drosophila melanogaster* (also known thereafter as only '*Drosophila*' or 'the fly') has been the model organism of choice for many genetic researchers, leading to several Nobel prizes and, more importantly, an understanding of several key genes and their role in development (Jennings 2011). In regards to neuroscience, *Drosophila* studies have uncovered key proteins involved in neurogenesis (Notch) and nerve function (TRP, Sh, eag) and have been used to model synaptic transmission at the neuromuscular junction (Bellen, Tong et al. 2010). *Drosophila*'s long history as a model organism provides many research advantages due to its fully sequenced genome, well-studied anatomy and the broad range of genetic tools which can be used to probe the system, as outlined in Table 2 (Prüßing, Voigt et al. 2013). From a practical side, they can also be reared cheaply and *en-mass*, allowing for sizeable experimental screening. Experiments also have fast turnaround times, as *Drosophila*'s lifespan is in the region of 120 days (Prüßing, Voigt et al. 2013). This means that 'old age' in a fly is achieved in around two months, whereas most Tau studies in mice require ageing to around two years, dramatically increasing the rate at which data can be generated. The key advantages and disadvantages of using *Drosophila* for modelling Tau spread are listed in Table 2.

Table 2: The relative advantages and disadvantages of *Drosophila melanogaster* as a model organism for studying Tau propagation and seeding

Advantage	Disadvantage
Well-defined neuroanatomical connections	Very different anatomy
GAL4.UAS system allows for spatiotemporally-controlled protein expression	Living stocks must be maintained, and flies cannot viably be frozen and thawed
Extensive library of existing transgenes	Less complex/adaptive immune system
New transgene expression is fast and inexpensive	The effect of drug trials may not translate to humans
Short experimental turnaround times (adults eclose in around ten days) due to a 120-day lifespan	Short lifespan
Behavioural assays allow for consequences of pathological Tau propagation to be investigated	Challenging to carry out behavioural assays
Easy/cheap to maintain large numbers allowing for high numbers of biological repeats	
Conservation of basic signalling pathway and cellular processes	
Balancer chromosomes allow for genetic tractability	

1.12.1 Specificity of connections

The key to research on Tau propagation is the detailed knowledge of circuitry within the *Drosophila* brain. Focused ion beam–scanning electron microscopy (FIB-SEM) and computer-aided reconstruction have led to the development of the adult *Drosophila* brain atlas, in which many circuits have been studied down to the EM level (Scheffer and Meinertzhagen 2019). These connectomes are constantly progressing, with detailed connectomes now available for olfactory, thermosensory, hygrosensory and memory systems (Li, Lindsey et al. 2020, Lizbinski and Jeanne 2020, Marin, Büld et al. 2020). In certain tissues

(such as the olfactory or gustatory systems) external stimuli are characterised, meaning that odour perception have been mapped onto functional neuronal circuits (Vosshall and Stocker 2007) offering physiological stimulation or behavioural outputs (Kirkhart and Scott 2015). This is reviewed further by Ugur *et al* (2016). This offers not only a well-defined circuit, but also the ability to further interrogate the health of the neurons present based on preserved functionality.

A number of experiments in *Drosophila* have also used a variety of techniques, fluorescent reporters and dyes to investigate neuronal connections (Marin, Jefferis *et al.* 2002, Tanaka, Suzuki *et al.* 2012, Talay, Richman *et al.* 2017). The injection of dyes into flies has provided further information on downstream connections and activity. Dyes include calcium-binding molecules for studying neuron signalling and the larval NMJ (Macleod 2012), fluorescent dyes to visualize the giant fibre (Boerner and Godenschwege 2011) and lipophilic dyes in larvae and adult flies to investigate downstream connections (Tanaka, Suzuki *et al.* 2012, Inal, Banzai *et al.* 2020).

Fluorescent markers, genetically expressed using the Gal4:UAS system, can also label neuronal populations and their downstream connections with greater accuracy and less physical damage to the fly than using injections (Salvaterra and Kitamoto 2001, Talay, Richman *et al.* 2017). Whilst visualisations are not as detailed as in EM studies, fluorescent reporters such as GFP are easily combined with Tau expression to identify circuits or act as controls.

1.12.2 The UAS:GAL4 system

UAS:GAL4 is a yeast transcriptional activator system utilized in *Drosophila* to express the desired protein in a subset of cells (Brand and Perrimon 1993). It is an incredibly useful system; many of the experiments outlined in previous sections, such as section 1.8, would not have been possible without this system. GAL4 is a *Saccharomyces cerevisiae* transcriptional activator that binds to four related upstream activating sites (known as UAS) of the genes GAL10 and GAL1. In *Drosophila*, this system can be split into two parts to localize the desired protein expression to selected tissue. Tissue selection is achieved via a driver line in which the transcription factor GAL4 is expressed under the control of a regulatory sequence only found in the selected tissue. This achieves specificity as the protein of interest is downstream of the UAS promoter region, controlling its expression. Translation and subsequent protein synthesis can occur only in tissue with Gal4 expression. The selection of the targeted tissue can be as broad as every neuron or glia in the brain (Wittmann, Wszolek *et al.* 2001, Colodner and Feany 2010) down to drivers of specific cell types, such as motor or sensory neurons (Williams, Tyrer *et al.* 2000, Mudher, Shepherd *et al.* 2004). Alternatively, GAL4 drivers can be selected for regions of the flies' brain such as in the eyes (Glass Multiple Reporter; GMR) or mushroom bodies (Aso, Grübel *et al.* 2009, Li, Li *et al.* 2012).

Other expression systems exist that can be used alongside GAL4, such as the Q-system (Potter and

Luo 2011) and LexA (Kockel, Huq et al. 2016), to facilitate the co-expression of other proteins of interest. Furthermore, spatio-temporal control can be achieved with the UAS.GAL4 system by the co-expression of the repressor GAL80 which inhibits GAL4 activity (Eliason, Afify et al. 2018). The use of a temperature-sensitive (ts) GAL80 variant allows for Gal80ts to repress GAL4 activity when flies are reared at 18°C. However, when flies are reared at 29°C, GAL80ts is inactivated, and the protein of interest can be expressed (Parkhitko, Ramesh et al. 2020). These systems offer a powerful toolkit to fly geneticists to create complex models, allowing for tight expression profiles of multiple genes of interest.

1.12 *Drosophila* Tau and other homologues

The UAS.GAL4 system allows for the expression of proteins relevant to AD within the *Drosophila* brain, but importantly these human proteins are not completely novel to the *Drosophila*. 60% of *Drosophila* genes are homologous to humans, with 75% human disease-related genes also having homologues in flies (Reiter, Potocki et al. 2001, Chiang, Ho et al. 2022). Importantly, *Drosophila* genomes have equivalents of human APP and A β (Carmine-Simmen, Proctor et al. 2009) and Tau (Heidary and Fortini 2001). Expression of human APP in the fly can ameliorate the deficits caused by *APPI* (the *Drosophila* APP homologue) knockdown, suggesting that conserved pathways are present in the fly (Luo, Tully et al. 1992). There is a single Tau gene in the fly, producing a protein 66% similar to human Tau. This dTau consists of five highly conserved MTBD regions (one more than the largest human Tau isoform) and lacks N-terminal functional domains (Heidary and Fortini 2001). Overexpression in the mushroom bodies of either human or *Drosophila* Tau leads to learning deficits in the fly, (Mershin, Pavlopoulos et al. 2004). However, no seeding of *Drosophila* Tau misfolding by human Tau has been reported, unlike in mouse models where human Tau can seed misfolding of murine Tau (Narasimhan, Guo et al. 2017). Whilst the physiology and gross structure of the neuronal anatomical connections may differ, the underlying physiology is conserved and for investigating basic or singular aspects of AD the fly can provide translatable insights (Pandey and Nichols 2011).

1.12.3 *Drosophila's* use in modelling other prion-like proteins

Drosophila melanogaster is well suited to model Tau propagation as it has already been utilized to gain a mechanistic understanding of the spread of prion-like proteins in Parkinson's and

Huntington's disease (Feany and Bender 2000, Gunawardena, Her et al. 2003). In two separate studies of Huntington's disease, the spread of the mutant Htt protein has been tracked from an initial site in *Drosophila's* olfactory bulb throughout the system into selectively vulnerable neurons. In both cases, the spread of the Htt protein was also shown to cause neuronal dieback and, eventually death of the organism (Gunawardena, Her et al. 2003, Babcock and Ganetzky 2015). In addition, recent work using small circuits within the olfactory bulb (targeting single olfactory neuron classes and their connections) has shown that glia are intermediates in the transmission of mutant Htt protein across the synapse (Donnelly, DeLorenzo et al. 2020). These studies demonstrate that *Drosophila* can be effectively used to model Tau's prion-like spread across the synapse, having already been employed to understand another prion-like proteinopathy.

1.13 Proposed model

1.13.1 Odorant receptors

The proposed *Drosophila* model utilizes olfactory receptors and their associated circuitry to provide specific connections across which Tau spread can be investigated, linking Gal4 promoter expression to olfactory receptors to drive UAS.Tau expression in specific circuits. The Gal4:UAS system can then also be used to express other proteins that will affect Tau spread, such as activity mutants in order to investigate their effects.

Discovered in 1999, *Drosophila* odorant receptors have been mapped to 60 odorant genes, encoding 62 receptors (the extra two result from alternate splicing) (Robertson, Warr et al. 2003). These genes encode a 7-transmembrane domain protein that is evolutionary distinct from G-coupled receptors, forming independently of chemosensory systems present in other animals (Vosshall, Amrein et al. 1999). These genes are expressed in a defined spatial pattern between olfactory receptor neurons within one of three distinct regions of the fly brain; antennae, maxillary pulp and larval dorsal organs (only found in larvae). The exception to this rule is Or83b, a co-receptor expressed in all olfactory receptor neurons. Or83b is expressed alongside only one of the other 62 receptor types and the resulting complex defines each olfactory receptor neuron (Vosshall, Amrein et al. 1999). In the majority of olfactory neurons, only a single receptor type is expressed in that neuron. However there are exceptions to this rule 13 olfactory receptor neurons express two or three olfactory receptors in a single neuron, although the resulting function of this is currently unknown.

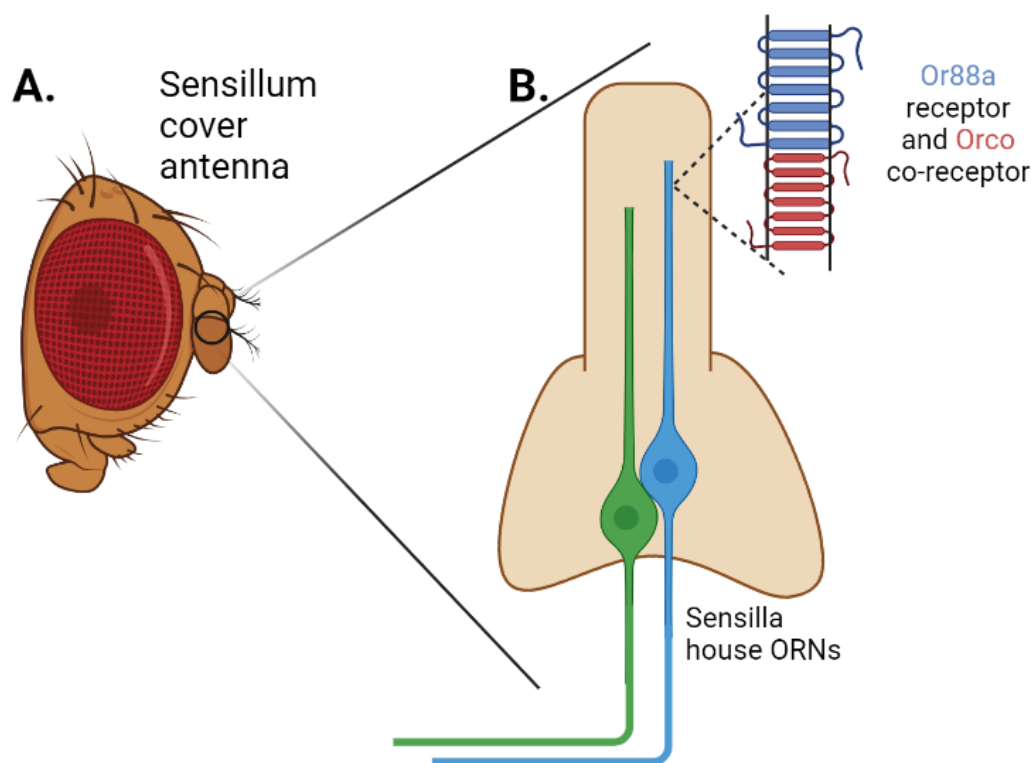


Figure 6. Diagram of the olfactory receptor neurons in the antennae

- A) *Drosophila* antenna are covered in tiny hairs called sensillum
- B) These sensillum contain a combination of olfactory receptor neurons (green and blue). Each of these olfactory receptor neurons only contain one type of olfactory receptor (such as Or88a) and the co-receptor Orco (Or83b)

1.13.2 Olfactory circuitry

The location of each olfactory receptor neuron within individual sensillum on the antennae and olfactory organs have been elucidated (Vosshall and Stocker 2007). The use of fluorescent tracers to label these olfactory neurons has shown that olfactory receptor neurons target one or two glomeruli within the antennal lobe, depending on which olfactory neuron is expressed (Fishilevich and Vosshall 2005). The glomeruli that the olfactory neurons target are distinct, well-defined microareas of the antennal lobe which are formed of synapses between olfactory neurons, local interneurons and their corresponding projection neurons (Vosshall and Stocker 2007). The synapsing of a particular olfactory neuron to its corresponding projection neuron in a specific glomerulus creates a “glomerular code” of the odor being received. The projection neuron then carries this pattern to higher brain regions, such as the calyx and lateral horn, where the axons converge and diverge to stimulate a variety of terminal fields in both of these brain regions (Vosshall and Stocker 2007).

In this way, olfactory circuitry in the fly can be loosely generalized by the one-receptor-one-neuron and the one-neuron-one-glomeruli rules. The first of these rules is outlined in the previous

section, with one olfactory receptor (and corresponding co-receptor Or85b, known as ORCO) being expressed in a single olfactory neuron type. These olfactory receptor neurons will then target one (in some exceptions two, as outlined previous) glomeruli within the antennal lobe (Fishilevich and Vosshall 2005).

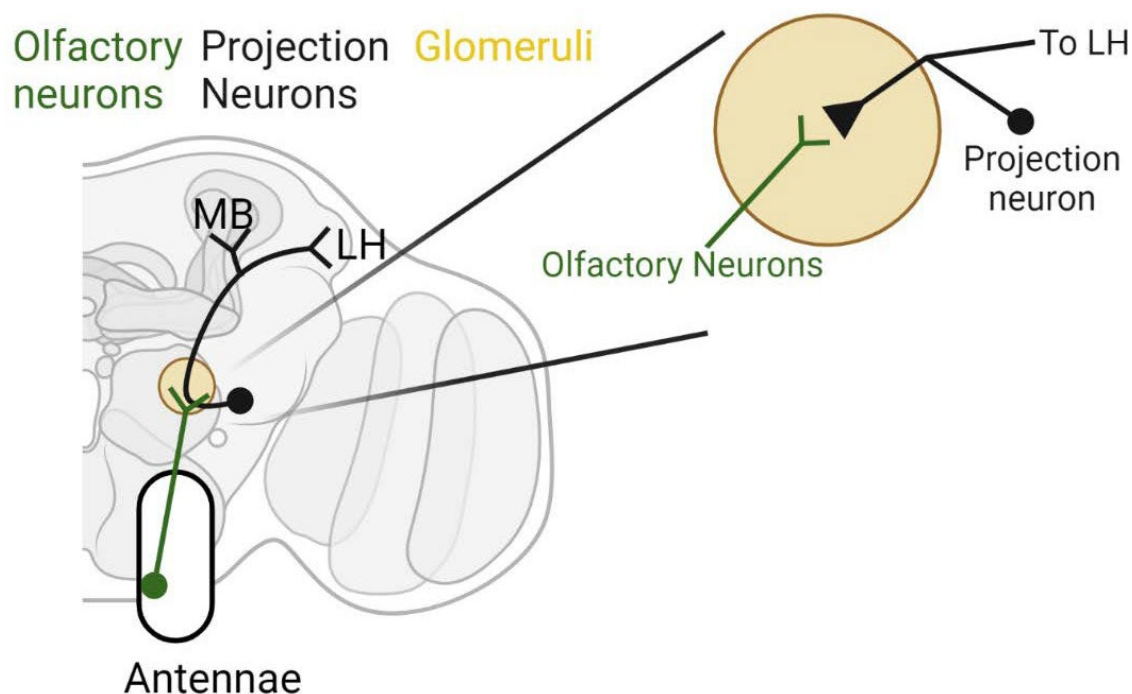


Figure 7: Diagram of olfactory circuitry in the *Drosophila melanogaster* brain

In the antennae a single olfactory neuron class (green) projects its axons to the olfactory bulb. Within the olfactory bulb these olfactory neurons target a specific glomerulus (shown in beige) where they synapse onto projection neurons (shown in black) within a specific glomeruli (as indicated).

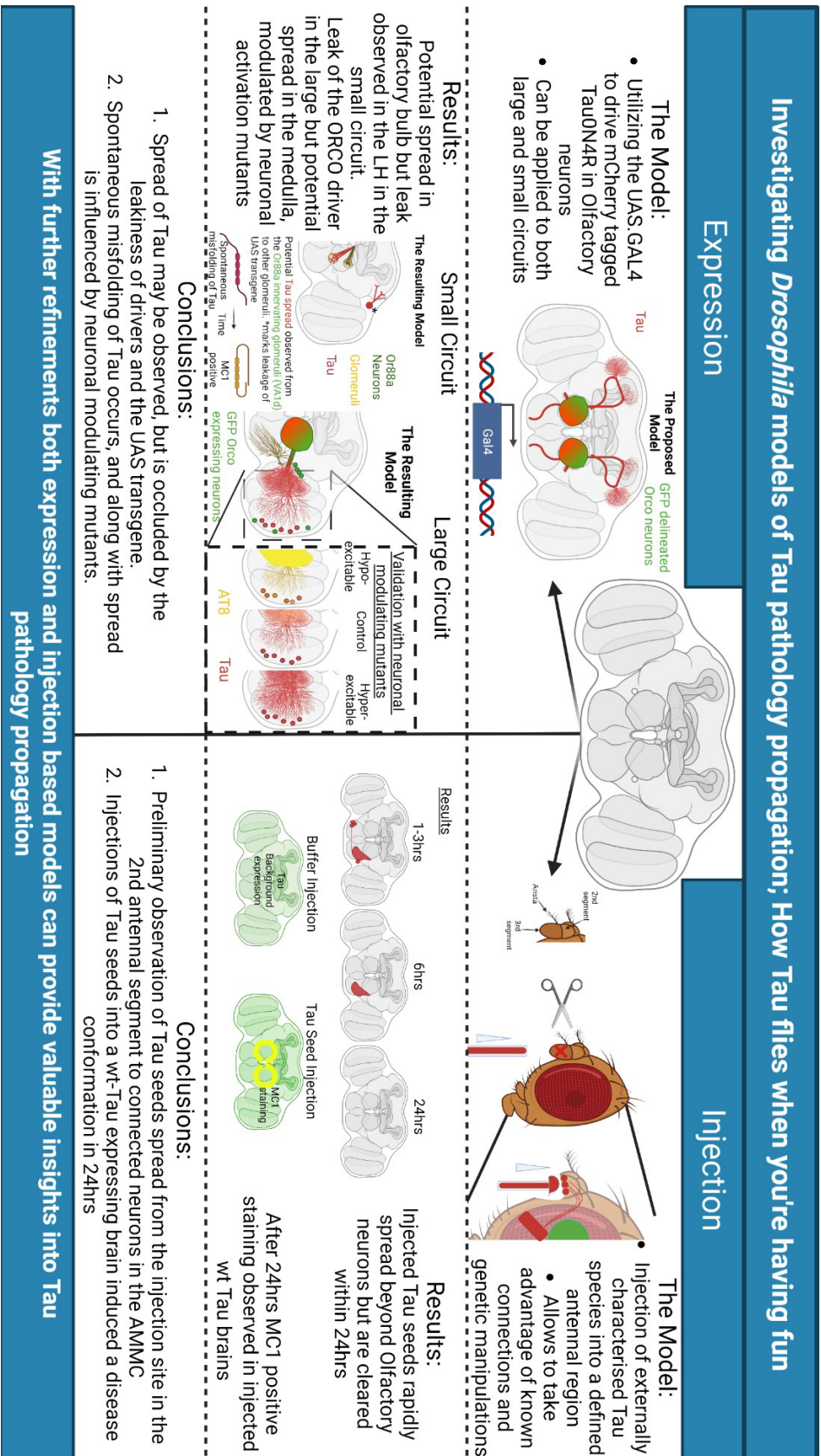
1.13.3 Utilizing the *Drosophila* model

The discrete connections offered by the olfactory neurons and their post-synaptic partners, combined with the ability to express Tau only in select groups of olfactory neurons using the UAS.GAL4 system, provide a specific circuit within which to investigate Tau that retains the complexity of an *in-vivo* system. This occurs as GAL4 lines can be selected that express in the pattern of specific olfactory receptors, driving Tau in those corresponding neurons. In this way Tau expression can be driven in a collection of olfactory neurons. From there, its spread to the post-synaptic projection neuron can be observed. The molecular identity of many post-synaptic projection neurons are also known and are targetable using the GAL4 system (Das, Sen et al. 2008), allowing for the manipulation or marking of the post-synaptic neurons. The range of genetic tools and methods available for *Drosophila* researchers allows for more complex models and

experiments to be built on this circuit. For example, by changing the neuronal firing rate of the circuit by overexpression of sodium channels to investigate the interaction of neuronal activity on Tau spread (Pooler, Phillips et al. 2013). Or, alternatively, by expressing $A\beta_{42}$, APOE4 or other associated factors of AD (Busche, Eichhoff et al. 2008). Furthermore, these olfactory circuits have known olfactory stimulants and can be linked to behavioral assays, providing greater information on the modulators and consequences of Tau spread.

Chapter 2 Aims

2.1 Thesis Summary



2.2 Thesis Aims

Objective: To Develop a *Drosophila* model to study tau spread

Aim 1: To simulate Tau spread in a small circuit *in-vivo*

Simulating Tau spread in a small circuit *in-vivo* would allow for the investigation of mechanisms and actors influencing Tau spread across a few synapses, creating a specific system that still retained the complexity of an *in-vivo* system. This can be achieved by taking advantage of the specific connections offered by the *Drosophila* olfactory system and the UAS.GAL4 expression system to drive Tau in pre-synaptic compartments. This work will aim to identify specific small circuits within the olfactory bulb and investigate the consequences of expressing Tau in the pre-synaptic compartment, looking for Tau spread to downstream connections and its conformation to establish which species are spreading.

Aim 2: To simulate tau spread in a large population of neurons *in-vivo*

By driving Tau expression in all olfactory neurons spread between tissues and the functional consequences for the receiving circuits and the organisms as a whole can be modelled to better understand the effects of Tau spread on receiving post synaptic partners. The UAS.GAL4 system allows for the expression of Tau within a starting tissue from which Tau spread can be observed.

Aim 3: To validate these models by utilising known modulators of spread

Evidence points to the role of synaptic activity playing a role in Tau spread. By using UAS.GAL4 to induce synaptic activity modulating mutants to the above models, changes in Tau spread can be investigated. These activity modulating mutants can then be used in the model to investigate the interactions based on pathological neuronal excitation by A β and its effect on pathological Tau spread. Adding deeper understanding to the interplay of these two key hallmarks of AD

Aim 4: To develop an injection based *Drosophila* model to allow for the relationship between Tau seed competency and its ability to spread to be investigated

Many techniques exist to uncover the structure and seeding potential of Tau seeds derived artificially or from patient brains. The ability to combine these highly characterised Tau seeds with an *in-vivo* system for studying aspects of both spread and Tau seeding would provide a powerful model in which to study the relationship between Tau seeding potential and spread, as well as validation of these external assays.

Chapter 3 Materials & methods

3.1 Fly stocks

Table 3. Fly lines used in this thesis, (BL = Bloomington *Drosophila* stock centre and Allan lab (University of British Columbia))

Fly Genotype	Fly Phenotype	Origin
W; <u>UAS.mCherryTau^{ON4R}</u> CyO	Expresses human Tau ^{ON4R} fused with an N terminal mCherry tag under the control of a UAS promoter on Chromosome II Balanced over Curly of Oster	Allan Lab, UBC
P{w[+mC]=Orco-Gal4.C} (2022)142t52.1, w[*]	Expresses Gal4 in all olfactory tissues expressing the olfactory co-receptor ORCO (Or85e). Insert is on the x chromosome	Bloomington <i>Drosophila</i> Stock Center. Catalogue number 23909
Y'w*;UAS.cd8::GFP	Expresses membrane tagged GFP under the control of a UAS promoter on Chromosome II.	Allan Lab, UBC
w[1118]/Dp(1;Y)y[+]; CyO/nub[1] b[1] sna[Sco] lt[1] stw[3]; MKRS/TM6B, Tb[1]	Fly with balancers on the 2 nd and 3 rd chromosome, used for creating recombinant flies from existing lines	Bloomington <i>Drosophila</i> Stock Centre. Catalogue number 3703
w[*]; P{w[+mC]=Or88a-Mmus\Cd8a.GFP}2	Expresses membrane-targeted GFP in the pattern of the Or88a gene. Insert is on the 2 nd chromosome	Bloomington <i>Drosophila</i> Stock Centre. Catalogue number 52644

OR47b-Gal4, UAS.cd8::GFP/CyO	Expresses membrane-targeted GFP in the pattern of the Or47b gene. Insert is on the 2 nd chromosome	Allan Lab, UBC
; P{w[+mC]=Or23a-Mmus\Cd8a.GFP}2	Expresses membrane-targeted GFP in the pattern of the Or23a gene. Insert is on the 2 nd chromosome	Bloomington <i>Drosophila</i> Stock Center. Catalogue number 52622
W;Or88a.Gal4, UAS.cd8::GFP / Cyo	Recombinant fly, Expresses membrane-targeted GFP in the pattern of the Or88a gene using a Gal4 driver, allowing for combination with UAS.Tau flies. Insert is on the 2 nd chromosome	Mudher lab, UoS
w;UAS.Tau ^{ON4R} /[CDGY]	Expresses human Tau ^{ON4R} under the control of a UAS promoter on Chromosome II Balanced over Curly of Oster	Allan Lab, UBC
P{w[+mC]=Orco-Gal4.K]142t52.1, w[*] ; UAS.mCherryTau ^{ON4R} / CyO	Expresses Gal4 in all olfactory tissues containing the olfactory co-receptor ORCO (Or85e). Insert is on the x chromosome recombined with mCherry N terminal tagged human Tau ^{ON4R} under the control of a UAS promoter on Chromosome II Balanced over Curly of Oster	Allan Lab, UBC
y[1] w[*]; P{y[+*]=ET-mCD8-GFP}Mz19	Expresses a CD8-GFP fusion protein in antennal glomeruli, antennocerebral tract neurons	Bloomington <i>Drosophila</i> Stock Centre. Catalogue number 23300

	and in the mushroom body. Inserted on Chromosome II	
W; Mz19.Gal4 / CyO	Expresses Gal4 in a subset of olfactory projection neurons. on Chromosome II Balanced over Curly of Oster	Allan Lab, UBC
w[1118]; PBac{Disc\RFP[DsRed2.3xP3]=GH146-QF.P}53 P{w[+mC]=QUAS-mtdTomato-3xHA}24	Expresses QF and HA-tagged Tomato under QUAS control in subsets of projection neurons. Inserted on Chromosome III	Bloomington <i>Drosophila</i> Stock Centre. Catalogue number 30037
w[*]; P{w[+mC]=UAS-TeTxLC.(-)V}A2	Expresses a scrambled mutant of the light chain of tetanus toxin under UAS control. Inserted on Chromosome II	Expresses the light chain of tetanus toxin under UAS control. Number 28840
w[*]; P{w[+mC]=UAS-TeTxLC.tnt}G2	Expresses the light chain of tetanus toxin under UAS control. Inserted on Chromosome II	Bloomington <i>Drosophila</i> Stock Centre. Catalogue number 28838
w;;[NSYB-EGFPTau ^{ON4R}]attp2 /TDGY	Expresses in all neurons EGFP N-terminal tagged human Tau ^{ON4R} on Chromosome III Balanced over Tm6B and the phenotypic marker tubby	Allan Lab, UBC
w[*];UAS.Abeta 42 arc/CyO; +/-	Expression of the Aβ ₄₂ ARTIC fragment under control of UAS. Insertion on Chromosome II	Crowther lab, Cambridge

<p>w[*]; P{w[+mC]=UAS(FRT.stop)Hsap\KCNJ2-19A/CyO</p>	<p>Hypo-polarizing, Expresses human KCNJ2 (Kir2.1), an inwardly-rectifying potassium channel, under UAS control after FLP-mediated removal of a stop cassette. Insertion on Chromosome II</p>	<p>Bloomington <i>Drosophila</i> Stock Centre. Catalogue number 67686</p>
<p>w[z]; P{w[+mC]=UAS-eag.DN.EKI}2/CyO</p>	<p>Expresses a truncated eag potassium channel protein resulting in neuronal hyper excitability under the control of UAS. Insertion on Chromosome II</p>	<p>Bloomington <i>Drosophila</i> Stock Centre. Catalogue number 8187</p>
<p>w; UAS.cd8.GFP/cyO; OrcoGal4/TM3; Ser AG</p>	<p>Expresses Gal4 in all olfactory tissues containing the olfactory co-receptor ORCO (Or85e) Balanced over TM3 with the phenotypic markers Serate and GFP tagged Actin. Insert is on the III chromosome cd8::GFP under the control of a UAS promoter on Chromosome II Balanced over Curly of Oster</p>	<p>Allan Lab, UBC</p>

3.1.1 Fly husbandry

Assays were conducted by crossing the appropriate UAS and Gal4 lines from Table 3 and collecting male progeny bearing the correct markers. Collection of male offspring was carried out whilst the flies were still virgins and for zero day time points flies were dissected immediately in order for the T=0 timepoint to be as close to eclosion as possible. All *Drosophila* were raised on standard Bloomington media at 23°C in a 12/12 hour light/dark cycle unless otherwise stated hereafter.

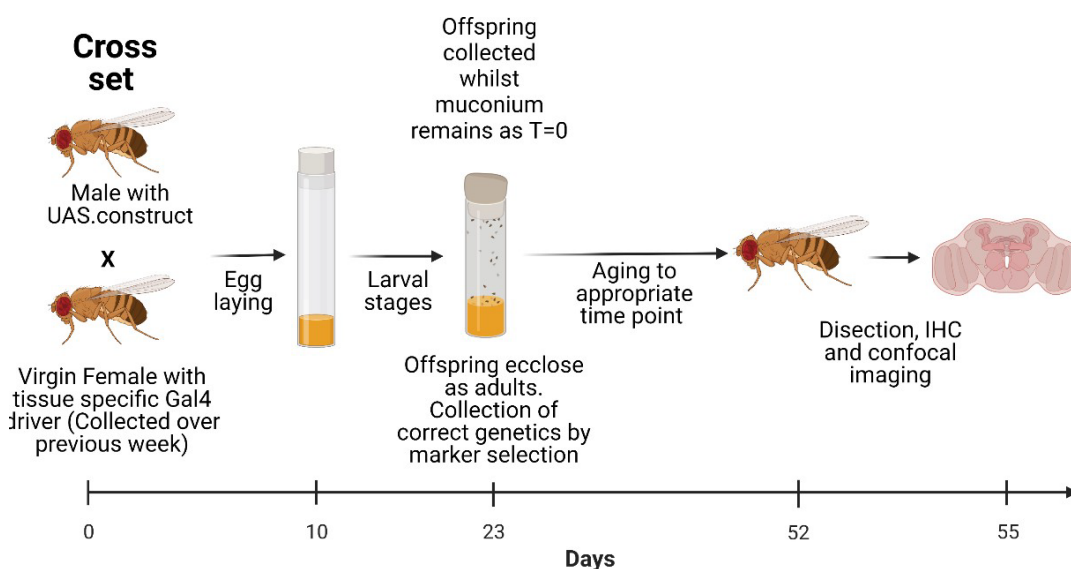


Figure 8: Schematic outlining the time taken to carry out an experimental time course from the setting of genetic crosses to final confocal imaging.

3.2 Recombinant fly generation

In order to generate flies with genetic compositions that are not available from stocks or collaborators, recombination of existing lines was carried out by the Allan lab in the University of British Columbia (UBC) or the Mudher lab at the University of Southampton (UoS). This was carried out by selecting virgin female progeny of crossed UAS and Gal4 lines (see Appendix 1 for lines used) and crossing these with males of double balancer line 3703 ($w;Cyo/Sco;Tm3/Tm6$). From this second cross, potential recombinant males containing both the UAS and Gal4 insertions on the same chromosome were selected and backcrossed with virgins from the double balancer line 3703 to create a stable recombinant stock. These potential recombinant flies were then screened for GFP expression by confocal microscopy. As the recombinant should result in a constitutive expression of the fluorophore, its presence in the stock line indicates a successful recombination. These stocks are listed above as having the origin from Allan Lab, UBC or Mudher lab, UoS in Table 3. For example, a cross sheet detailing the creation of Or88a.Gal4 recombined with UAS.cd8::GFP is shown in Appendix 1

3.3 Experimental Crosses

Table 4: Table of fly crosses, parents and offspring genotype in the results of this thesis.

Figure number(s)	Male parent genotype	Virgin female parent genotype	Male Offspring genotype
Figure 13 (Or23a)	w* ; P{w[+mC]=Or23a-Mmus\Cd8a.GFP}2	w* ; P{w[+mC]=Or23a-Mmus\Cd8a.GFP}2	w* ; P{w[+mC]=Or23a-Mmus\Cd8a.GFP}2
Figure 13 (Or88a)	P{w[+mC]=Or88a-Mmus\Cd8a.GFP}2	P{w[+mC]=Or88a-Mmus\Cd8a.GFP}2	P{w[+mC]=Or88a-Mmus\Cd8a.GFP}2
Figure 13 (Or47b)	OR47b-Gal4, UAS.cd8::GFP/CyO	OR47b-Gal4, UAS.cd8::GFP/CyO	OR47b-Gal4, UAS.cd8::GFP
Figure 13 (Or85e)	w; Or85e-Gal4.UAS- CD8.GFP Allen lab (UBC)	w; Or85e-Gal4.UAS- CD8.GFP Allen lab (UBC)	w; Or85e-Gal4.UAS- CD8.GFP
Figure 13 (ORCO)	w; UAS.cd8::GFP	P{w[+mC]=Orco-Gal4.K]142t52.1, w[*]	P{w[+mC]=Orco-Gal4.K]142t52.1, w[*]/w ; UAS.cd8::GFP/+
Figure 14	w1118;P{w[+mC]=Or88a-Gal4.W}88.II.	w; UAS-mCherry: Tau ^{ON4R} / CDGY	w; Or88a-Gal4.W}88.II./ UAS-mCherry: Tau ^{ON4R}
Figure 15	W;Or88a.Gal4, UAS.cd8::GFP / Scu	w; UAS-mCherry: Tau ^{ON4R} / CDGY	w; Or88a.Gal4, UAS.cd8::GFP/ UAS-mCherry: Tau ^{ON4R}

Figure 16	W;Or88a.Gal4, UAS.cd8::GFP / Scu	w; UAS-mCherry: Tau ^{ON4R} / CDGY	w; Or88a.Gal4, UAS.cd8::GFP / UAS- mCherry: Tau ^{ON4R}
Figure 17	w; UAS-mCherry: Tau ^{ON4R} / CDGY	w; UAS-mCherry: Tau ^{ON4R} / CDGY	w; UAS-mCherry: Tau ^{ON4R}
Figure 20	P{w[+mC]=Orco- Gal4.K]142t52.1, w[*]	P{w[+mC]=Orco- Gal4.K]142t52.1, w[*]	P{w[+mC]=Orco- Gal4.K]142t52.1, w[*]
Figure 20	w; UAS-mCherry: Tau ^{ON4R} / CDGY	w; UAS-mCherry: Tau ^{ON4R} / CDGY	w; UAS-mCherry: Tau ^{ON4R} / CDGY
Figure 20	P{w[+mC]=Orco- Gal4.K]142t52.1, w[*]	w; UAS-mCherry: Tau ^{ON4R} / CDGY	P{w[+mC]=Orco- Gal4.K]142t52.1, w[*] ; UAS-mCherry: Tau ^{ON4R}
Figure 21 Figure 22 Figure 25 Figure 26	P{w[+mC]=Orco- Gal4.K]142t52.1, w[*] ; UAS.mCherryTau ^{ON4R} / CyO	w; UAS.cd8::GFP	P{w[+mC]=Orco- Gal4.K]142t52.1, w[*] ; UAS.mCherryTau ^{ON4R} / w; UAS.cd8::GFP
Figure 23 Figure 24 Figure 25	P{w[+mC]=Orco- Gal4.K]142t52.1, w[*] ; UAS.mCherryTau ^{ON4R} / CyO	P{w[+mC]=UAS(FRT.stop) Hsap\KCNJ2}VIE-19A / CyO	P{w[+mC]=Orco- Gal4.K]142t52.1, w[*] ; UAS.mCherryTau ^{ON4R} / P{w[+mC]=UAS(FRT.stop)

			Hsap\KCNJ2}VIE-19A
Figure 24 Figure 25 Figure 26	P{w[+mC]=Orco-Gal4.K]142t52.1, w[*] ; UAS.mCherryTau ^{ON4R} / CyO	w[z]; P{w[+mC]=UAS-eag.DN.EKI}2/CyO	P{w[+mC]=Orco-Gal4.K]142t52.1, w[*] ; UAS.mCherryTau ^{ON4R} / P{w[+mC]=UAS-eag.DN.EKI}2
Figure 29 Figure 30 Figure 31 Figure 32	w; UAS.cd8.GFP/cyO; OrcoGal4/TM3; Ser AG	w; UAS.cd8.GFP/cyO; OrcoGal4/TM3; Ser AG	w; UAS.cd8.GFP/cyO; OrcoGal4/TM3; Ser AG
Appendix 2	w1118;P{w[+mC]=Or88a-Gal4.W}88.II. / CyO	w; UAS.cd8.GFP	w1118;P{w[+mC]=Or88a-Gal4.W}88.II. / UAS.cd8.GFP
Appendix 3	W; Mz19.Gal4 / CyO y[1] w[*]; P{y[+*]=ET-mCD8-GFP}Mz19	w; UAS.cd8.GFP y[1] w[*]; P{y[+*]=ET-mCD8-GFP}Mz19	W; Mz19.Gal4 / UAS.cd8.GFP y[1] w[*]; P{y[+*]=ET-mCD8-GFP}Mz19
Appendix 4	P{w[+mC]=Orco-Gal4.K]142t52.1, w[*]	P{w[+mC]=Orco-Gal4.K]142t52.1, w[*]	P{w[+mC]=Orco-Gal4.K]142t52.1, w[*]
Appendix 5	P{w[+mC]=Orco-Gal4.K]142t52.1, w[*] ; UAS.mCherryTau ^{ON4R} / CyO	w; UAS.cd8::GFP	P{w[+mC]=Orco-Gal4.K]142t52.1, w[*] ; UAS.mCherryTau ^{ON4R} / UAS.cd8::GFP

Appendix 6	W;Or88a.Gal4, UAS.cd8::GFP / Scu	w; UAS.Tau ^{ON4R} / CDGY	w; Or88a.Gal4, UAS.cd8::GFP / UAS.Tau ^{ON4R}
Appendix 7	W;Or88a.Gal4,mCD8- GFP} Mz19	w; UAS-mCherry: Tau ^{ON4R} / CDGY	W;Or88a.Gal4,mCD8-GFP} Mz19 / UAS-mCherry: Tau ^{ON4R}
Appendix 8	w[*]; P{w[+mC]=UAS- TeTxLC.(-)V}A2 w[*]; P{w[+mC]=UAS- TeTxLC.tnt}G2	P{w[+mC]=Orco- Gal4.K]142t52.1, w[*] ; UAS.mCherryTau ^{ON4R} / CyO P{w[+mC]=Orco- Gal4.K]142t52.1, w[*] ; UAS.mCherryTau ^{ON4R} / CyO	P{w[+mC]=Orco- Gal4.K]142t52.1, w[*] ; UAS.mCherryTau ^{ON4R} / P{w[+mC]=UAS-TeTxLC.(-)V}A2 P{w[+mC]=Orco- Gal4.K]142t52.1, w[*] ; UAS.mCherryTau ^{ON4R} / P{w[+mC]=UAS- TeTxLC.tnt}G2
Appendix 10 Appendix 11	w; UAS.cd8.GFP/cyO; OrcoGal4/TM3; Ser AG	w; UAS.cd8.GFP/cyO; OrcoGal4/TM3; Ser AG	w; UAS.cd8.GFP/cyO; OrcoGal4/TM3; Ser AG

3.4 Longevity Assays

Male offspring which had eclosed within 0-3 days were isolated from each genotype, forming ten groups of ten flies per individual genotype. The number of dead flies in each vial was assessed three times a week and kept on standard Bloomington media at 23°C and 12/12 hour light/dark cycle. The surviving flies were moved to a new vial of food once a week. The recorded number of surviving flies was used to carry out a survival analysis using GraphPad Prism where a Kaplan-Meier curve was plotted to determine median life expectancy. A Mantel-cox Log-rank test was then used to determine the significance of any differences in survivability.

3.5 Injections

Progeny from the experimental stocks were selected for both sex and correct marker gene expression. Males were isolated into groups of ten and aged until appropriate time points (0, 3, 7 and 14 days) at which point they were anaesthetised with CO₂. Once anaesthetised, a small nick was made in the right-hand side 2nd or 3rd antennal lobe using dissecting scissors (see Figure 9 below). A pulled capillary tube needle was then placed into this nick. Capillary action drew the contents of the needle into the 3rd antennal lobe. The fly was then transferred immediately to a fresh food vial to recover and age to the appropriate time point.

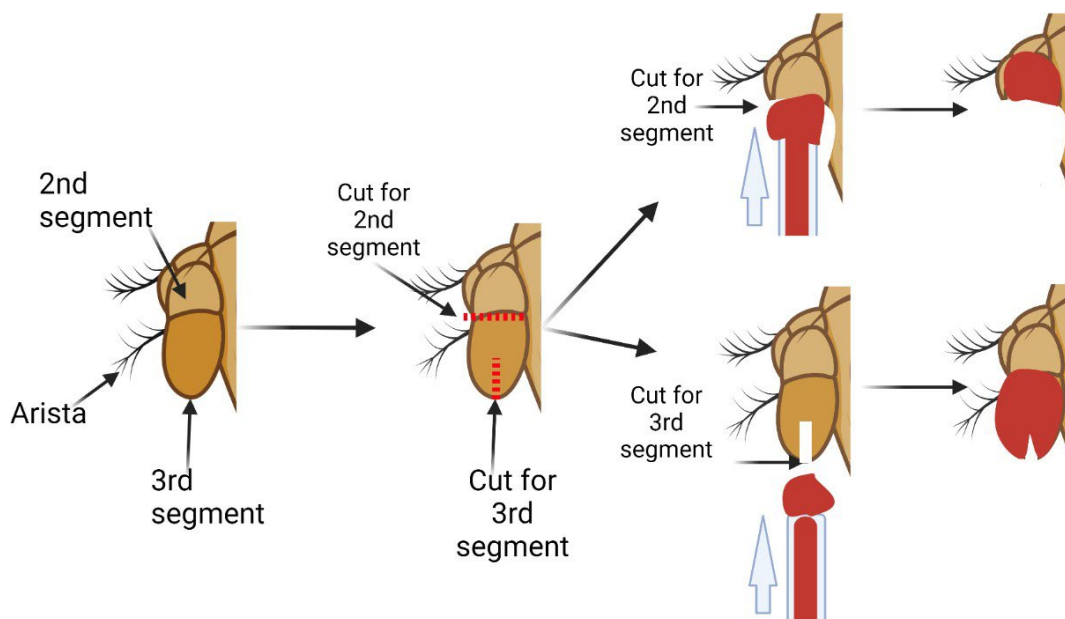


Figure 9: Schematic of injections into the 2nd or 3rd antennal segment.

Either a small cut was made into the tip of the 3rd antennal segment, or the entire 3rd segment was completely removed using dissecting scissors, as shown by the dotted line. A pulled glass capillary needle was placed into this cut containing Tau (red). Capillary action drew either the Dextran or Tau into the antennae, producing a visible colour change in this antennae (red).

3.6 Dissections

Progeny from the experimental stocks were selected for both sex and correct marker gene expression. Males were isolated into groups of ten and aged until appropriate time points (0, 3, 7 and 14 days), at which point they were anaesthetised with CO₂. Individuals were decapitated using a pair of tweezers (Fisherbrand™ Dumont #5 Fine Tip Tweezers) to pull on the flies' proboscis. The heads were then immediately transferred to a watch glass with 100µl of PBST and dissected at room temperature by gripping the carapace in the gap left by the removal of the proboscis and peeling back tissue surrounding the brain. The trachea and remaining eye pigment were removed before the dissected brain was placed in 4% PFA for twenty minutes with gentle agitation. After 20 minutes, the PFA was removed and the brains washed three times for 20 minutes with 1000µl of PBST.

3.7 Immunohistochemistry (IHC)

All steps were carried out at room temperature with gentle agitation. Dissected brains were blocked in 3% NGS for one hour and then a primary antibody (Table 3) was added and left overnight at room temperature. The brains were then washed three times for 10 minutes in 1000 μ l phospho-buffered saline with Triton X-100 (PBST) before being re-suspended in 200 μ l of 3% normal goat serum (NGS) and the appropriate secondary antibody (Table 3) for 2 hours. After this, the secondary antibody was washed off with a brief PBS wash.

Table 5: Description of all antibodies and their dilutions used in experiments within this thesis

Name	Target	Species	Dilution in 3% NGS	Supplier/Catalogue Number
Anti-Tau	Human Tau	Rabbit pAb	1:1000	Dako A0024
Anti-GFP	GFP	Chicken	1:1000	Abcam ab13970
Anti-mCherry	mCherry	Rabbit pAb	1:1000	Abcam ab167453
AT8	Tau phosphorylation at Ser202 and Thr 205	Mouse	1:1000	ThermoFisher Scientific MN1060
MC1	Tau Misfolding (conformation-dependent antibody (epitope within aa312-322))	Mouse	1:200	DSHB
nc82*	Bruchpilot (a scaffold protein found in the pre-synapse of <i>Drosophila</i>)	Mouse	1:50	DSHB
Anti-Chicken Alexa 488	Chicken	Goat	1:500	Invitrogen A11039
Anti-rabbit Alexa 555	Rabbit	Goat	1:500	Abcam ab150078
Anti-mouse Alexa 647	Mouse	Goat	1:500	Abcam ab150115

*nc82 was deposited to the DSHB by Buchner, E. (DSHB Hybridoma Product nc82)

3.7.1 Vectashield Mount

Upon completion of immunohistochemistry the brains were transferred into a well on a premade lysine-coated slide (Superfrost Plus Adhesion microscope slides, eprelia, J1800AMNZ). The brains were placed into a well created by two coverslips (Cover Glass, 22x22mm 200pcs, 0.13-0.17mm thick), attached by nail varnish. Forceps were used to ensure correct orientation of the brain for imaging and the remaining PBS was aspirated with a P200 (Gilson pipetman) 50 μ l Vectashield anti-fade mounting media (Vectashield Vibrance with DAPI, H-1800). This covered the brains and left on for 2 minutes to allow the brains to resettle. The brains were then sealed in place with nail varnish (see Figure 10)

3.7.2 DPX Mount

Alternatively, upon completion of immunohistochemistry, the brains were transferred onto Lysine-coated coverslips made by dipping coverslips (Cover Glass, 22x22mm 200pcs, 0.13-0.17mm thick) sequentially in 70% ethanol, deionised water, Lysine solution (0.1 % (w/v) in H₂O) for 5 minutes and then deionised water again. These slips were then placed in a watch glass and taken through a series of 5 minute dehydration steps (30%, 50%, 70%, 95% and 100% ethanol:deionised water) and then three 5 minute clearance steps using Xylene (Sigma-Aldrich, 214736-1L) (50:50 Xylene:Ethanol, 100% Xylene, 100% Xylene). After this brains were immediately mounted in DPX in a coverslip well and placed upon a microscope slide, as shown in Figure 10. These slides were then left to dry at room temperature for 7 days.

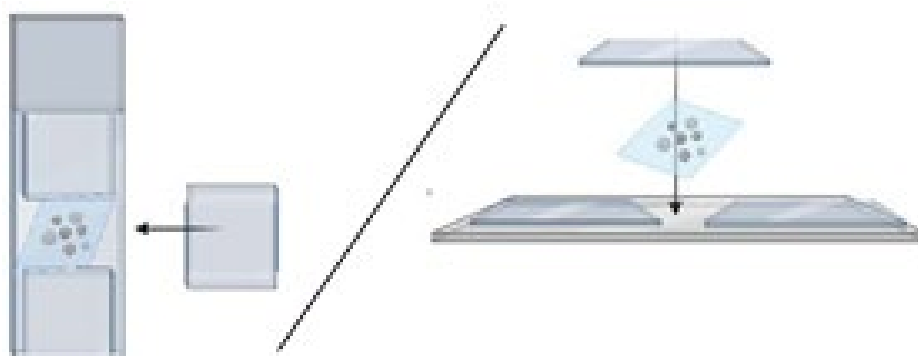


Figure 10: Schematic of wells created atop slides using cover slips into which stained *Drosophila* brains are mounted

3.8 Confocal imaging

Confocal microscopy was chosen due to the highly 3D structure of the fly brain, requiring a technique that allows for optically sectioning of tissue. A pinhole was used to block out of focus light, permitting an optical slice of the specimen to be taken. Multiple optical slices taken by confocal microscopy can be built up into z-stacks, allowing for a 3D reconstruction of the fly brain in ImageJ. The use of multiple detectors and sequential scanning also allows for the separation of multiple fluorescently- tagged proteins and stains within the sample.

Using a Leica SP8 Inverted scanning confocal microscope, 12-bit depth stacks were taken across the whole brain at either 20x (dry) or 63x (oil) magnification. These stacks were taken at 1024x1024 resolution at 400Hz line average 2. Sequential excitation steps were used to minimize bleed through between channels which were detected on a Leica HyD hybrid detector.

Image processing was carried out using ImageJ Fiji 1.53e to apply colour tables and scale bars.

Table 6: A table outlining the fluorescent tags used in this thesis and the corresponding excitation and collection parameters used to image them on a Leica SP8 Inverted scanning confocal microscope

Fluorescent label	Laser (nm)	Laser power (%)	Smart Gain (%)	Collection bracket (nm)
DAPI	405	5	100%	450-480
Alexa 555	561	5	100%	570-590
Alexa 488	496	5	200%	510-530
Alexa647	633	5	200%	660-680

3.9 Analysis

The area coverage of GFP, mCherry and MC1 was measured using (Fiji is Just) ImageJ 1.53e by thresholding the channel using auto-setting and adjusting to remove excess background. This allowed for a measurement of the area coverage of signal. Measurements of fluorescence were avoided due to conditions during slide preparations causing a variability in this signal, given that some of these experiments occurred across multiple weeks. Area coverage is also more relevant to

Tau spread as it should only increase as Tau moves into new neuronal populations. However, some of this signal will be attributable to Tau signal moving throughout (e.g. from somatodendritic to axonal).

3.10 Statistics

Differences between the area coverage of tested fluorophores was analysed using a t-tests and one-way ANOVAs followed by Dunnett's multiple comparisons test or two-way ANOVAs followed by Tukeys mixed-effects analysis. These were performed using GraphPad Prism version 9.4.1 for Windows 64-bit, GraphPad Software, San Diego, California USA, www.graphpad.com.

3.11 Figures and Diagrams

All Diagrams and figures in this thesis were "Created with BioRender.com" under an academic subscription.

3.12 Reagents

Table 7: Reagents, their ingredients and suppliers used in experiments this thesis

Reagent	Ingredients	Supplier
PBST	PBS	Building 85 media kitchen
	0.1% Triton X-100	SigmaUltra T9284
4% PFA	20% Paraformaldehyde, EM Grade	Electron Microscopy Sciences 15713-S
	PBST	-
3% NGS	Goat Serum	Sigma –aldrich G9023
	PBST	-

Dextran, tetramethylrhodamine and biotin, 3000mw 1:100 solution	Dextran, tetramethylrhodamine and biotin, 3000mw 5mg crystals	Invitrogen D7162
	3%NGS	-
Ethanol	N/A	
Xylenes	N/A	Sigma-Aldrich, 214736-1L
VECTASHIELD® Vibrance™ Antifade Mounting Medium H-1700	N/A	Vector Laboratories H-1700-2

Chapter 4 Simulating Tau spread in a small number of olfactory neurons by expressing mCherryTau^{ON4R} in Or88a olfactory circuitry

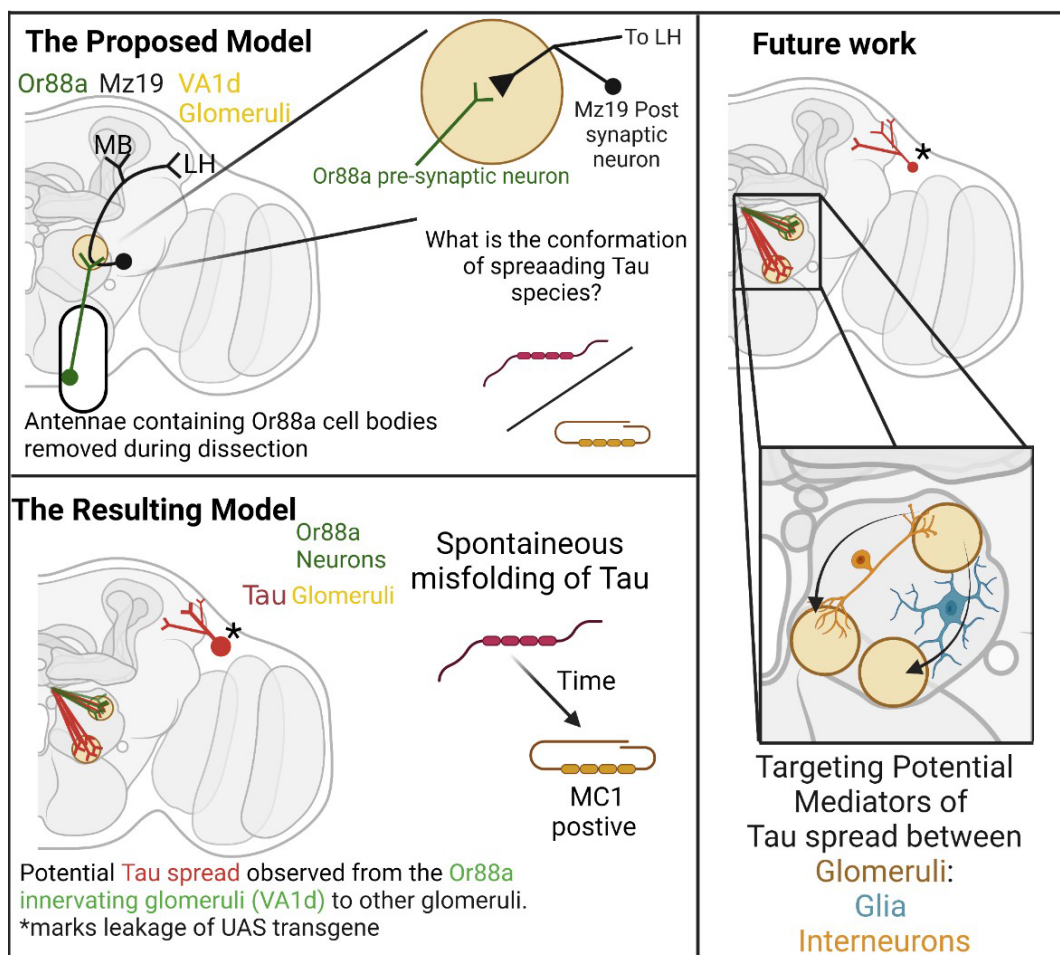


Figure 11: Graphical abstract of Chapter 4; Simulating Tau spread in a small number of olfactory neurons by expressing mCherryTau^{ON4R} in Or88a olfactory circuitry

The proposed model in which Tau spread is simulated (red) from a delineated expression site within a small group of olfactory neurons (green), and the investigation of the conformation of spreading Tau species. The model resulted in two apparent areas of spread within the glomeruli and lateral horn (*). The latter Tau population was found to result from leakage of the UAS transgene and could therefore not be considered spread. Another observation was that the Tau construct can spontaneously adopt a misfolded conformation with time, something not seen in other models of Tau pathology. Future work should aim to refine the expression of the construct and confirm the spread of Tau in the olfactory bulb. It would then be possible to use readily available *Drosophila* mutants to investigate mediators of Tau spread.

4.1 Introduction

The primary aim of this thesis is to develop a *Drosophila* model to study Tau spread. In creating such a model, it will be possible to take advantage of the flies' well-understood anatomy and wide range of genetic tools to further probe the unknown mechanisms used in Tau spread *in vivo*, both in a physiological and pathological context.

This chapter addresses this thesis's first aim: to simulate Tau spread in a small group of neurons *in vivo* by characterising the expression profile of various olfactory receptors and, after this, precisely express mCherryTau^{ON4R} in the Or88a expressing neurons.

4.1.1 The mechanisms behind the prion-like spread of Tau are unknown

Tau spread through the brain is thought to occur in a prion-like manner between connected neurons, with much evidence to support this (Clavaguera, Bolmont et al. 2009, Lasagna-Reeves, Castillo-Carranza et al. 2012, Liu, Drouet et al. 2012, Wegmann, Bennett et al. 2019). However, the precise mechanisms underpinning this prion-like spread remain unknown. Pre-synaptically, Tau release is thought to occur through exosomes (Saman, Kim et al. 2012, Simón, García-García et al. 2012, Wang, Balaji et al. 2017, Yan and Zheng 2021), ectosomes (Dujardin, Bégard et al. 2014) and even as free Tau (Dujardin, Bégard et al. 2014, Wang, Balaji et al. 2017). Post synaptically, the picture remains unclear, with diffusion and micropinocytosis proposed but with evidence primarily pointing to endocytosis via receptor-mediated uptake via LRP1 (Christianson and Belting 2014, Calafate, Flavin et al. 2016, Rauch, Luna et al. 2020). Furthermore, the functional consequences for the postsynaptic neurons and, consequently, the behavioural consequences for the organism as a whole are not always apparent (as reviewed in (Pernègre, Duquette et al. 2019)).

Current models of Tau propagation are based upon one of two systems, either *in vitro* mammalian cell culture or *in vivo* rodent models (transgenic or ic/ip injections). Each model has advantages and disadvantages; *in vitro* cell models, for example, can investigate Tau spread over a single synapse but in a vastly reduced system. In contrast, *in vivo* mouse models offer the complexity of a complete living organism but are limited to regional promoters. As such, it is not possible to directly investigate synaptic connections. Both types of models and the insights they offer have provided many insights as outlined in Introduction 1.11. However, much remains unknown in the field about the molecular mechanisms enabling Tau spread and a new model is needed to uncover these synaptic players. *Drosophila* offers both the opportunities for complexity and specificity in a genetically tractable organism where it is possible to manipulate wide range of genetic tools.

4.1.2 *Drosophila's* suitability to model Tau spread

Neuronal circuitry in the *Drosophila* brain has been extensively mapped in detail, with research and resources widely available that detail the fly's neuronal connections down to EM level for many circuits (Vosshall and Stocker 2007, Zheng, Lauritzen et al. 2018, Scheffer and Meinertzhagen 2019, Lizbinski and Jeanne 2020). Not only are the physical connections understood, but also the neurotransmitters involved are also known, providing further information on the neuronal connections in which Tau spread can be studied. This mapping extends beyond individual connections, providing a circuit-wide understanding of neuronal connections. The functional outputs of many neurons are also readily available, offering measurable phenotypes to assay (Talay, Richman et al. 2017). These known neuronal groupings are targetable due to the UAS:GAL4 system. By linking the expression of the GAL4 promotor to tissue-specific proteins the promotor is only found in these associated tissues. Whilst a protein of interest, in this case Tau, is placed downstream of the UAS region and is found in all tissues, it is only in those tissues in which the GAL4 promotor is expressed, and therefore can bind to and activate the UAS sequence that expression of the protein of interest can occur. This system allows for the expression of Tau (under UAS control) within any discrete well-studied neuronal circuit whose structure (such as primary pre- and post- synaptic neurons and secondary modulatory inputs), neurotransmitter profile and behavioural function is not only known but is also amenable to genetic manipulation.

Drosophila's genetic tools are vital to this model and allow for the expression of Tau at a number of tissue resolutions. For instance, broad expression profiles have been created across all neuronal and glial cells using the Elav and Repo drivers respectively (Wittmann, Wszolek et al. 2001, Colodner and Feany 2010). Specific drivers have been developed to target individual cell types including motor and sensory neurons (Williams, Tyrer et al. 2000, Mudher, Shepherd et al. 2004). An intermediate resolution exists with tissue-specific drivers which, by nature, are expressed in a tight spatial pattern. The two primary tissues used in fly models are the eyes (GMR) and mushroom bodies. However, this model aims to drive Tau expression in the olfactory system, which uses both tissue-specific and cell-type drivers within a common system.

4.1.2 A small number of neurons within *Drosophila's* olfactory system to study Tau spread

The olfactory system offers a tight grouping of neurons with known connections and functions that can be further subdivided into small neuronal groups (Vosshall and Stocker 2007). These olfactory receptor neurons target one (or rarely two) glomeruli within the antennal lobe, offering around 62 candidate olfactory receptor neurons which could be tested (Vosshall and Stocker 2007). At the glomeruli, the olfactory receptor neurons synapses onto a corresponding projection neuron based upon the receptor expressed, creating a 'glomerular code' from the smell being received. These

projector neurons carry this code to higher brain regions such as the calyx and lateral horn, where the axons converge and diverge to stimulate a variety of terminal fields.

Connections between the olfactory neurons, targetable both individually and as a group through the expression of specific receptors in each subgroup, are well-mapped, with known connections between each olfactory neuron and its projection neuron (Vosshall and Stocker 2007). This offers a system in which the spread of Tau can occur across a small number of well-defined synapses and where observable behavioral outputs, such as attraction to apple cider vinegar (Semmelhack, J., Wang, J. 2009) are known for use in assay design.

4.1.3 The Tau construct used to investigate Tau spread

Fluorescently-tagged Tau or Tau fragments are a common substrate in both cellular and mouse models of Tauopathies, with a variety of different fluorophores available to visualise the spreading of Tau species (Kfoury, Holmes et al. 2012, Sanders, Kaufman et al. 2014, Gibbons, Banks et al. 2017, Wegmann, Bennett et al. 2019). For the present system, a monomeric mCherry tag was selected due to its N-terminal stability and increased photostability over mRFP1 (Shaner, Campbell et al. 2004). The red emission spectra allows the use of mCherry-tagged Tau^{ON4R} alongside a range of GFP- tagged olfactory drivers and mCherry can even be co-expressed with GFP-tagged Tau species to compare the interaction of two different Tau populations or conformations within the brain. The mCherry construct, specifically built for this study by our collaborators at the Allan lab (UBC), was inserted into the attP40 insertion site on the 2nd chromosome. This common insertion site allows for a specific landing site that results in a strong, reproducible expression of the gene of interest (Pfeiffer, Ngo et al. 2010). The advantage of this system over older P-element type insertions is the ability to place the transgene in a specific chromosomal location. In doing so, other Tau species can be placed in the same location in future studies, leading to comparable expression levels. This is important to ensure inserts have comparable activity, as expression levels are known to affect Tau misfolding (von Bergen, Barghorn et al. 2005, Povellato et al 2014).

This chapter investigates the potential to model Tau spread from a small number of neurons to surrounding regions. This utilizes a small discrete circuit made up of the olfactory receptor neuron and its post synaptic projection neuron through which to investigate Tau propagation within the complexity of an *in- vivo* model.

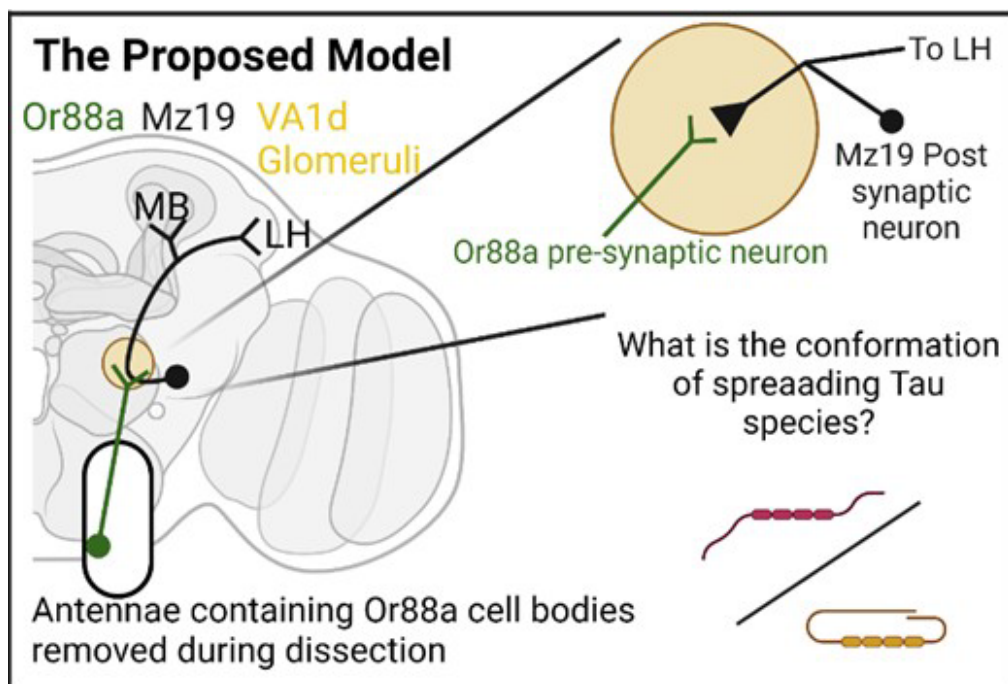


Figure 12: The proposed model in which to simulate Tau spread

Expression of mCherryTau^{ON4R} within the small Or88a population of antennal olfactory neurons (green) will create a system in which to simulate Tau spread between the Or88a neurons and its post synaptic partners Mz19 (black) within the VA1d glomeruli (yellow). The conformation of these spreading species is investigated using the conformationally dependent MC1 antibody against misfolded species.

4.2 Summary of Aims and Objectives:

Aim 1: To simulate Tau spread in a small number of neurons *in-vivo*

Objectives:

1. Identify candidate olfactory receptor neurons

By crossing a panel of potential olfactory receptor neuron GAL4 drivers with UAS.cd8::GFP, the selection of a driver with a clear glomeruli location and well defined postsynaptic partner can be carried out.

2. Preliminary expression of Tau construct in the identified circuitry

With an olfactory receptor neuron GAL4 driver selected, initial experiments looking at Tau spread from the expressing neurons into downstream connections can be carried out.

3. Refine the resulting potential model

Adjustments can be made to the model in order to maximise spread and clearly delineate expressing circuitry by co-expressing GFP markers. This would build a model in which to study Tau spread.

4. Investigate the nature of Tau species in the model

Whilst the model has so far been built to investigate spread, the pathological nature of Tau within the system, and therefore its relevance to AD, can be assessed through the use of conformational dependent antibodies. This includes MC1, which only stains pathological Tau species. The use of MC1 would provide insights into the nature of Tau spread within this system, be it physiological or pathological.

4.3 Results

4.3.1 Selection of the Or88a olfactory receptor neuron

To identify potentially amenable neuronal circuitry, a membrane-bound GFP (cd8::GFP) construct was expressed under the control of a selection of olfactory receptor-linked GAL4 promoters, allowing for the confirmation of expression sites and any potential miss-expression of the driver. This experiment was carried out at 23°C, and flies were dissected at seven days old.

Olfactory co-receptor Orco (Or83b) GAL 4 was used to drive cd8::GFP expression in all neurons in the olfactory bulb (Figure 13 AI). The long projections from the olfactory bulb's base are the axonal tracts from the antennae where the olfactory neuron's cell bodies are located. As the antennae are removed as part of the dissection protocol, it is impossible to visualise any of the cell bodies in this confocal image. The postsynaptic partner of olfactory neurons are projection neurons, of which GH146.Gal4 targets around 60% of olfactory projection neurons (Shang, Claridge-Chang et al. 2007). GH146.Gal4 was used to drive UAS.cd8::GFP, delineating these projection neurons. Figure 13 AII shows a high-magnification image of a single olfactory bulb displaying GFP around the glomeruli where cell bodies would be expected as well as staining the glomeruli where the projection neurons connect to the olfactory neurons, as shown by the white circle in Figure 13 AII.

GFP expression within individual olfactory receptor drivers shows that the signal can be mapped to single distinct glomeruli within the olfactory bulb (Figure 13 B). The three-dimensional position of these glomeruli is unique for each driver, with Or88a (Figure 13 BI) and its postsynaptic partner Mz19 (Figure 13 BII) selected. Or88a cd8::GFP expression can be seen to be prominent on the surface of the glomeruli and localised to the VA1d glomeruli. Meanwhile its postsynaptic partner, Mz19, has a cd8::GFP signal in projection neuron cell bodies located above and on the outside edge of the glomeruli. Dendritic projects are also highlighted which overlap with the glomeruli of both Or88a and Or47b. GFP can also be detected in higher brain regions of the *Drosophila* brain as the axons of Mz19 project into these areas, as shown by the white arrows in Figure 31 B II. Or88a and its postsynaptic partner were selected because they offer a clear glomerulus (VA1d) on the olfactory bulb's surface, with an easily visualised postsynaptic connection and known odorants and downstream read-outs offering a versatile neuronal circuit to study.

Other olfactory receptor drivers were tested as part of these experiments (Figure 13 C), with Or47b (Figure 13 CIII) also being on the surface of the olfactory bulb and offering a potential control to Or88a as both Or88a and Or47b synapses with Mz19 projection neurons. Or22a (Figure 13 CII) and Or85e (Figure 13 CIII) are smaller and deeper within the structure and are not as well suited to the

developing model as they are hard to discern within the olfactory bulb in images.

Together, the olfactory drivers Orco and Or88a represent upstream expression sites, or presynaptic neurons, where Tau can be expressed. With potential olfactory receptor neuron identified, the next step is to express the mCherryTau^{ON4R} construct from these olfactory receptor neurons, and observe their spread through the neuronal circuits of the *Drosophila* brain.

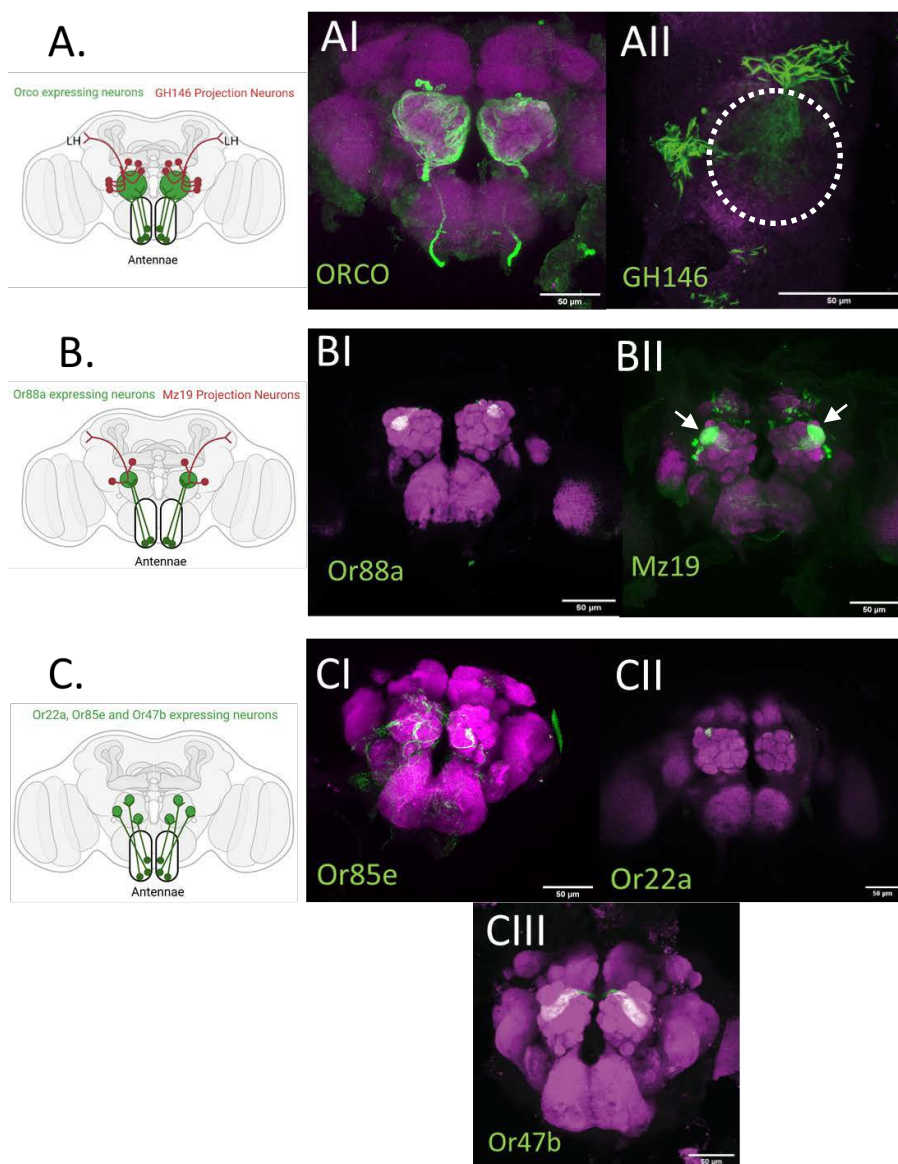


Figure 13: UAS.cd8.GFP expression driven in different olfactory subunit and projection neuron-targeted GAL4 drivers.

Confocal images of membrane-bound cd8.GFP fluorescence (green) allow for comparison of potential olfactory neuron and projection neuron GAL4 drivers. Nc82 staining of *Drosophila* synaptic active zone protein Bruchpilot (magenta) allows for navigation in the brain and identification of glomeruli. **A**) Shows GFP expression (green) in Orco olfactory co-receptor, delineating the entire olfactory bulb (**AI**) and a higher magnification image of a single olfactory bulb showing the postsynaptic GH146 neurons delineated with GFP (green), with their dendritic field outlined by the white circle (**AII**). **B**) Demonstrates the selected olfactory receptor neuron Or88a (**BI**) and its downstream partner MZ19 (**BII**), Both delineated with GFP (green) **C**) Images of a selection of other olfactory subunit drivers whose expression, as delineated by GFP (green), is localised to smaller regions of the olfactory bulb but were not selected to drive mCherryTau^{ON4R} in. Images were taken on a Leica SP8 confocal microscope with a 20x air objective (GH146 image taken using 63x oil objective with digital zoom applied using Leica Application Suite X (LAS X)). Scale bar = 50µm.

4.3.2 Spread from Or88a olfactory receptor neurons at 23°C

Or88a is expressed in 25 different neurons innervating the glomeruli VA1d (Berdnik, Chihara et al. 2006), offering a small number of neurons with specific connections in a prominent location on the olfactory bulb that is clear to image, as previously characterised at 23°C in section 4.3.1

Expression of the mCherryTau^{ON4R} construct in Or88a neurons at 23°C was hard to discern at the zero-day time point indicating expression is not present in larval and pupal developmental stages. However, either expression appears to increase post-eclosion or Tau has accumulated to detectable levels, as a weak mCherryTau^{ON4R} expression can be observed within the VA1d glomeruli by seven days. The amount of mCherryTau^{ON4R} increases with time, however this remains localised within the VA1d glomeruli across the entire 42 day time course (Fig 14 B I-IV).

By day 42 the expression pattern within the glomeruli has become punctate, potentially suggesting aggregation of the mCherryTau^{ON4R} construct. The area occupied by the mCherryTau^{ON4R} signal within the Or88a was quantified and analysed by one-way ANOVA, comparing the effect of time on the area of signal. The results showed that the area of the mCherryTau^{ON4R} signal is not significantly different ($F_{(4,10)} = 0.6465$, $p = 0.6533$) providing evidence that Tau is not spreading beyond the initial expression site in the VA1d glomeruli.

These results indicated that the spread of the mCherryTau^{ON4R} construct was not observed when expressed in the Or88a olfactory receptor neurons. However, we can see a potential aggregation of mCherryTau^{ON4R} at late time points. It is possible that, due to lower expression levels, whilst most Tau remains localised to the expression site a small amount below the detectable threshold may be spreading beyond the initial expression site. Therefore, an improvement to this experimental approach is required to enhance the detection levels of the system and possibly increase total Tau expression to boost the possibility of spread.

Comparable results were also seen in secondary confirmational experiments when mCherryTau^{ON4R} and GFP were expressed in another small group of neurons, Mz19, which is the projection neuron of Or88a (shown in Appendix 3). The Mz19 population only consists of 12 projection neurons whose cell bodies lie to the side and above the olfactory bulb. From here, the dendrites of Mz19 synapse in VA1d and VA1v glomeruli with Or88a and the Mz19 axons projecting to higher brain regions. However, GFP-positive cells and processes were also observed in both the bottom of the brain (prow) and the higher brain region, suggesting that the Mz19 driver expresses beyond the expected projection neurons due to expression of GFP beyond the expected Mz19 location (4A). When mCherryTau^{ON4R} is expressed in Mz19-positive neurons the signal is weak at zero days, becoming more robust by seven days. As with the Or88a experiments, this signal remains localised to GFP-positive regions identified in the separate Mz19.GAL4 UAS.cd8::GFP flies.

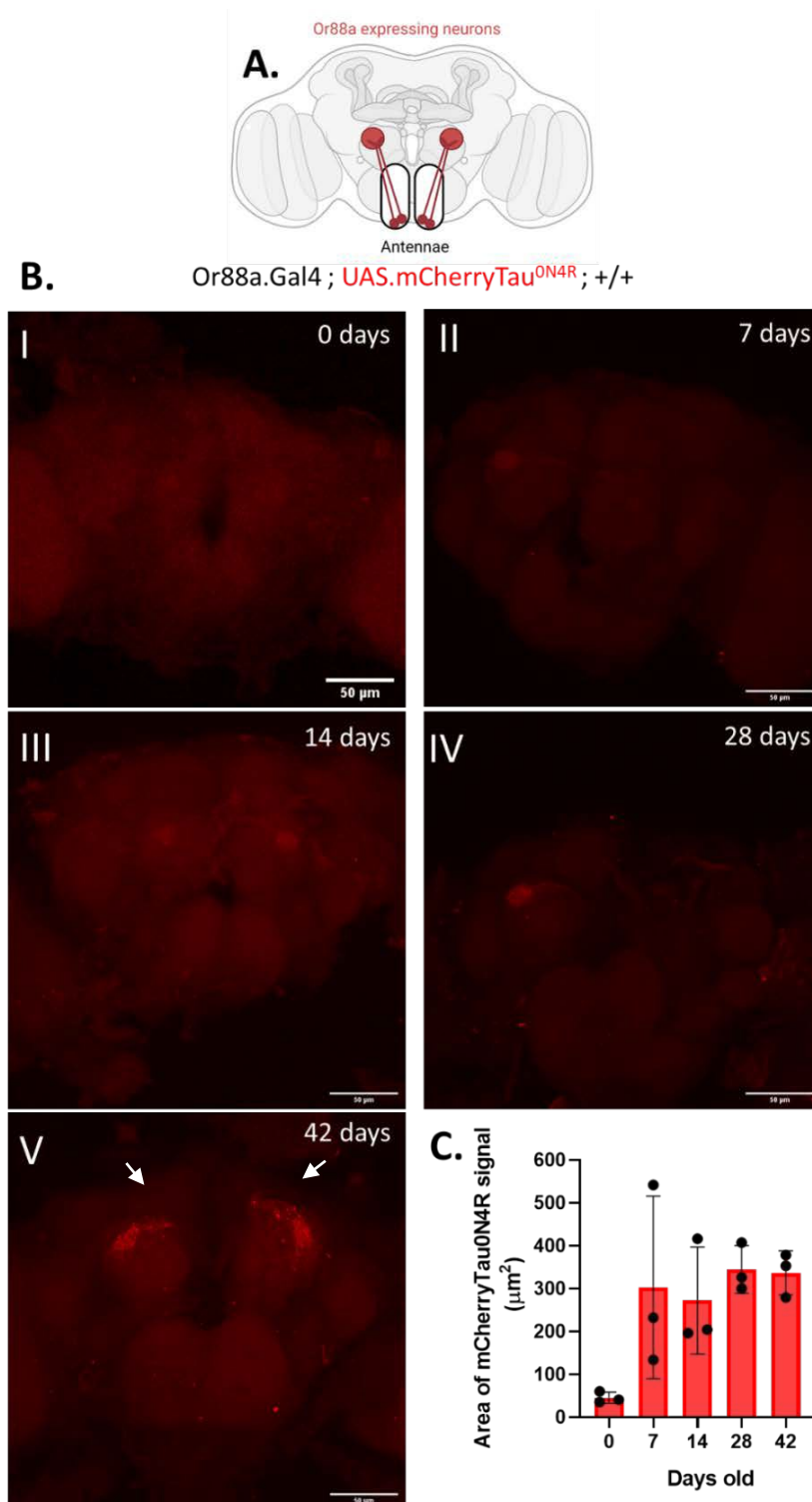


Figure 14: mCherryTau^{ON4R} does not spread from Or88a olfactory receptor neurons at 23°C

Expression of mCherryTau^{ON4R} construct (red) within the 25 Or88a olfactory-expressing neurons over 42 days. At zero days, the mCherry signal is barely detectable but remains localised to the VA1d glomeruli in which the Or88a neurons are located (BI) and at each point across the whole time course (BI–V). There is no significant difference between the mCherry coverage across the whole time course ($n=3$, $F_{(4,10)} = 0.6465$, $p = 0.6533$) (C). Of interest is the punctate morphology (arrows) of the mCherry signal by 42 days, potentially indicative of Tau aggregation (BV). Images were taken on a Leica SP8 confocal microscope with a 40x oil objective. Scale bar = 50μm.

4.3.3 Refining the model; stimulating spread from Or88a neurons at 29°C

In order to increase the amount of mCherryTau^{ON4R} present in the Or88a neurons, the flies were raised at 29°C to enhance protein expression due to enhanced molecular and enzymatic activity. In addition, immunohistochemistry was performed against the mCherry tag in order to detect even low levels of the construct.

To further refine the system, the Or88a.GAL4 driver was recombined with a UAS.cd8:GFP expressing fly. This resulted in a fly in which the Or88a.GAL4 expression site was constitutively delineated with GFP, into which the mCherryTau^{ON4R} construct could be expressed. In doing so, the GFP can outline the Or88a.GAL4 expression site and give confidence as to where expression is occurring, allowing for differentiation between this and local spread.

The cd8::GFP signal marked with a * in Figure 15AIII is the result of a surface trachea that was not completely cleared from the brain. Taking this into account, as shown in Figure 15A below, the recombined flies' GFP signal remains localised to the area of the Or88a glomeruli across a two-week course (Figure 15AIII). To demonstrate that the Or88a.GAL4 driver remains localised throughout this time course the area covered by the cd8::GFP signal in microns was measured at each time point. As shown in Figure 15B, the area coverage of cd8::GFP signal remains consistent between the three time points, as no significant difference in the area of the cd8::GFP signal between 0 and 7 days ($p = 0.9360$) and 7 and 14 days ($p = 0.9839$) is reported. This suggests that the expression of cd8::GFP is not observed beyond the Or88a expressing cells with time.

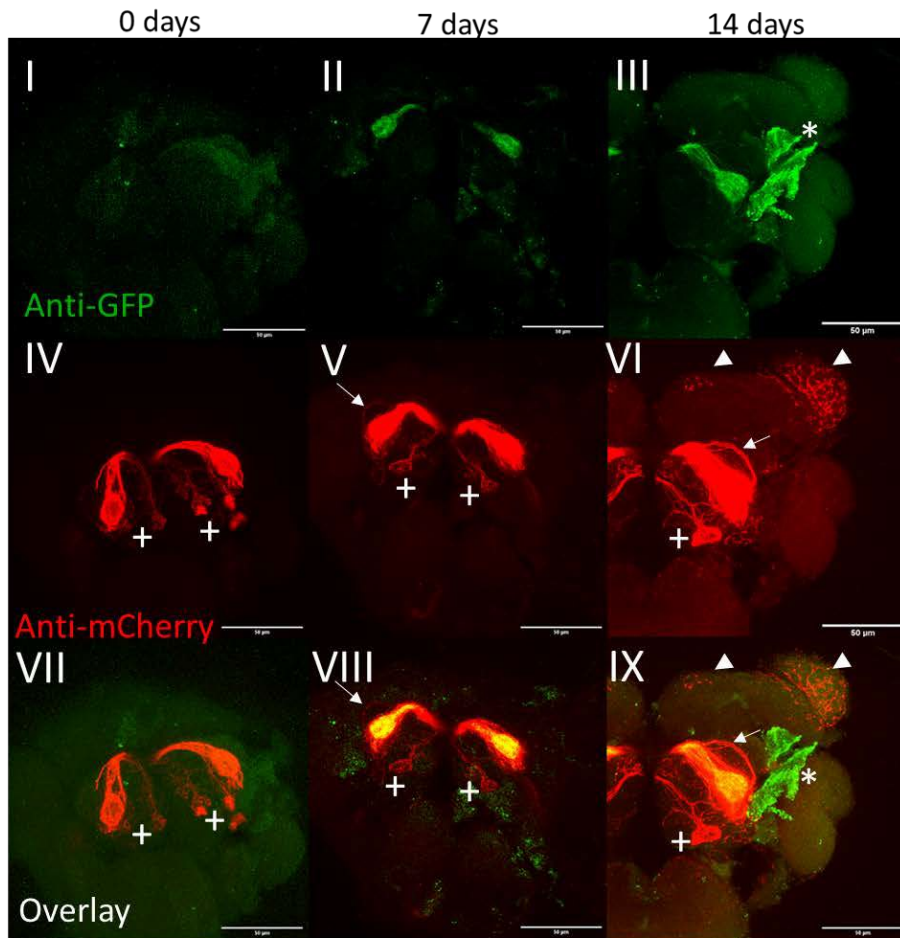
In contrast, in Figure 15 AIV, the mCherry signal is not only localised to the Or88a glomeruli but also appears in other glomeruli (+). The commissure of these glomeruli projects into a similar region to that of Or88a, potentially forming connections between the two. There are also signs of a loss of structure in the Or88a neurons in the appearance of mCherry positive tracts arching up from the Or88a glomeruli at days seven and fourteen, as indicated by the arrows in Figure 15 AV and VI. This loss appears more extensive at fourteen days than seven and mCherry signal appeared in other parts of the olfactory bulb at this point (Figure 15 AV and VI). The extent to which the mCherry signal extends beyond the GAL4 expression site is shown in the overlay in the final row of Figure 15 A(VII – IX). Here, it can be seen that the mCherry signal associated with the GFP-delineated expression area appears orange; this is most evident at seven and fourteen days when the GFP signal is most prominent. At the fourteen-day point, a population of mCherry-positive neurons is visible mainly in the higher brain region. The expression occurs primarily in the lateral horn region with a smaller population, more centrally, near the mushroom bodies as indicated by the white arrowheads in Figure 15 AVI. This population in the LH corresponds with the expected pattern of the postsynaptic Mz19 projection neurons, as diagrammatised in Figure 13 above. This

is potentially suggestive of trans-synaptic spread of the mCherryTau^{ON4R}. However, as the axonal tract linking the olfactory bulb to the lateral horn is not evident in any of the images, it raises the question as to how the signal has spread to those afferent regions.

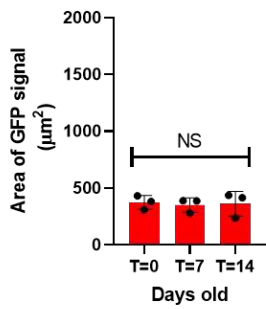
The area of mCherry signal beyond regions delineated by GFP, as shown in Figure 15C), shows no significant difference between non-GFP-associated Tau on zero to seven days ($F=0.060603$, $p = 0.6580$) but a significant increase between 7 and 14 days is observed ($F=0.0060$, $p = 0.0011$). This corresponds with the appearance of the mCherry signal in the higher brain regions at 14 days as shown in Figure 14 B and E, and together suggest that the mCherryTau^{ON4R} construct is moving beyond its expression site in the lateral horn. However, the area of mCherry beyond GFP remains consistent within the antennal lobe (Figure 15D) indicating that, over the entire time course, spread within the antennal lobe has not increased beyond those glomeruli that were mCherryTau^{ON4R} positive at the beginning.

This signal in the other glomeruli remains the same levels as day zero even if the flies are reared at 18°C until they eclose as adults. After this which point they are returned to 29°C to limit expression post-eclosion (Appendix 5). Signal in the other glomeruli is also present when DAKO anti-Tau was used in place of anti-mCherry where an untagged UAS.Tau^{ON4R} was crossed into the recombinant fly (full results shown in Appendix 6).

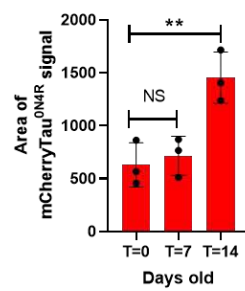
A Or88a.Gal4 ; UAS.mCherryTau^{ON4R} / UAS.cd8::GFP ; +/-



B Area of GFP signal in the fly brain

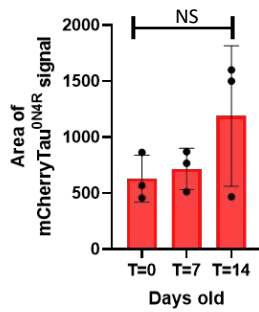


C Area of mCherryTau^{ON4R} beyond GFPdelimited areas



D

Area of mCherryTau^{ON4R} in the Glomeruli



E

Area of mCherryTau^{ON4R} in the Lateral horn

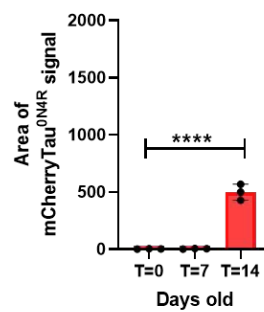


Figure 15: Characterising mCherryTau^{ON4R} expression in Or88a olfactory receptor neurons at 29°C

A time course of Or88a.GAL4-driven expression of UAS.mCherryTau^{ON4R} and UAS.cd8::GFP in the same fly. At zero days GFP signal (green) is weak, but is visible by seven days in the region associated with the Or88a glomeruli. At the 14 day time point surface trachea create noise in the GFP channel (green), as delineated by the white asterisk in **A(iii)**. The mCherry signal (red) is visible from zero days and appears to be located outside of the Or88a site in different glomeruli within the olfactory bulb to those containing GFP, as denoted by + symbols in **A(iv)**. This signal remains throughout the time course and at day 14 the mCherry signal can be observed in the lateral horn (**A(iv)** arrowheads). At day seven, neuronal processes appear that are connected to the Or88a neurons which seem to be coming away slightly from the glomeruli, perhaps indicating a loss of structure (shown by arrows in **A(v)**).

Analysis of the area covered with GFP signal (n=3) remains consistent over the 14 days, with no significant difference in area of GFP signal between zero and seven days ($p = 0.9360$) and 7 and 14 days ($p = 0.9839$), as shown in **(B)**. When analysing the area of mCherry beyond the GFP expression site (n=3), there no significant difference in non-GFP associated mCherry between zero to seven days is observed ($p = 0.6580$) but a marked increase between seven and 14 days is present ($p = 0.0011$) **(C)**. When analysing the spread regions separately, however, no significant difference in mCherryTau^{ON4R} is seen any of the time points when focusing on the glomeruli ($p = 0.2256$) **(D)** whereas in the lateral horn a significant difference is recorded between zero and 14 days ($p < 0.0001$) **(E)**. Images were taken on a Leica SP8 confocal microscope with a 63x oil objective. Scale bar = 50 μ m

4.3.4 Investigating the mCherryTau^{ON4R} conformation in Or88a olfactory receptor neurons

So far, this work has aimed to characterise the spread of the mCherryTau^{ON4R} without investigating whether the Tau present is of a pathological nature. This is key to understanding whether Tau spread is a purely pathological process, since most spreading species are believed to be misfolded and therefore seed competent.

One way to investigate whether the Tau species expressed in the Or88a olfactory receptor neurons has become misfolded is to use MC1, a conformational-dependent antibody that only detects pathological misfolded Tau (Jicha, Bowser et al. 1997). Figure 16 shows a time course of Or88a.GAL4-driven mCherryTau^{ON4R} stained with anti-mCherry (Figure 16 A(ii), (v), (vii) and (xi)) and MC1 (Figure 16 A(iii), (vi), (ix) and (xii)). At zero days post-eclosion mCherry signal is detectable in the Or88a glomeruli, as delineated by GFP co-expression, but no MC1 signal is present (Figure 16 A(i), (ii) and (iii)). By day three, a very weak MC1 signal can be observed in the glomeruli. However, the low levels of signal makes it hard to distinguish it above background levels. Despite this, MC1 appears to not be present in neurons that appear to have come out from above and below the glomeruli, as marked by arrows in the mCherry channel (Figure 16 A(v) and A(vi)). This could potentially be due to defasciculating of the neuronal bundle, or from the invasion of neighboring glomeruli. After seven days, the MC1 signal has spread upwards into the arch of the commissure, although it still remains weak (Figure 16 A(viii)). At fourteen days the majority of Or88a neurons, including those that have separated from the main bundle, have become MC1-positive (Figure 16 A(x), (xi) and (xii)). This is also seen in the graph in Figure 16 B, where a significant difference between zero and 14 days is shown in the MC1 signal ($F_{(3,8)}=11.82$, $p=0.0026$). This collectively implies that a time-dependent misfolding of the mCherryTau^{ON4R} construct is occurring in the Or88a olfactory receptor neurons, but that it has not spread.

From 7 days onwards MC1 signal can be observed more clearly in the Or88a neurons, as delineated in the anti-GFP channel. However, no conclusion can be drawn about whether the spreading Tau species is misfolded as Tau spread, either within other glomeruli or to the LH, was not observed in this set of experiments. The area of Tau is very similar to the cd8::GFP area and, indeed, matches the coverage of the cd8::GFP area at 14 days (Figure 16), suggesting that the significant difference in mCherryTau^{ON4R} signal observed ($F_{(3,8)} = 42.36$, $p < 0.0001$) is due to a delay in the expression and accumulation of neurons expressing cd8::GFP. As discussed previously, there is potential evidence of a breakdown in neuronal structure as the anti-mCherry signal in all 3 brains tested can be seen in the neuronal tracts that have separated from the main group of Or88a neurons (Figure 16 A(v) and (viii) arrows). These tracts appear to be Or88a neurons, as the bottom one is cd8::GFP-positive, suggesting that this neuron is part of the expressing population (Figure 16 A(iv) and (vii)).

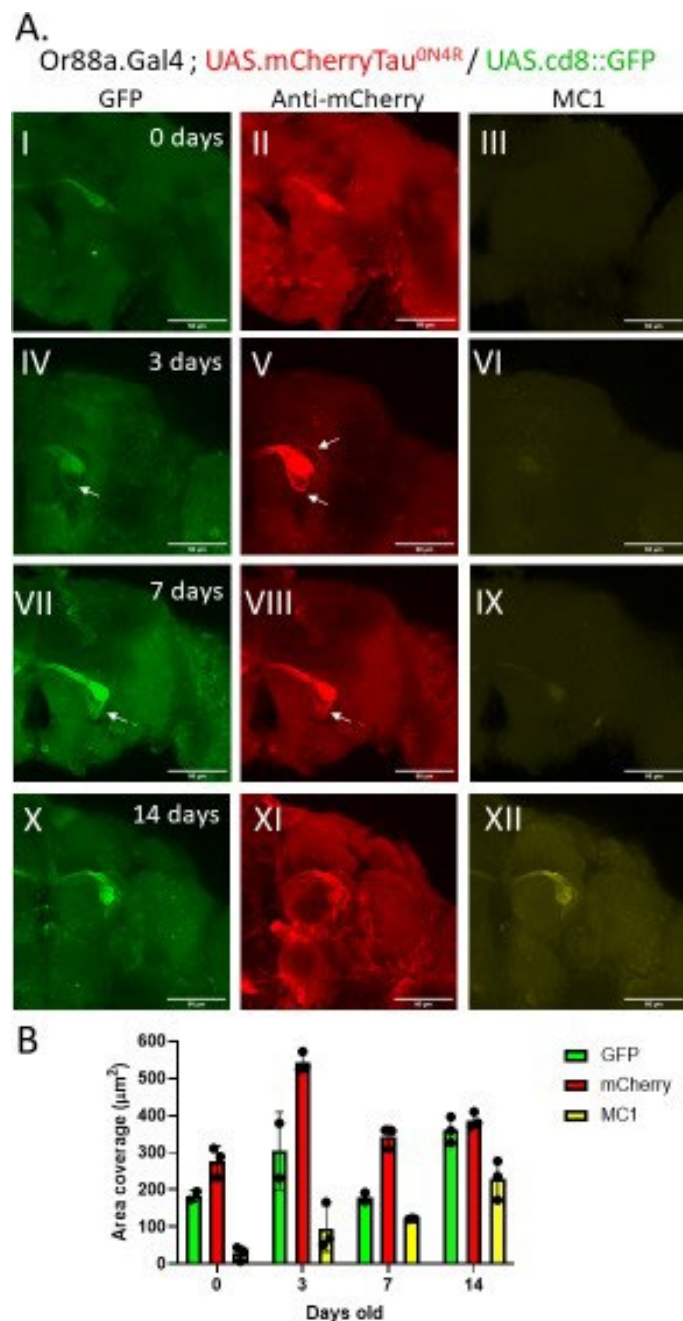


Figure 16 Investigating the conformation of mCherryTau^{ON4R} in the Or88a olfactory receptor neurons .

(A) At zero days post-eclosion mCherryTau^{ON4R} (red) is not MC1 positive (yellow), indicating that Tau^{ON4R} is not in a disease relevant conformation. The mCherryTau^{ON4R} signal that is present is restricted to the OR88a expression site (green), as is indicated by the GFP co-expression without previously observed spread to the LH and other glomeruli. At three days a loss of structure in the Or88a glomeruli is evident in the neuronal strands above and below the Or88a glomeruli and a very weak MC1 signal, barely above background levels is observable in only the Or88a glomeruli. This MC1 signal spreads to the commissure by day seven and becomes clearer in the glomeruli. By 14 days the MC1 signal is much stronger and covers a greater proportion of the Or88a glomeruli. **(B)** Quantification of the area coverage of this signal shows a significant difference between the GFP and mCherry coverage only at seven days (*) ($n=3$, $p = 0.0087$). Images were taken on a Leica SP8 confocal microscope with a 63x oil objective. Scale bar = 50μm

4.3.5 Is the observed spread real?

To be certain whether the spread of mCherryTau^{ON4R} beyond the Or88a-expressing neurons observed in Figure 15 is real, more stringent controls were necessary. This is key as either the Or88a.GAL4 driver is expressing beyond the expected olfactory neurons or the UAS transgene is mis-expressing, resulting in the appearance of mCherryTau^{ON4R} beyond the expected expression site and giving the appearance of spread. Furthermore, non-specific binding of either the primary or secondary antibodies used to assist with visualising the mCherryTau^{ON4R} may also result in signal beyond the expected expression site and, thus, the appearance of spread.

To test if the Or88a.GAL4 driver is expressed beyond the expected olfactory neurons the Or88a driver was crossed with cd8::GFP to delineate its expression site. When this was done, no expression into other glomeruli or the lateral horn was observed from the Or88a neurons over a 28-day time course (Appendix 2). This time course demonstrated that the expression pattern of Or88a does not change with time and remains localised to the VA1d glomeruli. Therefore, the driver expresses within the expected area and so is not mis-expressing into other brain regions. To account for non-specific binding the primary-secondary antibody combination for the anti-mCherry antibodies was tested on ORCO.GAL4 before its use on the experimental fly (Appendix 4). When primary and secondary antibodies were tested on Orco.GAL4, no observable structures were observed over a 21-day time course (Appendix 4). These results suggested non-specific staining from the primary or secondary antibody is not occurring.

Whilst the co-expression of cd8::GFP in previous results confirmed the driver's specificity, the UAS construct's specificity was not shown. Whilst theoretically, there should be no expression of a yeast promoter-controlled protein within a *Drosophila* brain, previous work with transgene expression systems in mice has shown that the transgene leaks when not driven (Costello, Lao et al. 2019). Furthermore, whilst other studies have shown that the attP40 site selected for the UAS insert is not leaky, other attP sites were shown to leak in the lateral horn (Pfeiffer, Ngo et al. 2010).

To test whether the potential 'spread' observed in the LH and glomeruli in Figure 15 is actually a result of this UAS leak, the UAS.mCherryTau^{ON4R}-only fly was tested with the same parameters as Figure 15. This revealed that a cell body and its projections in the top of the *Drosophila* brain can be observed faintly at zero days and the intensity of this increases at three, seven and 14 days (Figure 17A, with an arrow delineating the top of the brain). However, at 14 days signal in the projections is no longer visible. This suggests that there is some ectopic expression of the construct, confirming that this signal is the UAS.mCherryTau^{ON4R} construct and not non-specific binding of the primary antibody. Further evidence comes from staining with both anti-mCherry and anti-human Tau primary antibodies (Figure 17 A and B), showing that the signal in this area is a result of both human Tau and mCherry. This cell body and its projections failed to produce a signal when an anti-

Drosophila Tau antibody was used (Figure 17 C) nor when this experiment was carried out in the Orco.GAL4 control, where no UAS construct is present (Appendix 4). Further optimisation was trialled by raising the flies at 18°C until eclosion then transferring them to 29°C in order to limit expression pre-eclosion and potentially remove this ectopic signal. However, the cell body and its projections in the lateral horn remain (Appendix 5), suggesting the expression here is independent of temperature. This implies that the signal in this regions does not result from raising the flies at 29°C.

The leakage of the construct is apparent within the same area that spread into the lateral horn is seen in Figure 15, raising doubts about the validity of this observation. However, at no time point did anti-Tau or anti-mCherry stain the olfactory bulb in the UAS fly. This supports that the spread observed in the glomeruli is real and not an artefact of leaky expression.

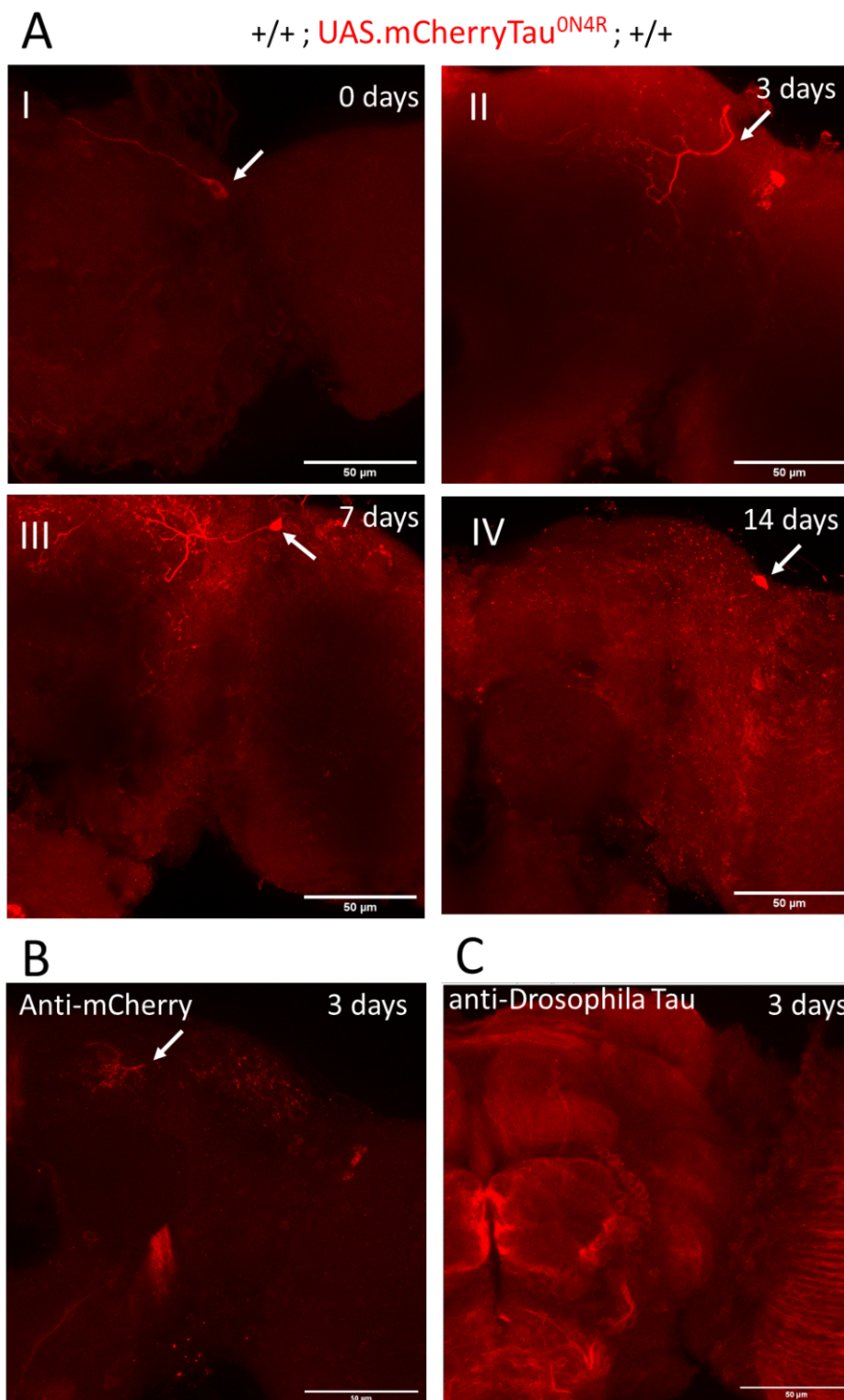


Figure 17 Staining of the UAS.mCherryTau^{ON4R} construct alone at 29°C

(A I,II,III,IV) In the non-driven UAS.mCherryTau^{ON4R} fly anti-Tau antibodies (red) stain a cell body and its projections in the lateral horn, as marked with arrows across 0-14 days. **(B)** These projections are also positive for anti-mCherry antibodies (red) (delineated with an arrow). **(C)** They are not stained by endogenous anti *Drosophila* Tau antibodies (red), suggesting that there is ectopic expression of the UAS.mCherryTau^{ON4R} construct in this region. Images were taken on a Leica SP8 confocal microscope with a 63x oil objective. Scale bar = 50µm.

4.4 Discussion

4.4.1 Summary

This work sought to investigate the spread of Tau in a small number of olfactory neurons by expressing the mCherryTau^{ON4R} construct in Or88a olfactory receptor neurons. Having characterised several other olfactory receptor neurons and selecting Or88a, the next step was to express the mCherryTau^{ON4R} construct at 23°C. In doing so an aggregate phenotype, in which the mCherry Tau signal became punctate with time, was observed but no spread was evident. Increasing the temperature at which the experiments were carried out, alongside boosting signal using antibodies against the mCherryTau^{ON4R} construct, enabled the observation of potential spread to both higher brain regions and to neighboring glomeruli. This was accompanied by potential degeneration in the expressing Or88a neurons and evidence of the mCherryTau^{ON4R} construct adopting a pathological confirmation over time. However, further controls identified that the spread found in the higher brain regions originated from ectopic expression of the UAS.mCherryTau^{ON4R} construct over time. This ruled out spread occurring in the lateral horn, however no leakage was observed in the olfactory bulb supporting the idea that spread into this region is real.

4.4.2 Selection and optimization of a small number of olfactory receptor neurons in which to model Tau spread

Selection of the olfactory receptor neurons

Or88a.GAL4 was chosen to be the driver over Or47b due to the productivity of the stock. Both Or88a and Or47b are located in a prominent position on the surface of the olfactory bulbs (Figure 13). Both odorant receptors are involved in the mating process, giving a well 92tilized92ized physiological input and output with which to further manipulate the model in future studies. Furthermore, they share a common projection neuron subclass, Mz19, although they each innervate separate glomeruli, VA1d and VA1v, for Or88a and Or47b respectively (Jefferis, Vyas et al. 2004, Dweck, Ebrahim et al. 2015). This offers a specific synaptic connection across which Tau spread can be studied. A further advantage is that the neuronal driver, Or88a, and non-Tau expressing partner, Or47b, share a common downstream target in Mz19. This allows for physiological studies to be carried out to assess the health and function of the downstream projection neurons as the presence of a non-Tau expressing pre-synaptic neuron will act as an inbuilt control. The inability of the fly in being able to sense both Or88a and Or47b odorants in a Or88a Tau expressing fly would confirm that Tau is causing dysfunction in the downstream Mz19 neurons and this dysfunction is not just coming from the expression of Tau within the Or88a population.

Amplifying Tau signal in the Or88a olfactory receptor neurons to observe spread beyond GFP-delineated expression sites

When expressed from the Or88a neurons, the mCherry signal in Figure 14 is relatively weak and does not spread beyond the Or88a glomeruli even after 42 days, as delineated by GFP in Appendix 2. The concentration of Tau is known to play a role in its pathology (von Bergen, Barghorn et al. 2005), so an increase in expression levels may succeed in inducing spread in this model.

Furthermore, given the weakness of the mCherry signal detected and the small number of neurons expressing the construct compared to the overall olfactory circuitry co-expressing Orco (~20 vs ~2000) (Vosshall and Stocker 2007), some of the mCherryTau^{ON4R} population might have been spreading. However, the fluorescence level may be too low and below detection limits. To address this issue, increased temperature and amplification to the immunohistochemical signal were attempted to enhance protein expression and boost the fluorescence signal (Figure 15). As flies are ectotherms, an increase in the rearing temperature will increase body temperature and so lead to higher protein expression (Robinson, Kellie et al. 2010).

The above improvements with the system 93tilized by recombining the Or88a.GAL4 driver with UAS.cd8::GFP. This results in the presynaptic neuronal population that would be expressing Tau becoming delineated and making it easier to ascertain if any Tau is spreading beyond this initial expression site, a common control employed in mouse models (Rauch, Luna et al. 2020). When crossed with the UAS.mCherryTau^{ON4R} construct, this resulting fly expresses both cd8::GFP and mCherryTau^{ON4R} in the Or88a neurons in the same individual. As well as delineating the pre-synaptic neuron in which the Tau is expressed, this cd8::GFP also serves to identify any ectopic GAL4 activity in neurons other than OR88a.

Implementing these improvements to the system resulted in a clear delineation of the Or88a-expressing populations from seven day old flies (Figure 15). Alongside this was observed mCherryTau^{ON4R} signal, seen not only the GFP-positive glomeruli, but also in another glomeruli lacking GFP co-expression. Furthermore, mCherryTau^{ON4R} was observed in the lateral horn from 14 days. The lateral horn is a tissue connected to the olfactory bulb via the Mz19 projection neuron which carries olfactory inputs to higher brain areas (Ito, Suzuki et al. 1998). A signal in the lateral horn was not observed at early time points. Still, a signal appeared in a time- dependent manner (Figure 15) with both tagged and untagged Tau variants (Appendix 6), although this signal is weaker when flies are first reared in 18°C and transferred to 29°C.

These results suggest two potential locations where spread occurred; the lateral horn and the glomeruli. However, as discussed later on, the Tau population within the lateral horn is most likely due to miss-expression of the driver. However, the potential spread within the olfactory bulb remains.

4.4.3 Evidence for and against the Tau spread within the glomeruli

If spread into other glomeruli is indeed occurring, what mechanisms are present that could facilitate this movement from the Or88a neurons laterally into other glomeruli?

The case for glia in mediating Tau spread

A potential pathway for Tau spread between the glomeruli is via the ensheathing glia surrounding each glomeruli (Sen, Shetty et al. 2005). These glia play an active role in *Drosophila* synapse homeostasis and can clear debris and excess neurotransmitters, potentially including Tau, from the synaptic cleft (Doherty, Logan et al. 2009). Such a 'lateral' Tau spread in humans has been suggested to exist alongside a trans-synaptic pathway, in which glia take up phosphorylated Tau species and release them via exosomes (Asai, Ikezu et al. 2015). Whilst such a lateral move may explain why other glomeruli are Tau-positive, previous *Drosophila* studies using mutant Htt, another prion-like protein, have shown a much more punctate and dispersed signal due to the physiology of glial cells (Pearce, Spartz et al. 2015). More recent work has utilized a smaller number of neurons, like the one in the present study, and found that whilst glia do play a role in mutant Htt protein spread, they are from an intermediate, uptaking and releasing Htt, allowing the crossing of Htt from an olfactory receptor neuron into the post-synaptic projection neuron (Donnelly, DeLorenzo et al. 2020). The patterns described in these works do not correlate with the axonal processes observed in other glomeruli, as observed in this model, as (Donnelly, DeLorenzo et al. 2020) found spread of Htt in the projection neuron within the same glomeruli. This suggests that glia are not involved in mediating spread to the projection neuron. However another connection is present from the Or88a neurons – the interneurons.

The case for interneurons mediating Tau spread in the glomeruli

In Figure 15, it is only within glomeruli associated with the expression site where Tau-positive neurons are observed. This could indicate that mCherryTau^{ON4R} is entering olfactory interneurons, which connect between olfactory neurons and projection neurons with a function to synchronise projection neuron firing (Vosshall and Stocker 2007, Das, Sen et al. 2008). The role of interneurons in mediating spread of Tau has been reported in mouse models where AD patient-derived extracellular vesicles were injected into the outer molecular layer of the dentate gyrus (Ruan, Pathak et al. 2021). In particular, phosphorylated Tau accumulated in GABAergic interneurons (Ruan, Pathak et al. 2021). In *Drosophila*, the interneurons' neurotransmitters are diverse, consisting of both GABAergic and cholinergic neurons (Das, Sen et al. 2008). The VA1d glomeruli into which Or88a neurons innervate are also innervated by GABAergic local interneurons (Liou, Lin et al. 2018). This suggests that the Tau signal within glomeruli which do not express cd8::GFP, as observed in Figure 15, could result from an early and preferential spread. This could be facilitated

by GABAergic local interneurons that connect between the VA1d and these glomeruli. Whilst the interneurons are not the primary postsynaptic partner of Or88a, the conformation of the Tau protein may confer a preference for particular neuronal circuitry, explaining spread in this direction. A potential confounding factor to this theory is the lack of Tau signal in the interneuron cell bodies located around the edge of the antennal lobe, similar to those of the projection neurons (Das, Sen et al. 2008). However, it is possible that, as a predominantly axonal-located protein, mCherryTau^{ON4R} has not spread out into the cell bodies of these neurons during this time course.

Evidence against spread in the glomeruli: mis-targeting of OR88a neurons

A very recent pre-print paper on BioRxiv has highlighted a potential complication of the attP40 insertion site used to create the transgenic lines utilized in the present study, which could provide an alternative explanation for the results seen in the present chapter (Duan, Estrella et al. 2022). This paper found that homozygous attP40, or interaction between attP40 and second chromosome GAL4, resulted in altered olfactory glomeruli structure. Interestingly, this was independent of the MSP 300 gene that attP40 inserts into, suggesting that there may be other local effects generated by the insertion (Duan, Estrella et al. 2022). Duan *et al* used another small ORN driver, Or47b.GAL4, to drive other genes from the attP40 locus. This led to these neurons invading surrounding glomeruli, causing the Or47b GFP signal to become distorted and mis-localized into neighbouring glomeruli (Duan, Estrella et al. 2022). There is potential that such mis-localisation also occurs in the present system, potentially accounting for the small protrusions of the mCherry signal seen at the bottom of the Or88a glomeruli which could be manifesting as “defasculations” of the Or88a axon bundles (Figure 16B). The flies in this experiment are heterozygous for attP40 as Or88a.Gal4 is a P-element insertion, but the mCherryTau^{ON4R} is an attP40 insertion. The effect of this could be tested by repeating the experiment using a different insertion site for Tau. If these protrusions did not appear with a different insertion site, then they are the result of the attP40 insertion. The presence of cd8::GFP in some of these same neurons (Figure 16B) supports the idea that perhaps some miss-targeting of neurons is occurring as a result of the attP40 insertion site. However, it is clear that cd8::GFP is not observed in some of these tracts (Figure 16) suggesting that these neurons do express Tau and that Tau spread and its’ toxicity may be causing this potential “defasculation”. Furthermore, the complete miss- targeting of Or88a neurons into glomeruli other than VA1d, as observed in Figure 15 makes this possibility unlikely. However, the expression of a toxic construct, such as the mCherryTau^{ON4R}, can exacerbate these phenotypes.

Whilst the attP40 insertion site may have some effect on the shape of the VA1d glomeruli it remains unlikely that this alone could explain the presence of Tau in adjacent glomeruli. Overall, the two different pathways described, via the glomeruli or interneurons, may facilitate the transfer of Tau from the Or88a neurons in the VA1d glomerulus to adjacent, non-cd8::GFP expressing glomeruli,

although further work is required to confirm this.

4.4.4 Evidence against Tau spread into the lateral horn; UAS transgene leakage

In the Or88a-driven mCherryTau^{ON4R} fly spread of mCherry Tau^{ON4R} appears to occur in the lateral horn after 14 days (Figure 15B). However, in later experiments, no signal could be detected in the lateral horn (Figure 16). Experiments on control Orco.GAL4 flies ruled out the possibility of higher rearing temperatures and anti-mCherry antibodies causing non-specific staining in the brain which may appear as spread (Appendix 4). It has been reported in other attP drivers that leakage of the UAS transgene can occur, particularly in the lateral horn (Pfeiffer, Ngo et al. 2010). Whilst this has not been reported for the attP40 insertion site, to be confident in the system another control experiment was carried out using the undriven UAS.mCherryTau^{ON4R} fly. When primary and secondary fluorescent staining were applied in the UAS.mCherryTau^{ON4R} flies, a cell body and its' projections were visible in the region of the lateral horn (Figure 15A). These were immunopositive for mCherry and human Tau, indicating that non-specific binding of the primary antibodies had not occurred but result from ectopic expression of the UAS.mCherryTau^{ON4R} construct in this region. This is further supported by the absence of staining of *Drosophila* Tau in UAS.mCherry brains (Figure 15C).

As previously stated, leakiness of UAS transgenes has been reported in other insertion sites, with the extent of the leak varying depending on the tissue it is expressed in, due to the different genetic background flanking the insertion site (Pfeiffer, Ngo et al. 2010, Mao, Xiong et al. 2014). Pfeiffer *et al* observed ectopic expression in the lateral horn using a GFP construct in other attP insertion sites but not in attP40, as can be seen in their supplementary dataset (Pfeiffer, Ngo et al. 2010). Given that many of these attP drivers express ectopically in the LH, the signal observed in Figure 14 is likely a leak of the UAS transgene. The fact that an attP40 leak is not seen in the Pfeiffer, Ngo *et al* (2010) paper when using a UAS.GFP construct may suggest that it is the Tau construct being inserted into the attP40 site which is playing a role in its leakage in Figure 17. This leakage appears in the cell body and processes observed could be either Lateral Horn Output Neurons (LHONs) or Lateral Horn Local Neurons (LHLNs), AV4a1 or Av7a1 respectively (Dolan, Frechter et al. 2019). However, without the co-expression of specific GFP drivers for these prospective neuronal populations, it is impossible to say with certainty which neuron contains the ectopic expression. Therefore, this cell body and its' projections shall be referred to as the lateral horn cell body from here on. The mCherryTau^{ON4R} ectopic expression seen in the lateral horn cell body is low given the inability to detect it without using Tau or mCherry-specific antibodies. However, Figure 17 revealed that any signal detected in this region is confounded by ectopic expression and its labelling as spread cannot be certain.

4.4.5 Evidence against Tau spread into the lateral horn; Lack of Mz19 staining

Further evidence against the Tau population in the LH originating from the Or88a neurons comes from the lack of mCherry signal between the olfactory bulb and the lateral horn. Connecting the two tissues is the Mz19 projection neuron, as characterised with GFP in Appendix 2, yet in all images Mz19 cell bodies do not appear to contain mCherry signal. In addition, there is no evidence of signal in the projection neuron axons connecting to the LH at either day seven or 14. There is potential that the Mz19 projection neuron is selectively vulnerable to degradation from Tau, resulting in its death and making it appear as if the two tissues are not connected. Such selective vulnerability has been reported by Babcock & Ganetzky (2015) in their model of mutant Huntington's spread. This model saw the loss of vulnerable neurons between the olfactory bulb and more resistant cells in the posterior of the brain (Babcock and Ganetzky 2015). Such a selective loss may occur here; preliminary work where an Or88a.GAL4, Mz19::GFP fly was created and crossed with the UAS.mCherryTau^{ON4R} construct found that the cell bodies for the Or88a innervating Mz19 neurons were not present. In their place were some cells that appeared to be apoptotic (Appendix 6) whilst the Or47b-innervating Mz19 neurons remained. This work remained preliminary as it was not possible to detect the GFP signal enough to reliably observe the axons of the Mz19 projection neuron. This potentially suggests the loss of the Or88a-innervating Mz19 neurons but, conversely, could be due to issues with the levels produced by the Mz19-GFP fusion construct. These constructs produce much less GFP than a UAS/GAL4 system due to the lack of amplification from the multiple GAL4 bindings. However, without further studies, for instance using a cell death marker such as DCP-1 (Song, McCall et al. 1997), it cannot be concluded that the Mz19 projection neurons have died and so no conclusive evidence is present suggesting Tau has spread to the lateral horn via Or88a's post-synaptic partner.

Overall, the signal in the lateral horn is unlikely to be a result of spread, despite its' time dependent appearance and downstream location, due to the low leakage of the transgene into this region. However, this leakage was not observed in the olfactory bulb itself and so insights gained from the olfactory bulb are unmarred by this leakage.

4.4.6 Pathogenic aspects of Tau in this model; evidence of toxicity

Much of the work discussed so far focuses on the spread of the mCherry-tagged Tau^{ON4R}. Yet, spread is only one part of AD pathology. Tau misfolds in AD, adopting a pathogenic conformation that allows it to aggregate into larger structures. Such misfolding and aggregation is present in the *Drosophila* model.

In many of the Tau-expressing brains (Figure 15 and Figure 16) axons separate from the Or88a inverted glomeruli (VA1d), or from other glomeruli that are expressing Tau, can be seen with time.

These neurons often contain cd8::GFP, suggesting that they are Or88a expressing neurons that have detached from the main bundle. A similar phenotype has been reported previously in models expressing Tau in *Drosophila* sensory neurons (Williams, Tyrer et al. 2000). In addition, in Figure 14, the mCherry signal appeared clumped together within the Or88a neuron at 42 days, suggesting accumulation and, potentially, aggregation of Tau within Or88a neurons. Aggregation of Tau is usually seen in pathology-mimicking designer or diseased-derived mutants in other models (see Intro 1.9.3), and such a spontaneous aggregation is uncommon. Nonetheless, the accumulation of Tau suggests that some of the Tau in this model is acquiring pathogenic properties, though without clear degeneration of those neurons in which it is found.

4.4.7 Pathogenic aspects of Tau in this model; MC1 staining of neurons

To confirm the pathological nature of the mCherryTau^{ON4R} construct in this system, staining with an MC1 antibody was used to detect the misfolding of Tau. This antibody is conformationally-dependent on misfolded Tau, recognising amino acids 7–9 in the N terminus and amino acids 313–322 in the third microtubule-binding domain, which are brought into close proximity by the pathological Tau fold (Jicha, Bowser et al. 1997). The lack of staining at day zero is a positive indication that time-dependent misfolding of the mCherryTau^{ON4R} is being observed. This is also supported by the steady increase in signal area and intensity seen in Figure 15. The appearance of misfolding with time is pathologically relevant and confirms that such misfolding is not a consequence of human Tau expression within the *Drosophila's* olfactory neurons. The spontaneous appearance of MC1-positive Tau species is somewhat surprising, given that many other models of Tauopathies require Tau mutants or co-factors when using wild-type Tau species in order to induce Tau aggregation. Some success with spontaneous misfolding has been found in mouse and rat models, although these take 8-24 months to show a weak pathological phenotype (Dujardin, Lécolle et al. 2014, Dujardin, Bégard et al. 2018). The MC1 staining always co-localised with the mCherryTau^{ON4R} signal but never fully covered the mCherryTau^{ON4R} positive area (Figure 15), suggesting that a proportion of the Tau was becoming progressively misfolded. At none of the time points studied did the MC1 signal spread beyond the GFP-delineated area, raising doubts as to whether or not the misfolded Tau species was the one spreading into the adjacent glomeruli. However, insights into the nature of spreading Tau species cannot be gained from these results as spread into adjacent glomeruli did not appear to occur in the flies tested with MC1 (Figure 15).

In summary, the time-dependent appearance of MC1 staining in the fly suggests a spontaneous misfolding of the wt-Tau species attached to the mCherry tag. This recapitulates the spontaneous misfolding of Tau observed in the majority of AD cases in way that is, perhaps, more relevant than using Tau mutants to induce aggregation (Dujardin, Lécolle et al. 2014).

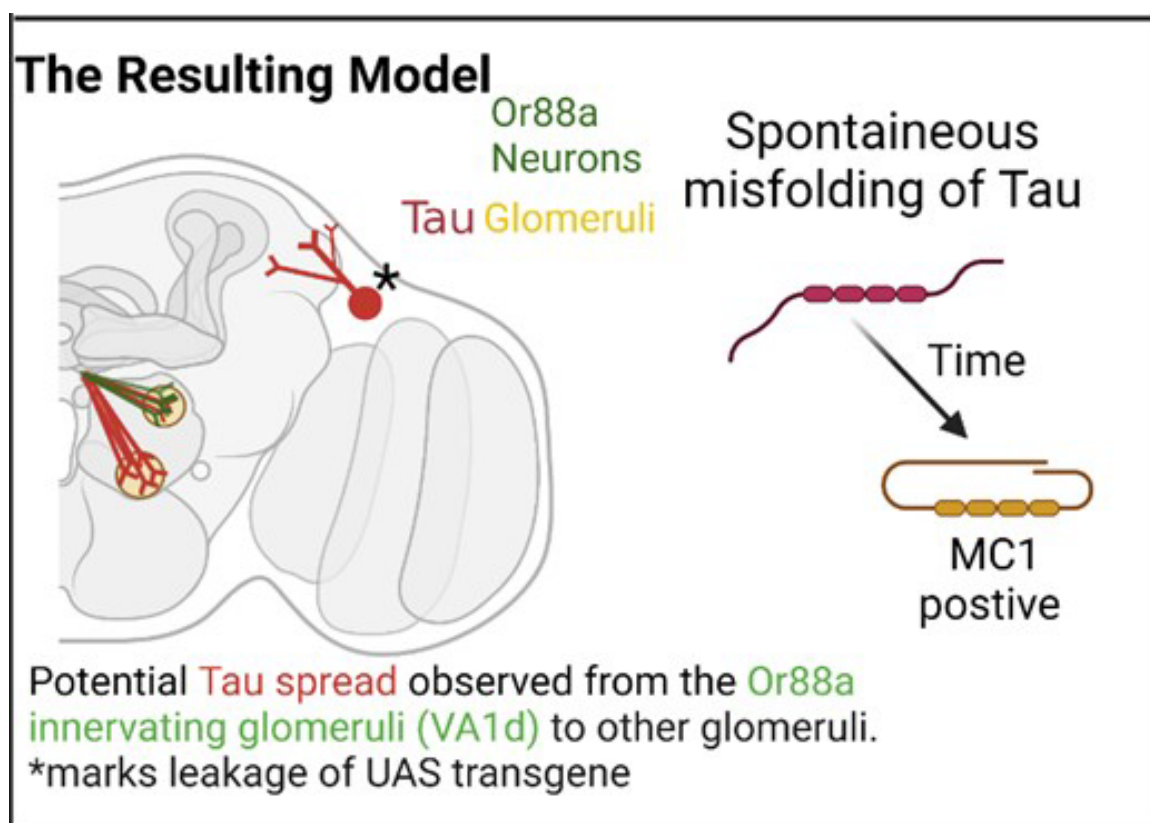


Figure 18: Schematic of the results found in this chapter, showing the spontaneous misfolding of Tau and spread into adjacent glomeruli

Potential spread was observed to occur from the Or88a expression site of UAS.mCherryTau^{ON4R} (green and red) to other olfactory glomeruli (red). mCherry signal was also detected in the lateral horn (*), however results (either directly, through expression, or spread) from a leakage of the UAS.mCherryTau^{ON4R} construct. It was also found that the Tau in this system spontaneously adopted a misfolded conformation, via MC1, with time.

4.4.8 Conclusion and future directions

This chapter has demonstrated a spontaneous time-dependent adoption of a pathological confirmation of the mCherryTau^{ON4R} with time, with potential consequences for where it is expressed. Furthermore, there may be a spread of Tau from the Or88a neurons into other nearby glomeruli. However, careful consideration of confounding factors must be considered before drawing such conclusions from this model. Insertion of the mCherryTau^{ON4R} in the attP40 site appears to lead to ectopic expression in a lateral horn neuron and may also independently impact the glomerular organisation. Despite this, potential spread may still occur via local interneurons into non-cd8::GFP expressing glomeruli when mCherryTau^{ON4R} is driven in Or88a neurons at 29°C. It can also be seen that the mCherryTau^{ON4R} spontaneously adopts a pathological confirmation with

time, as shown by MC1 staining. This is an important area to investigate further as work in microfluidic models has shown that phosphorylation-mimicking Tau mutants are capable of spreading across synapses and inducing misfolding in the downstream neuron (Hallinan, Vargas-Caballero et al. 2019). This raises the question that if MC1 staining is observed in the expressing neurons, whether these misfolded species are capable of spreading to downstream connections.

Refinement of the model

The small number of Or88a olfactory receptor neurons offers the ability to investigate the effect of mCherryTau^{ON4R} on a small population of neurons, making it suitable for observing pathological differences between different Tau species expressed in these neurons. The potential Tau spread phenotype observed should be investigated further, aiming to identify whether the mCherryTau^{ON4R} signal in the olfactory bulb is the result of glia, interneurons or potentially mistargeting during development caused by the transgenes attP insertion site. This could be achieved using *Drosophila's* genetic and molecular tools to probe each of these in turn. A new genetic landing site for the UAS.mCherryTau^{ON4R} should be the first experimental factor to be modulated, ensuring that these observations are not due to the misexpression or mistargeting of Or88a neurons. Insertions into new genetic landing sites are relatively simple, with a potential candidate being attP2, located on the 3rd chromosome. Whilst a reported leak of UAS transgenes into the lateral horn has been observed previously from this landing site (Pfeiffer, Ngo et al. 2010), the insertion will be on a separate chromosome. Therefore, if the Tau signal is the result of the insertion site, a change to a different chromosome will change its phenotype. Another experiment with an older P-element insertion site would help to confirm that these effects are not simply due to the attP system.

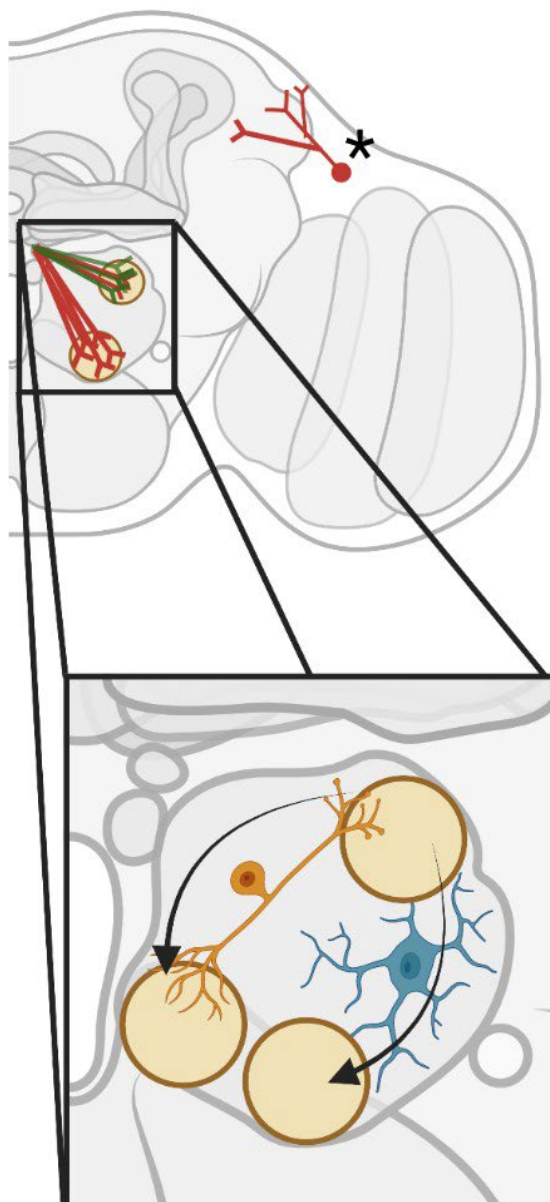
Future uses of this model

If local spread seen within the olfactory bulb is confirmed, several mutants are readily available in the fly to investigate the mechanisms of Tau spread via the interneurons or glia. Repo is a transcription factor, expressed in all glial cells (Alfonso and Jones 2002) whose targeting via antibodies may co-localise with the mCherryTau^{ON4R} signal. However, being a global receptor, it may not be informative due to the high prevalence of signal occluding specific information. Glial targeting lines exist that allow the expression of fluorescent tags or knockdown/knockout of the glial genes in the fly. In such flies, the ability of expressed mCherryTau^{ON4R} to still spread to other glomeruli in the system would indicate the glia's role in this process, as it could still occur in the absence or reduced presence of glia at a similar rate. A similar approach can be taken when investigating the effect of local interneurons with NP3056.GAL4 (Chou, Spletter et al. 2010). This would allow for the targeting of fluorescent proteins to the GABAergic interneurons that connect Or88a in the VA1d glomeruli to other glomeruli positively identifying them as intermediaries if

found to co-localise with mCherry Tau^{ON4R} signal. The presence of these interneurons could also be decreased or removed through the use of RNAi's. If spread is reduced or ablated in these experiments then the role of interneurons would become apparent.

In the next chapter, the aim is to characterise the phenotypes of the mCherryTau^{ON4R} construct further when driving from a larger number of olfactory neurons using Orco and to trial the effect of various neuronal activity-modulating mutants.

Future work



Targeting Potential
Mediators of
Tau spread between
Glomeruli:
Glia
Interneurons

Figure 19: Schematic outlining future directions from this chapter

Future work should aim to refine the expression of the construct and confirm the spread of Tau in the olfactory bulb. With this it is then possible to use readily available mutants in *Drosophila* to investigate mediators of Tau spread.

Chapter 5 Modelling Tau spread in all *Drosophila* olfactory neurons

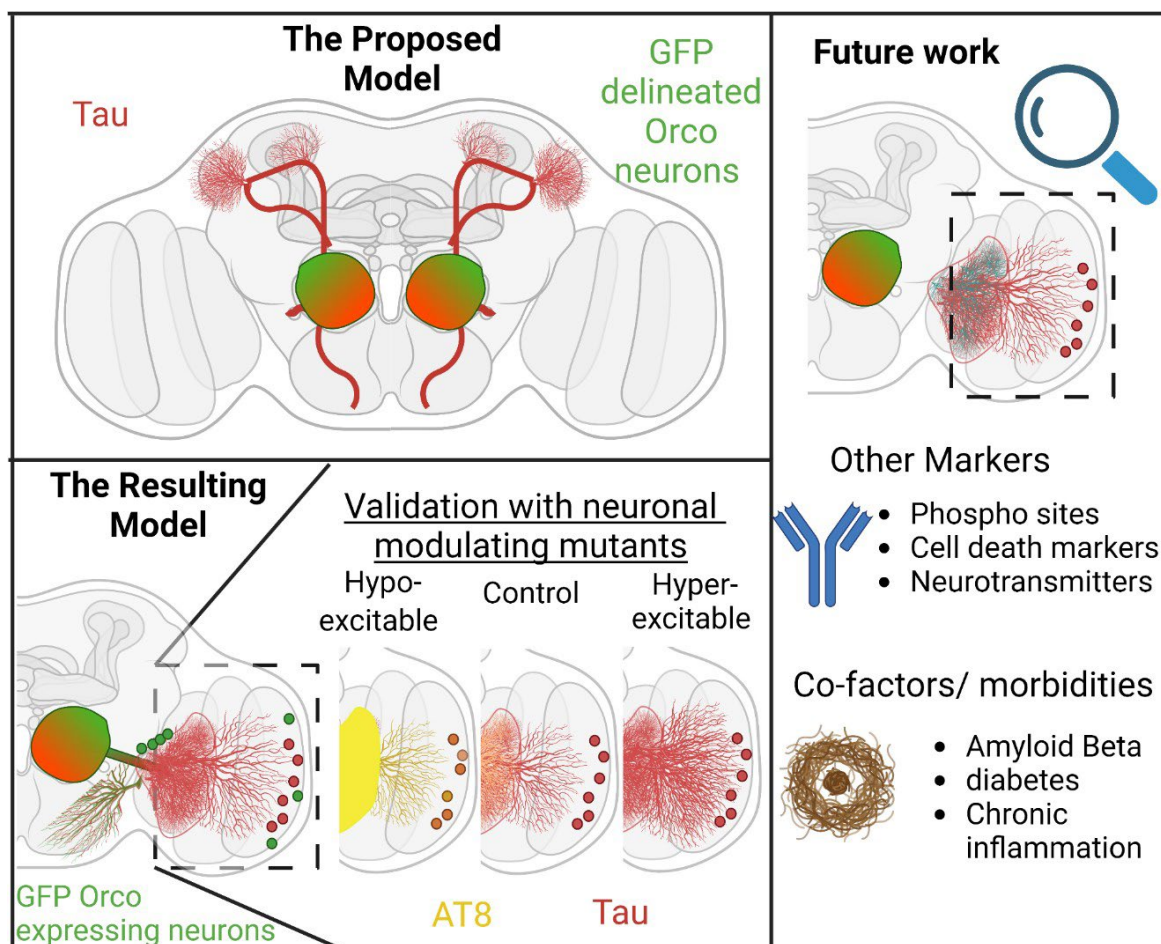


Figure 20 Graphical abstract of Chapter 5; Simulating Tau spread in all olfactory neurons by expressing mCherryTau^{ON4R} in Orco expressing neurons

Tau spread is simulated (red) with a delineated expression site (green). The Orco driver appears to mis-express into areas outside of the olfactory bulb, with GFP expression found throughout the central brain region and in the lobular plate. However, spread does appear to be happening in the medulla, with only a small amount of GFP signal present in this area that does not co-localise with Tau. This spread is modified by the co-expression of neuronal activity modulating mutants supporting the observation that the Tau signal in the medulla is actual spread. The co-expression of these mutants resulted in changes to both area coverage of Tau and its phosphorylation state. Future work should aim to identify more specific drivers from which to express Tau from, with these drivers it would be possible to delve deeper into the mechanisms underlying the effect of neuronal excitation on Tau spread. It would also be possible to investigate the impact of other co-factors and morbidities on Tau spread.

5.1 Introduction

The primary aim of this thesis is to develop a *Drosophila*-based model to study Tau spread. In creating such a model, it will be possible to take advantage of the flies' well-understood anatomy and wide range of genetic tools to probe further the unknown mechanisms involved in Tau spread in-vivo, in both a physiological and pathological context.

This chapter addresses the 2nd aim of this thesis; to simulate Tau spread in a large number of olfactory neurons in-vivo by utilising insights gained in previous chapters and applying them to the Orco Gal4 driver, which is expressed in all olfactory receptor neurons. This chapter also addresses this thesis's 3rd aim: to validate the model by utilising neuronal activity mutants to modulate the suspected spread observed from Orco-expressing neurons.

5.1.1 Orco; a larger number of neurons

The outcome of the previous chapter suggested the possibility of Tau spreading into neighbouring glomeruli when the UAS.mCherryTau^{ON4R} is expressed in the Or88a neurons. In the present chapter, a larger number of neurons comprising all olfactory receptor neurons is used to model Tau spread. This aims to express Tau within the circuitry that is amenable to spread beyond the olfactory bulb.

Orco was chosen for this purpose for several reasons. It is a co-receptor expressed in all olfactory neurons and has been used to model the spread of the mutant Htt protein, as previously discussed (Babcock and Ganetzky 2015). Orco-expressing neurons have been well-characterised in experiments investigating olfactory function in *Drosophila*, providing many opportunities for physiological manipulations (Schneider, Ruppert et al. 2012, Ronderos, Lin et al. 2014, Task, Lin et al. 2022). Importantly for this model, Orco's downstream connections are well known, having been mapped with fluorescent staining (Talay, Richman et al. 2017) and an established connectome (Scheffer and Meinertzhagen 2019). Fluorescent staining provides a clear pathway of downstream connections in the *Drosophila* brain, marking cell bodies around the antennal lobe and projecting axons into the lateral horn, mushroom bodies and the prow of the fly brain. These all receive input from Orco-expressing neurons, totalling around 182 post-synaptic neurons in each hemisphere in male flies (Talay, Richman et al. 2017).

5.1.2 The uncertain mechanisms of trans-synaptic Tau spread

Understanding downstream connections of Orco is important in modelling AD as Tau is theorized to spread trans-synaptically between connected regions in prion-like propagation. This has been evidenced in many prior studies, (Braak and Braak 1991, Duyckaerts, Uchihara et al.

1997, de Calignon, Polydoro et al. 2012, Sanders, Kaufman et al. 2014), The mechanisms of this trans-synaptic spread remain unclear, with evidence that the synaptic release of Tau occurs in both vesicle-mediated and free forms (Saman, Kim et al. 2012, Dujardin, Bégard et al. 2014). Whilst the mechanisms remain unknown, there is evidence that suggests Tau release increases with increased neuronal activity (Pooler, Phillips et al. 2013, Yamada, Holth et al. 2014, Wu, Hussaini et al. 2016). *Drosophila* is well suited to investigating the effects of neuronal excitation with mutants that affect neuronal activity readily available (Hodge 2009). Alternatively, known odorants can stimulate activity in a physiological manner (Schneider, Ruppert et al. 2012, Ronderos, Lin et al. 2014, Task, Lin et al. 2022). However, whilst more physiologically relevant external variables can be more challenging to regulate, further insights into the effects of Tau spread on neuronal excitation can be obtained through electrophysiological studies. These can provide a deeper understanding of the events affecting Tau spread and the consequences of Tau spread on downstream connections (Mershin, Pavlopoulos et al. 2004, Bykhovskaia and Vasin 2017).

A deeper understanding of the mechanisms of Tau spread is crucial for therapeutic design but also for the field's understanding of the disease itself, where increased neuronal activity is clinically observed very early on in AD, before neuronal hypoactivity and neuronal death (Bassett, Yousem et al. 2006, Filippini, MacIntosh et al. 2009). The other essential protein in AD, A β , has a potential link to this; increased neuronal activity has been reported near A β plaques both clinically (Busche, Eichhoff et al. 2008, Busche, Chen et al. 2012) and in cell and mouse models (Busche, Chen et al. 2012, Ghatak, Dolatabadi et al. 2019). Therefore, A β may cause the hyperexcitation of neurons, leading to greater Tau release.

To test the effects of the neuronal environment, this chapter characterises Orco-driven mCherryTau^{ON4R} before crossing in mutations that affect neuronal activity.

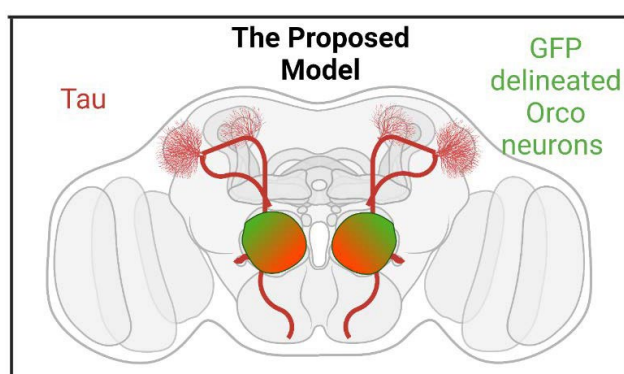


Figure 21 Diagram of the proposed model in which to simulate Tau spread in a large number of neurons.

Expression of mCherryTau^{ON4R} within the ~2000 Orco neurons (shown in black green) will create a system in which to simulate Tau spread between the olfactory neurons and downstream tissues into which Tau may spread (red). The lack of GFP in these downstream tissues will confirm that this is spread, and not expression.

5.2 Aims and hypothesis

Aim 1: To simulate Tau spread, in-vivo, in a large number of neurons

Objectives:

1. To express the mCherryTau^{ON4R} construct in the large number of neurons expressing Orco

By expressing the mCherryTau^{ON4R} construct alongside cd8::GFP within the Orco neuronal circuitry, spread into amenable downstream connections will be identified by the presence of mCherry and absence of GFP in downstream neurons. The resulting model would use a time course to observe the rate of Tau spread from the olfactory neurons, giving a system which can then be manipulated to ask questions about spread.

2. To clarify the consequences of Tau expression.

This will be investigated using a longevity assay to understand the overall effect on the flies' lifespan. By comparing the longevity of the UAS.mCherryTau^{ON4R} fly with the Orco-driven mCherryTau^{ON4R} fly the toxicity, or lack thereof, of driven Tau expression can be compared with that of the leakage of the UAS.mCherryTau^{ON4R} construct, as seen in the results in the previous chapter.

Aim 2: To validate the above models by utilising known modulators of spread

Objectives:

1. To express a neuronal activity-modulating mutation to observe effects on potential Tau spread

The expression of a neuronal modulating mutation should influence Tau spread, as suggested by prior Tau research. If Tau spread is genuine, then the introduction of modulating factors should lead to a change in Tau spread. If introducing these factors fails to change the observed 'spread', then the origin of that Tau signal is more likely to be a miss-expression. It is hypothesised that hyper excitability mutants will increase Tau spread, whilst hypo excitability mutants will decrease Tau spread.

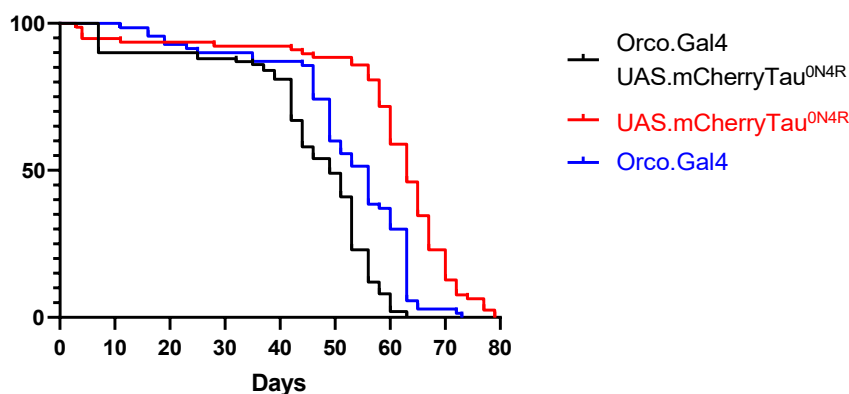
5.3 Results

5.3.1 Unpicking the consequences of ectopic Tau expression and driven Tau expression on fly lifespan

To establish if the baseline leakage of the UAS.mCherryTau^{ON4R} transgene, as seen in Chapter 4, is of a higher detriment than the Orco.Gal4-driven transgene, a longevity assay was used to determine if leakage of the transgene results in a more toxic phenotype than just the driven transgene alone. This is important to unpick the effects of driven Tau expression from the baseline leakage. Figure 22 shows a significant difference in the lifespans of each parent line and the offspring where Tau is driven (LogLog- rank, Mantel-Cox test $p < 0.0001$). The median lifespan of Orco.Gal4-driven UAS.mCherryTau^{ON4R} flies were 49 days, whilst the median lifespan of the UAS.mCherryTau^{ON4R} flies was 63 days. Suggesting the background leak of Tau observed in previous sections from the UAS-only fly is not as toxic as targeted expression. Interestingly, the Orco.Gal4 driver was found to have toxicity, resulting in a lower median lifespan of 56 days. This suggests a component of the toxicity, and therefore reduced lifespan in the driven flies, results from the driver itself.

However, the driven UAS.mCherryTau^{ON4R} still has the shortest survival curve, suggesting Tau expression has an effect beyond the Orco.Gal4 toxicity.

Survival proportions of the ORCO.Gal4 UAS.mCherryTau^{ON4R} fly and its parent genotypes



	Orco.Gal4 UAS.mCherryTau ^{ON4R}	UAS.mCherryTau ^{ON4R}	Orco.Gal4
Median survival	49	63	56

Figure 22: Longevity assay of the Orco.Gal4-driven UAS.mCherryTau^{ON4R} offspring and its parent genotypes Orco.Gal4 and UAS.mCherryTau^{ON4R}

Survival curve for Orco.Gal4-driven UAS.mCherryTau^{ON4R}, Orco. Gal4 and UAS.mCherryTau^{ON4R} (n=100) showed a significant difference in lifespan between the three genotypes (LogLog-rank, Mantel-Cox test $p < 0.0001$). The shortest lifespan is in the ORCO.Gal4-driven UAS.mCherryTau^{ON4R} flies, with the median survival of flies 49 days, versus the UAS.mCherryTau^{ON4R}, where the median survival of flies was 63 days. The longevity of Orco.Gal4 flies are between the other two genotypes, with the median being 56 days.

5.3.2 Spread of Tau from the large number of Orco neurons

To ensure that a non-specific driver line is not the cause of the Tau spread, an Orco.Gal4 and UAS.mCherryTau^{ON4R} recombinant fly was crossed with UAS.cd8::GFP to identify all Orco-expressing neurons, including those beyond the targeted region (diagrammatised in Figure 23 A). In this recombined fly, staining against both GFP and mCherry showed that the expression of both GFP and mCherry appears substantial, with both being clearly visible at zero days (Figure 23 B II and III). Looking at the whole brain, the distribution of mCherry signal has also spread further than expected at this early time point, with the GFP signal appearing in the prow, AMMC and beyond into the optic region, with several cell bodies within the lobular plate. All GFP-positive tracts and cell bodies appear to co-localise with the mCherry signal, as seen in the overlay of the two channels (Figure 23 B IV). At 7 days, the cd8::GFP signal in the lobular is localised to the tracts rather than cell bodies (Figure 23 B VII). This wide distribution of GFP signal beyond the olfactory bulb is indicative of the x-linked Orco.Gal4 driver expressing beyond the expected sites in the olfactory bulb. This also suggests that much of the mCherry signal in the central brain region and lobular results from expression by the non-specific Orco driver, even if this expression is transient like in the lobular cell bodies.

Despite this non-specific leak, a number of tracts, particularly those projecting into the medulla, are only mCherry positive (Figure 23 B VIII arrow). With time, more mCherry signal appears in the medulla, as does cd8::GFP. However, the two signals rarely overlap (Figure 23 B XII). There appears to be no difference in the cd8::GFP signal across the entire time course (Figure 23 C). However, at 14 days, the cd8::GFP signal remains similarly distributed but with more GFP-positive cell bodies in the medulla. Importantly few of these co-localise with mCherry, and no significant increase in GFP signal over 14 days is observed across the whole brain ($F_{(2,6)} = 0.5992$, $p = 0.591$). This suggests that spread may still occur into the medulla with time due to the lack of co-localisation of mCherry with cd8::GFP and the increasing mCherry signal in this region.

In this work not only potential spread was investigated, but also the disease relevance of the Tau species present. AT8 staining can be seen at an early time point, matching much of the mCherry signal but not in the outer reaches of the eye (Figure 23 I). However, by seven days, a small amount of AT8 signal can now be detected in the medulla and in a greater number of optic nerves within the lobular (Figure 23 V arrow head). However, when quantifying the area coverage, no significant change in the AT8 signal was observed across the entire time course ($F_{(2,6)} = 1.326$, $p = 0.333$). This may be due to most of the area coverage coming from the glomeruli. An enlargement of the glomeruli due to sample preparations may occlude subtler changes in the olfactory bulb, as may be the case at 7 days where the glomeruli appear to have a different shape to 0 and 14 days. In contrast, mCherry signal is also significantly increased in the fly brain ($F_{(2,6)}$

=63.85, $p < 0.001$) between 0 and 7 days, covering large regions of the central brain and more tracts in the lobular and medulla. The mCherry signal now covers almost all of the optic and lower brain regions, with several tracts also present in the higher brain regions, although these stain for AT8, unlike much of the rest of the mCherry positive regions. This suggests that the majority of the Tau in the system is not AT8 positive, especially considering the lower total area coverage found for AT8 compared to Tau (Figure 23 C).

Orco.Gal4 ; UAS.mCherryTau^{ON4R} / UAS.cd8::GFP ; +/+

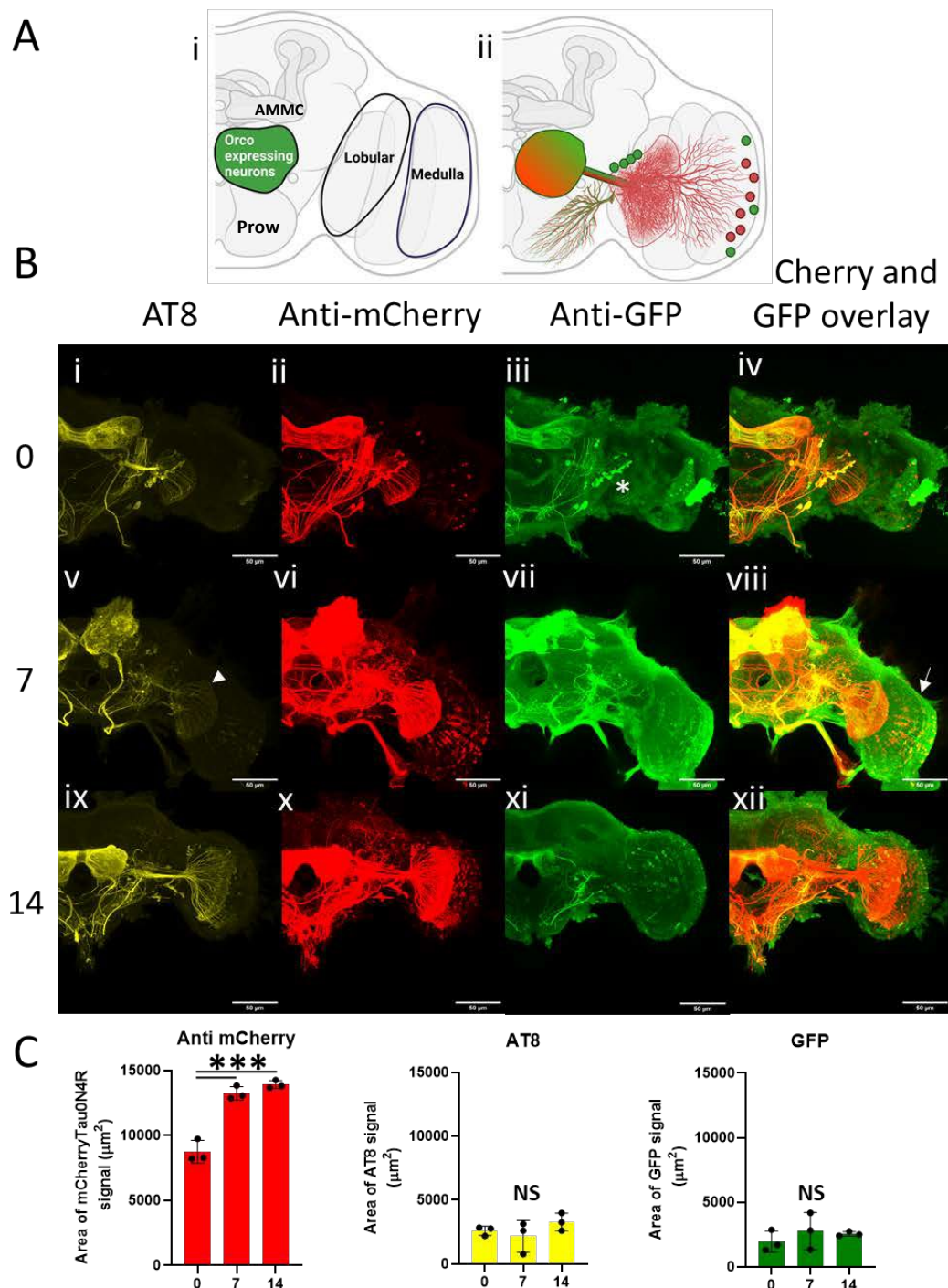


Figure 23 Orco.Gal4 driving expression of both UAS.mCherryTau^{ON4R} and UAS.cd8::GFP at 25°C over a two-week time course. Fly brains stained with anti-GFP, anti-mCherry and AT8 antibodies.

A i shows the theorized expression site of Orco.Gal4 in the olfactory neurons (green), as well as delineating the optical regions, whilst Figure A ii diagrammatizes the regions of Orco expression that were observed in this work (green) as well as the areas where Tau was observed (red). **Figure B (iii, vii, xi)** shows that Orco expression beyond the expected area does not always overlap with mCherry signal, which can often be found outside these regions (**iv, viii, xii**). However, there is overlap in the lobular,

particularly at day 0 (*) where GFP can be seen in the cell body of LC neurons, although not in their dendrites. The coverage of mCherry signal increases with time, particularly into the medulla. This is reflected in Figure C where a significant increase in the mCherry signal coverage occurs between 0 and 7 days ($n=3$ $p < 0.001$). There is no significant difference in the total coverage of AT8 and cd8::GFP signal however ($n=3$, $p = 0.561$ and $p = 0.293$), despite the appearance of AT8 staining in the medulla with time in **Figure B (I, IV, IX)** where no GFP signal is detected, suggesting that some of the spreading Tau may be hyperphosphorylated. Images were taken on a Leica SP8 confocal microscope with a 63x oil objective. Scale bar = 50 μ m

5.3.3 Spread of Tau from the large number of Orco neurons, focusing on the medulla region

As the medulla was identified as the most likely location of Tau spread due to it having many mCherry tracts that are not also GFP positive (Figure 22 A & B), further analysis was carried out focusing on this area. Focusing on a smaller region potentially reduces noise from the Orco driver, which was found to be expressing Tau beyond the expected sites in the olfactory bulb, by looking at the area coverage of mCherryTau^{ON4R} and cd8::GFP. A similar pattern of increasing mCherryTau^{ON4R} signal with time is observed in this analysis. Although in the medulla, a significant increase in mCherry Tau does not occur until 14 days ($p < 0.001$) compared with the whole brain analysis in Figure 22 that identified a significant increase at 7 days. A similar pattern is observed with the cd8::GFP coverage, showing a significant increase between 0 and 14 days ($p = 0.013$). However, the microscope images present little-to-no overlap of cd8::GFP with the mCherry signal, suggesting that most of the mCherry signal is independent of the cd8::GFP (Figure 24). Therefore, the mCherry signal in those neurons is not a result of expression from the driver and, therefore may be a product of Tau spread.

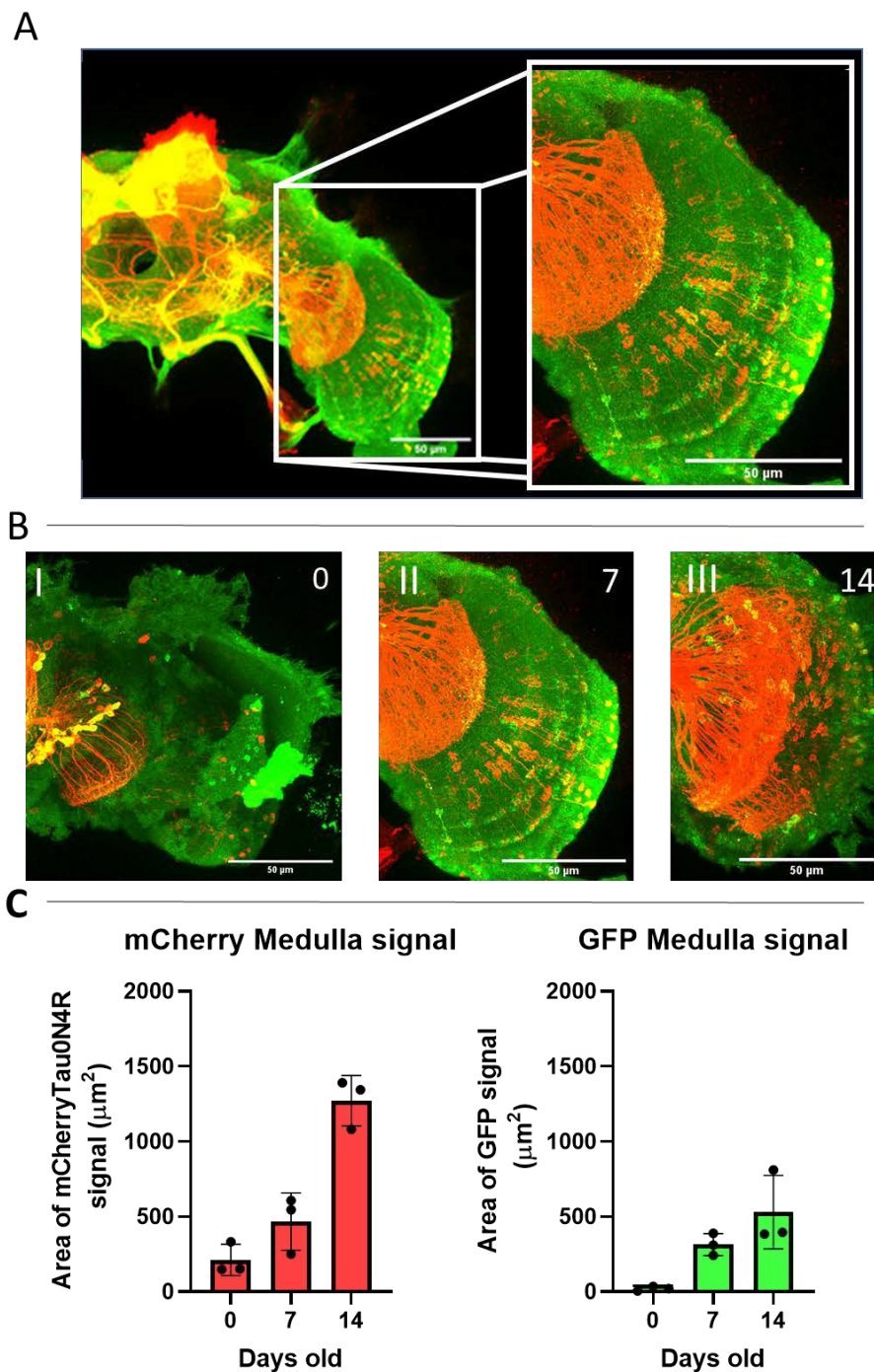


Figure 24 Analysis of signal in the medulla in the brains from Figure 23

- A)** A magnified region of the lobular and medulla from Figure 22 at 7 days.
- B)** Representative images of this region across the three time points tested. At each time point it can be seen that the majority of Tau and GFP do not co-localise in the medulla, suggesting that the signal here is not due to it being driven.
- C)** Analysis of these regions, excluding the lobular, for mCherry and cd8::GFP ($n=3$). For both mCherry and cd8::GFP a significant increase is observed between 0 and 14 days ($p = 0.0004$ and $p = 0.0128$). Images were taken on a Leica SP8 confocal microscope with a 63x oil objective. Scale bar = 50μm

5.3.4 Effect of neuronal hyperactivity on Tau spread and phosphorylation across the whole brain

Despite the recombinant flies examined in Figure 23 revealing that the Orco driver expression is not as specific as initially thought, mCherryTau^{ON4R} can still be detected outside of GFP-positive neurons, suggesting that spread may be occurring. To test if spread is occurring, it was investigated whether this spread could be modulated. As changes to the amount of spread by mutations affecting potential mechanisms of Tau spread, would further support the observations that spread in the medulla is real spread rather than tau expression due to the increased area of ORCO expression or leak of the UAS.Tau transgene. Increased neuronal firing in other models results in greater Tau spread and less Tau phosphorylation. Expressing mutant proteins that recreate increased neuronal firing to the *Drosophila* model could identify if the spread is indeed occurring, as increased spread could be recapitulated in the fly.

UAS-eag.DN.EKI, expresses a truncated eag potassium channel protein which results in neuronal hyperexcitability. This mutated protein has previously resulted in increased neuronal firing in Orco neurons (Hodge 2009). As this mutation is also on the 2nd chromosome, GFP co-expression could not be used in these experiments. Figure 25 demonstrates the expression of mCherryTau^{ON4R} and levels of AT8 in animals expressing UAS-eagDN. When comparing the total area covered by mCherry Tau^{ON4R} and AT8 signal (Figure 25 B & C), a similar pattern to Figure 23 C emerges, with an increase in the area of mCherry signal between 0 and 7 days ($F_{3,7} = 9.122$, $p = 0.0081$). This is reflected in Figure 25 A with an apparent increased signal in the medulla. This increase in mCherry signal occurs at an earlier time point than the brain in Figure 22 where the neuronal firing was not affected and is therefore suggestive of increased spread. This shows that increased neuronal firing in Tau expressing neurons leads to an increased area of spread at early time points compared to Figure 23.

Also investigated was the phosphorylation state of Tau present, throughout the 14-day time course, a low level of AT8 staining is seen, which presents no significant change with time (Figure 25 C; $F_{3,7} = 0.8149$, $p = 0.5252$). However, analysis of the medulla singularly shows an increase of mCherry signal between 0 and 7 days, suggestive of an increased level of spread. As there was no corresponding increase in AT8 signalling. If there is real spread here, then the spreading species may not be hyperphosphorylated.

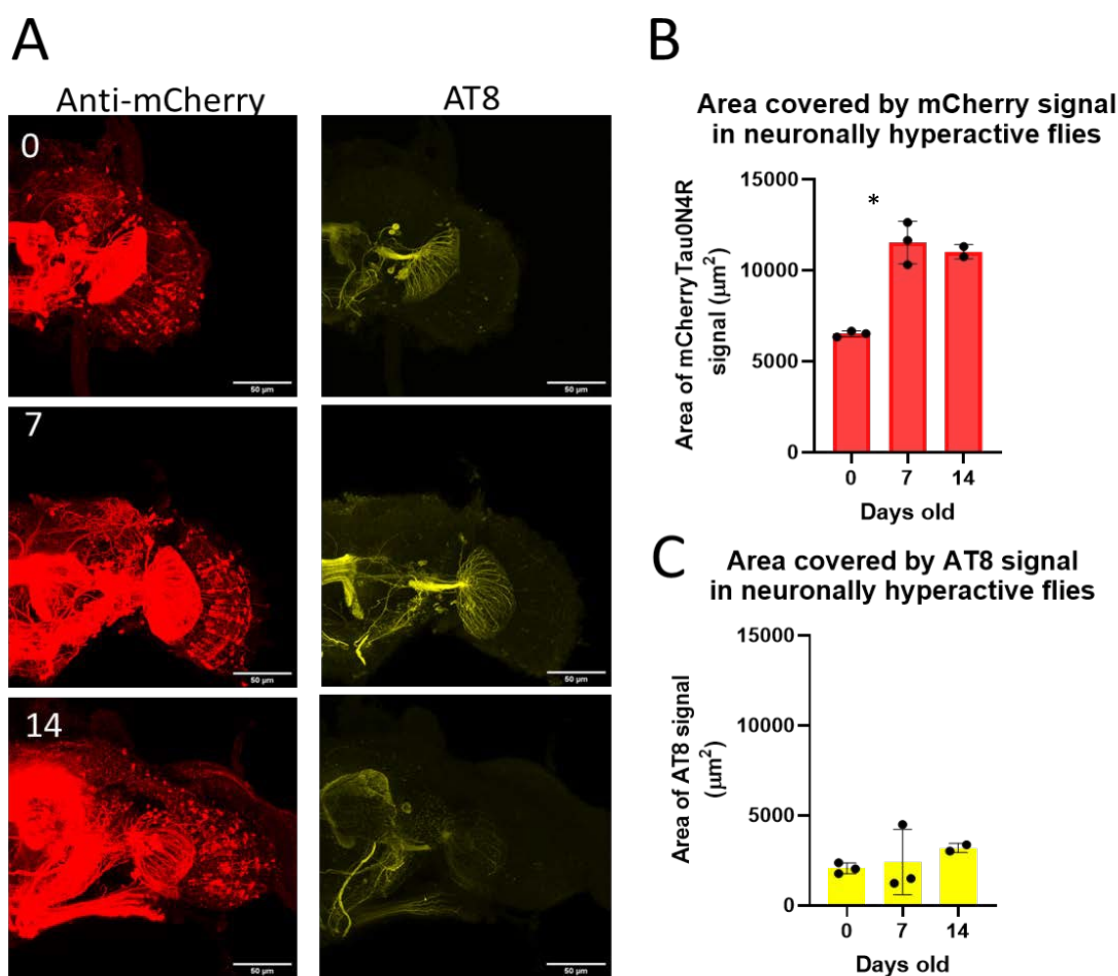


Figure 25 Orco.Gal4 driving mCherryTau^{ON4R} and the hyperactivity mutant Kir2.1 in Orco- expressing neurons at 25°C, stained with anti-mCherry and AT8

A) When the neuronal hyperactivity mutant is crossed into these flies anti-mCherry staining is extensive throughout the brain and eyes from 0 days (red). The amount of anti-mCherry staining increases with time, particularly in the medulla at 7 and 14 days. However, the intensity in the lobular is higher, even at zero days, than in Figure 23, although it appears less at 14. AT8 signal (yellow) appears absent in the medulla.

B) The total area covered by mCherry signal and AT8 in these neuronally-hyperactive flies shows an increase in mCherry signal between 0 and 7 days (shown by the *) ($n=3$ $F=9.122$, $p = 0.0081$), whilst AT8 signal remains constant (20 C). However, the distribution of the mCherry signal differs to previous observations, with more signal being present in the medulla.

Images were taken on a Leica SP8 confocal microscope with a 63x oil objective. Scale bar = 50µm

5.3.5 Effect of neuronal hypoactivity on Tau spread and phosphorylation across all Orco-expressing neurons

A neuronal hypoactive mutation was introduced to confirm the effects of decreased neuronal activity, by expressing the inwardly rectifying potassium channel Kir2.1. This potassium channel localized neurons were used to reduce neuronal activity in Orco-expressing neurons. When this mutated protein is crossed into the fly's genome in place of the hyperactive mutation, differences in the pattern and coverage of AT8 and mCherry are observed (Figure 26).

The AT8 signal detected is low at 0 days but rapidly increases at 7 and 14 days and corresponds with most of the mCherry signal (Figure 26 A and C). The intensity of the AT8 signal appears very strong at the later time points and, given its greater coverage than observed in previous experiments (Figure 23, Figure 25), suggests that a greater proportion of the mCherryTau^{ON4R} population is phosphorylated.

The AT8 coverage in the mutant fly increases gradually across the 0, 7 and 14 days (Figure 26 C). This pattern differs from prior results as there is no sudden increase at a single time point. Instead, a more graduated increase appears, primarily due to increases in AT8 in the region surrounding the olfactory bulb . rather than the increased signal in the medulla observed previously. This may be due to increased local spread but could be due to a potential differences in the tissue morphology caused during preparation of the brain,. Regardless, it is clear that there is a significant increase in the AT8 signal when the Orco neurons are hypoactive.

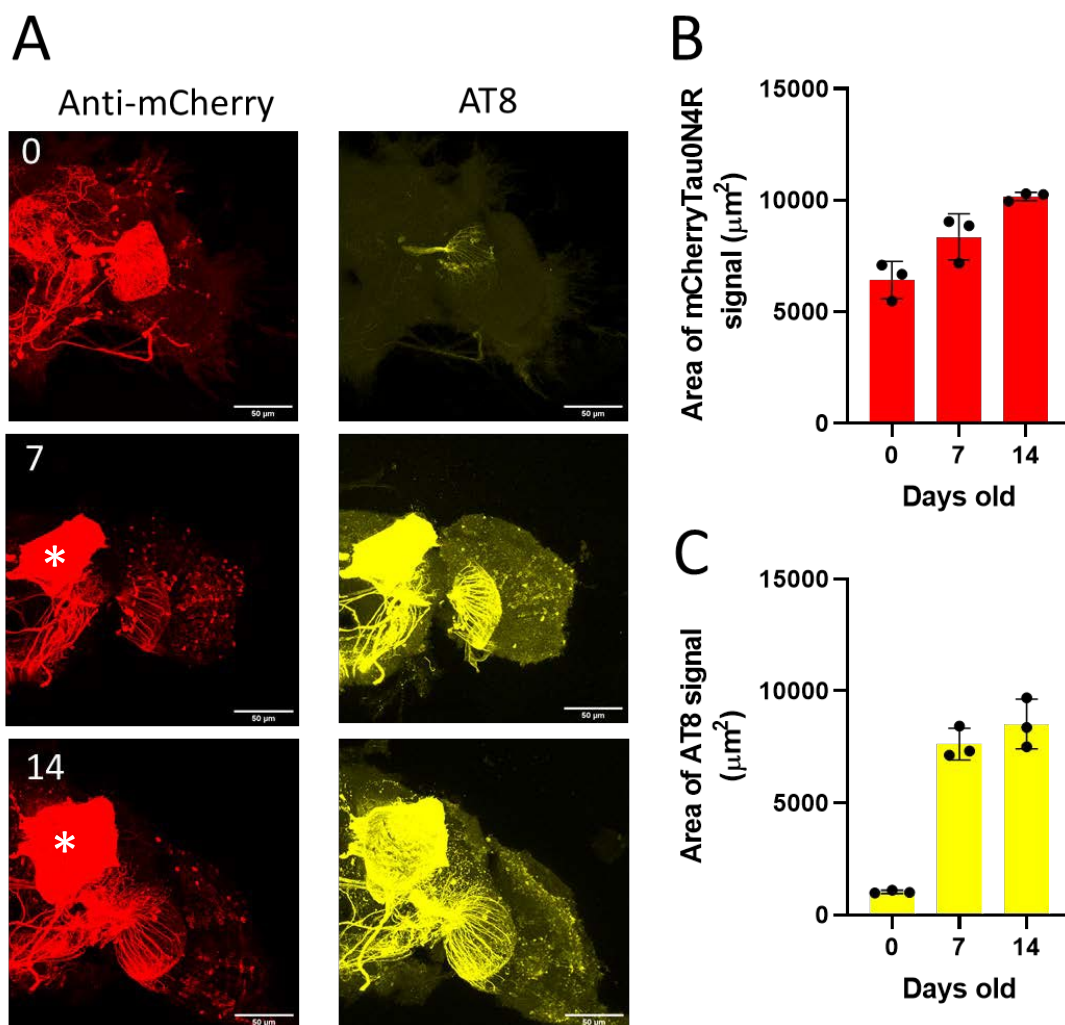


Figure 26 Orco.Gal4 driving mCherryTau^{0N4R} and the hypo-active mutant NaV1.1 in Orco expressing neurons at 25°C, stained with anti-mCherry and AT8

The expression of the hypoactive mutation results, initially, in a lower coverage of AT8-stained phosphorylated Tau at 0 days (n=3 yellow). This staining appears to have rapidly increased at 7 and 14 days, demonstrating that the majority of Tau in mCherry-positive regions (red) is phosphorylated at the key disease sites (**A**, **C**). The increase in mCherry coverage is more gradual than in prior experiments, with the area surrounding the olfactory bulb(*) increasing in signal with time as opposed to the medulla, whose signal remains fairly consistent throughout.

Images were taken on a Leica SP8 confocal microscope with a 63x oil objective. Scale bar = 50 μm

5.3.6 Comparing the effects of neuronal hypoactivity and hyperactivity on Tau spread and phosphorylation across the brain

To further clarify the effects of the neuronal modulating mutations on Tau spread and phosphorylation, a two-way ANOVA was used to compare the areas of Tau and AT8 coverage of each mutant and the brains from Figure 23. By placing the quantifications of the previous two neuronal modulating flies alongside that of the unmodulated Orco, mCherryTau^{ON4R} recombinant GFP cross of Figure 23 comparisons on the area coverage of mCherry and AT8 signal between the genotypes and at each time point can be made.

A two-way ANOVA was performed to analyse the effect of time and neuronal modulation on the area coverage of the mCherry Tau^{ON4R} signal. A statistically significant interaction between the effects of time and neuronal modulation was observed ($F_{(4, 11)} = 7.445, p = 0.004$). Simple main effects analysis showed that time ($p < 0.001$) and neuronal modulation ($p < 0.001$) both have a statistically significant effect on the area coverage of the mCherry signal. Further mixed-effects analysis comparing flies with the hypoactive and hyperactive mutations with the unmodulated flies from Figure 22 at each time point shows a significant effect for the hypoactive mutation at 0, 7 and 14 days ($p = 0.048, p = 0.009$ and $p < 0.001$ respectively). However, for the hyperactive mutant, only at day 14, a significant difference to the unmodulated flies was recorded ($p = 0.026$).

These results suggest that both the hyper- and hypoactive mutations affected the mCherryTau^{ON4R} coverage. For hypoactive individuals, area coverage when compared to the unmodulated brains was reduced at all-time points, suggesting consistently less spread over time. This data suggests that both the hyper and hypo modulators of neuronal activity reduces mCherryTau^{ON4R} coverage, compared to the unmodulated brains, but localised of the hypoactivity mutation decreases this coverage to a greater extent.

To understand how these neuronal activity-modulating mutations affect Tau hyperphosphorylation a two-way ANOVA was used to analyse the effect of time and neuronal modulation on the area coverage of the AT8 signal. It was revealed that there is a statistically significant interaction between time and neuronal modulation on the AT8 signal ($F_{(4, 17)} = 16.95, p < 0.001$). Simple main effects analysis showed that both time ($p < 0.001$) and neuronal modulation ($p < 0.001$) significantly affects the area coverage of the AT8 signal. Further mixed-effects analysis comparing flies with the hypo- and hyperactive mutations to unmodulated flies at each time point shows a significant effect for hypopolarising at 0, 7 and 14 days ($p = 0.0214, p = 0.0100$ and $p = 0.0071$ respectively) leading to an increase of AT8 signal in the hypopolarised flies when compared to the unmodulated controls. For localised mutants, no significant difference was found in comparison to the unmodulated genotype was recorded at 0, 7 and 14 days ($p = 0.1856,$

$p = 0.9742$ and $p = 0.9705$ respectively).

These results suggest that both the hyper- and hypoactive mutations influenced AT8 coverage and therefore Tau hyperphosphorylation. For the hypoactive mutants this resulted in a significant increase in AT8 staining at all-time points, suggesting much more of the Tau in the hypoactive flies is hyperphosphorylated. Conversely, no increase or decrease was observed in AT8 coverage in the neuronally hyperactive flies. This suggests that Tau phosphorylation is not a requirement for Tau spread, as an increase in phosphorylation was associated with decreased Tau spread.

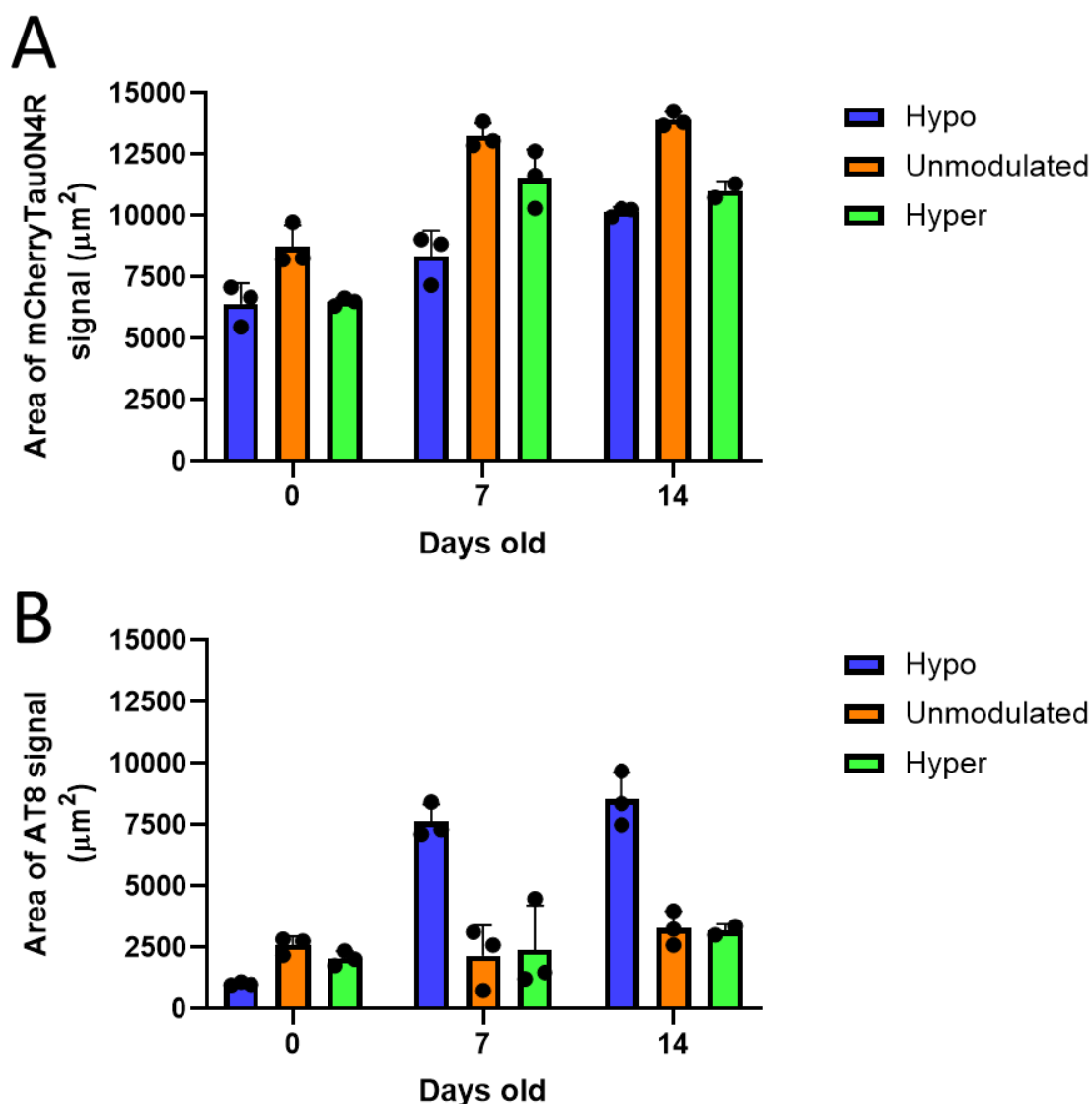


Figure 27: Quantification of AT8 and mCherry coverage in Orco.Gal4UAS.mCherryTau0N4R recombinant flies with either a neuronal hyper- or hypoactive mutation compared with the recombinant line without any neuronal modulation at 25°C.

An increase in the mCherry coverage with time is observed across all genotypes (n=3), however at each time point the neuronal hypoactivity mutant has less coverage than the unmodulated flies ($p=0.0482$, $p=0.009$ and $p<0.001$). Whilst a significant difference between the hyper and the unmodulated did not occur until 14 days ($p=0.0261$) (A). AT8 coverage was significantly increased in the hypoactive mutants compared to the unmodulated at all-time points ($p=0.0214$, $p=0.0100$ and $p=0.0071$) but no significant difference was observed when comparing the hyperactive mutants with the control (B).

5.3.7 Comparing the effects of neuronal hypo- and hyperactivity on Tau spread and phosphorylation in the medulla.

Previous sections of this chapter have identified that the most likely location for Tau spread is to be into the medulla. To further clarify the effects of these neuronal modulating mutations, a two-way ANOVA was used to compare the quantifications of mCherry and AT8 coverage in each mutant and the brains from Figure 25. This analysis focused on the medulla as the area where spread is most likely to be occurring. When analysing the medulla solely, excluding the lobular, as seen in 30, it can be observed that the coverage of mCherry in the medulla increases with time across all genotypes, although by differing amounts. The most significant differences appear at 7 days, as shown in Figure 30 A. Images at the 7 day time point show the mCherry and AT8 channels overlaid. The hyperexcitability mutant appears to have a high density of neurons that are mCherry positive in the medulla compared with the unmodulated background, whilst the hypo excitability mutant AT8 staining is much more intense than the unmodulated fly in Figure 29 and co-localises with much of the mCherry signal (Figure 30).

For mCherry coverage, a two-way ANOVA was performed to analyse the effect of time and neuronal modulation on the area coverage of the mCherry signal in the medulla. This revealed a statistically significant interaction between the effects of time and neuronal modulation ($F_{(4, 11)} = 8.282, p = 0.003$). Simple main effects analysis showed that both time ($p < 0.001$) and neuronal modulation ($p=0.003$) individually have a statistically significant effect on the area coverage of the mCherry signal. Further mixed-effects analysis comparing hypo- and hypermutants with the unmodulated flies at each time point showed a significant effect for hyper excitable mutants only at 7 days ($p = 0.033$). No significant difference was recorded between any of the other time points and the hypo-polarising mutant fly. In each case, this may be due to the more stringent test conditions used in the mixed-effect analysis, resulting in a lack of significance despite the ANOVA finding a significant effect from the presence of neuronal modulating mutants. This data still shows a significant increase in mCherryTau^{ON4R} coverage in the hyperactive fly for a single time point, but not in the hypoactive fly, in the medulla where spread is thought to be occurring. This is a polar opposite to the previous sections' findings when looking at the whole brain. Spread is believed to be occurring in the medulla, due to the lack of GFP signal observed in Figure 23, which would otherwise indicate that the Tau in this region is the result of expression, but not in the whole brain where GFP signal in Figure 22, indicates that this Tau is the result of expression. This observation of a significant increase in mCherryTau^{ON4R} coverage in the medulla appears to be the more relevant finding for investigating to spread.

For AT8 staining, a two-way ANOVA was performed to analyse the effect of time and neuronal modulation on the area coverage of the AT8 signal in the medulla. A statistically significant interaction

between the effects of time and neuronal modulation was seen ($F_{(4, 11)} = 6.443, p = 0.0064$). Simple main effects analysis showed that time ($p = 0.0010$) and neuronal modulation ($p = 0.0090$). Both separately have a statistically significant effect on the area coverage of the mCherry signal. Further mixed-effects analysis comparing hypo- and hypermutants with the unmodulated flies at each time point did not show a significant effect for either the hypo- or hyperpolarising mutant despite the ANOVA showing a significant effect of genotype on time. The results of the two-way ANOVA do show that the expression of a hyper- or hypopolarising mutant have an effect on the AT8 staining in the medulla of the fly brain. With Hyper active mutations appearing to have a decrease compared to the unmodulated and Hypoactive mutations causing an increase in AT8 staining, however further insights are limited by the more stringent mixed effect analysis.

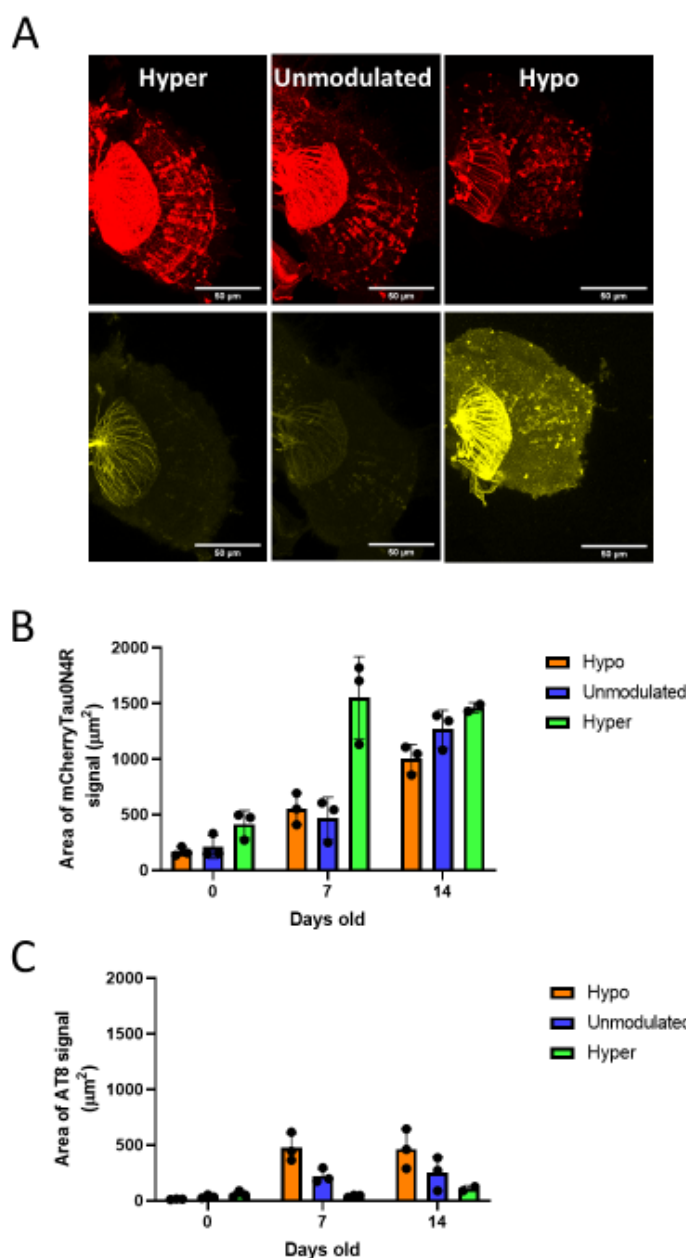


Figure 28: Quantification of AT8 and mCherry coverage in the medulla of Orco.Gal4 UAS.mCherryTau^{ON4R} recombinant flies crossed with either a neuronal hyper or hypoactive mutant compared with the recombinant line crossed with an unmodulated fly at 25°C (n=3)

Figure A shows the medulla of each of the genotypes at 7 days old. Here the largest differences can be seen, with extensive mCherry (red) coverage in the hyper-excitability flies and an intense and high coverage of AT8 staining (yellow) in the hypo-excitability fly when compared to the unmodulated. An increase in mCherry signal is observed with time, although varying based on the genotype ($F(4,11)=8.282$, $p=0.0025$). Mixed effect analysis showed a significant difference between the Hyper mutant and unmodulated at 7 days ($p=0.0330$) but not at other timepoints nor genotypes (B). Similarly AT8 staining increases with time, with the coverage differing between genotypes ($F(4,11)=6.443$, $p=0.0064$) however no significant difference is observed between genotypes at each timepoint in mixed effect analysis

5.4 Discussion

5.4.1 Summary

This series of experiments sought to investigate the spread of Tau in *Drosophila*'s large number of olfactory neurons by expressing the mCherryTau^{ON4R} construct in Orco neurons. Having established that Orco- driven UAS.mCherryTau^{ON4R} causes greater toxicity than the transgene by itself, a recombinant fly expressing cd8::GFP and UAS.mCherryTau^{ON4R} was used to delineate the extent of expression of the Orco-expressing neurons and the spread of Tau beyond them. This recombinant fly showed that Orco-expressing neurons extended beyond the olfactory bulb and covered much of the fly brain, deeming this Orco insertion on the x chromosome rather unsuitable for identifying large number of neurons from which to study propagation due to this large amount of expression beyond the expected olfactory neurons . However, Tau is also found within the medulla which increases in concentration with time and co-localises minimally with GFP suggesting that its presence is not due to mis- expression. Furthermore, expressing neuronal modulating mutants in the expressing neurons leads to an increase in Tau spread in the medulla if a hyperexcitable mutation is utilized. In addition, it can increase AT8 phosphorylation in the medulla population of Tau if hypomutants are used. This implies that the Tau in the medulla may be due to spread because the known modulators of spread result in corresponding changes in this population. Expression of Tau using Orco to express in a large number of olfactory neurons, despite leakage and expression beyond the expected olfactory neurons, offers a model in which Tau spread into the medulla can be studied, using genetically controlled modulators of Tau spread.

5.4.2 Orco.Gal4 driven UAS.mCherryTau^{ON4R} spread

5.4.2.1 Understanding the effects of ectopic and driven Tau expression

Due to the leak reported in Chapter 4, each parent line was tested to investigate the consequences that this leak has on the fly's lifespan. Figure 21 demonstrates that flies expressing both the Orco.Gal4 and UAS.mCherryTau^{ON4R} have a reduced lifespan compared to either constituent part in the parent line. Previous Tau research has shown similar results, with the shortening of lifespan seen in flies using Gal4 driven expression of human Tau isoforms 3R and 4R (Folwell, Cowan et al. 2010, Sealey, Vourkou et al. 2017). It is apparent that the Orco-driven Gal4 is toxic to the fly and does represent a component of the decreased longevity, as seen in Figure 22 early studies on Tau in flies have found a genomic response to Gal4 expression, independent of UAS transgenes, on stress and immune response pathways when Gal4 is expressed at high levels

in larval salivary glands (Liu and Lehmann 2008), which may contribute to its' toxicity. When Gal4 is driven using the GMR driver, it has been shown that it alone is capable of causing developmental defects and apoptosis in the eye (Kramer and Staveley 2003). However, a more recent meta-analysis has shown that UAS or Gal4 constructs extend lifespan significantly in w1118 flies (Ziehm, Piper et al. 2013). The w1118 fly was used as the basis for the insertion of our genes of interest for this work, including for UAS and Gal4 components. The results observed in these experiments appear to have many interplays affecting them, with Gal4 and UAS inserts having potentially toxic and protective effects depending on location and concentration. This, alongside background leakage of Tau from the UAS.mCherryTau^{ON4R} fly alone, complicates interpreting results from the fly brain. However, what is clear is that when the Orco.Gal4 and UAS.mCherryTau^{ON4R} are combined in a single fly, the toxic effect is greater than Orco.Gal4 alone, implying that expression of the UAS.mCherryTau^{ON4R} in this system is pathological independent of Gal4 toxicity.

5.4.3 Tau spread from the large number of Orco expressing olfactory neurons in the whole brain compared to the medulla in isolation

The advantage of expressing both cd8::GFP and the mCherryTau^{ON4R} construct within a single fly is that the areas where Tau is expressed are delineated by GFP and so it is possible to see if Tau in an area is the result of expression or spread. In doing so, greater confidence in the origin of that mCherry signal can be gained, identifying if it is the result of expression or spread based on whether the cd8::GFP and Tau co-localise or not.

Figure 23 shows the importance of using such a system as the cd8::GFP signal was detected in the lobula columnar (LC) neuronal cell bodies in the medulla, as shown by the *. Comparable results have been observed in other datasets, showing a similar expression pattern (Wu, Nern et al. 2016). Without the cd8::GFP signal highlighting the leaky expression beyond olfactory bulb spread appears to be occurring outside the known downstream connections mapped with *trans-tango* (Talay, Richman et al. 2017). The *trans-tango* method comprises of a synthetic signaling pathway that is activated upon ligand binding, resulting in expression of a fluorescent reporter. This pathway is expressed pan-neuronally whilst the ligand that activates it is expressed only pre-synaptically, meaning only post-synaptic neurons signaling pathways are activated (Talay, Richman et al. 2017). Whilst this cd8::GFP signal is strongest in the cell bodies, it does appear faintly in the dendrites of the LC neurons where mCherryTau^{ON4R} has been observed at the early time point (Figure 22). Whilst the cd8::GFP signal in the cell bodies appears to be transient and is not present at 7 days, cd8::GFP remains in the axonal projection of the LC neurons as well as with the prow AMMC and VLP. Much of this signal co-localises with mCherry, as can be seen by the orange colouring in the overlay. This shows that the mCherry signal in these regions is due to a

result of miss-expression rather than spread. Taken together with previous controls in Figure 17, and excluding the possibility of Tau spread into the lateral horn, there appears to be a large amount of noise in the system, occluding the possibility of spread in the central brain region and lobula.

However, even at day 0, a population of mCherryTau^{ON4R}-positive cell bodies can be seen in the medulla which does not appear to overlay with the cd8::GFP signal, suggesting that spread may have occurred into these cells. However, the presence of cd8::GFP-positive cells in the medulla complicates the picture by suggesting that there is some miss-expression of the mCherryTau^{ON4R} into these cells and what is observed in Figure 23 may be a leak of either the cd8::GFP or the mCherryTau^{ON4R} transgene. By 7 days, cd8::GFP-positive cell bodies in the medulla are also mCherry positive but the apparent increase in cells only showing mCherry could indicate spread from nearby cells into the medulla. Interestingly, when looking at the brain as a whole, none of the Tau in the medulla is AT8- positive and both this and the area coverage of GFP remains constant whilst the area of mCherry coverage increases, suggesting mCherry spread into new areas but no spread of cd8::GFP. However, when focusing only on the medulla (excluding the lobular regions), as in Figure 24, a significant increase in cd8::GFP signal is reported between 0 and 14 days, suggesting that a temporal change in the expression profile of GAL4 has led to expression in other cells with time. However, the majority of the Tau signal remains separate from this cd8::GFP signal in these images suggesting that its presence in the medulla is not due to miss-expression.

A recent paper also using a *Drosophila* model observed trans-cellular propagation of human Tau aggregates in a similar region. However, the direction of spread in this study followed from the eye toward the brain, using the GMR driver to express Tau species in the retina and measuring the distance from the lamina into the optic lobe over a similar timeframe (Aqsa and Sarkar 2021). This study observed the Tau signal migrating away from the lamina in a time-dependent manner between 5 and 15 days, a similar timeframe to what was observed in this study. However, the measurement of the distance of Tau signal from the medulla is open to confusing Tau distribution with spread along axons, particularly with the physiology of optic neurons. Area coverage of Tau in the optic lobe was also reported to increase with time by this group (Aqsa and Sarkar 2021). This was observed in the present study and better averages Tau spread into neuronal populations, localised the effects of different axonal lengths in the up taking neurons or physical differences resulting from brain preparations. Regardless, the results from this prior work and the present study suggest that the neuronal circuitry in the *Drosophila* eye is amenable to modelling Tau spread with time.

Aqsa and Sarkar also looked at the phosphorylation state of Tau in the system using the antibody AT180, which also showed that the Tau was phosphorylated at early time points. However, these

experiments showed an increase in Tau phosphorylation in spreading species with time, not seen in the present study. Indeed, the paper suggests a relationship between Tau phosphorylation via GSK-3 β and spread (Aqsa and Sarkar 2021). Conversely, Tau phosphorylation in the spreading species with time is not apparent in the present study, where Tau in the medulla is not AT8-positive, whilst much of the rest of the brain is. This suggests that Tau phosphorylation is occurring in neurons where Tau is expressed, but this phosphorylation is not seen in the spreading Tau.

5.4.4 Modulating Tau spread from the large number of Orco expressing neurons, whole brain analysis compared to analysis of the medulla.

Neuronal activity has been shown to effect models of Tau propagation (Pooler, Phillips et al. 2013, Yamada, Holth et al. 2014, Wu, Hussaini et al. 2016). Therefore, by crossing in excitability mutants into the system modulation of any potential spread should be possible. This appears to be the case with the hyperexcitability mutant causing a significant increase in mCherryTau^{ON4R} spread at the 7-day time point (Figure 28). This is in line with previously reported research which identified neuronal hyperexcitability resulting in increased Tau release and uptake in multiple models (Pooler, Phillips et al. 2013, Yamada, Holth et al. 2014, Wu, Hussaini et al. 2016) provides confidence that spread seen in the present study may indeed be occurring in the system. Interestingly, the high AT8 staining in the hypoexcitability mutation further supports Pooler's data by producing an opposite overall effect, in this study neuronal activation, caused the release of de-phosphorylated Tau species (Pooler, Phillips et al. 2013). The amount of phosphorylated Tau increased dramatically in the hypoactive mutant lines, possibly due to the higher dwell time of Tau monomers in the neuron which allows for increased concentrations and therefore aggregation (von Bergen, Barghorn et al. 2005)., The effects of this hypoactive mutant are also interesting given previous work showing that neuronal activation has a protective effect, promoting the clearance of Tau (Mann, Gondard et al. 2018, Akwa, Di Malta et al. 2022). This all suggests that the neuronal environment in which Tau exists plays a role in its pathology, and possibly in its ability to spread.

Conversely, with the hyperactive mutant, Tau phosphorylation does not differ to the unmodulated fly (Figure 23), suggesting no difference in the phosphorylation state of the potentially spreading Tau species. However, low AT8 levels were also seen in the unmodulated fly, suggesting that the spreading Tau under regular neuronal activity was not greatly phosphorylated to begin with in line with other research findings (Pooler, Phillips et al. 2013). The findings of other studies and these highlight the question of whether the spread of Tau between neurons is a purely pathological aspect of Tau or a physiological role hijacked in disease. As discussed in the introduction 1.9.

Further research directions could involve co-expressing A β alongside the recombinant Tau line to compare the effects with hyperexcitability and hypoexcitability mutants. A number of A β ₄₂ expressing flies have been characterized and these flies, combined with this model, would build upon observations of A β 's excitatory effect, as discussed previously, and findings that A β 's presence can accelerate Tau propagation (Pooler, Polydoro et al. 2015). A reduction in neuronal activity can attenuate A β 's catalysing of Tau pathology (Rodriguez, Barrett et al. 2020) while an increase in neuronal activity can rescue A β pathology (Ramirez, Pacheco et al. 2014) suggesting a complex interplay. If, in this model, A β co-expression causes an increase or decrease in Tau spread then introducing the corresponding excitability mutant could rescue this effect, providing mechanistic insights. Unfortunately, the A β line tested for this thesis was found to be contaminated, with genetic material from another fly line and experiments could therefore not continue. However, another aspect of Tau spread was investigated using a genetically expressible tetanus toxin light chain, which is shown to eliminate synaptic transmission in *Drosophila* (Sweeney, Broadie et al. 1995, Cao, Yang et al. 2017). If Tau release is linked to neuronal activation, then a likely mechanism for this is release via synaptic vesicles, as observed in cell models (Pooler, Phillips et al. 2013). Difficulties arose while collecting the progeny of the recombinant fly crossed with the UAS tetanus toxin line due to the expression of another toxic protein within the fly. Due to the high mortality of this line, it was not possible to exclude a survivorship bias as a factor affecting the results. Appendix 8 shows the single time point recovered from these flies at 14 days compared to a control line, consisting of a scrambled primary amino acid sequence of tetanus toxin light chain. No significant differences were seen between the mCherryTau^{ON4R} coverage or AT8 coverage, with almost all of the signal localised within the olfactory bulb. This is in contrast to results by Pooler *et al* results, which found the tetanus toxin to attenuate Tau release, though not remove it entirely (Pooler, Phillips et al. 2013). Given the difficulties in collecting progeny, survivorship bias may be at play or the results may also be due to testing only at the 14-day time. Previous results such as Figure 23 and Figure 25 have shown the largest differences between genotypes at the 7-day time point before a convergence of the area of Tau spread at 14 days, which may also explain the lack of significance if this result followed a similar pattern.

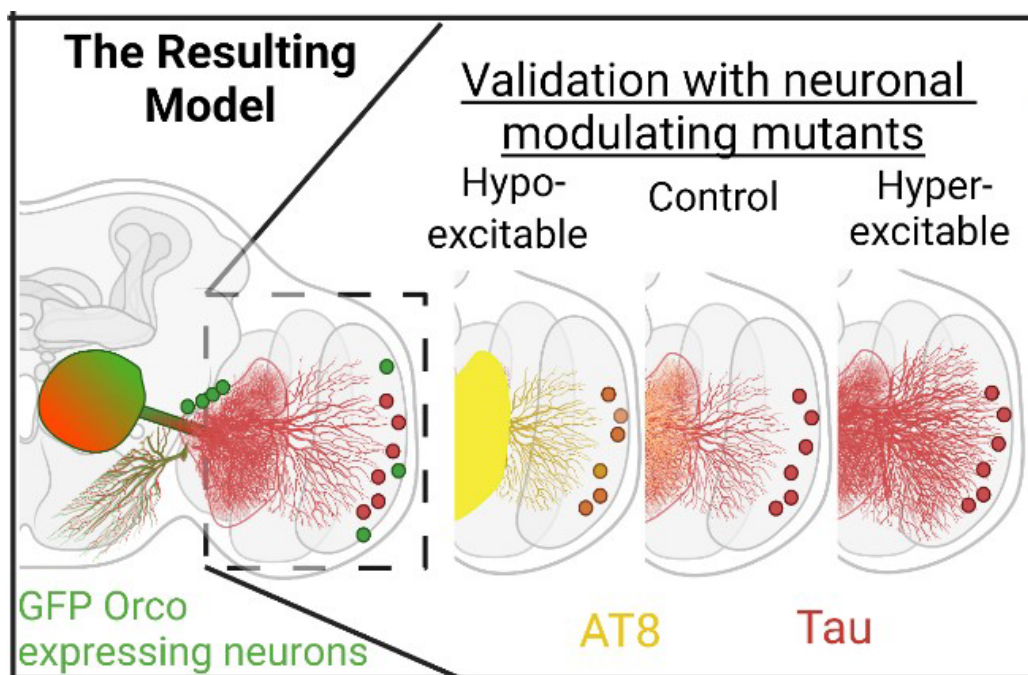


Figure 29 Diagram of the results found in this chapter.

The Orco driver appears to drive expression in additional areas beyond the olfactory neurons, with GFP expression found throughout the central brain region and in the lobula. Spread does appear to be happening however in the medulla, with only a small amount of GFP signal present in the medulla that does not co-localise with Tau. The fact that this is spread is supported by the Tau signal in the medulla is modulateable by the co-expression of neuronal activity modulating mutants. The co-expression of these mutants resulted in changes to both area coverage of Tau and its phosphorylation state

5.4.5 Conclusion and future directions

The evidence presented so far points to evidence that Tau spread may be occurring from the large number of ORCO-expressing olfactory neurons but it is occluded by the non-specific driver expression observed with this driver line. Figure 23 highlights the broad expression profile of both the Gal4 and the UAS construct, which together place uncertainty in results seen throughout the whole brain and lobular. However, evidence of spread is present in the medulla, where neither a UAS construct leak has been observed, nor has Orco-driven GFP expression mapped onto the majority of mCherryTau^{ON4R} detected increased with time. Given that the coverage of this mCherryTau^{ON4R} signal is modulateable using neuronal excitability mutants that have been shown to affect Tau spread, it is not unreasonable to assume Tau spread between cells is occurring. Still, the caveat is that the current system's leakiness prevents precise information from being extracted.

To this end, future work needs to identify clean drivers and insertion sites to cut down the leak of UAS expression and improve the specificity of the GAL4 driver line. Other Orco lines exist, with Orco Gal4 inserted on the 2nd and 3rd Chromosome. However, the 3rd Chromosome insertion of Orco.Gal4 appears to drive expression in projection neurons (see Chapter 6 Figure 34). These should be tested with antibodies against GFP and mCherry (or Tau) to maximise signal collection. This is necessary to identify low-level background expression which, with time, may result in a neuron becoming positive for the respective signal and so giving the appearance of spread. The identification of these specific drivers should occur both in the olfactory system and in other regional promoters, such as LC neurons, which are analogues to the glomeruli system of the olfactory bulb (Wu, Nern et al. 2016).

Another key conclusion, as mentioned previously, is that neuronal activity appears to moderate Tau spread and pathology. Further insights can be gained through the use of a more comprehensive panel of antibodies, such as those against different Tau phosphorylation sites (e.g. AT100) or cell death markers (e.g. DCP-1), to get information on how the change in firing rate and spread affects the toxicity of the Tau construct. Techniques to investigate neurotransmitter release and clearance can also be applied in *Drosophila* to understand any feedback loops from Tau release on neuronal firing. This could unlock insights into the progression from neuronal hyperexcitability to hypoexcitability seen in the advancement of AD (Bassett, Yousem et al. 2006, Filippini, MacIntosh et al. 2009). Furthermore, the many mutants readily available in the fly will allow a deeper dive into precise mechanisms. For example, using tetanus toxin light chain, to prevent neuronal vesicle binding and observe the effect on Tau spread. However, to observe the potentially subtle effects, these experiments need to occur in the cleaner system, as outlined above, to achieve a signal-to-noise ratio that allows for detecting subtle changes. Such a clean

system can also be used to investigate the role of other co-factors and co-morbidities that may affect pathological Tau propagation, such as $A\beta$, age, Diabetes, epilepsy and chronic inflammation. This, in combination with the extensive catalogue of mutants discussed prior, will allow for the mechanisms of the co-factors and morbidities to be dissected in detail.

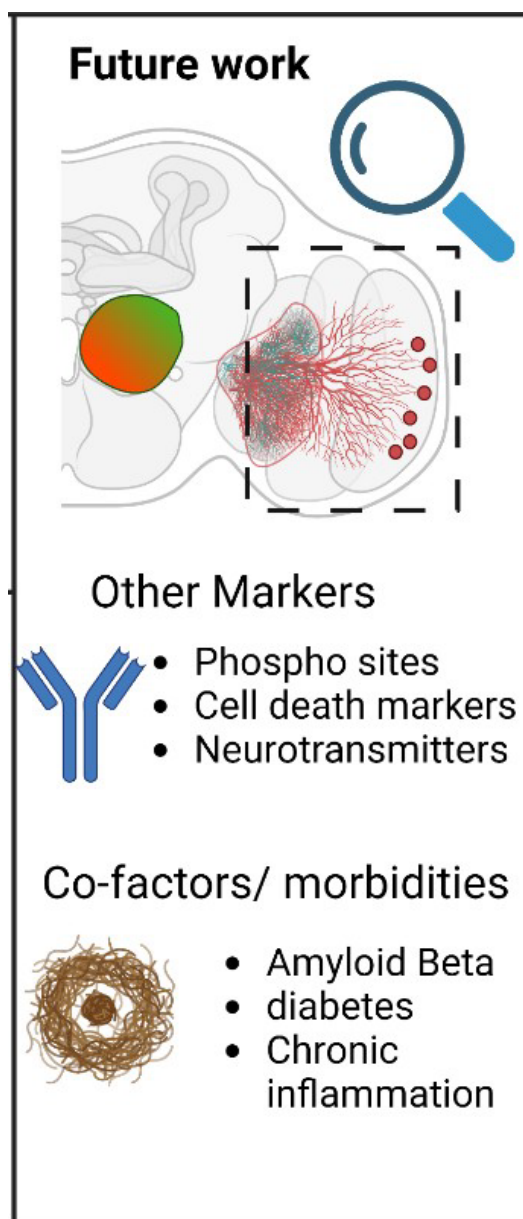


Figure 30: Diagram of the future directions offered in this chapter

Future work should aim to identify cleaner drivers from which to express Tau from, with these drivers it would be possible to delve deeper into the mechanisms underlying the effect of neuronal excitation on Tau spread. It would also be possible to investigate the impact of other co-factors and morbidities on Tau spread.

Chapter 6 Injections of externally characterised Tau species into the *Drosophila* brain

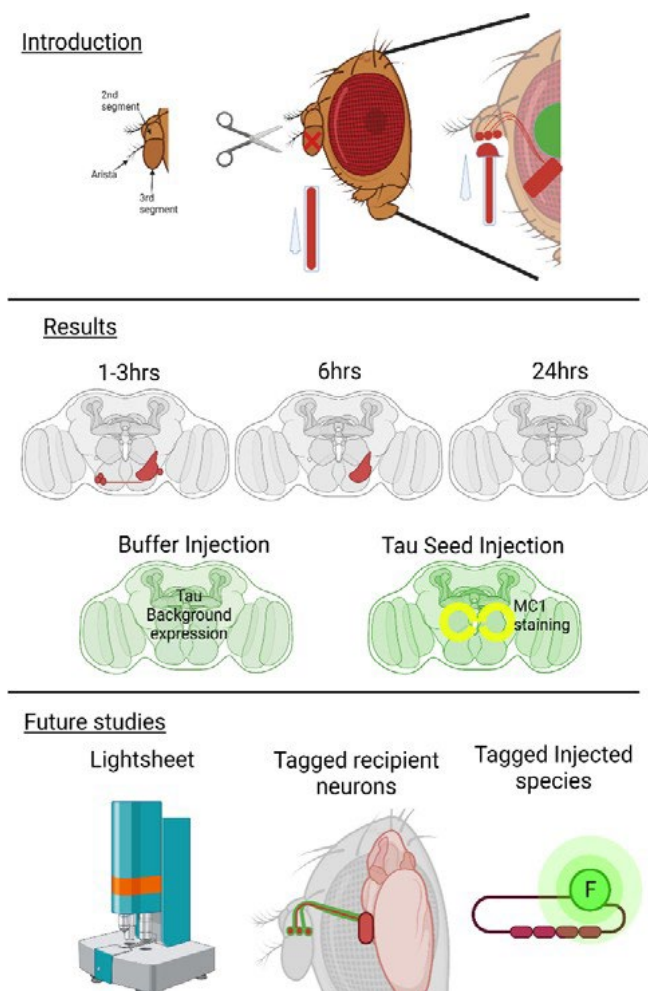


Figure 31 Graphical abstract of Chapter 6 Injecting externally characterised Tau species into the *Drosophila* brain

This chapter focuses on injecting externally characterised Tau species into the 2nd antennal segment, from which tau enters the Johnston's body organs which project into the AMMC. This Tau signal resulted in staining of the AMMC, VLP and IVLP along with associated cell bodies, however much of this signal was cleared at 6hrs and completely cleared by 24hrs. When injected into a human Tau expressing fly MC1 staining was seen 24hrs after injection indicating that seeding was occurring. Future work should focus on tagging the injected Tau and recipient neurons and using advanced microscopy techniques to better visualise the fly brain.

6.1 Introduction

The primary aim of this thesis is to develop a *Drosophila* model to study Tau spread. Previous chapters have sought to do this using genetic tools to express Tau and observe its spread. This chapter focuses on simulating spread from an injection site into the connected circuitry. Such a system is necessary in order to take advantage of the range of *in-vitro* structural and seeding assays that are available, allowing for a direct transference and interrogation of externally characterised species into a living system. The Mudher lab uses a biophysical toolkit that uses Atomic force microscopy (AFM) and Raman spectroscopy to distinguish conformational different Tau strains in AD with different seeding potentials (Devitt, Crisford et al. 2021). By introducing externally characterised Tau of differing seeding potentials into the *Drosophila* brain, a link between spread and seeding potential could be established. This chapter focuses on optimization of the delivery of Tau fibrils into the *Drosophila* brain by injection. In order to do this, Tau monomers seeded with heparin and formed into fibres as characterised by AFM and seeding assays were used (Appendix 9).

Injections are a common method of Tau delivery in mouse models (see Intro 1.11.2) and have been used to study the propagation of distinct strains across multiple mouse brains (Sanders, Kaufman et al. 2014). These mice were 3 months old and expressed the mutant P301S form of Tau for the inoculated material to seed. The flies used in this experiment were one to seven days old and expressed a wild-type form of Tau with a fluorescent reporter, offering a more efficient system and a more disease relevant substrate for Tau seeds to convert, recapitulating the more common, spontaneous AD. Furthermore, as the antenna is the selected injection site, any damage or mosaicism in Tau uptake will not be transferred to the central brain region. Injections of dyes into the fly brain have been published (Stork, Engelen et al. 2008, Au – Nazario-Toole and Au – Wu 2019, Pogodalla, Kranenburg et al. 2021), specifically the injection a of trans-synaptic dye into *Drosophila's* olfactory system (Tanaka, Suzuki et al. 2012) offers a map of downstream sites. This work builds on these findings, adapting techniques and methodologies to using Tau seeds to drive Tau spread.

The injection site will be In the antennae, offering two potential downstream circuits to which the Tau can propagate based on which segment is injected. The 3rd antennal segment contains the dendrites and cell bodies of the majority of olfactory neurons (Vosshall and Stocker 2007) investigated in previous chapters. Here it hypothesized that injections into these neurons will lead to a spread of Tau into the olfactory bulb and its downstream connections. Whereas injections into the 2nd antennal segment will target the Johnston's organs whose projections join those of the olfactory system in forming the antennal nerve (Kamikouchi, Shimada et al. 2006). However instead

of entering the olfactory bulb these Johnston's organ projections innervate the ipsilateral AMMC projection neuron and from there the inferior ventrolateral protocerebrum and ventrolateral protocerebrum (Lai, Lo et al. 2012).

By injecting into antenna, non-specific uptake of injected Tau into potential downstream tissue should be minimized whilst also providing clear neuronal populations for uptake with clear downstream targets. Further advantages are found in *Drosophila's* genetic tractability allowing for a low background expression of human Tau substrate, the conversion of which will provide evidence of seeding and spread potential of injected species. To allow for such an investigation this chapter identifies potential injection sites within the *Drosophila* antennae and shows Tau seed uptake, spread and clearance.

Introduction

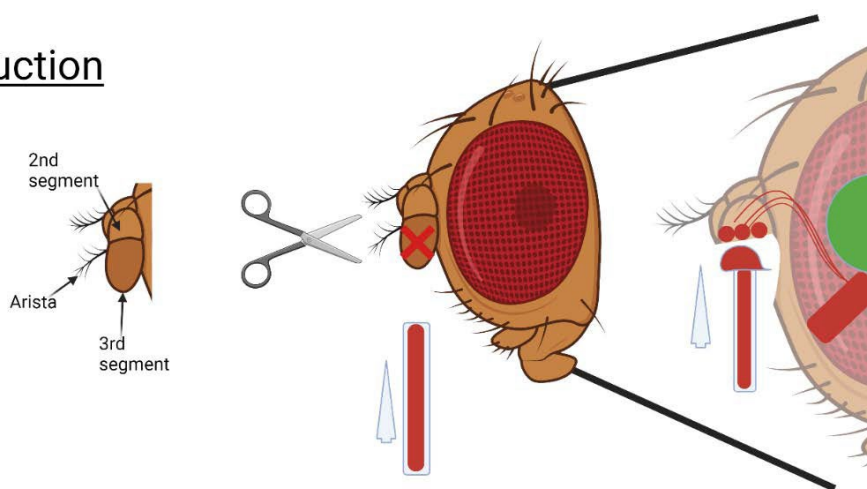


Figure 32 Graphical abstract of the methodology used in Chapter 6; Injecting externally characterised Tau species into the *Drosophila* brain

This chapter focuses on injecting externally characterised tau species into the 2nd antennal segment, from which tau enters the Johnston's body organs which project into the AMMC

6.2 Aims and hypothesis

Aim 4: To develop an injection based *Drosophila* model to allow for the relationship between Tau seed competency and its ability to spread to be investigated

Objectives:

1. To identify injection sites in the antennae and their downstream connections

The 2nd and 3rd antennal segments offer 2 potential injection sites in the antennae. To identify the best site, a dextran-based dye will be injected. This dye is capable of crossing synapses and has been used by previous groups (Tanaka, Suzuki et al. 2012) to identify downstream connections from the olfactory bulb.

2. To inject externally characterised Tau seeds into the antennae and observe the spread and perdurance in a “Blank” fly brain

Tau seeds will be injected into the injection site identified above. Using a fly that expresses only *cd8::GFP* in ORCO neurons to aid with orientation and potentially stain the receiving neurons. Doing so will give an indication of the spreading capability of the Tau seed along with how long it lasts in the system.

3. To inject the Tau seeds into the antennae of a fly brain expressing a wt-hTau population to observe seeding of this wt-hTau population by the externally characterize seed.

With an understanding of Tau spread and perdurance from the injection site, and using the *nSyb* promoter to express wt-hTau at a low level background throughout the fly brain, injection of the hTau seed will allow for the link between seeding and spread to be investigated

6.3 Results

6.3.1 Characterisation of the injection site using a dextran based dye

The proposed injection sites selected were in the 3rd and 2nd antennal segments to take advantage of the known circuitry of the olfactory receptor neurons and Johnston's organs respectively (Figure 33 A). As outlined in Methods 3.5, the 3rd antennal segment was either removed, exposing the 2nd antennal segment (Figure 33 B), or a large incision was made into it (Figure 33 C). Dextran was injected into these using a pulled glass capillary needle and capillary action allowed the filling of the segment with purple dextran dye, as seen in Figure 33 B I and C I. The conjugated micro-Ruby tag on the dye allows for the injection sites to be imaged in greater detail under fluorescence and bright field microscopy once the remains of the antennae are removed during the dissection protocol. In both injection types an Orco.GFP fly was used, meaning that the cell bodies were removed in Figure 33 B I, hence the lack of GFP signal. In Figure 33 C I the cell bodies were not removed but there did appear to be a reduction in GFP positive cell bodies in the injected left-hand 3rd antennal segment as marked by *. The staining of the 3rd or 2nd antennal segment after injection is a positive indicator that exogenous material can be taken up into the antennal segment, providing a platform for the injection of Tau fibrils.

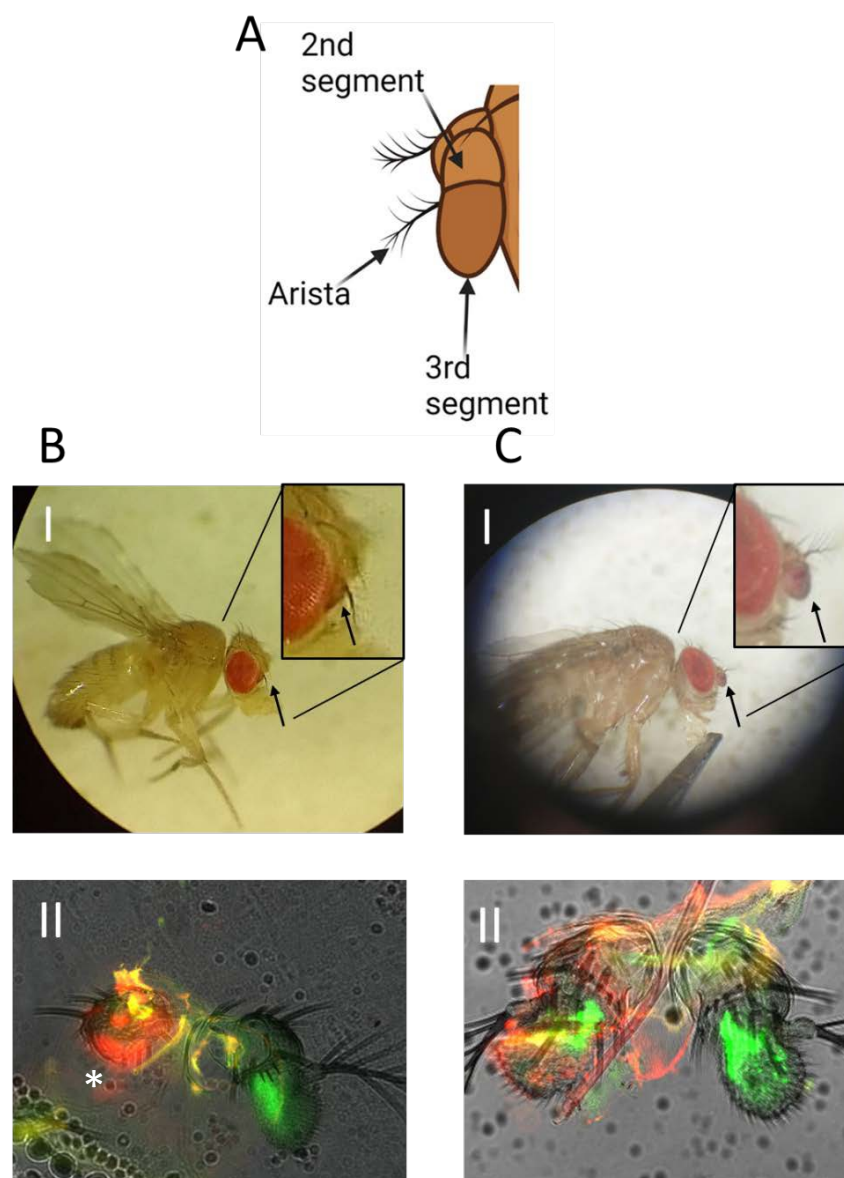


Figure 33 The injection sites used, located in the 2nd and 3rd antennal segments

An illustration of the *Drosophila* antennae denotes the relevant antennal segments **(A)**. Flies injected in the 2nd antennal segment with the Dextran dye have a purple stained 2nd antennal segment in the nearside antennae **(BI, arrow)**. Whilst flies injected in the 3rd antennal segment have a purple staining in the 3rd segment **(CI, arrow)**. When this is visualised using bright field and fluorescence microscopy, the lack of the 3rd antennal segment (*) and its GFP-positive Orco cell bodies (green) is clearly visible **(BII)** compared to the third antennal segment injection in **(CII)**. Shown in red is the fluorescent micro-ruby tag attached to the Dextran dye. Images were taken on a benchtop light microscope Zeiss Axioplan 2 with a 20x air objective.

6.3.2 Injection of dextran conjugate and Tau fibrils to identify the most suitable antennal segment for targeting

The previous section showed that it was possible to introduce the dextran dye into the antennae where it stained the receiving antennal segment. However key to this model is the dye or Tau being taken up by those neurons within the antennal segment, which then project to the brain. When focusing on the central brain region, it is possible to detect the micro-Ruby tag of the dextran conjugate both below and either side of the olfactory bulbs (Figure 34 A). These experiments were carried out on line *w*; UAS.cd8.GFP/cyO; OrcoGal4/TM3; Ser AG which constitutively expresses GFP in Orco-positive neurons (Figure 34 A I). 1 week old flies were anaesthetised and injected with the dextran conjugate. Flies were incubated at room temperature on fresh food to recover from a for one hour and immediately dissected and fixed. Interestingly, despite only being injected into one antennae, both olfactory bulbs and AMMC's contained micro-ruby signal. The AMMC appears to have a higher intensity signal than the olfactory bulbs. These have a low signal in comparison, aligning with the fact these flies were injected into the 2nd antennae where the majority of connections are to the AMMC. As the dextran conjugate is capable of moving across synapses into new neurons, its presence in a neuronal population does not necessarily mean that it was injected into this area.

The generation of Tau seeds for use in these experiments was carried out with help from Dr George Devitt (UoS). To generate the Tau seeds used for injections, recombinant Tau^{2N4R} was combined with the cofactor heparin to induce aggregation. This Tau and heparin mix was incubated at 37°C for 12 days under constant shaking. The fibrillar morphology of Tau was confirmed using atomic force microscopy (AFM) and the characteristic amyloidogenic cross- β -core structure was confirmed by the binding of fluorescent thioflavin T (ThT) dye, as demonstrated in Devitt et al, 2019. To increase the seed competency of these fibres, ultrasonication was used to break down the fibres into smaller fibrils as fibrillar Tau seeding occurs by elongation at the fibril ends (Milto, Michailova et al. 2014). The seed competency of these sheared T fibrils (referred to as Tau seeds or Tau Fibrils) was demonstrated using an *in vitro* ThT seeding assay (Appendix 9). These Tau seeds were subsequently used for antennal injection experiments.

When antennal injection was repeated with Tau seeds the majority of Tau deposition, as shown by the antibody DAKO, was found to be in a single brain hemisphere 1 hour after injection (Figure 34 B). Again, this uptake appeared to be localised to the AMMC (Figure 34 B I). The Tau signal could also be detected higher into the inferior ventrolateral protocerebrum (IVLP) as well as in structures appearing to be cell bodies (marked with arrows in Figure 34) to the right of the AMMC and in the opposite side of the prow. The staining of

these cell bodies, along with the increased coverage of the Tau staining compared to the dextran injection, may be indicative of spread into new neurons.

Injection of buffer used in the fibril formation process into the 2nd antennal region did not result in Tau staining in the fly brain (Appendix 11). Furthermore, despite multiple injections of both dextran and Tau into the 3rd antennal segment, no visible signal of either substrate was detected in the central brain region (Appendix 10). Together, these results suggest that an injection into the 2nd antennal region is the best candidate for modelling Tau spread using this method.

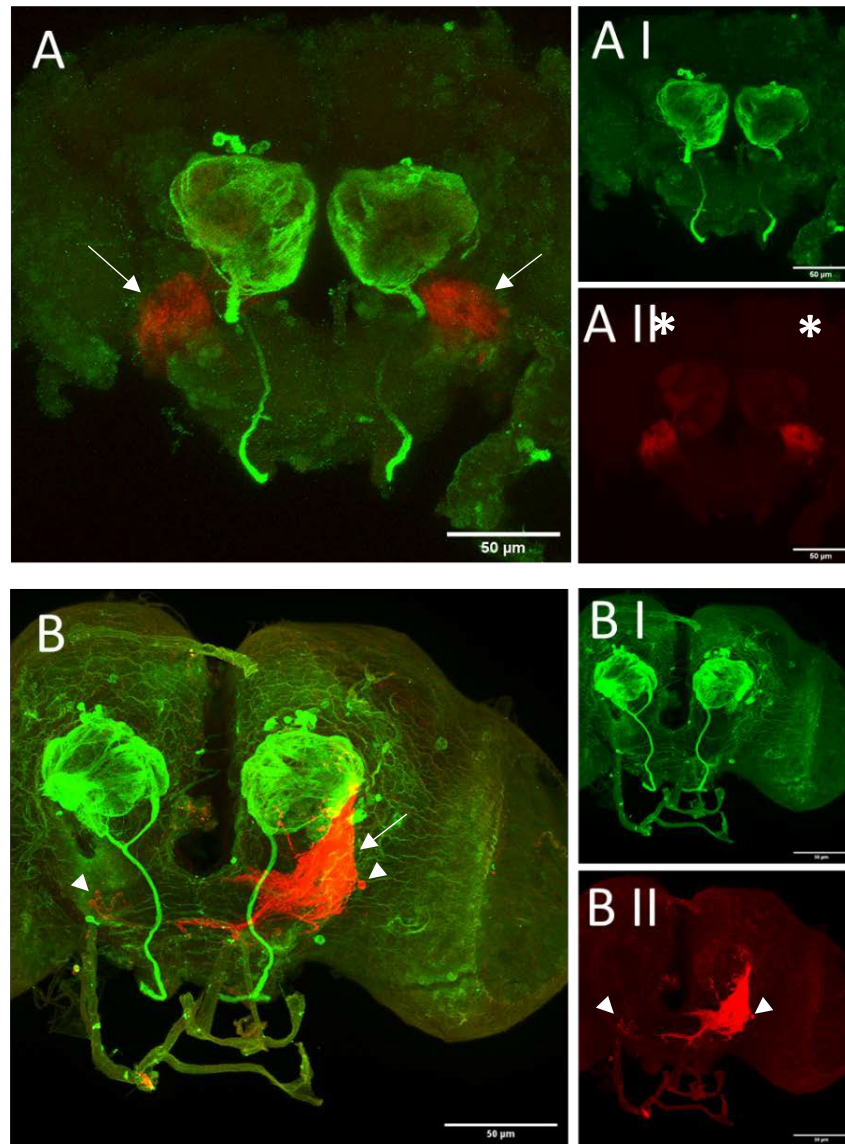


Figure 34: Injection of Dextran or Tau seed into Orco GFP brains

Overlay of GFP (green) and micro-Ruby signal (red) from the dextran conjugate **(A)** reveals a weak fluorescence signal from the micro-Ruby tag (red) in the olfactory bulbs (*) and stronger staining in the AMMC (arrows) **(AII)** on both hemispheres of the brain 1hr after injection. In contrast, 1hr after sonicated Tau fibrils were injected into the same genetic background, extensive Tau staining (red) was detected in one hemisphere of the brain in the AMMC (arrow) and IVLP (arrowheads), but not in the olfactory bulb **(B)**. When looking at individual channels visible are cell bodies that are positive for Tau, marked by arrow heads **(B and BII)**. Images were taken on a Leica SP8 confocal microscope with a 63x oil objective. Scale bar = 50 μ m

6.3.3 Clearance of sonicated Tau fibrils from the system after 6 hours

To investigate the spread of injected Tau fibrils beyond the sites identified above, brains of flies subjected to Tau injections were imaged at one, three, six and twenty four hours post-injection (Figure 35). After 3 hours, the DAKO staining appeared comparable in location to those at 1 hour with signal seen in the AMMC and IVLP. However, by 6hrs this signal had vastly reduced and appeared localised to the AMMC before appearing completely absent at 24 hours. This absence could also be seen in the dextran-injected flies at 24 hours (Appendix 11), suggesting a general clearance mechanism of the injected compounds with time.

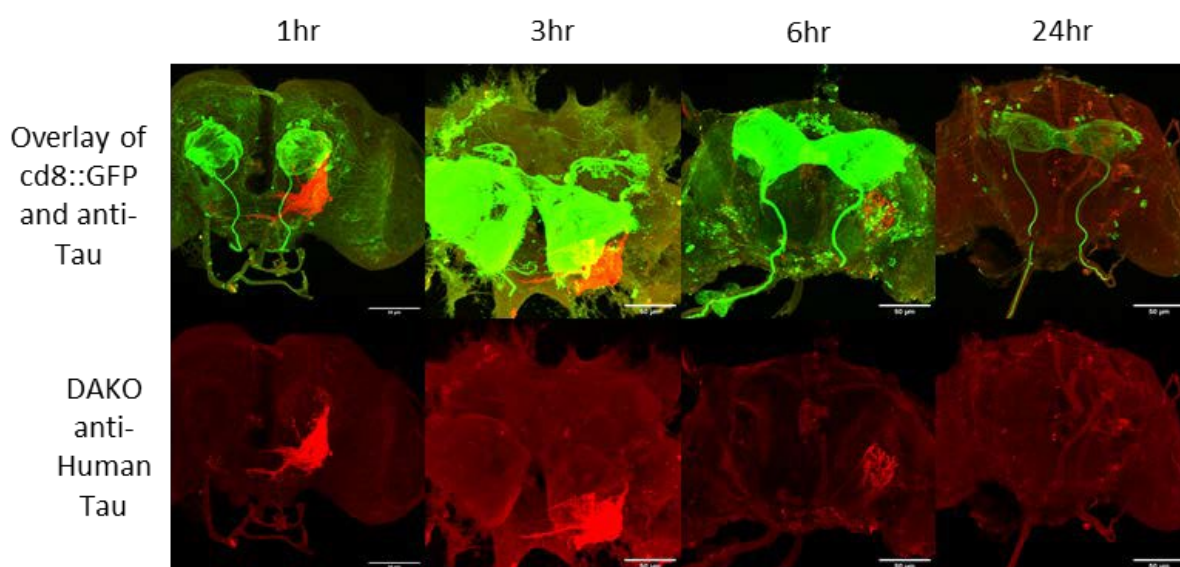


Figure 35: A time course of brains injected with sonicated Tau fibrils into the 2nd antennal segment between 1 and 24 hours.

Drosophila brains expressing GFP in Orco neurons (green), were injected with sonicated Tau fibrils (red) 1, 3, 6 and 24 hours before dissection. The intensity and distribution of the anti-Tau signal (red) remains similar at 3 hours to that of 1 hour old brain shown in Figure 34. By **6 hours** the anti-Tau signal is much reduced and no longer in projections that cross to the opposite hemisphere. By **24 hours** the anti-Tau signal is no longer appears distinguishable form background in the *Drosophila* brain. Images were taken on a Leica SP8 confocal microscope with a 63x oil objective. Scale bar = 50µm

6.3.4 Injected sonicated Tau Fibrils appear capable of seeding human Tau expressed at low levels in the fly

Section 6.3.3 demonstrates that, once injected, Tau fibrils are cleared within 24 hours. The next step is to establish whether, within this timeframe, the sonicated fibrils can induce their misfolded conformation in a native Tau population. Flies with EGFP tagged Tau^{ON4R} driven in neurons by the nSyb promotor, result in weak Tau expression in every neuron in the fly brain (Figure 35). Tau fibrils were injected in these flies which were dissected and fixed after 24hrs. The injected Tau could not be distinguished from the endogenously expressed Tau due to both being human Tau and so therefore both are recognized by the anti-human Tau antibody used. MC1 staining was greater after 24 hours in injected brains compared to in control brains where only the buffer that the Tau seeds were suspended in was injected into the 2nd antennal segment. However, this MC1 staining diffused throughout the fly brain and appeared most intense in the cell bodies around the glomeruli. When the area coverage of the EGFP signal was analysed by an unpaired t-test no significant difference was found ($F_{(2, 2)}=1.179$, $p= 0.4868$). However, a significant difference between MC1 coverage in injected and control brains was seen ($p=0.0002$). It is important to highlight the difference in scale bars of the two graphs as coverage of MC1 is much less overall ($\sim 1500\mu\text{m}^2$) than seen in the EGFP::Tau^{ON4R} ($\sim 12000\mu\text{m}^2$).

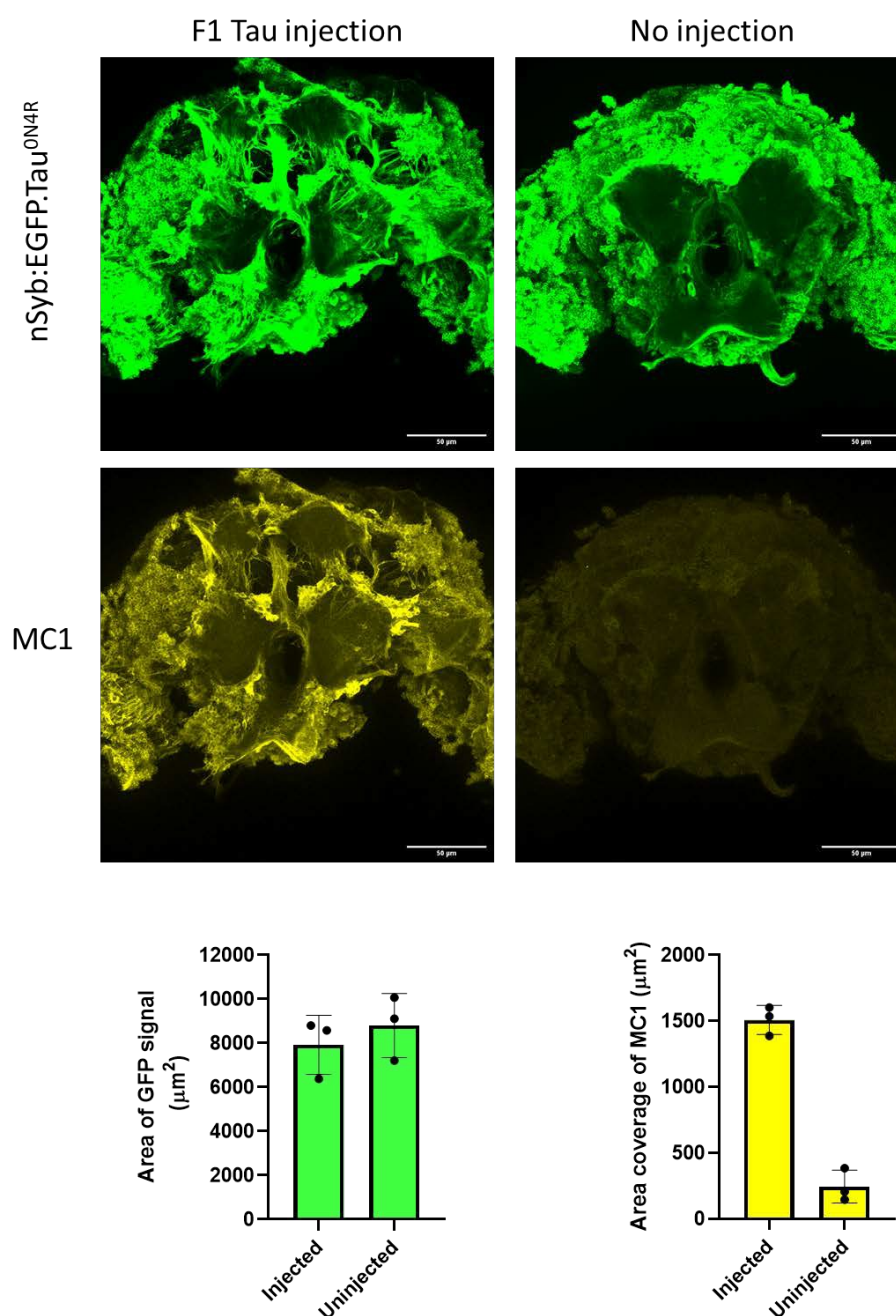


Figure 355: Injection of Tau Fibrils vs a control injected brains expressing nSyb:EGFP:Tau^{ON4R} after 24 hours (n=3)

The nSyb promoter drives a low level of EGFP tagged Tau^{ON4R} (GFP) in all neurons at similar level in both the injected and control brains, as determined by an unpaired t-test ($F_{(2, 2)}=1.179$, $p=0.4868$). In brains injected with Tau fibril, however, a significant increase in MC1 staining (yellow) is observed ($F_{(2, 2)}=1.263$ $p=0.0002$) particularly around the olfactory bulb. It should be noted that the total MC1 staining is approximately 4x less than the EGFP staining. Images were taken on a Leica SP8 confocal microscope with a 63x oil objective. Scale bar = 50μm

6.4 Discussion

6.4.1 Summary

This chapter aimed to create a model which would allow for the probing of the relationship between Tau seeding and spread by injecting externally characterised species into a fly expressing a naïve (Wt conformation) Tau population. This work found that it was possible to introduce a neuronal dye and a Tau seed into the 2nd segment of the antennae and, from this, signal could be observed in the brain. However, no signal was observable in the central brain when injecting into the 3rd antennal segment. Successful injections into the 2nd antennal segment showed dextran staining of the AMMC. Tau seeding was also observed staining beyond the AMMC into the IVLP and crossing the prow into the other hemisphere 1 hour after injection, with a small number of few cell bodies potentially associated with the AMMC and IVLP projection neurons also seen stained. Overall staining appeared much reduced 6 hours after injection and had completely disappeared by 24 hours for both Tau and dextran.

In preliminary experiments these Tau seeds were then injected into a fly genetically expressing GFP-tagged Tau^{ON4R} at low levels throughout the brain. This injection resulted in an increase in MC1 staining after 24 hours upon comparison to non-Tau injected controls. These results show that it is possible to inject pre-characterised Tau species into the fly brain where they are potentially capable of spreading beyond the injection site and converting locally expressed Tau^{ON4R} species to a disease-relevant conformation. Further work would be able to build a spatio-temporal picture of these events, creating a rapid and versatile model of Tau spread and seeding.

6.4.2 Characterisation of two distinct injection sites in the antennae for delivery of exogenous dyes and Tau species

Injection of Tau, A β and other AD relevant substrates have been used to model different aspects of AD in mice with great effect (Götz, Chen et al. 2001, Clavaguera, Bolmont et al. 2009, Sanders, Kaufman et al. 2014). However, these systems retain a number of limitations as discussed in introduction 1.11.3. Whilst damage of the injection site will always be present in any injection models, the *Drosophila* model described isolates the site from the rest of the brain by injecting into the antennae. This also brings the added advantage of the injection site being in a spatially-controlled population of cells with known downstream connections, providing a specific system in which to investigate spread and seeding.

As demonstrated in Figure 34: two potential injection sites within the fly antennae offer a specific cell population to inject into, with the 3rd and 2nd antennal segments containing the olfactory

neuron cell bodies and Johnston's organ cell bodies respectively (Eberl and Boekhoff-Falk 2007, Vosshall and Stocker 2007). Both of these neuronal types project to distinct and characterised brain regions (the olfactory bulb and AMMC respectively), offering distinct populations in which to investigate Tau further.

Previous research has utilised a dextran conjugate dye to visualise connections of the antennal lobe but the dye was instead introduced by opening up the fly head and directly piercing the antennal lobe (Tanaka, Suzuki et al. 2012). However, such a method is not conducive to aging studies and can create an altered brain environment in response to such injuries. Instead, the present study utilised a method of creating small incisions into the antennae and introducing dextran dye via capillary action from a pulled capillary tube needle, resulting in a purple injection site (Figure 34). By only making an incision into the antennae, this method limits both the damage and the cells that are capable of incorporating the dye. When observed using a bright field and fluorescence microscope technique, it can be observed that none of the GFP positive Orco cell bodies remain in flies with the 2nd antennal injection whilst most still appear present in flies subject to the 3rd antennal injection. This ability to mark recipient cells with GFP made the 3rd antennal injection site appear the most amenable to the model. However, despite the antennal segment turning purple (Figure 34), dextran was not found to be in any brains tested (Appendix 10), despite its use in the olfactory system in Tanaka, Suzuki et al. 2012. However, in the present study injections occurred directly into the antennal lobe. Not only are the olfactory neurons axonal terminals located here but the projection neurons' dendritic terminals are also present. Therefore, injecting here may have resulted in the staining of projection neurons as opposed to the olfactory. In contrast, the 2nd antennal segment also stained purple (Figure 34) but time-dependent staining was observed within the AMMC and, to a lesser extent, the olfactory bulb. This may be, in part, due to the 2nd antennal segment being smaller than the 3rd and so resulting in a higher local concentration enabling uptake. As the injection of the dye is down to capillary action, injecting a greater quantity into the 3rd antennal segment is not possible, however a greater volume would suggest greater action. This work shows that it is possible to inject the Dextran dye into the 2nd antennal segment, but not the 3rd, marking the 2nd antennal segment as the better candidate in which to inject Tau seeds.

6.4.3 Spread of Tau from the Injection site, followed by its rapid clearance.

The dextran dye not only marks the injection site but, due to its ability to cross synapse in either direction, it is also capable of marking up sites that are downstream of the injection. The successful uptake of dextran from the 2nd antennal segment led to staining in both hemispheres, predominantly of the AMMC but also of a small amount in the olfactory bulbs. There are two potential causes of the staining of both the AMMC and olfactory bulbs; one possibility is that this

dye spreads across neuronal connections, with the stronger signal in the AMMC suggesting that the dye spreads from the AMMC to the olfactory bulb in this way. Dextran is capable of spreading both retro-grade and antero-retrograde through neuronal connections (Tanaka, Suzuki et al. 2012) and once the signal is within a glomeruli within the olfactory bulb, potential spread through interneurons would ensure the staining of a other glomeruli within the bulb as observed. Another possibility is that the dextran dye is taken up by the olfactory neuron's axons which form a bundle with the Johnston's organ's axons through the 2nd antennal segment, collectively known as the antennal nerve (Kamikouchi, Shimada et al. 2006). The potential cause of this uptake could be that the injection process may have nicked or exposed the antennal nerve to the dye, hence why both olfactory bulb and AMMC contain signal. The appearance of a signal in both olfactory bulbs is unusual and may be a property of the dye rather than the injection method. This theory is supported by the results of sonicated Tau fibril injections, where only staining of a single AMMC is observed, with no staining in the olfactory bulb detected. This is more closely aligns with other work demonstrating known connections from the Johnston's organs to the AMMC (Kamikouchi, Shimada et al. 2006).

The large area of signal seen when sonicated Tau fibrils are injected into the brain is suggestive of spread beyond the AMMC, although this pattern is not dissimilar to those produced by dextran. The pattern of Tau signal in these brains suggests presence not only in the AMMC but its projection neurons, alongside those of the inferior ventrolateral protocerebrum (IVLP). These are known downstream connections of the Johnston's organs, but were not stained by dextran from these injections. Further evidence of Tau spread is shown in the staining of cell bodies shown with arrows in Figure 34. The Johnston's cell bodies are located in the antennae (Kamikouchi, Shimada et al. 2006) which are removed as part of the dissection process. Therefore, the presence of staining in these unidentified cell bodies is indicative of potential Tau spread in new neurons. Upon comparing the patterning of signal with other studies of *Drosophila* brains it can be seen that the stained cell bodies and associated neurons are located in areas possibly downstream of the injection site, namely the AMMC, ventrolateral protocerebrum (VLP), IVLP and projection neurons which make up *Drosophila's* 2nd and 3rd order auditory connections (Lai, Lo et al. 2012). However, without markers for both these regions and neuronal populations a definitive answer as to the identity of the Tau-positive regions remains unclear. Regardless, the wider area stained compared to the dextran and the staining of these unidentified cell bodies is strong evidence for spread having occurred.

If spread has indeed been observed then it has occurred within an hour of injection, as seen in Figure 34. This suggests that spread is occurring very rapidly, faster than in microfluidic devices in where the crossing of a single synapse is measured with MC1 staining after 8 days. Mouse models

where recombinant Tau seeds were injected report potential spread around the injection site by one month using MC1 staining (Iba, Guo et al. 2013). By measuring MC1 staining as an output, these experiments have measured the time taken for Tau to spread into and converted local Tau populations in these neurons. Whereas the work here has measured the spread of Tau directly and the appearance of Tau in new neurons is only dependent on its spread, not spread and conversion of naïve Tau species, which may explain the time differences. However, the study did find small populations of MC1-positive neurons close to the injection site even at 2 weeks, suggesting that the spread and seeding does rapidly occur (Iba, Guo et al. 2013). This work also found that the spread and seeding ability was dose- and time-dependent (Iba, Guo et al. 2013). This may explain the rapid spread observed in the present study as it was not possible to control dosage, meaning a large dose may have been delivered relative to the size of the fly brain.

Whilst the spread occurred rapidly it also appeared to have also reached its furthest reaches of spread in the first hour, with no further signal detected at the 3 hour time point in Figure 35. A finer time course would help to confirm the theory of spread is correct by providing evidence of a progressive filling of the neurons in question. However, the time required to carry out each injection complicates this method. The speed of spread observed, which plateaus at the third hour, may be caused by the initial high concentration of Tau injected into the antennae overcoming barriers to Tau spread. Over time, however, the concentration of Tau decreases until spread is no longer possible or, potentially, detectable.

Regardless of this, a rapid clearance of injected Tau occurs between 3 and 6 hours and is completely removed by 24 hours (Figure 35). This clearance within 24 hours was also seen with the dextran injections (Appendix 11). Clearance could be due to the degeneration of any cut neurons as reported in other studies occurring over a 24 hour period (MacDonald, Beach et al. 2006). If this is the case then the signal observed is not actually spread as Tau signal loss could correspond with the degeneration of the injected neuron rather than its transfer to other healthy neurons. Other studies using mice have reported clearance of injected Tau species in their models, with clearance from extracellular space observed within 48 hours (Ishida, Yamada et al. 2022) and from cells within a 1 month post-injection (Bassil, Meymand et al. 2020). The results described here match more closely with the time taken for clearance from the extracellular space; however in the *Drosophila* model Tau signal was seen within cell bodies. Whilst the rapid loss of Tau signal was not recorded in earlier chapters, this may be a due to its continual expression via the UAS.Gal4 system in comparison to its short, high intensity delivery using the injection method.

This work shows that Tau seeds can be injected into the fly and, from there, potentially spread into downstream neurons. It also shows that the injected Tau population is fully cleared for the system within 24hrs.

6.4.4 Injection of Tau seeds causes seeding of the MC1 conformation into naïve Tau populations

To create a model in which both seeding and spread could be observed, a pool of naïve Tau had to be present in the fly from which the injected template could induce the misfolded conformation. A *Drosophila* Tau homologue does exist, however cross-seeding between human and *Drosophila* Tau is unknown. The nSyb promotor drove a background of expression of human Tau^{ON4R} for this purpose. Some spontaneous misfolding in this species has been described in previous chapters, however this was caused by a higher expressing driver leading to increased local concentrations of Tau, resulting in an accelerated effect on misfolding. In the present study flies 1 day old flies were selected to minimise the chances for misfolding to occur. This resulted in little to no spontaneous misfolding observed in controls 24 hours after injection of the Tau buffer (PBS with 2mM DTT) (Figure 35). To further this model's physiological relevance, future work could focus upon creating a fly where *Drosophila* Tau is substituted for human Tau under the same promotor.

In this current work, however, the difference between sonicated Tau seed injected brains and the control brain is evident (Figure 35). The increase in MC1 signal was more global in nature and did not bear a direct correlation with areas positive for injected Tau in Figure 34. However, by 24 hours Figure 35 shows that injected material was no longer detectable in the system, meaning that in Figure 35 the MC1 signal detected did not originate from the injected material. As with the potential spread described Figure 34 here the potential seeding activity is significantly faster than spread reported by other groups using recombinant Tau injections in mice, whose measurement of spread was MC1 or AT8 staining within the naïve Tau population (Iba, Guo et al. 2013, Iba, McBride et al. 2015, Peeraer, Bottelbergs et al. 2015). The rapid spread and seeding, leading to the global Tau MC1 staining seen could be due to the sonicated Tau species used here which has been shown to increase aggregation propensity through an increase in β -sheet content (Stathopoulos, Scholz et al. 2004) but also by sonication breaking up the Tau fibrils as fibrillar Tau seeding occurs by elongation at the fibril ends (Milto, Michailova et al. 2014). However, in the mice injection studies sonication of the Tau seeds is also a common practice. Further adding to the rapid spread seen is the difficulties in controlling the concentration and amount of Tau seed injected, both of which are known to play a role in seeding (King, Ahuja et al. 1999, Rankin, Sun et al. 2005). Furthermore, very high local concentrations may be reached at the injection site, giving an early accelerated spread.

Whilst this spread is easy to follow when human Tau^{2N4R} seeds are injected into a blank brain, they become much harder to observe when injected onto a human Tau^{ON4R} background. In order to clarify the spread of the injected species and the conversion of the human Tau^{ON4R} background the use of a marker for the injected species more specific than anti-human Tau antibodies is needed. The use of 2N4R for seed formation offers the possibility of an N-terminal targeting antibody (For example ab218316), specific for the seeded species, however this may produce a seeding barrier. Another possibility is the use of Dylight Antibody Labelling, which allows for the labelling of Tau seeds before its injection in order to differentiate it from the expressed background Tau (Evans, Wassmer et al. 2018).

Critically, this work shows that the presence of a Tau seed may accelerate aggregate formation, as measured by MC1, *in-vivo*, similar to the effect these Tau seeds had in the *in-vitro* ThT seeding assay (Appendix 9). Future efforts to distinguish the injected human Tau species from those expressed would allow for a readout of spread, alongside the seeding activity shown here. Other groups have injected different Tau species from different Tauopathies into mice, recapitulating the associated Tau inclusions in the naïve human Tau populations, complete with Tau hyperphosphorylation, a prerequisite to misfolding in AD (Clavaguera, Akatsu et al. 2013). This shows a potential future direction in which injections of Tau enriched and characterised human brain tissue from various Braak stages and Tauopathies can be used to ascertain the relationship between Tau structure, seeding and spreading in a high throughput manner *in-vivo*. Furthermore thanks to the Cryo-EM structures of Tau filaments (Fitzpatrick, Falcon et al. 2017), newly designed inhibitors of Tau aggregation can be rapidly tested alongside the injection of various pathogenically relevant Tau seeds in a timely manner.

6.5 Conclusion and future directions

Whilst Tau spread is seen to occur at a different rate from other injection models, in this model it appears possible to map both spread and, seeding of naïve human Tau species when compared to a control. Further refinement of this model could offer a system that provides insight into Tau seed structure which can be tested within a modifiable neuronal environment, albeit within a potentially limited timeframe.

The further refinement of this model should focus on confirming if the recipient neurons in the antennae are, in fact, the Johnston's organs. A GFP marker could be used to delineate the receptor neurons in the antennae and, in doing so, would also highlight their projections in the central brain region, clarifying what proportion of signal is spread. To this extent a change in microscopy technique may also yield a better model; light sheet microscopy in combination with a chemical depigmentation and clearing protocol (Pende, Becker et al. 2018) would allow for greater throughput

and imaging of the injection site in the antennae, alongside the rest of the brain. Such a system would also lead to quicker turnaround times per brain and so allow for a time course that occurs within less than an hour, alongside the visualisation of uptake neurons at the injection site and transfer to downstream connections.

Further refinements will be required to best utilise the spread and seeding model, with two more markers needed. One marker as a positive control that can be injected alongside the Tau seed to confirm success of the injection and to quantify the loading. This is because despite many repeats at negative time points, the potential for incorrect loading of the antennae remains. Another key marker required will be for that of Tau itself, as both the injected seed species and the recipient naïve species are both human. Differentiating between the two is therefore difficult and may lead

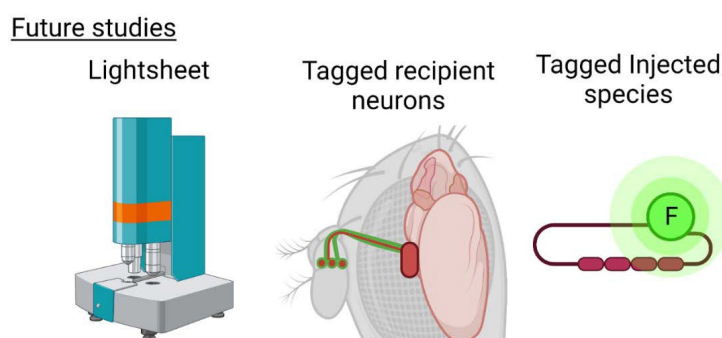


Figure 36 Graphical abstract of Chapter 6's Future work, injecting externally-characterised Tau species into the *Drosophila* brain

Future work should focus on tagging the injected Tau and recipient neurons and using advanced microscopy techniques to better visualise the fly brain. With these refinements in place, the full potential of *Drosophila's* genetic tractability can be brought to bear when investigating Tau seeding and spread.

to naïve neurons being classified as diseased due to the presence of injected species that have not induced the disease conformation. Fluorescent dyes exist that can be used to stain these externally characterised species. Dyes such as Dylight Antibody Labelling, allow for the labelling of these Tau before its injection in order to differentiate it from the expressed background Tau (Evans, Wassmer et al. 2018). Investing energy in refining the proposed model will yield a system in which insights into Tau seed structure can be tested in a modifiable neuronal environment. To this end, a large number of prefabricated mutants and unbiased screening panels exist to probe mechanisms of seeding and spread. These include A β co-expression, vesicle trafficking, Tau uptake and activity mutants alongside mutants and techniques that recreate co-morbidities, such as diabetes and traumatic brain impact.

Chapter 7 Overall conclusions and future directions

7.1 Summary

The spread of Tau throughout the brain correlates with disease progression (Arriagada, Growdon et al. 1992, Van Rossum, Visser et al. 2012, Rolstad, Berg et al. 2013). This spread is thought to be prion-like, as evidence suggests Tau seeds move through neuronal connections to convert naïve Tau populations to the disease conformation (Clavaguera, Bolmont et al. 2009, Vogel, Iturria-Medina et al. 2020). Whilst mouse and cell models of Tau spread exist, each have their own advantages and disadvantages when it comes to modelling Tau spread. The overall aim of this thesis was to develop a *Drosophila* model to study Tau spread, taking advantage of the specific and well mapped olfactory anatomy and powerful genetics available in *Drosophila*. This work resulted in a split into three separate potential models of Tau spread, each with their own advantages, but also with further work required to refine each model.

7.2 Modelling Tau spread in a small number of olfactory neurons using *Drosophila's* olfactory system

Modelling Tau spread in a small number of olfactory neurons would allow a model to recapitulate the spread of Tau between neurons in complexity of an in-vivo system. In doing so specific questions about the mechanisms of Tau spread could be asked, but also given wider context of neuronal dysfunction and death, along with the resulting consequences for the organism. For the small number of olfactory neurons model Or88a.Gal4 was selected as the best olfactory driver due to its prominent and therefore easy to visualise position on the olfactory bulb and for its potential use in behavioral assays.. This was used to drive UAS.mCherry tagged Tau and cd8::GFP which showed mCherry Tau signal in glomeruli that did not contain GFP, suggesting spread. This spread is potentially occurring via GABAergic inhibitory interneurons which have been reported to show preferential uptake of Tau in mice (Ruan, Pathak et al. 2021). When these brains were stained with MC1, spontaneous misfolding of Tau within the Or88a neurons was found with time. A leak of the UAS transgene was observed in the lateral horn. This UAS leak is likely due to attP40 insertion site as other attP lines have also shown leak in this area (Pfeiffer, Ngo et al. 2010).

This model, using a small number of neurons in the olfactory bulb may be useful to investigate the role of inhibitory interneurons in Tau spread as when using Orco to drive expressing in a large number of olfactory neurons this would be occluded by Tau expression in all glomeruli within the olfactory bulb. However further work is needed to improve the specificity of the UAS line by using different insertion sites. Confirmation that spread is indeed occurring through the interneurons

can be achieved by using olfactory interneuron specific Gal4 drivers to express *cd8::GFP* within the interneurons, or by using olfactory interneuron knockout lines to remove this potential avenue of Tau spread.

The use of *Drosophila* to model pathological Tau spread in AD has shown further advantages in the spontaneous misfolding of human Tau in fly brains, which is more relevant to the spontaneous forms of AD than the hereditary mutant Tau variants used to induce misfolding in other models. The rapid spontaneous misfolding of human Tau species in *Drosophila* neurons presents both an opportunity to understand the factors around Tau misfolding and spread, but also a limitation in the study of physiological Tau spread due to the rapid and spontaneous misfolding.

7.3 Modelling and modulating Tau spread in a large number of neurons using *Drosophila's* olfactory system

This chapter utilised the Orco.GAL4 to drive mCherryTau^{ON4R} expression in all olfactory neurons to model Tau spread through a large number of olfactory neurons. In this way targeting amenable connections that would allow Tau spread between known connected regions of the brain. Neuronal excitability is thought to have a role in modulating Tau spread and so was used to investigate potential spread further using *Drosophila's* genetic tools.

This work found that the Orco-driver on the X chromosome drove expression beyond the olfactory bulb, with *cd8::GFP* signal being detected throughout the brain and lobula. Despite this, spread may be occurring within the medulla, where mCherryTau^{ON4R} signal was detected, but not co-localised with *cd8::GFP*. The use of Hyper excitation mutants increased the area coverage of Tau in the medulla, whilst hypo active flies increased AT8 staining throughout the brain in line with previous findings (Pooler, Phillips et al. 2013).

By driving Tau in Orco neurons, this work has shown a decrease in median life expectancy, spontaneous hyperphosphorylation (a pre-requirement of aggregation) and potential spread of mCherryTau^{ON4R} into the medulla. However, these results are occluded by the non-specificity of the driver. Identifying a more specific driver in the LC neurons would give a clear expressing population, beyond which Tau spread into the medulla could be studied with greater certainty.

There are advantages to developing Orco.GAL4 as a separate model to the small number of olfactory neurons targeted by Or88a.GAL4. By using a larger number of neurons in which to study Tau spread, potential consequences for the fly are more obvious, given the higher Tau burden, facilitating electrophysiological or behavioural readouts. Orco.Gal4 driven Tau has also shown the ability to modulate potential Tau spread through the use of excitability mutants, suggesting that other readily available fly mutants, targeting different mechanisms of Tau spread may also be used with this model.

7.4 Injecting externally characterised Tau species into the *Drosophila* brain to model spread and seeding of Tau seeds

Injection of Tau species is used as a vector in mouse models (Sanders, Kaufman et al. 2014) and in flies is used for loading of various dyes (Tanaka, Suzuki et al. 2012). Tau species produced in-vitro, can be characterised by a range of structural and seeding assays, to determine conformation and seeding properties (Devitt, Crisford et al. 2021). These can be injected into the flies antennae using pulled capillary tube needles, to observe spread and seeding activity when introduced to a wt-Tau population. This allows for questions on interaction of seeding and spread to be asked. The *Drosophila* antennae offer a well-defined injection site separate to, but connected to the central brain, isolating the possible neuronal populations that can take up the injected Tau.

It was found that Injected Tau seeds or Dextran dye was successfully taken up when injected into the 2nd antennal segment, but not the 3rd. This led to the injected Tau seeds being taken up into the Johnston body organs. Tau seeds seemed to spread beyond these neurons to the AMMC and LVLP very rapidly, though a rapid clearance is also observed. When injected into flies expressing background Tau, Tau seed uptake appears to cause misfolding of wt-Tau in seed injected brains vs buffer injected brains. Though given both seeds and wt-Tau are human it is difficult to observe injected species within the wt-Tau background.

This work shows that it is possible to inject and observe externally characterised Tau seeds in the *Drosophila* brain. This method of introducing Tau to the fly brain complements the two genetic approaches, described above, offering a greater understanding of the Tau conformation and seeding ability that is being introduced to the system. Whilst still retaining the many advantages of working in *Drosophila*, such as the specific circuitry and powerful genetics. Further work is needed to use genetic markers to delineate the extent of the injection site and uptaking neurons. Cd8::GFP expression in the Johnston organs would allow for understanding of the extent of spread from these neurons. Further markers for the injected species will help differentiate seeded Tau from the injected species.

7.5 Future directions for *Drosophila* models

This thesis has described 3 models with each showing the potential to model different aspects of Tau spread.

Expression of mCherryTau^{ON4R} within a small number of olfactory neurons has potential for investigating the role of interneurons in Tau spread. In *Drosophila* Gal4 lines exist to specifically target olfactory interneurons through which spread may be occurring. NP1227.Gal4 and NP2426

label large numbers of inhibitory interneurons (Das, Sen et al. 2008) individual groupings of olfactory interneurons are also targetable, although these will require some further investigation to find out which innervate the Or88a glomeruli (Chou, Spletter et al. 2010). These interneuron specific lines would best be used with the parallel to UAS.Gal4, but non-interacting Q expression system (Potter and Luo 2011). This would allow for separate expression of markers or for down regulation in the olfactory interneurons, without changing the expression site of UAS.mCherryTau^{ON4R} or UAS.cd8::GFP. These studies can't be carried out using the Orco driver as Tau is expressed in all olfactory bulbs and so occludes spread within the bulb that is potentially mediated by this driver. The investigation of spread via interneurons and identification of mechanisms or influencing factors is important as evidence suggests GABAergic interneurons are vulnerable to neurofibrillary tangles and phosphorylated Tau (Zheng, Li et al. 2020, Ruan, Pathak et al. 2021).

Whilst the large number of olfactory neurons targeted by Orco.GAL4 may not be useful for investigating spread via these interneurons, it has been shown to be amenable to neuronal activity-modulating mutants. Once a suitable driver has been found, offering specific expression in either olfactory neurons or in LC neurons, further mutants can be crossed in alongside the neuronal modulating mutants, to derive a greater understanding of the mechanisms of Tau spread. The combination of activity mutants with Tetanus toxin light chain expression for example would block neuronal vesicle binding. If Tau release in response to neuronal activation was mediated by the neurotransmitter vesicle binding then the co-expression of Tetanus toxin would reduce Tau spread. In this way, neuronal activity and tetanus toxin light chain expressing mutants can be used with this model can be used to understand how co-expression of A β influence Tau spread. A reduction in neuronal activity can attenuate A β 's catalysing of Tau pathology (Rodriguez, Barrett et al. 2020). If A β expression caused an increase or decrease in Tau spread, then introducing the corresponding excitability mutant could rescue this effect, providing mechanistic insights alongside functional consequences for the organism, assessed by longevity or learning and memory assays all in a single model.

This model of spread through a large number of olfactory neurons can also be combined with other co-morbidities that effect AD, such as diabetes, depression and gut microbiome (Santiago and Potashkin 2021). Models of these morbidities exist already in *Drosophila* and can be induced without using genetic manipulation via additives to the diet (Ludington and Ja 2020, Chen, Yang et al. 2021, Moulin, Ferro et al. 2021). Furthermore, by introducing the Gal80 expression alongside that of Gal4, GAL80 binds to the Gal4 transcriptional activation domain, inhibiting its activity, thereby giving temporal control of expression and allowing for investigation of one of the biggest potential risk factors in AD, age (Eliason, Afify et al. 2018). By delaying Tau expression until later life stages the effect of the age of the neuronal circuit on Tau spread and pathology is possible to

be investigated.

By modelling Tau spread in *Drosophila* questions not just about the spread of Tau can be asked, but also its seeding potential. Using the injection method a range of externally characterized Tau conformers of different seeding potentials can be introduced to a flies expressing background levels of human Tau to compare how changes to the structure of Tau affect its ability to spread from the injection site. This can also be carried out with patient derived fibrils from different Braak stages to understand how the seeding and spreading competency of Tau changes over the course of the disease. Due to the wide range of genetic tools in *Drosophila* the injected fly brain itself can be adapted to the experimental needs, with potential pathways or interacting factors targetable with markers or modulators.

Gaining an understanding of the mechanisms of Tau spread and seeding is key to understanding the pathological progression of Tau throughout AD. In doing so it will provide better diagnosis, treatments and prognosis to those affected by this disease.

7.6 Presentations of this work

This work has been presented in poster format at the Coldspring Harbour Neurobiology of *Drosophila* 2021, Tau 2022 Global Conference in Washington DC, for which it secured a Tau 2022 Global Conference Fellowship and at ARUK 2022 in Brighton where it won the ARUK Conference Poster Prize. At the ARUK 2022 conference this work was also presented as a talk during the early careers day.

Appendix

Making Or88a-Gal4,UAS-cd8::GFP

We have: Or88a-Gal4 on Chromosome 2 [23294]
: UAS-cd8::GFP on Chromosome 2 (provided by Herman [Wijger](#))

We want flies [having](#) both Or88a-Gal4 and UAS-cd8::GFP on same arm of ch2 à +/+; Or88a-Gal4,UAS-cd8::GFP so that in this fly the Or88a driver cells are green indicating the extent of driver-dependent expression.

1) Cross Or88a-Gal4 flies with UAS-cd8::GFP

$\frac{x}{x} \frac{+}{+} \frac{OR88a-Gal4}{OR88a-Gal4} \times \frac{y}{y} \frac{+}{+} \frac{UAS-cd8::GFP}{UAS-cd8::GFP}$

	$\frac{s}{s} \frac{+}{+} \frac{OR88a-Gal4}{OR88a-Gal4}$	$\frac{s}{s} \frac{+}{+} \frac{OR88a-Gal4}{OR88a-Gal4}$
$\frac{z}{z} \frac{+}{+} \frac{UAS-cd8::GFP}{UAS-cd8::GFP}$	$\frac{z}{z} \frac{+}{+} \frac{OR88a-Gal4}{UAS-cd8::GFP}$	$\frac{z}{z} \frac{+}{+} \frac{OR88a-Gal4}{UAS-cd8::GFP}$
$\frac{w}{w} \frac{+}{+} \frac{UAS-cd8::GFP}{UAS-cd8::GFP}$	$\frac{w}{w} \frac{+}{+} \frac{OR88a-Gal4}{UAS-cd8::GFP}$	$\frac{w}{w} \frac{+}{+} \frac{OR88a-Gal4}{UAS-cd8::GFP}$

2) Cross selected progeny (20-30 virgin females) from (1) with 20 males of 3709 ([scd/CyQ](#); TMS/TM6) to put marker over [tubby](#)

$\frac{x}{x} \frac{+}{+} \frac{OR88a-Gal4}{UAS-cd8::GFP} \times \frac{y}{y} \frac{Cyo}{Cyo} \frac{TMS}{TM6} \frac{Sb}{Tb}$

	X; CyQ	Y; CyQ	X; Scd	Y; Scd
$\frac{z}{z} \frac{+}{+} \frac{OR88a-Gal4}{UAS-cd8::GFP}$ those will be light red eyes	$\frac{z}{z} \frac{+}{+} \frac{OR88a-Gal4}{UAS-cd8::GFP}$ Y CyQ	$\frac{z}{z} \frac{+}{+} \frac{OR88a-Gal4}{UAS-cd8::GFP}$ Y CyQ	$\frac{z}{z} \frac{+}{+} \frac{OR88a-Gal4}{UAS-cd8::GFP}$ X Scd	$\frac{z}{z} \frac{+}{+} \frac{OR88a-Gal4}{UAS-cd8::GFP}$ Y Scd
$\frac{w}{w} \frac{+}{+} \frac{UAS-cd8::GFP}{UAS-cd8::GFP}$ those will be light red eyes	$\frac{w}{w} \frac{+}{+} \frac{UAS-cd8::GFP}{UAS-cd8::GFP}$ X CyQ	$\frac{w}{w} \frac{+}{+} \frac{UAS-cd8::GFP}{UAS-cd8::GFP}$ Y CyQ	$\frac{w}{w} \frac{+}{+} \frac{UAS-cd8::GFP}{UAS-cd8::GFP}$ X Scd	$\frac{w}{w} \frac{+}{+} \frac{UAS-cd8::GFP}{UAS-cd8::GFP}$ Y Scd
$\frac{v}{v} \frac{+}{+} \frac{UAS-cd8::GFP;OR88a-Gal4}{UAS-cd8::GFP}$ those will be dark red eyes	$\frac{v}{v} \frac{+}{+} \frac{UAS-cd8::GFP;OR88a-Gal4}{UAS-cd8::GFP}$ X CyQ	$\frac{v}{v} \frac{+}{+} \frac{UAS-cd8::GFP;OR88a-Gal4}{UAS-cd8::GFP}$ Y CyQ	$\frac{v}{v} \frac{+}{+} \frac{UAS-cd8::GFP;OR88a-Gal4}{UAS-cd8::GFP}$ X Scd	$\frac{v}{v} \frac{+}{+} \frac{UAS-cd8::GFP;OR88a-Gal4}{UAS-cd8::GFP}$ Y Scd
		Red eyed/CyQ MALES And TMS (stubby)		

Pick CyQ males making sure they are dark red eyed + stubby

Red eye male fly selected for X2



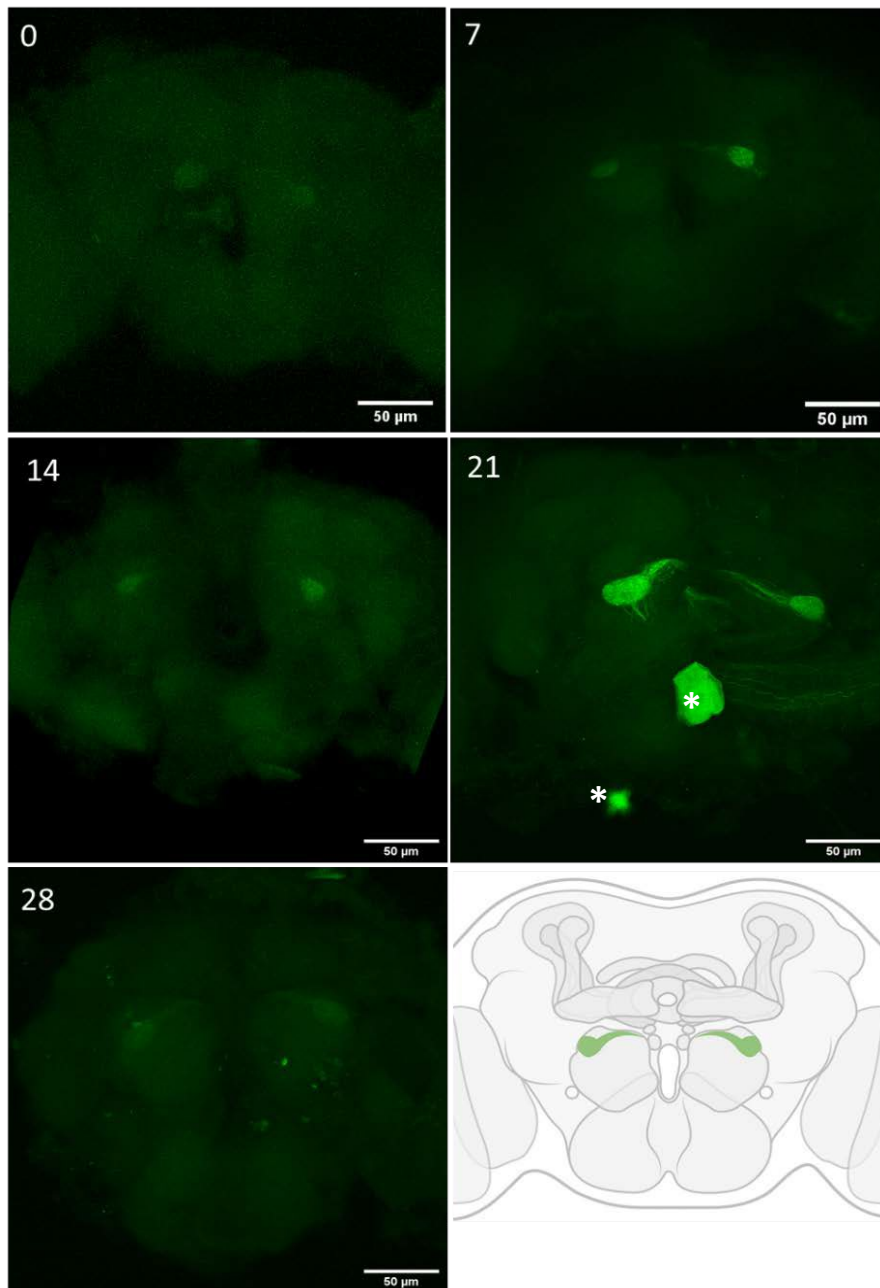
3) cross selected progeny from X2, generating small stocks of potentially recombinant males to test

$\frac{x}{x} \frac{+}{+} \frac{UAS-cd8::GFP;OR88a-Gal4}{UAS-cd8::GFP} \frac{TMS}{TM6} \times \frac{y}{y} \frac{+}{+} \frac{Scd}{Scd} \frac{TMS}{TM6}$
1 male only 5 female virgins

ChrII	Scd	Scd
$\frac{z}{z} \frac{+}{+} \frac{UAS-cd8::GFP;OR88a-Gal4}{UAS-cd8::GFP}$	$\frac{z}{z} \frac{+}{+} \frac{UAS-cd8::GFP;OR88a-Gal4}{Scd}$	$\frac{z}{z} \frac{+}{+} \frac{UAS-cd8::GFP;OR88a-Gal4}{Scd}$
CyQ	X	Scd CyQ

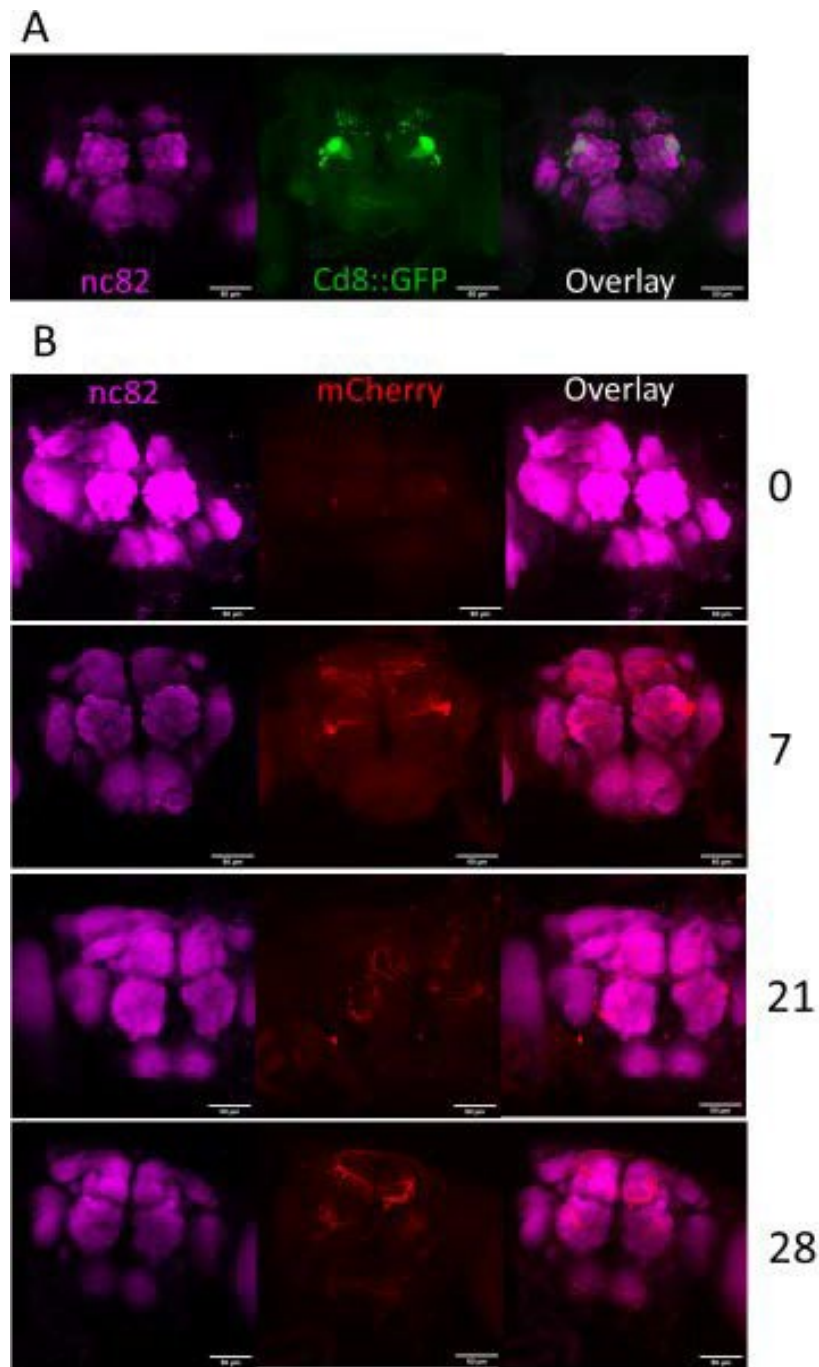
4) Potential recombinant male offspring from the above cross were then tested by looking for GFP expression in fly brains under confocal microscopy.

Appendix 1: Cross sheet outlining the steps taken to generate the recombinant Or88a.Gal4 UAS.cd8::GFP flies



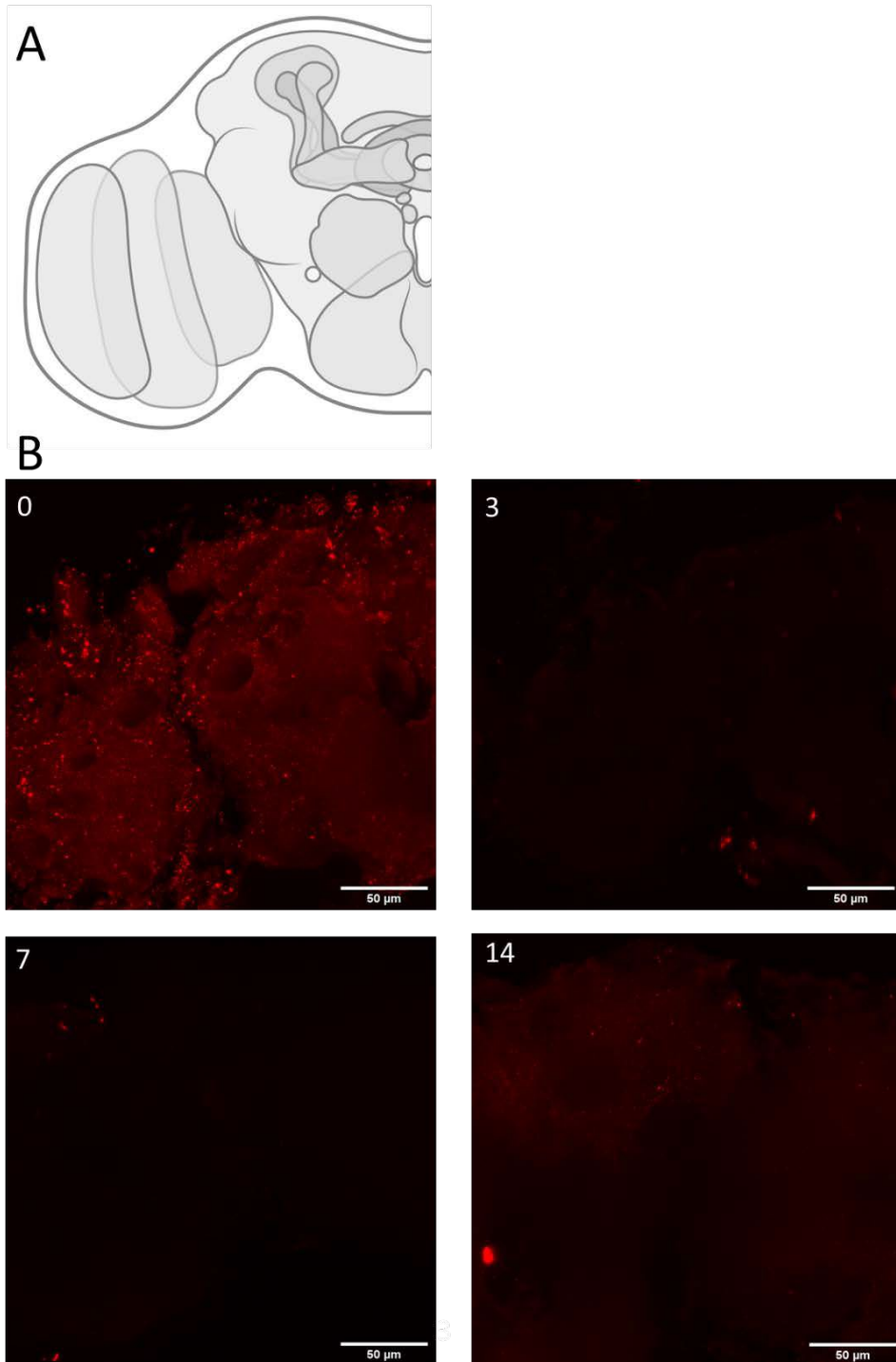
Appendix 2: Or88a.GAL4 driven UAS.cd8::GFP at 23°C over 28 days

A timecourse of Or88a.GAL4-driven UAS.cd8::GFP expression at weekly time points over 28 days shows that the GFP expression remains localised to the VA1d glomeruli. * Indicates surface contaminants that are autofluorescent in the GFP collection band.



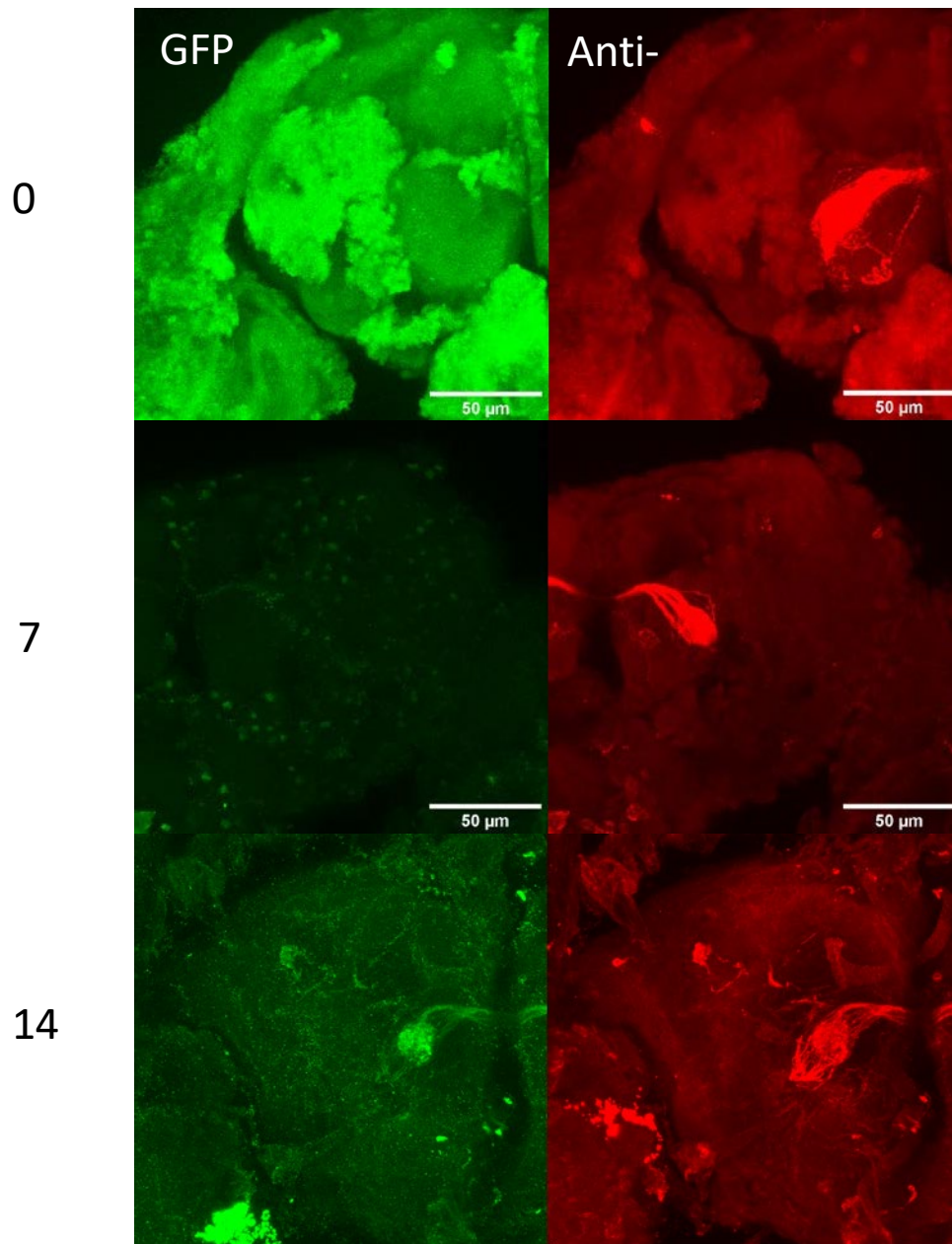
Appendix 3: Mz19.GAL4 driven UAS.mCherryTau^{ON4R} at 23°C over 28 days

To investigate if spread was possible in the downstream connection, we tested Mz19.GAL4 driven UAS.mCherryTau^{ON4R} over 28 days (B) and compared this to Mz19.GAL4 driven UAS.cd8::GFP (A). The Mz19 population only consists of 12 projection neurons whose cell bodies lie to the side and above the olfactory bulb and axons project to higher brain regions. However this driver also appears to be expressed in the prow and a number cell bodies in the higher brain region, suggesting that driver is not specific to the projection neurons (A). When mCherryTau^{ON4R} is expressed in Mz19 positive neurons the mCherry Tau signal appears localised to regions that were GFP positive in the separate Mz19.GAL4 UAS.cd8::GFP flies (B)



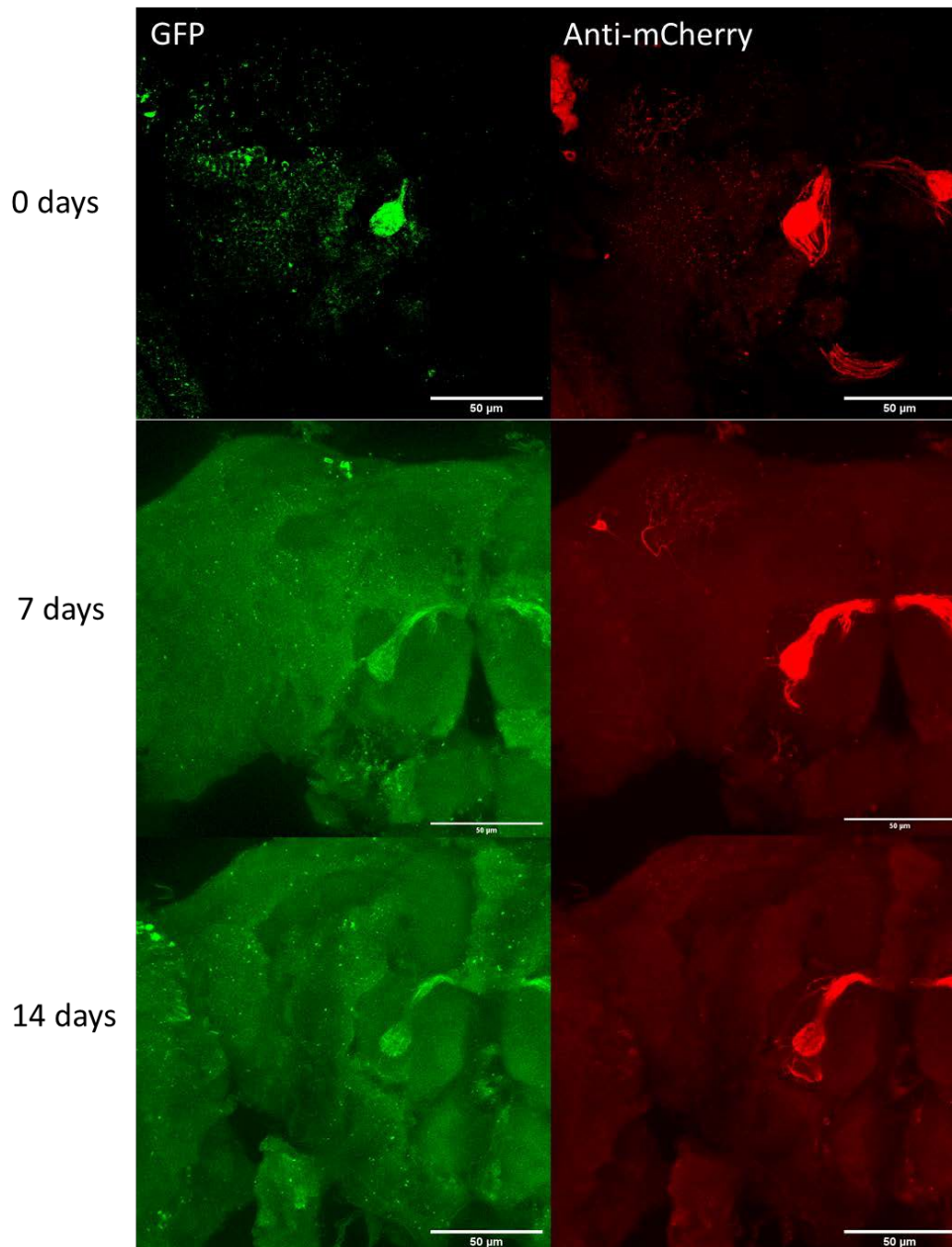
Appendix 4: Anti-mCherry staining of ORCO.GAL4 control brain at 29°C

IHC of a “Blank” ORCO.GAL4 expressing brain was carried out to account for any non-specific binding of either the primary Donkey anti-mCherry antibody or the secondary fluorescent Goat anti-Donkey Alexa 555 antibody conjugate. Schematic of the brain region imaged created with BioRender.com (A). A low, nonspecific background signal can be seen across the 14day time-course but staining of neurons and cell bodies does not appear (B).



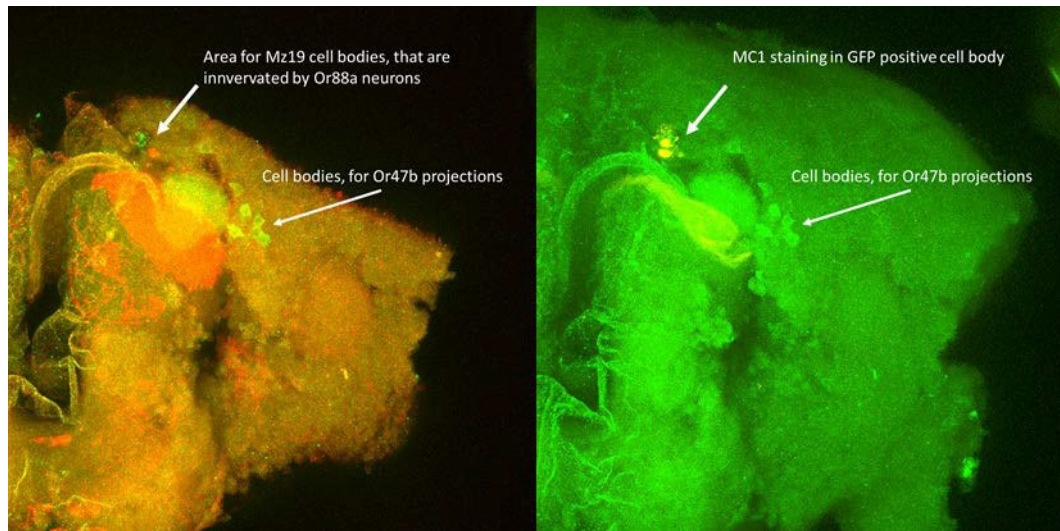
Appendix 5: Or88a.GAL4 driving UAS.mCherryTau^{ON4R} expression, offspring kept at 18°C until eclosion, then moved to 29°C

Staining with anti-GFP failed to detect any above background signal in brains until 14 days at which point the VA1d glomeruli and commissure become clear, meanwhile anti-mCherry staining reveals a similar pattern to those flies raised throughout life at 29°C, with day zero spread into other glomeruli. However in these flies a cell body that lights up in the lateral horn (indicated with white arrow) is also observable from day zero. This cell body matches that which is seen in section 4.3.3 which is a result of ectopic expression of the UAS.mCherryTau^{ON4R} construct.



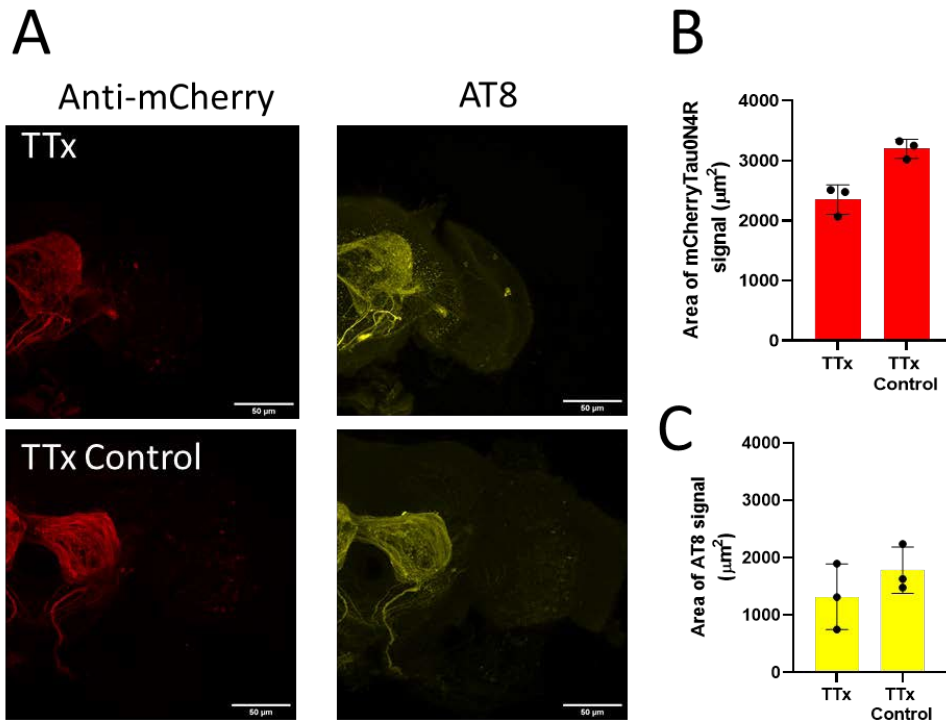
Appendix 6: Or88a.GAL4 recombined with UAS.cd8::GFP and crossed with untagged UAS.Tau^{ON4R}

Repeating the crosses for Figure 15 with an untagged version of the Tau construct used, inserted into the attP40 site. This repeat demonstrated the lateral horn cell body and invasion of other glomeruli within the antennal lobe that is seen with the mCherry tagged Tau^{ON4R} suggesting that the tag is not playing a key role in the observations reported.



Appendix 7: Tau expression driven in Or88a neurons whilst the postsynaptic partner Mz19 is marked with cd8::GFP

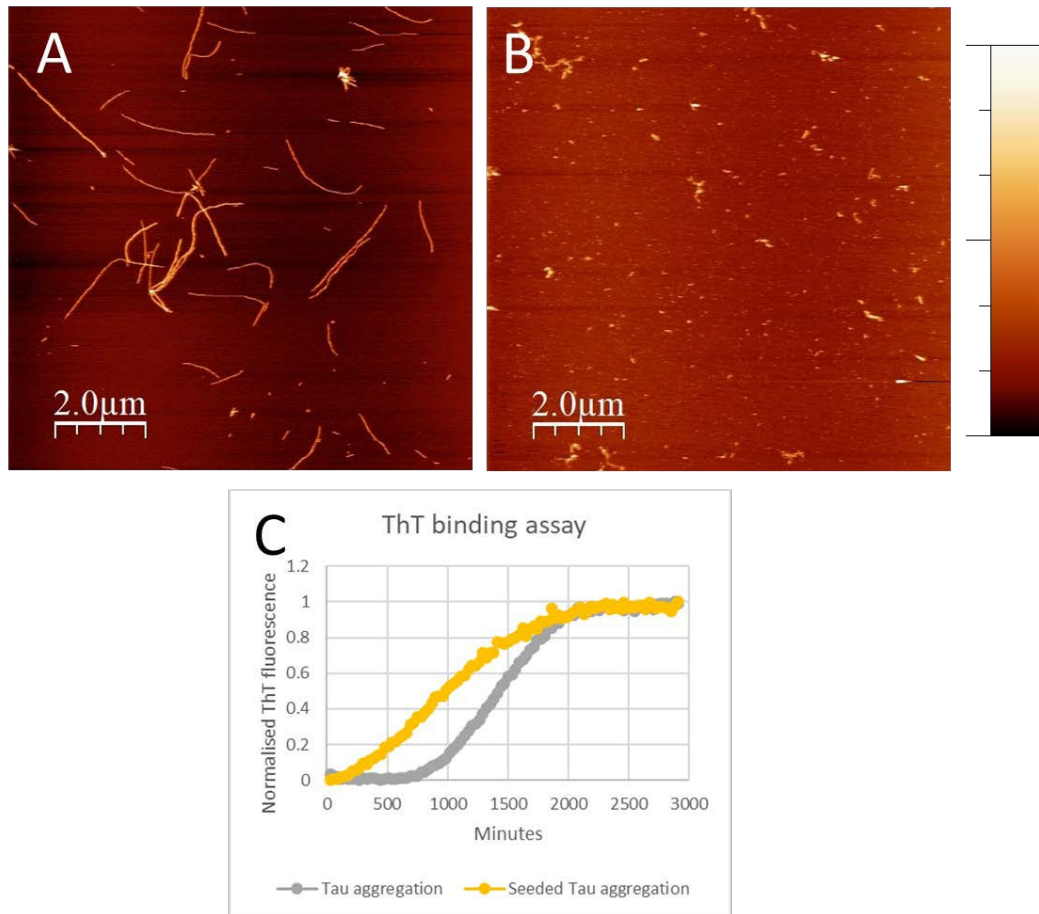
- A. When GFP and Tau signals are overlaid the Mz19 cell bodies that are innervated by the Or88a neurons appear to be apoptotic and contain Tau
- B. MC1 staining of this area corresponds with the area where these cell bodies are expected to be.



14

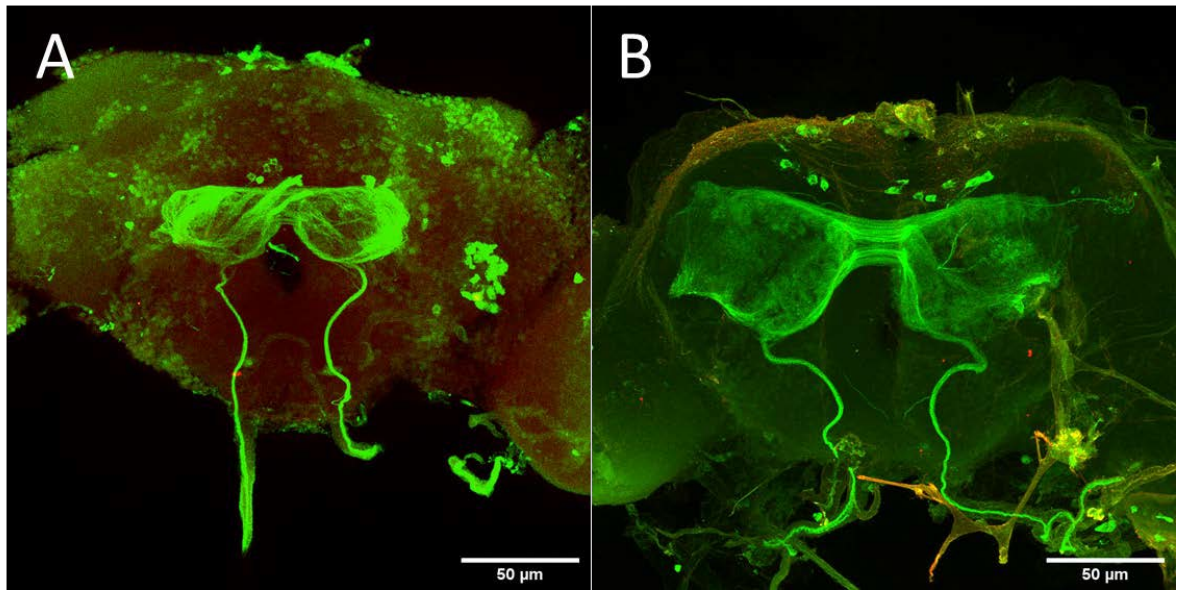
Appendix 8: Orco.Gal4, UAS.mCherryTau^{ON4R} recombinant flies crossed with Tetanus toxin.

Only a 14 day old time point was recovered from this cross for both the tetanus toxin (TTx) and its scrambled protein control (TTx control). In both cases almost all mCherry and AT8 signal was localised to the olfactory bulb and no significant difference was reported between the mCherryTau^{ON4R} coverage nor the AT8 coverage.



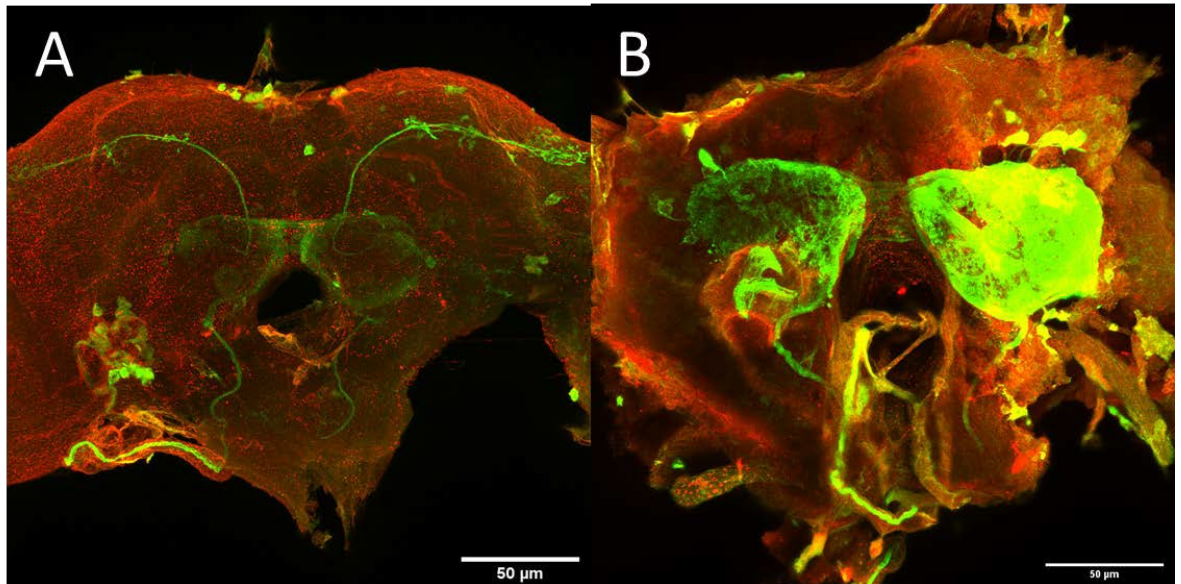
Appendix 9: Assays to determine seed competence of fibrils used for injection experiment, this work was carried out jointly with fellow lab member Dr George Devitt, UoS

- (A) Atomic force microscopy (AFM) image of Tau Fibrils formed by aggregation using Heparin as a co-factor. this 2D representation shows the long thin fibres formed from Tau aggregation. z scale bar = 0 – 15 nm, x scale bar = 2 μ m.
- (B) AFM image of Tau fibrils after sonication, this 2D image show small and fragments of the fibrils shown previously that have stronger seeding potential. These sonicated tau fibrils were used for *Drosophila* injection.
- (C) ThT seeding assay using the sonicated fibrils. ThT binds to tau fibrils as it aggregates providing a readout of aggregation. ThT fluorescence for Tau aggregation in the presence of heparin is shown in grey, whilst ThT fluorescence for seeded aggregation using sonicated tau seeds is shown in yellow. ThT kinetics demonstrate that sonicated tau fibrils used for *Drosophila* injection are seed competent and demonstrate that seeded aggregation is faster than aggregation with Heparin alone.



Appendix 10: Injections into the 3rd antennae did not result in uptake to the central brain of either Tau or Dextran

- A. Example image of a brain into which Tau has been injected into the 3rd antennal segment 1hr before dissection. No Dako anti-Tau signal is detected throughout the brain
- B. Example image of a brain into which Dextran dye conjugated with micro-Ruby has been injected into the 3rd antennal segment 1hr before dissection. No micro-Ruby signal is detected throughout the brain



Appendix 11: Control brains showing a lack of Dako staining in Buffer injected brains and the loss of Dextran from the brains after 24hrs.

- A. Example image of a brain into which the buffer in which the Tau seed is suspended in has been injected into the 2nd antennal segment 1hr before dissection. No Dako anti-Tau signal is detected throughout the brain
- B. Example image of a brain into which Dextran dye conjugated with micro-Ruby has been injected into the 2nd antennal segment 24hr before dissection. No micro-Ruby signal is detected throughout the brain

Bibliography

(2022). "Lecanemab." 2022, from <https://www.alzforum.org/therapeutics/lecanemab>.

Akwa, Y., C. Di Malta, F. Zallo, E. Gondard, A. Lunati, L. Z. Diaz-de-Grenu, A. Zampelli, A. Boiret, S. Santamaria, M. Martinez-Preciado, K. Cortese, J. H. Kordower, C. Matute, A. M. Lozano, E. Capetillo-Zarate, T. Vaccari, C. Settembre, E. E. Baulieu and D. Tampellini (2022). "Stimulation of synaptic activity promotes TFEB-mediated clearance of pathological MAPT/Tau in cellular and mouse models of tauopathies." *Autophagy*: 1-18.

Alfonso, T. B. and B. W. Jones (2002). "gcm2 promotes glial cell differentiation and is required with glial cells missing for macrophage development in *Drosophila*." *Dev Biol* **248**(2): 369-383.

Alonso, A., T. Zaidi, M. Novak, I. Grundke-Iqbal and K. Iqbal (2001). "Hyperphosphorylation induces self-assembly of tau into tangles of paired helical filaments/straight filaments." *Proc Natl Acad Sci U S A* **98**(12): 6923-6928.

Alyenbaawi, H., W. T. Allison and S. A. Mok (2020). "Prion-Like Propagation Mechanisms in Tauopathies and Traumatic Brain Injury: Challenges and Prospects." *Biomolecules* **10**(11).

Amatniek, J. C., W. A. Hauser, C. DelCastillo-Castaneda, D. M. Jacobs, K. Marder, K. Bell, M. Albert, J. Brandt and Y. Stern (2006). "Incidence and predictors of seizures in patients with Alzheimer's disease." *Epilepsia* **47**(5): 867-872.

Aqsa and S. Sarkar (2021). "Age dependent trans-cellular propagation of human tau aggregates in *Drosophila* disease models." *Brain Research* **1751**: 147207.

Arriagada, P. V., J. H. Growdon, E. T. Hedley-Whyte and B. T. Hyman (1992). "Neurofibrillary tangles but not senile plaques parallel duration and severity of Alzheimer's disease." *Neurology* **42**(3): 631-631.

Asai, H., S. Ikezu, S. Tsunoda, M. Medalla, J. Luebke, T. Haydar, B. Wolozin, O. Butovsky, S. Kügler and T. Ikezu (2015). "Depletion of microglia and inhibition of exosome synthesis halt tau propagation." *Nat Neurosci* **18**(11): 1584-1593.

Asai, H., S. Ikezu, S. Tsunoda, M. Medalla, J. Luebke, T. Haydar, B. Wolozin, O. Butovsky, S. Kügler and T. Ikezu (2015). "Depletion of microglia and inhibition of exosome synthesis halt tau propagation." *Nature Neuroscience* **18**(11): 1584-1593.

Aso, Y., K. Grübel, S. Busch, A. B. Friedrich, I. Siwanowicz and H. Tanimoto (2009). "The mushroom body of adult *Drosophila* characterized by GAL4 drivers." *J Neurogenet* **23**(1-2): 156-172.

Au - Nazario-Toole, A. E. and L. P. Au - Wu (2019). "Assessing the Cellular Immune Response of the Fruit Fly, *Drosophila melanogaster*, Using an In Vivo Phagocytosis Assay." *JoVE*(146): e59543.

Audouard, E., S. Houben, C. Masaracchia, Z. Yilmaz, V. Suain, M. Authelet, R. De Decker, L. Buée, A. Boom, K. Leroy, K. Ando and J.-P. Brion (2016). "High-Molecular-Weight Paired Helical Filaments from Alzheimer Brain Induces Seeding of Wild-Type Mouse Tau into an Argyrophilic 4R Tau Pathology in Vivo." *The American Journal of Pathology* **186**(10): 2709-2722.

Babcock, D. T. and B. Ganetzky (2015). "Non-cell autonomous cell death caused by transmission of Huntingtin aggregates in *Drosophila*." *Fly* **9**(3): 107-109.

Babcock, D. T. and B. Ganetzky (2015). "Transcellular spreading of huntingtin aggregates in the *Drosophila* brain." *Proceedings of the National Academy of Sciences of the United States of America* **112**(39): E5427-E5433.

- Bassett, S. S., D. M. Yousem, C. Cristinzio, I. Kusevic, M. A. Yassa, B. S. Caffo and S. L. Zeger (2006). "Familial risk for Alzheimer's disease alters fMRI activation patterns." Brain **129**(5): 1229-1239.
- Bassil, F., E. Meymand, H. Brown, H. Xu, T. Cox, S. Pattabhiraman, C. Maghames, Q. Wu, B. Zhang, J. Trojanowski and M. Y. Lee (2020). " α -Synuclein modulates tau spreading in mouse brains." Journal of Experimental Medicine **218**.
- Bellen, H. J., C. Tong and H. Tsuda (2010). "100 years of *Drosophila* research and its impact on vertebrate neuroscience: a history lesson for the future." Nature reviews. Neuroscience **11**(7): 514-522.
- Berdnik, D., T. Chihara, A. Couto and L. Luo (2006). "Wiring Stability of the Adult *Drosophila* Olfactory Circuit after Lesion." The Journal of Neuroscience **26**(13): 3367-3376.
- Biernat, J. and E.-M. Mandelkow (1999). "The Development of Cell Processes Induced by tau Protein Requires Phosphorylation of Serine 262 and 356 in the Repeat Domain and Is Inhibited by Phosphorylation in the Proline-rich Domains." Molecular Biology of the Cell **10**(3): 727-740.
- Boerner, J. and T. A. Godenschwege (2011). "Whole mount preparation of the adult *Drosophila* ventral nerve cord for giant fiber dye injection." J Vis Exp(52).
- Braak, H. and E. Braak (1991). "Neuropathological staging of Alzheimer-related changes." Acta neuropathologica **82**(4): 239-259.
- Bramblett, G. T., M. Goedert, R. Jakes, S. E. Merrick, J. Q. Trojanowski and V. M. Lee (1993). "Abnormal tau phosphorylation at Ser396 in Alzheimer's disease recapitulates development and contributes to reduced microtubule binding." Neuron **10**(6): 1089-1099.
- Brand, A. H. and N. Perrimon (1993). "Targeted gene expression as a means of altering cell fates and generating dominant phenotypes." development **118**(2): 401-415.
- Brandt, R. and G. Lee (1993). "Functional organization of microtubule-associated protein tau. Identification of regions which affect microtubule growth, nucleation, and bundle formation in vitro." Journal of Biological Chemistry **268**(5): 3414-3419.
- Brion, J. P., A. M. Couck, E. Passareiro and J. Flament-Durand (1985). "Neurofibrillary tangles of Alzheimer's disease: an immunohistochemical study." J Submicrosc Cytol **17**(1): 89-96.
- Brothers, H. M., M. L. Gosztyla and S. R. Robinson (2018). "The Physiological Roles of Amyloid- β Peptide Hint at New Ways to Treat Alzheimer's Disease." Frontiers in Aging Neuroscience **10**(118).
- Brunello, C. A., M. Merezko, R.-L. Uronen and H. J. Huttunen (2019). "Mechanisms of secretion and spreading of pathological tau protein." Cellular and Molecular Life Sciences. 2020 May;77(9):1721-1744. doi: 10.1007/s00018-019-03349-1. Epub 2019 Oct 30. PMID: 31667556; PMCID: PMC7190606.
- Busche, M. A., X. Chen, H. A. Henning, J. Reichwald, M. Staufienbiel, B. Sakmann and A. Konnerth (2012). "Critical role of soluble amyloid- β for early hippocampal hyperactivity in a mouse model of Alzheimer's disease." Proceedings of the National Academy of Sciences **109**(22): 8740-8745.
- Busche, M. A., G. Eichhoff, H. Adelsberger, D. Abramowski, K.-H. Wiederhold, C. Haass, M. Staufienbiel, A. Konnerth and O. Garaschuk (2008). "Clusters of hyperactive neurons near amyloid plaques in a mouse model of Alzheimer's disease." Science **321**(5896): 1686-1689.
- Busche, M. A., S. Wegmann, S. Dujardin, C. Commins, J. Schiantarelli, N. Klickstein, T. V. Kamath, G. A. Carlson, I. Nelken and B. T. Hyman (2019). "Tau impairs neural circuits, dominating amyloid- β effects, in Alzheimer models in vivo." Nature neuroscience **22**(1): 57-64.
- Butner, K. and M. W. Kirschner (1991). "Tau protein binds to microtubules through a flexible array

of distributed weak sites." The Journal of cell biology **115**(3): 717-730.

Bykhovskaia, M. and A. Vasin (2017). "Electrophysiological analysis of synaptic transmission in *Drosophila*." Wiley Interdiscip Rev Dev Biol **6**(5).

Calafate, S., A. Buist, K. Miskiewicz, V. Vijayan, G. Daneels, B. de Strooper, J. de Wit, P. Verstreken and D. Moechars (2015). "Synaptic Contacts Enhance Cell-to-Cell Tau Pathology Propagation." Cell Reports **11**(8): 1176-1183.

Calafate, S., W. Flavin, P. Verstreken and D. Moechars (2016). "Loss of Bin1 promotes the propagation of tau pathology." Cell reports **17**(4): 931-940.

Cao, L.-H., D. Yang, W. Wu, X. Zeng, B.-Y. Jing, M.-T. Li, S. Qin, C. Tang, Y. Tu and D.-G. Luo (2017). "Odor-evoked inhibition of olfactory sensory neurons drives olfactory perception in *Drosophila*." Nature Communications **8**(1): 1357.

Carmine-Simmen, K., T. Proctor, J. Tschäpe, B. Poeck, T. Triphan, R. Strauss and D. Kretzschmar (2009). "Neurotoxic effects induced by the *Drosophila* amyloid- β peptide suggest a conserved toxic function." Neurobiology of disease **33**(2): 274-281.

Cash, A. D., G. Aliev, S. L. Siedlak, A. Nunomura, H. Fujioka, X. Zhu, A. K. Raina, H. V. Vinters, M. Tabaton and A. B. Johnson (2003). "Microtubule reduction in Alzheimer's disease and aging is independent of τ filament formation." The American journal of pathology **162**(5): 1623-1627.

Celone, K. A., V. D. Calhoun, B. C. Dickerson, A. Atri, E. F. Chua, S. L. Miller, K. DePeau, D. M. Rentz, D. J. Selkoe and D. Blacker (2006). "Alterations in memory networks in mild cognitive impairment and Alzheimer's disease: an independent component analysis." Journal of Neuroscience **26**(40): 10222-10231.

Chai, X., J. L. Dage and M. Citron (2012). "Constitutive secretion of tau protein by an unconventional mechanism." Neurobiology of Disease **48**(3): 356-366.

Chen, D., J. Yang, Z. Xiao, S. Zhou and L. Wang (2021). "A diet-induced type 2 diabetes model in *Drosophila*." Science China Life Sciences **64**(2): 326-329.

Chen, J., Y. Kanai, N. J. Cowan and N. Hirokawa (1992). "Projection domains of MAP2 and tau determine spacings between microtubules in dendrites and axons." Nature **360**(6405): 674-677.

Chen, Q., Z. Zhou, L. Zhang, Y. Wang, Y.-w. Zhang, M. Zhong, S.-c. Xu, C.-h. Chen, L. Li and Z.-p. Yu (2012). "Tau protein is involved in morphological plasticity in hippocampal neurons in response to BDNF." Neurochemistry international **60**(3): 233-242.

Chételat, G. (2013). "Alzheimer disease: A β -independent processes-rethinking preclinical AD." Nature reviews. Neurology **9**(3): 123-124.

Chiang, M. H., S. M. Ho, H. Y. Wu, Y. C. Lin, W. H. Tsai, T. Wu, C. H. Lai and C. L. Wu (2022). "*Drosophila* Model for Studying Gut Microbiota in Behaviors and Neurodegenerative Diseases." Biomedicines **10**(3).

Chiarini, A., U. Armato, E. Gardenal, L. Gui and I. Dal Prà (2017). "Amyloid β -Exposed Human Astrocytes Overproduce Phospho-Tau and Overrelease It within Exosomes, Effects Suppressed by Calcilytic NPS 2143—Further Implications for Alzheimer's Therapy." Frontiers in Neuroscience **11**(217).

Cho, J. H. and G. V. Johnson (2004). "Primed phosphorylation of tau at Thr231 by glycogen synthase kinase 3 β (GSK3 β) plays a critical role in regulating tau's ability to bind and stabilize microtubules." Journal of neurochemistry **88**(2): 349-358.

- Chou, Y.-H., M. L. Spletter, E. Yaksi, J. C. S. Leong, R. I. Wilson and L. Luo (2010). "Diversity and wiring variability of olfactory local interneurons in the *Drosophila* antennal lobe." Nature Neuroscience **13**(4): 439-449.
- Christianson, H. C. and M. Belting (2014). "Heparan sulfate proteoglycan as a cell-surface endocytosis receptor." Matrix Biology **35**: 51-55.
- Cicognola, C., G. Brinkmalm, J. Wahlgren, E. Portelius, J. Gobom, N. C. Cullen, O. Hansson, L. Parnetti, R. Constantinescu and K. Wildsmith (2019). "Novel tau fragments in cerebrospinal fluid: relation to tangle pathology and cognitive decline in Alzheimer's disease." Acta neuropathologica **137**(2): 279-296.
- Cieri, D., M. Vicario, F. Vallese, B. D'Orsi, P. Berto, A. Grinzato, C. Catoni, D. De Stefani, R. Rizzuto, M. Brini and T. Cali (2018). "Tau localises within mitochondrial sub-compartments and its caspase cleavage affects ER-mitochondria interactions and cellular Ca²⁺ handling." Biochimica Et Biophysica Acta-Molecular Basis of Disease **1864**(10): 3247-3256.
- Clavaguera, F., H. Akatsu, G. Fraser, R. A. Crowther, S. Frank, J. Hench, A. Probst, D. T. Winkler, J. Reichwald, M. Staufenbiel, B. Ghetti, M. Goedert and M. Tolnay (2013). "Brain homogenates from human tauopathies induce tau inclusions in mouse brain." Proceedings of the National Academy of Sciences **110**(23): 9535-9540.
- Clavaguera, F., H. Akatsu, G. Fraser, R. A. Crowther, S. Frank, J. Hench, A. Probst, D. T. Winkler, J. Reichwald, M. Staufenbiel, B. Ghetti, M. Goedert and M. Tolnay (2013). "Brain homogenates from human tauopathies induce tau inclusions in mouse brain." Proc Natl Acad Sci U S A **110**(23): 9535-9540.
- Clavaguera, F., T. Bolmont, R. A. Crowther, D. Abramowski, S. Frank, A. Probst, G. Fraser, A. K. Stalder, M. Beibel and M. Staufenbiel (2009). "Transmission and spreading of tauopathy in transgenic mouse brain." Nature cell biology **11**(7): 909-913.
- Colodner, K. J. and M. B. Feany (2010). "Glial fibrillary tangles and JAK/STAT-mediated glial and neuronal cell death in a *Drosophila* model of glial tauopathy." Journal of Neuroscience **30**(48): 16102-16113.
- Colonna, M. and O. Butovsky (2017). "Microglia Function in the Central Nervous System During Health and Neurodegeneration." Annu Rev Immunol **35**: 441-468.
- Costello, A., N. T. Lao, C. Gallagher, B. Capella Roca, L. A. N. Julius, S. Suda, J. Ducrée, D. King, R. Wagner, N. Barron and M. Clynes (2019). "Leaky Expression of the TET-On System Hinders Control of Endogenous miRNA Abundance." Biotechnol J **14**(3): e1800219.
- Cubinková, V., B. Valachová, V. Brezováková, R. Szabó, I. Zimová, Z. Kostecká and S. Jadhav (2017). "Next generation tau models in Alzheimer's disease research - virus based gene delivery systems." Acta Virol **61**(1): 13-21.
- Cullen, W. K., Y. H. Suh, R. Anwyl and M. J. Rowan (1997). "Block of LTP in rat hippocampus in vivo by beta-amyloid precursor protein fragments." Neuroreport **8**(15): 3213-3217.
- Cummings, J., P. Aisen, C. Lemere, A. Atri, M. Sabbagh and S. Salloway (2021). "Aducanumab produced a clinically meaningful benefit in association with amyloid lowering." Alzheimer's research & therapy **13**(1): 98-98.
- Das, A., S. Sen, R. Lichtneckert, R. Okada, K. Ito, V. Rodrigues and H. Reichert (2008). "*Drosophila* olfactory local interneurons and projection neurons derive from a common neuroblast lineage specified by the empty spiracles gene." Neural Dev **3**: 33.

- Das, A., S. Sen, R. Lichtneckert, R. Okada, K. Ito, V. Rodrigues and H. Reichert (2008). "*Drosophila* olfactory local interneurons and projection neurons derive from a common neuroblast lineage specified by the empty spiracles gene." Neural Development **3**(1): 33.
- Dassie, E., M. R. Andrews, J. C. Bensadoun, M. Cacquevel, B. L. Schneider, P. Aebischer, F. S. Wouters, J. C. Richardson, I. Hussain, D. R. Howlett, M. G. Spillantini and J. W. Fawcett (2013). "Focal expression of adeno-associated viral-mutant tau induces widespread impairment in an APP mouse model." Neurobiol Aging **34**(5): 1355-1368.
- Dawson, H. N., V. Cantillana, M. Jansen, H. Wang, M. P. Vitek, D. M. Wilcock, J. R. Lynch and D. T. Laskowitz (2010). "Loss of tau elicits axonal degeneration in a mouse model of Alzheimer's disease." Neuroscience **169**(1): 516-531.
- de Calignon, A., M. Polydoro, M. Suárez-Calvet, C. William, D. H. Adamowicz, K. J. Kopeikina, R. Pitstick, N. Sahara, K. H. Ashe, G. A. Carlson, T. L. Spires-Jones and B. T. Hyman (2012). "Propagation of tau pathology in a model of early Alzheimer's disease." Neuron **73**(4): 685-697.
- de Calignon, A., M. Polydoro, M. Suárez-Calvet, C. William, David H. Adamowicz, Kathy J. Kopeikina, R. Pitstick, N. Sahara, Karen H. Ashe, George A. Carlson, Tara L. Spires-Jones and Bradley T. Hyman (2012). "Propagation of Tau Pathology in a Model of Early Alzheimer's Disease." Neuron **73**(4): 685-697.
- Dejanovic, B., M. A. Huntley, A. De Mazière, W. J. Meilandt, T. Wu, K. Srinivasan, Z. Jiang, V. Gandham, B. A. Friedman and H. Ngu (2018). "Changes in the synaptic proteome in tauopathy and rescue of tau-induced synapse loss by C1q antibodies." Neuron **100**(6): 1322-1336. e1327.
- Devitt, G., A. Crisford, W. Rice, H. A. Weismiller, Z. Fan, C. Commins, B. T. Hyman, M. Margittai, S. Mahajan and A. Mudher (2021). "Conformational fingerprinting of tau variants and strains by Raman spectroscopy." RSC Advances **11**(15): 8899-8915.
- Devkota, S., T. D. Williams and M. S. Wolfe (2021). "Familial Alzheimer's disease mutations in amyloid protein precursor alter proteolysis by γ -secretase to increase amyloid β -peptides of ≥ 45 residues." Journal of Biological Chemistry **296**.
- Doherty, J., M. A. Logan, Ö. E. Taşdemir and M. R. Freeman (2009). "Ensheathing Glia Function as Phagocytes in the Adult *Drosophila* Brain." The Journal of Neuroscience **29**(15): 4768- 4781.
- Dolan, M.-J., S. Frechter, A. S. Bates, C. Dan, P. Huoviala, R. J. V. Roberts, P. Schlegel, S. Dhawan, R. Tabano, H. Dionne, C. Christoforou, K. Close, B. Sutcliffe, B. Giuliani, F. Li, M. Costa, G. Ihrke, G. W. Meissner, D. D. Bock, Y. Aso, G. M. Rubin and G. S. X. E. Jefferis (2019). "Neurogenetic dissection of the *Drosophila* lateral horn reveals major outputs, diverse behavioural functions, and interactions with the mushroom body." eLife **8**: e43079.
- Donnelly, K. M., O. R. DeLorenzo, A. D. Zaya, G. E. Pisano, W. M. Thu, L. Luo, R. R. Kopito and M. M. Panning Pearce (2020). "Phagocytic glia are obligatory intermediates in transmission of mutant huntingtin aggregates across neuronal synapses." Elife **9**. 2020 May 28;9:e58499. doi: 10.7554/eLife.58499. PMID: 32463364; PMCID: PMC7297539.
- Duan, Q., R. Estrella, A. Carson, Y. Chen and P. C. Volkan (2022). "*Drosophila* attP40 background alters glomerular organization of the olfactory receptor neuron terminals." bioRxiv: 2022.2006.2016.496338.
- Dugger, B. N. and D. W. Dickson (2017). "Pathology of Neurodegenerative Diseases." Cold Spring Harb Perspect Biol **9**(7).
- Dujardin, S., S. Bégard, R. Caillierez, C. Lachaud, S. Carrier, S. Lieger, J. A. Gonzalez, V. Deramecourt, N. Déglon, C.-A. Maurice, M. P. Frosch, B. T. Hyman, M. Colin and L. Buée (2018).

- "Different tau species lead to heterogeneous tau pathology propagation and misfolding." Acta Neuropathologica Communications **6**(1): 132.
- Dujardin, S., S. Bégard, R. Caillierez, C. Lachaud, L. Delattre, S. Carrier, A. Loyens, M.-C. Galas, L. Bousset and R. Melki (2014). "Ectosomes: a new mechanism for non-exosomal secretion of tau protein." PloS one **9**(6): e100760.
- Dujardin, S., S. Bégard, R. Caillierez, C. Lachaud, L. Delattre, S. Carrier, A. Loyens, M.-C. Galas, L. Bousset, R. Melki, G. Aurégan, P. Hantraye, E. Brouillet, L. Buée and M. Colin (2014). "Ectosomes: A New Mechanism for Non-Exosomal Secretion of Tau Protein." PLOS ONE **9**(6): e100760.
- Dujardin, S., C. Commins, A. Lathuiliere, P. Beerepoot, A. R. Fernandes, T. V. Kamath, M. B. De Los Santos, N. Klickstein, D. L. Corjuc, B. T. Corjuc, P. M. Dooley, A. Viode, D. H. Oakley, B. D. Moore, K. Mullin, D. Jean-Gilles, R. Clark, K. Atchison, R. Moore, L. B. Chibnik, R. E. Tanzi, M. P. Frosch, A. Serrano-Pozo, F. Elwood, J. A. Steen, M. E. Kennedy and B. T. Hyman (2020). "Tau molecular diversity contributes to clinical heterogeneity in Alzheimer's disease." Nature Medicine **26**(8): 1256-1263.
- Dujardin, S., K. Lécolle, R. Caillierez, S. Bégard, N. Zommer, C. Lachaud, S. Carrier, N. Dufour, G. Aurégan, J. Winderickx, P. Hantraye, N. Déglon, M. Colin and L. Buée (2014). "Neuron-to-neuron wild-type Tau protein transfer through a trans-synaptic mechanism: relevance to sporadic tauopathies." Acta Neuropathologica Communications **2**(1): 14.
- Dujardin, S., K. Lécolle, R. Caillierez, S. Bégard, N. Zommer, C. Lachaud, S. Carrier, N. Dufour, G. Aurégan, J. Winderickx, P. Hantraye, N. Déglon, M. Colin and L. Buée (2014). "Neuron-to-neuron wild-type Tau protein transfer through a trans-synaptic mechanism: relevance to sporadic tauopathies." Acta Neuropathol Commun **2**: 14.
- Duyckaerts, C., T. Uchihara, D. Seilhean, Y. He and J.-J. Hauw (1997). "Dissociation of Alzheimer type pathology in a disconnected piece of cortex." Acta neuropathologica **93**(5): 501-507.
- Dweck, H. K., S. A. Ebrahim, M. Thoma, A. A. Mohamed, I. W. Keeseey, F. Trona, S. Lavista-Llanos, A. Svatoš, S. Sachse, M. Knaden and B. S. Hansson (2015). "Pheromones mediating copulation and attraction in *Drosophila*." Proc Natl Acad Sci U S A **112**(21): E2829-2835.
- Eberl, D. F. and G. Boekhoff-Falk (2007). "Development of Johnston's organ in *Drosophila*." Int J Dev Biol **51**(6-7): 679-687.
- Eidenmüller, J., T. Fath, T. Maas, M. Pool, E. Sontag and R. Brandt (2001). "Phosphorylation-mimicking glutamate clusters in the proline-rich region are sufficient to simulate the functional deficiencies of hyperphosphorylated tau protein." The Biochemical journal **357**(Pt 3): 759-767.
- Eliason, J., A. Afify, C. Potter and I. Matsumura (2018). "A GAL80 Collection To Inhibit GAL4 Transgenes in *Drosophila* Olfactory Sensory Neurons." G3 (Bethesda) **8**(11): 3661-3668.
- Evans, L. D., T. Wassmer, G. Fraser, J. Smith, M. Perkinson, A. Billinton and F. J. Livesey (2018). "Extracellular Monomeric and Aggregated Tau Efficiently Enter Human Neurons through Overlapping but Distinct Pathways." Cell Reports **22**(13): 3612-3624.
- Falcon, B., A. Cavallini, R. Angers, S. Glover, T. K. Murray, L. Barnham, S. Jackson, M. J. O'Neill, A. M. Isaacs, M. L. Hutton, P. G. Szekeres, M. Goedert and S. Bose (2015). "Conformation determines the seeding potencies of native and recombinant Tau aggregates." The Journal of biological chemistry **290**(2): 1049-1065.
- Falcon, B., W. Zhang, A. G. Murzin, G. Murshudov, H. J. Garringer, R. Vidal, R. A. Crowther, B. Ghetti, S. H. W. Scheres and M. Goedert (2018). "Structures of filaments from Pick's disease reveal a novel tau protein fold." Nature **561**(7721): 137-140.

Falcon, B., J. Zivanov, W. Zhang, A. G. Murzin, H. J. Garringer, R. Vidal, R. A. Crowther, K. L. Newell, B. Ghetti, M. Goedert and S. H. W. Scheres (2019). "Novel tau filament fold in chronic traumatic encephalopathy encloses hydrophobic molecules." Nature **568**(7752): 420-423.

Fan, D.-Y. and Y.-J. Wang (2019). "Early Intervention in Alzheimer's Disease: How Early is Early Enough?" Neuroscience Bulletin. 2020 Feb;36(2):195-197. doi: 10.1007/s12264-019-00429-x. Epub 2019 Sep 7. PMID: 31494835; PMCID: PMC6977799.

Feany, M. B. and W. W. Bender (2000). "A *Drosophila* model of Parkinson's disease." Nature **404**(6776): 394-398.

Fichou, Y., Y. K. Al-Hilaly, F. Devred, C. Smet-Nocca, P. O. Tsvetkov, J. Verelst, J. Winderickx, N. Geukens, E. Vanmechelen, A. Perrotin, L. Serpell, B. J. Hanseeuw, M. Medina, L. Buée and I. Landrieu (2019). "The elusive tau molecular structures: can we translate the recent breakthroughs into new targets for intervention?" Acta Neuropathologica Communications **7**(1): 31.

Filippini, N., B. J. MacIntosh, M. G. Hough, G. M. Goodwin, G. B. Frisoni, S. M. Smith, P. M. Matthews, C. F. Beckmann and C. E. Mackay (2009). "Distinct patterns of brain activity in young carriers of the APOE- ϵ 4 allele." Proceedings of the National Academy of Sciences **106**(17): 7209-7214.

Fischer, I. and P. W. Baas (2020). "Resurrecting the mysteries of big tau." Trends in neurosciences **43**(7): 493-504.

Fishilevich, E. and L. B. Vosshall (2005). "Genetic and Functional Subdivision of the *Drosophila* Antennal Lobe." Current Biology **15**(17): 1548-1553.

Fitzpatrick, A. W. P., B. Falcon, S. He, A. G. Murzin, G. Murshudov, H. J. Garringer, R. A. Crowther, B. Ghetti, M. Goedert and S. H. W. Scheres (2017). "Cryo-EM structures of tau filaments from Alzheimer's disease." Nature **547**(7662): 185-190.

Folwell, J., C. M. Cowan, K. K. Ubhi, H. Shiabh, T. A. Newman, D. Shepherd and A. Mudher (2010). "A β exacerbates the neuronal dysfunction caused by human tau expression in a *Drosophila* model of Alzheimer's disease." Experimental Neurology **223**(2): 401-409.

Franzmeier, N., M. Brendel, L. Beyer, L. Slemann, G. G. Kovacs, T. Arzberger, C. Kurz, G. Respondek, M. J. Lukic, D. Biel, A. Rubinski, L. Frontzkowski, S. Hummel, A. Müller, A. Finze, C. Palleis, E. Joseph, E. Weidinger, S. Katzdobler, M. Song, G. Biechele, M. Kern, M. Scheifele, B.-S. Rauchmann, R. Perneczky, M. Rullman, M. Patt, A. Schildan, H. Barthel, O. Sabri, J. J. Rumpf, M. L. Schroeter, J. Classen, V. Villemagne, J. Seibyl, A. W. Stephens, E. B. Lee, D. G. Coughlin, A. Giese, M. Grossman, C. T. McMillan, E. Gelpi, L. Molina-Porcel, Y. Compta, J. C. van Swieten, L. D. Laats, C. Troakes, S. Al-Sarraj, J. L. Robinson, S. X. Xie, D. J. Irwin, S. Roeber, J. Herms, M. Simons, P. Bartenstein, V. M. Lee, J. Q. Trojanowski, J. Levin, G. Höglinger and M. Ewers (2022). "Tau deposition patterns are associated with functional connectivity in primary tauopathies." Nature Communications **13**(1): 1362.

Frost, B., R. L. Jacks and M. I. Diamond (2009). "Propagation of Tau Misfolding from the Outside to the Inside of a Cell." Journal of Biological Chemistry **284**(19): 12845-12852.

Gamblin, T. C., F. Chen, A. Zambrano, A. Abraha, S. Lagalwar, A. L. Guillozet, M. Lu, Y. Fu, F. Garcia-Sierra, N. LaPointe, R. Miller, R. W. Berry, L. I. Binder and V. L. Cryns (2003). "Caspase cleavage of tau: Linking amyloid and neurofibrillary tangles in Alzheimer's disease." Proceedings of the National Academy of Sciences **100**(17): 10032-10037.

Gauthier-Kemper, A., C. Weissmann, N. Golovyashkina, Z. Sebö-Lemke, G. Drewes, V. Gerke, J. J. Heinisch and R. Brandt (2011). "The frontotemporal dementia mutation R406W blocks tau's interaction with the membrane in an annexin A2-dependent manner." The Journal of cell biology **192**(4): 647-661.

- Ghatak, S., N. Dolatabadi, D. Trudler, X. Zhang, Y. Wu, M. Mohata, R. Ambasudhan, M. Talantova and S. A. Lipton (2019). "Mechanisms of hyperexcitability in Alzheimer's disease hiPSC-derived neurons and cerebral organoids vs isogenic controls." Elife **8**: e50333.
- Gibbons, G. S., R. A. Banks, B. Kim, H. Xu, L. Changolkar, S. N. Leight, D. M. Riddle, C. Li, R. J. Gathagan, H. J. Brown, B. Zhang, J. Q. Trojanowski and V. M. Lee (2017). "GFP-Mutant Human Tau Transgenic Mice Develop Tauopathy Following CNS Injections of Alzheimer's Brain-Derived Pathological Tau or Synthetic Mutant Human Tau Fibrils." J Neurosci **37**(47): 11485-11494.
- Goedert, M., R. Jakes, R. Crowther, J. Six, U. Lübke, M. Vandermeeren, P. Cras, J. Trojanowski and V. Lee (1993). "The abnormal phosphorylation of tau protein at Ser-202 in Alzheimer disease recapitulates phosphorylation during development." Proceedings of the National Academy of Sciences **90**(11): 5066-5070.
- Goedert, M., R. Jakes, M. Spillantini, M. Hasegawa, M. Smith and R. Crowther (1996). "Assembly of microtubule-associated protein tau into Alzheimer-like filaments induced by sulphated glycosaminoglycans." Nature **383**(6600): 550-553.
- Goedert, M., M. G. Spillantini, N. J. Cairns and R. A. Crowther (1992). "Tau proteins of Alzheimer paired helical filaments: abnormal phosphorylation of all six brain isoforms." Neuron **8**(1): 159-168.
- Goedert, M., M. G. Spillantini, R. Jakes, D. Rutherford and R. A. Crowther (1989). "Multiple isoforms of human microtubule-associated protein tau: sequences and localization in neurofibrillary tangles of Alzheimer's disease." Neuron **3**(4): 519-526.
- Götz, J., F. Chen, J. van Dorpe and R. Nitsch (2001). "Formation of Neurofibrillary Tangles in P301L Tau Transgenic Mice Induced by A β 42 Fibrils: It takes 42 to tangle.(From Science)." Science of Aging Knowledge Environment **2001**(1):
- Green, K. N., J. S. Steffan, H. Martinez-Coria, X. Sun, S. S. Schreiber, L. M. Thompson and F. M. LaFerla (2008). "Nicotinamide restores cognition in Alzheimer's disease transgenic mice via a mechanism involving sirtuin inhibition and selective reduction of Thr231-phosphotau." Journal of Neuroscience **28**(45): 11500-11510.
- Grundke-Iqbal, I., K. Iqbal, M. Quinlan, Y. C. Tung, M. S. Zaidi and H. M. Wisniewski (1986). "Microtubule-associated protein tau. A component of Alzheimer paired helical filaments." J Biol Chem **261**(13): 6084-6089.
- Grundke-Iqbal, I., K. Iqbal, Y. C. Tung, M. Quinlan, H. M. Wisniewski and L. I. Binder (1986). "Abnormal phosphorylation of the microtubule-associated protein tau (tau) in Alzheimer cytoskeletal pathology." Proc Natl Acad Sci U S A **83**(13): 4913-4917.
- Grundke-Iqbal, I., K. Iqbal, Y. C. Tung, M. Quinlan, H. M. Wisniewski and L. I. Binder (1986). "Abnormal phosphorylation of the microtubule-associated protein tau (tau) in Alzheimer cytoskeletal pathology." Proceedings of the National Academy of Sciences of the United States of America **83**(13): 4913-4917.
- Gunawardena, S., L.-S. Her, R. G. Bruschi, R. A. Laymon, I. R. Niesman, B. Gordesky-Gold, L. Sintasath, N. M. Bonini and L. S. B. Goldstein (2003). "Disruption of Axonal Transport by Loss of Huntingtin or Expression of Pathogenic PolyQ Proteins in *Drosophila*." Neuron **40**(1): 25-40.
- Guo, T., W. Noble and D. P. Hanger (2017). "Roles of tau protein in health and disease." Acta Neuropathol **133**(5): 665-704.

- Haass, C. and E. Mandelkow (2010). "Fyn-tau-amyloid: a toxic triad." Cell **142**(3): 356-358.
- Hallinan, G. I., A. P. Pitera, P. Patel, J. West and K. Deinhardt (2019). "Minimalistic in vitro systems for investigating tau pathology." Journal of Neuroscience Methods **319**: 69-76.
- Hallinan, G. I., M. Vargas-Caballero, J. West and K. Deinhardt (2019). "Tau Misfolding Efficiently Propagates between Individual Intact Hippocampal Neurons." The Journal of Neuroscience **39**(48): 9623-9632.
- Hanger, D. P., B. H. Anderton and W. Noble (2009). "Tau phosphorylation: the therapeutic challenge for neurodegenerative disease." Trends in Molecular Medicine **15**(3): 112-119.
- Heidary, G. and M. E. Fortini (2001). "Identification and characterization of the *Drosophila* tau homolog." Mechanisms of development **108**(1-2): 171-178.
- Hodge, J. J. (2009). "Ion channels to inactivate neurons in *Drosophila*." Front Mol Neurosci **2**: 13.
- Hoffmann, N. A., M. M. Dorostkar, S. Blumenstock, M. Goedert and J. Herms (2013). "Impaired plasticity of cortical dendritic spines in P301S tau transgenic mice." Acta neuropathologica communications **1**(1): 1-11.
- Hoover, B. R., M. N. Reed, J. Su, R. D. Penrod, L. A. Kotilinek, M. K. Grant, R. Pitstick, G. A. Carlson, L. M. Lanier, L.-L. Yuan, K. H. Ashe and D. Liao (2010). "Tau Mislocalization to Dendritic Spines Mediates Synaptic Dysfunction Independently of Neurodegeneration." Neuron **68**(6): 1067-1081.
- Hopp, S. C., Y. Lin, D. Oakley, A. D. Roe, S. L. DeVos, D. Hanlon and B. T. Hyman (2018). "The role of microglia in processing and spreading of bioactive tau seeds in Alzheimer's disease." Journal of neuroinflammation **15**(1): 1-15.
- Hou, Y., X. Dan, M. Babbar, Y. Wei, S. G. Hasselbalch, D. L. Croteau and V. A. Bohr (2019). "Ageing as a risk factor for neurodegenerative disease." Nature Reviews Neurology **15**(10): 565-581.
- Howitt, J. and A. F. Hill (2016). "Exosomes in the pathology of neurodegenerative diseases." Journal of Biological Chemistry **291**(52): 26589-26597.
- Hyman, B. T., G. W. Van Hoesen, B. L. Wolozin, P. Davies, L. J. Kromer and A. R. Damasio (1988). "Alz-50 antibody recognizes Alzheimer-related neuronal changes." Ann Neurol **23**(4): 371-379.
- Iba, M., J. L. Guo, J. D. McBride, B. Zhang, J. Q. Trojanowski and V. M.-Y. Lee (2013). "Synthetic tau fibrils mediate transmission of neurofibrillary tangles in a transgenic mouse model of Alzheimer's-like tauopathy." Journal of Neuroscience **33**(3): 1024-1037.
- Iba, M., J. D. McBride, J. L. Guo, B. Zhang, J. Q. Trojanowski and V. M.-Y. Lee (2015). "Tau pathology spread in PS19 tau transgenic mice following locus coeruleus (LC) injections of synthetic tau fibrils is determined by the LC's afferent and efferent connections." Acta neuropathologica **130**(3): 349-362.
- Inal, M. A., K. Banzai and D. Kamiyama (2020). "Retrograde Tracing of *Drosophila* Embryonic Motor Neurons Using Lipophilic Fluorescent Dyes." J Vis Exp(155).
- Ishida, K., K. Yamada, R. Nishiyama, T. Hashimoto, I. Nishida, Y. Abe, M. Yasui and T. Iwatsubo (2022). "Glymphatic system clears extracellular tau and protects from tau aggregation and neurodegeneration." Journal of Experimental Medicine **219**(3).
- Ismael S, Sindi G, Colvin RA, Lee D. Activity-dependent release of phosphorylated human tau from *Drosophila* neurons in primary culture. J Biol Chem. 2021 Oct;297(4):101108. doi: 10.1016/j.jbc.2021.101108. Epub 2021 Aug 30. PMID: 34473990; PMCID: PMC8455371.
- Ito, K., K. Suzuki, P. Estes, M. Ramaswami, D. Yamamoto and N. J. Strausfeld (1998). "The

- organization of extrinsic neurons and their implications in the functional roles of the mushroom bodies in *Drosophila melanogaster* Meigen." Learn Mem **5**(1-2): 52-77.
- Ittner, A., S. W. Chua, J. Bertz, A. Volkerling, J. van der Hoven, A. Gladbach, M. Przybyla, M. Bi, A. van Hummel, C. H. Stevens, S. Ippati, L. S. Suh, A. Macmillan, G. Sutherland, J. J. Kril, A. P. G. Silva, J. P. Mackay, A. Poljak, F. Delerue, Y. D. Ke and L. M. Ittner (2016). "Site-specific phosphorylation of tau inhibits amyloid- β toxicity in Alzheimer's mice." Science **354**(6314): 904-908.
- Ittner, L. M., Y. D. Ke, F. Delerue, M. Bi, A. Gladbach, J. van Eersel, H. Wölfing, B. C. Chieng, M. J. Christie and I. A. Napier (2010). "Dendritic function of tau mediates amyloid- β toxicity in Alzheimer's disease mouse models." Cell **142**(3): 387-397.
- Janning, D., M. Igaev, F. Sündermann, J. Brühmann, O. Beutel, J. J. Heinisch, L. Bakota, J. Piehler, W. Junge and R. Brandt (2014). "Single-molecule tracking of tau reveals fast kiss-and-hop interaction with microtubules in living neurons." Molecular biology of the cell **25**(22): 3541-3551.
- Jaworski, T., B. Lechat, D. Demedts, L. Gielis, H. Devijver, P. Borghgraef, H. Duimel, F. Verheyen, S. Kügler and F. Van Leuven (2011). "Dendritic degeneration, neurovascular defects, and inflammation precede neuronal loss in a mouse model for tau-mediated neurodegeneration." The American journal of pathology **179**(4): 2001-2015.
- Jefferis, G. S. X. E., R. M. Vyas, D. Berdnik, A. Ramaekers, R. F. Stocker, N. K. Tanaka, K. Ito and L. Luo (2004). "Developmental origin of wiring specificity in the olfactory system of *Drosophila*." Development **131**(1): 117-130.
- Jeganathan, S., M. Von Bergen, E.-M. Mandelkow and E. Mandelkow (2008). "The natively unfolded character of tau and its aggregation to Alzheimer-like paired helical filaments." Biochemistry **47**(40): 10526-10539.
- Jennings, B. H. (2011). "*Drosophila* – a versatile model in biology & medicine." Materials Today **14**(5): 190-195.
- Jicha, G. A., R. Bowser, I. G. Kazam and P. Davies (1997). "Alz-50 and MC-1, a new monoclonal antibody raised to paired helical filaments, recognize conformational epitopes on recombinant tau." J Neurosci Res **48**(2): 128-132.
- Jonsson, T., J. K. Atwal, S. Steinberg, J. Snaedal, P. V. Jonsson, S. Bjornsson, H. Stefansson, P. Sulem, D. Gudbjartsson, J. Maloney, K. Hoyte, A. Gustafson, Y. Liu, Y. Lu, T. Bhangale, R. R. Graham, J. Huttenlocher, G. Bjornsdottir, O. A. Andreassen, E. G. Jönsson, A. Palotie, T. W. Behrens, O. T. Magnusson, A. Kong, U. Thorsteinsdottir, R. J. Watts and K. Stefansson (2012). "A mutation in APP protects against Alzheimer's disease and age-related cognitive decline." Nature **488**(7409): 96-99.
- Kamenetz, F., T. Tomita, H. Hsieh, G. Seabrook, D. Borchelt, T. Iwatsubo, S. Sisodia and R. Malinow (2003). "APP processing and synaptic function." Neuron **37**(6): 925-937.
- Kamikouchi, A., T. Shimada and K. Ito (2006). "Comprehensive classification of the auditory sensory projections in the brain of the fruit fly *Drosophila melanogaster*." Journal of Comparative Neurology **499**(3): 317-356.
- Kampers, T., P. Friedhoff, J. Biernat, E.-M. Mandelkow and E. Mandelkow (1996). "RNA stimulates aggregation of microtubule-associated protein tau into Alzheimer-like paired helical filaments." FEBS letters **399**(3): 344-349.

- Karch, C. M., A. T. Jeng and A. M. Goate (2012). "Extracellular Tau Levels Are Influenced by Variability in Tau That Is Associated with Tauopathies." Journal of Biological Chemistry **287**(51): 42751-42762.
- Katsinelos, T., M. Zeitler, E. Dimou, A. Karakatsani, H.-M. Müller, E. Nachman, J. P. Steringer, C. R. de Almodovar, W. Nickel and T. R. Jahn (2018). "Unconventional secretion mediates the trans-cellular spreading of tau." Cell reports **23**(7): 2039-2055.
- Kent, S. A., T. L. Spires-Jones and C. S. Durrant (2020). "The physiological roles of tau and A β : implications for Alzheimer's disease pathology and therapeutics." Acta Neuropathologica **140**(4): 417-447.
- Kfoury, N., B. B. Holmes, H. Jiang, D. M. Holtzman and M. I. Diamond (2012). "Trans-cellular propagation of Tau aggregation by fibrillar species." J Biol Chem **287**(23): 19440-19451.
- Khatoon, S., I. Grundke-Iqbal and K. Iqbal (1992). "Brain levels of microtubule-associated protein τ are elevated in Alzheimer's disease: A radioimmuno-slot-blot assay for nanograms of the protein." Journal of neurochemistry **59**(2): 750-753.
- Kim, J., P. Chakrabarty, A. Hanna, A. March, D. W. Dickson, D. R. Borchelt, T. Golde and C. Janus (2013). "Normal cognition in transgenic BRI2-A β mice." Molecular neurodegeneration **8**: 15-15.
- Kimura, T., D. J. Whitcomb, J. Jo, P. Regan, T. Piers, S. Heo, C. Brown, T. Hashikawa, M. Murayama and H. Seok (2014). "Microtubule-associated protein tau is essential for long-term depression in the hippocampus." Philosophical Transactions of the Royal Society B: Biological Sciences **369**(1633): 20130144.
- King, M. E., V. Ahuja, L. I. Binder and J. Kuret (1999). "Ligand-dependent tau filament formation: implications for Alzheimer's disease progression." Biochemistry **38**(45): 14851-14859.
- Kirkhart, C. and K. Scott (2015). "Gustatory learning and processing in the *Drosophila* mushroom bodies." J Neurosci **35**(15): 5950-5958.
- Kobayashi, S., T. Tanaka, Y. Soeda, O. F. X. Almeida and A. Takashima (2017). "Local Somatodendritic Translation and Hyperphosphorylation of Tau Protein Triggered by AMPA and NMDA Receptor Stimulation." EBioMedicine **20**: 120-126.
- Kockel, L., L. M. Huq, A. Ayyar, E. Herold, E. MacAlpine, M. Logan, C. Savvides, G. E. S. Kim, J. Chen, T. Clark, T. Duong, V. Fazel-Rezai, D. Havey, S. Han, R. Jagadeesan, E. S. J. Kim, D. Lee, K. Lombardo, I. Piyale, H. Shi, L. Stahr, D. Tung, U. Tayvah, F. Wang, J.-H. Wang, S. Xiao, S. M. Topper, S. Park, C. Rotondo, A. E. Rankin, T. W. Chisholm and S. K. Kim (2016). "A *Drosophila* LexA Enhancer-Trap Resource for Developmental Biology and Neuroendocrine Research." G3 Genes|Genomes|Genetics **6**(10): 3017-3026.
- Kolata, G. (1985). "Down syndrome--Alzheimer's linked." Science **230**(4730): 1152-1153.
- Kopke, E., Y. C. Tung, S. Shaikh, A. C. Alonso, K. Iqbal and I. Grundke-Iqbal (1993). "Microtubule-associated protein tau. Abnormal phosphorylation of a non-paired helical filament pool in Alzheimer disease." J Biol Chem **268**(32): 24374-24384.
- Kramer, J. M. and B. E. Staveley (2003). "GAL4 causes developmental defects and apoptosis when expressed in the developing eye of *Drosophila melanogaster*." Genet Mol Res **2**(1): 43-47.
- Kutoku, Y., Y. Ohsawa, R. Kuwano, T. Ikeuchi, H. Inoue, S. Ataka, H. Shimada, H. Mori and Y. Sunada (2015). "A second pedigree with amyloid-less familial Alzheimer's disease harboring an identical mutation in the amyloid precursor protein gene (E693delta)." Intern Med **54**(2): 205-208.

- Lachenal, G., K. Pernet-Gallay, M. Chivet, F. J. Hemming, A. Belly, G. Bodon, B. Blot, G. Haase, Y. Goldberg and R. Sadoul (2011). "Release of exosomes from differentiated neurons and its regulation by synaptic glutamatergic activity." Molecular and Cellular Neuroscience **46**(2): 409-418.
- Lai, J. S.-Y., S.-J. Lo, B. J. Dickson and A.-S. Chiang (2012). "Auditory circuit in the *Drosophila* brain." Proceedings of the National Academy of Sciences **109**(7): 2607-2612.
- Lasagna-Reeves, C. A., D. L. Castillo-Carranza, U. Sengupta, M. J. Guerrero-Munoz, T. Kiritoshi, V. Neugebauer, G. R. Jackson and R. Kaye (2012). "Alzheimer brain-derived tau oligomers propagate pathology from endogenous tau." Scientific reports **2**(1): 1-7.
- Lauckner, J., P. Frey and C. Geula (2003). "Comparative distribution of tau phosphorylated at Ser262 in pre-tangles and tangles." Neurobiology of aging **24**(6): 767-776.
- Laurent, C., L. Buée and D. Blum (2018). "Tau and neuroinflammation: What impact for Alzheimer's Disease and Tauopathies?" Biomedical Journal **41**(1): 21-33.
- Lee, G., R. Thangavel, V. M. Sharma, J. M. Litersky, K. Bhaskar, S. M. Fang, L. H. Do, A. Andreadis, G. Van Hoesen and H. Ksiazek-Reding (2004). "Phosphorylation of tau by fyn: implications for Alzheimer's disease." Journal of Neuroscience **24**(9): 2304-2312.
- Leroux, E., R. Perbet, R. Caillierez, K. Richetin, S. Lieger, J. Espourteille, T. Bouillet, S. Bégard, C. Danis, A. Loyens, N. Toni, N. Déglon, V. Deramecourt, S. Schraen-Maschke, L. Buée and M. Colin (2022). "Extracellular vesicles: Major actors of heterogeneity in tau spreading among human tauopathies." Molecular Therapy **30**(2): 782-797.
- Li, F., J. W. Lindsey, E. C. Marin, N. Otto, M. Dreher, G. Dempsey, I. Stark, A. S. Bates, M. W. Pleijzier, P. Schlegel, A. Nern, S. Y. Takemura, N. Eckstein, T. Yang, A. Francis, A. Braun, R. Parekh, M. Costa, L. K. Scheffer, Y. Aso, G. S. Jefferis, L. F. Abbott, A. Litwin-Kumar, S. Waddell and G. M. Rubin (2020). "The connectome of the adult *Drosophila* mushroom body provides insights into function." Elife **9**.
- Li, W. Z., S. L. Li, H. Y. Zheng, S. P. Zhang and L. Xue (2012). "A broad expression profile of the GMR-GAL4 driver in *Drosophila melanogaster*." Genet Mol Res **11**(3): 1997-2002.
- Liou, N.-F., S.-H. Lin, Y.-J. Chen, K.-T. Tsai, C.-J. Yang, T.-Y. Lin, T.-H. Wu, H.-J. Lin, Y.-T. Chen, D. M. Gohl, M. Silies and Y.-H. Chou (2018). "Diverse populations of local interneurons integrate into the *Drosophila* adult olfactory circuit." Nature Communications **9**(1): 2232.
- Liu, L., V. Drouet, J. W. Wu, M. P. Witter, S. A. Small, C. Clelland and K. Duff (2012). "Trans-synaptic spread of tau pathology in vivo." PloS one **7**(2): e31302.
- Liu, Y. and M. Lehmann (2008). "A Genomic Response to the Yeast Transcription Factor GAL4 in *Drosophila*." Fly **2**(2): 92-98.
- Lizbinski, K. M. and J. M. Jeanne (2020). "Connectomics: Bringing Fly Neural Circuits into Focus." Curr Biol **30**(16): R944-r947.
- Ludington, W. B. and W. W. Ja (2020). "*Drosophila* as a model for the gut microbiome." PLoS Pathog **16**(4): e1008398.
- Lund, H., R. F. Cowburn, E. Gustafsson, K. Strömberg, A. Svensson, L. Dahllund, D. Malinowsky and D. Sunnemark (2013). "Tau-Tubulin Kinase 1 Expression, Phosphorylation and Co-Localization with Phospho-S er422 Tau in the Alzheimer's Disease Brain." Brain pathology **23**(4): 378-389.

- Luo, L., T. Tully and K. White (1992). "Human amyloid precursor protein ameliorates behavioral deficit of flies deleted for *appl* gene." Neuron **9**(4): 595-605.
- Ma, Q.-L., F. Yang, E. R. Rosario, O. J. Ubeda, W. Beech, D. J. Gant, P. P. Chen, B. Hudspeth, C. Chen, Y. Zhao, H. V. Vinters, S. A. Frautschy and G. M. Cole (2009). "Beta-amyloid oligomers induce phosphorylation of tau and inactivation of insulin receptor substrate via c-Jun N-terminal kinase signaling: suppression by omega-3 fatty acids and curcumin." The Journal of neuroscience : the official journal of the Society for Neuroscience **29**(28): 9078-9089.
- MacDonald, J. M., M. G. Beach, E. Porpiglia, A. E. Sheehan, R. J. Watts and M. R. Freeman (2006). "The *Drosophila* cell corpse engulfment receptor Draper mediates glial clearance of severed axons." Neuron **50**(6): 869-881.
- Macleod, G. T. (2012). "Direct injection of indicators for calcium imaging at the *Drosophila* larval neuromuscular junction." Cold Spring Harb Protoc **2012**(7): 797-801.
- Mandelkow, E.-M. and E. Mandelkow (2012). "Biochemistry and cell biology of tau protein in neurofibrillary degeneration." Cold Spring Harbor perspectives in medicine **2**(7): a006247-a006247.
- Mann, A., E. Gondard, D. Tampellini, J. A. Milsted, D. Marillac, C. Hamani, S. K. Kalia and A. M. Lozano (2018). "Chronic deep brain stimulation in an Alzheimer's disease mouse model enhances memory and reduces pathological hallmarks." Brain stimulation **11**(2): 435-444.
- Mao, C.-X., Y. Xiong, Z. Xiong, Q. Wang, Y. Q. Zhang and S. Jin (2014). "Microtubule-severing protein Katanin regulates neuromuscular junction development and dendritic elaboration in *Drosophila*." Development **141**(5): 1064-1074.
- Marin, E. C., L. Büld, M. Theiss, T. Sarkissian, R. J. V. Roberts, R. Turnbull, I. F. M. Tamimi, M. W. Pleijzier, W. J. Laursen, N. Drummond, P. Schlegel, A. S. Bates, F. Li, M. Landgraf, M. Costa, D. D. Bock, P. A. Garrity and G. Jefferis (2020). "Connectomics Analysis Reveals First-, Second-, and Third-Order Thermosensory and Hygrosensory Neurons in the Adult *Drosophila* Brain." Curr Biol **30**(16): 3167-3182.e3164.
- Marin, E. C., G. S. X. E. Jefferis, T. Komiyama, H. Zhu and L. Luo (2002). "Representation of the Glomerular Olfactory Map in the *Drosophila* Brain." Cell **109**(2): 243-255.
- Matsumoto, S.-E., Y. Motoi, K. Ishiguro, T. Tabira, F. Kametani, M. Hasegawa and N. Hattori (2015). "The twenty-four kDa C-terminal tau fragment increases with aging in tauopathy mice: implications of prion-like properties." Human molecular genetics **24**(22): 6403-6416.
- Meldolesi, J. (2018). "Exosomes and ectosomes in intercellular communication." Current Biology **28**(8): R435-R444.
- Merezhko, M., C. A. Brunello, X. Yan, H. Vihinen, E. Jokitalo, R.-L. Uronen and H. J. Huttunen (2018). "Secretion of tau via an unconventional non-vesicular mechanism." Cell reports **25**(8): 2027-2035. e2024.
- Mershin, A., E. Pavlopoulos, O. Fitch, B. C. Braden, D. V. Nanopoulos and E. M. Skoulakis (2004). "Learning and memory deficits upon TAU accumulation in *Drosophila* mushroom body neurons." Learn Mem **11**(3): 277-287.
- Michel, C. H., S. Kumar, D. Pinotsi, A. Tunnacliffe, P. St. George-Hyslop, E. Mandelkow, E.-M. Mandelkow, C. F. Kaminski and G. S. Kaminski Schierle (2014). "Extracellular Monomeric Tau Protein Is Sufficient to Initiate the Spread of Tau Protein Pathology." Journal of Biological Chemistry **289**(2): 956-967.

- Milto, K., K. Michailova and V. Smirnovas (2014). "Elongation of mouse prion protein amyloid-like fibrils: effect of temperature and denaturant concentration." PLoS One **9**(4): e94469.
- Mirbaha, H., B. B. Holmes, D. W. Sanders, J. Bieschke and M. I. Diamond (2015). "Tau trimers are the minimal propagation unit spontaneously internalized to seed intracellular aggregation." Journal of biological chemistry **290**(24): 14893-14903.
- Mitra, G., S. Gupta, A. Poddar and B. Bhattacharyya (2015). "MAP2c prevents arachidonic acid-induced fibril formation of tau: Role of chaperone activity and phosphorylation." Biophysical Chemistry **205**: 16-23.
- Miyamoto, T., L. Stein, R. Thomas, B. Djukic, P. Taneja, J. Knox, K. Vossel and L. Mucke (2017). "Phosphorylation of tau at Y18, but not tau-fyn binding, is required for tau to modulate NMDA receptor-dependent excitotoxicity in primary neuronal culture." Molecular Neurodegeneration **12**(1): 41.
- Mondragón-Rodríguez, S., E. Trillaud-Doppia, A. Dudilot, C. Bourgeois, M. Lauzon, N. Leclerc and J. Boehm (2012). "Interaction of Endogenous Tau Protein with Synaptic Proteins Is Regulated by N-Methyl-D-aspartate Receptor-dependent Tau Phosphorylation *." Journal of Biological Chemistry **287**(38): 32040-32053.
- Morfini, G. A., M. Burns, L. I. Binder, N. M. Kanaan, N. LaPointe, D. A. Bosco, R. H. Brown, H. Brown, A. Tiwari, L. Hayward, J. Edgar, K.-A. Nave, J. Garberrn, Y. Atagi, Y. Song, G. Pigino and S. T. Brady (2009). "Axonal Transport Defects in Neurodegenerative Diseases." The Journal of Neuroscience **29**(41): 12776-12786.
- Morsch, R., W. Simon and P. D. Coleman (1999). "Neurons May Live for Decades with Neurofibrillary Tangles." Journal of Neuropathology & Experimental Neurology **58**(2): 188-197.
- Moulin, T. C., F. Ferro, A. Hoyer, P. Cheung, M. J. Williams and H. B. Schiöth (2021). "The *Drosophila melanogaster* Levodopa-Induced Depression Model Exhibits Negative Geotaxis Deficits and Differential Gene Expression in Males and Females." Front Neurosci **15**: 653470.
- Mucke, L. and D. J. Selkoe (2012). "Neurotoxicity of amyloid β -protein: synaptic and network dysfunction." Cold Spring Harbor perspectives in medicine **2**(7): a006338-a006338.
- Mudher, A., M. Colin, S. Dujardin, M. Medina, I. Dewachter, S. M. Alavi Naini, E.-M. Mandelkow, E. Mandelkow, L. Buée, M. Goedert and J.-P. Brion (2017). "What is the evidence that tau pathology spreads through prion-like propagation?" Acta neuropathologica communications **5**(1): 99-99.
- Mudher, A., D. Shepherd, T. Newman, P. Mildren, J. Jukes, A. Squire, A. Mears, S. Berg, D. MacKay and A. Asuni (2004). "GSK-3 β inhibition reverses axonal transport defects and behavioural phenotypes in *Drosophila*." Molecular psychiatry **9**(5): 522-530.
- Mullan, M., F. Crawford, K. Axelman, H. Houlden, L. Lilius, B. Winblad and L. Lannfelt (1992). "A pathogenic mutation for probable Alzheimer's disease in the APP gene at the N-terminus of β -amyloid." Nature Genetics **1**(5): 345-347.
- Narasimhan, S., J. L. Guo, L. Changolkar, A. Stieber, J. D. McBride, L. V. Silva, Z. He, B. Zhang, R. J. Gathagan, J. Q. Trojanowski and V. M. Y. Lee (2017). "Pathological Tau Strains from Human Brains Recapitulate the Diversity of Tauopathies in Nontransgenic Mouse Brain." J Neurosci **37**(47): 11406-11423.
- Naseri, N. N., H. Wang, J. Guo, M. Sharma and W. Luo (2019). "The complexity of tau in Alzheimer's disease." Neuroscience letters **705**: 183-194.

- Otvos Jr., L., L. Feiner, E. Lang, G. I. Szendrei, M. Goedert and V. M.-Y. Lee (1994). "Monoclonal antibody PHF-1 recognizes tau protein phosphorylated at serine residues 396 and 404." Journal of Neuroscience Research **39**(6): 669-673.
- Ozcelik, S., F. Sprenger, Z. Skachokova, G. Fraser, D. Abramowski, F. Clavaguera, A. Probst, S. Frank, M. Müller, M. Staufenbiel, M. Goedert, M. Tolnay and D. T. Winkler (2016). "Co-expression of truncated and full-length tau induces severe neurotoxicity." Molecular psychiatry **21**(12): 1790-1798.
- Pandey, U. B. and C. D. Nichols (2011). "Human disease models in *Drosophila melanogaster* and the role of the fly in therapeutic drug discovery." Pharmacol Rev **63**(2): 411-436.
- Panza, F., Lozupone, M., Logroscino, G. & Imbimbo, B. (2019). A critical appraisal of amyloid- β -targeting therapies for Alzheimer disease. Nat Rev Neurol **15**, 73–88.
- Paonessa, F., L. D. Evans, R. Solanki, D. Larrieu, S. Wray, J. Hardy, S. P. Jackson and F. J. Livesey (2019). "Microtubules Deform the Nuclear Membrane and Disrupt Nucleocytoplasmic Transport in Tau-Mediated Frontotemporal Dementia." Cell Reports **26**(3): 582-593.e585.
- Park, J., I. Wetzel, I. Marriott, D. Dréau, C. D'Avanzo, D. Y. Kim, R. E. Tanzi and H. Cho (2018). "A 3D human triculture system modeling neurodegeneration and neuroinflammation in Alzheimer's disease." Nature Neuroscience **21**(7): 941-951.
- Parkhitko, A. A., D. Ramesh, L. Wang, D. Leshchiner, E. Filine, R. Binari, A. L. Olsen, J. M. Asara, V. Cracan, J. D. Rabinowitz, A. Brockmann and N. Perrimon (2020). "Downregulation of the tyrosine degradation pathway extends *Drosophila* lifespan." eLife **9**: e58053.
- Pearce, M. M. P., E. J. Spartz, W. Hong, L. Luo and R. R. Kopito (2015). "Prion-like transmission of neuronal huntingtin aggregates to phagocytic glia in the *Drosophila* brain." Nature Communications **6**(1): 6768.
- Peeraer, E., A. Bottelbergs, K. Van Kolen, I.-C. Stancu, B. Vasconcelos, M. Mahieu, H. Duytschaever, L. Ver Donck, A. Torremans and E. Sluydts (2015). "Intracerebral injection of preformed synthetic tau fibrils initiates widespread tauopathy and neuronal loss in the brains of tau transgenic mice." Neurobiology of disease **73**: 83-95.
- Peineau, S., C. Taghibiglou, C. Bradley, T. P. Wong, L. Liu, J. Lu, E. Lo, D. Wu, E. Saule, T. Bouschet, P. Matthews, J. T. Isaac, Z. A. Bortolotto, Y. T. Wang and G. L. Collingridge (2007). "LTP inhibits LTD in the hippocampus via regulation of GSK3beta." Neuron **53**(5): 703-717.
- Pende, M., K. Becker, M. Wanis, S. Saghafi, R. Kaur, C. Hahn, N. Pende, M. Foroughipour, T. Hummel and H. U. Dodt (2018). "High-resolution ultramicroscopy of the developing and adult nervous system in optically cleared *Drosophila melanogaster*." Nat Commun **9**(1): 4731.
- Pernègre C, Duquette A, Leclerc N. Tau Secretion: Good and Bad for Neurons. Front Neurosci. 2019 Jun 26;13:649. doi: 10.3389/fnins.2019.00649. PMID: 31293374; PMCID: PMC6606725.
- Pfeiffer, B. D., T.-T. B. Ngo, K. L. Hibbard, C. Murphy, A. Jenett, J. W. Truman and G. M. Rubin (2010). "Refinement of Tools for Targeted Gene Expression in *Drosophila*." Genetics **186**(2): 735-755.
- Povellato, G, Tuxworth R, Hanger D.P, Tear G, (2014). "Modification of the *Drosophila* model of in vivo Tau toxicity reveals protective phosphorylation by GSK3 β ". Biol Open **3** (1): 1–11.
- Pogodalla, N., H. Kranenburg, S. Rey, S. Rodrigues, A. Cardona and C. Klämbt (2021). "*Drosophila* β Heavy-Spectrin is required in polarized ensheathing glia that form a diffusion-barrier around the neuropil." Nature Communications **12**(1): 6357.

- Pooler, A. M., E. C. Phillips, D. H. Lau, W. Noble and D. P. Hanger (2013). "Physiological release of endogenous tau is stimulated by neuronal activity." EMBO reports **14**(4): 389-394.
- Pooler, A. M., M. Polydoro, E. A. Maury, S. B. Nicholls, S. M. Reddy, S. Wegmann, C. William, L. Saqran, O. Cagsal-Getkin, R. Pitstick, D. R. Beier, G. A. Carlson, T. L. Spires-Jones and B. T. Hyman (2015). "Amyloid accelerates tau propagation and toxicity in a model of early Alzheimer's disease." Acta Neuropathologica Communications **3**(1): 14.
- Potter, C. J. and L. Luo (2011). "Using the Q system in *Drosophila melanogaster*." Nat Protoc **6**(8): 1105-1120.
- Prüßing, K., A. Voigt and J. B. Schulz (2013). "*Drosophila melanogaster* as a model organism for Alzheimer's disease." Molecular Neurodegeneration **8**(1): 35.
- Qiang, L., X. Sun, T. O. Austin, H. Muralidharan, D. C. Jean, M. Liu, W. Yu and P. W. Baas (2018). "Tau Does Not Stabilize Axonal Microtubules but Rather Enables Them to Have Long Labile Domains." Current Biology **28**(13): 2181-2189.e2184.
- Quraishe, S., M. Sealey, L. Cranfield and A. Mudher (2016). "Microtubule stabilising peptides rescue tau phenotypes in-vivo." Sci Rep **6**: 38224.
- Ramachandran, G. and J. B. Udgaonkar (2011). "Understanding the kinetic roles of the inducer heparin and of rod-like protofibrils during amyloid fibril formation by Tau protein." Journal of biological chemistry **286**(45): 38948-38959.
- Ramirez, A., C. Pacheco, L. Aguayo and C. Opazo (2014). "Rapamycin protects against A β -induced synaptotoxicity by increasing presynaptic activity in hippocampal neurons." Biochimica et Biophysica Acta (BBA)-Molecular Basis of Disease **1842**(9): 1495-1501.
- Rankin, C. A., Q. Sun and T. C. Gamblin (2005). "Pseudo-phosphorylation of tau at Ser202 and Thr205 affects tau filament formation." Molecular Brain Research **138**(1): 84-93.
- Rauch, J. N., J. J. Chen, A. W. Sorum, G. M. Miller, T. Sharf, S. K. See, L. C. Hsieh-Wilson, M. Kampmann and K. S. Kosik (2018). "Tau Internalization is Regulated by 6-O Sulfation on Heparan Sulfate Proteoglycans (HSPGs)." Scientific Reports **8**(1): 6382.
- Rauch, J. N., G. Luna, E. Guzman, M. Audouard, C. Challis, Y. E. Sibih, C. Leshuk, I. Hernandez, S. Wegmann, B. T. Hyman, V. Gradinaru, M. Kampmann and K. S. Kosik (2020). "LRP1 is a master regulator of tau uptake and spread." Nature **580**(7803): 381-385.
- Regan, P., T. Piers, J.-H. Yi, D.-H. Kim, S. Huh, S. J. Park, J. H. Ryu, D. J. Whitcomb and K. Cho (2015). "Tau Phosphorylation at Serine 396 Residue Is Required for Hippocampal LTD." The Journal of Neuroscience **35**(12): 4804-4812.
- Reiter, L. T., L. Potocki, S. Chien, M. Gribskov and E. Bier (2001). "A systematic analysis of human disease-associated gene sequences in *Drosophila melanogaster*." Genome research **11**(6): 1114-1125.
- Robertson, H. M., C. G. Warr and J. R. Carlson (2003). "Molecular evolution of the insect chemoreceptor gene superfamily in *Drosophila melanogaster*." Proceedings of the National Academy of Sciences **100**(suppl_2): 14537-14542.
- Robinson, R. A., J. F. Kellie, T. C. Kaufman and D. E. Clemmer (2010). "Insights into aging through measurements of the *Drosophila* proteome as a function of temperature." Mech Ageing Dev **131**(9): 584-590.
- Rodriguez, G. A., G. M. Barrett, K. E. Duff and S. A. Hussaini (2020). "Chemogenetic attenuation of neuronal activity in the entorhinal cortex reduces A β and tau pathology in the hippocampus." PLoS biology **18**(8): e3000851.

- Rolstad, S., A. I. Berg, M. Bjerke, B. Johansson, H. Zetterberg and A. Wallin (2013). "Cerebrospinal fluid biomarkers mirror rate of cognitive decline." Journal of Alzheimer's Disease **34**(4): 949-956.
- Romero-Molina, C., V. Navarro, R. Sanchez-Varo, S. Jimenez, J. J. Fernandez-Valenzuela, M. V. Sanchez-Mico, C. Muñoz-Castro, A. Gutierrez, J. Vitorica and M. Vizuete (2018). "Distinct microglial responses in two transgenic murine models of TAU pathology." Frontiers in Cellular Neuroscience **12**: 421.
- Ronderos, D. S., C. C. Lin, C. J. Potter and D. P. Smith (2014). "Farnesol-detecting olfactory neurons in *Drosophila*." J Neurosci **34**(11): 3959-3968.
- Ruan, Z., D. Pathak, S. Venkatesan Kalavai, A. Yoshii-Kitahara, S. Muraoka, N. Bhatt, K. Takamatsu-Yukawa, J. Hu, Y. Wang, S. Hersh, M. Ericsson, S. Gorantla, H. E. Gendelman, R. Kaye, S. Ikezu, J. I. Luebke and T. Ikezu (2021). "Alzheimer's disease brain-derived extracellular vesicles spread tau pathology in interneurons." Brain **144**(1): 288-309.
- Salter, M. W. and L. V. Kalia (2004). "Src kinases: a hub for NMDA receptor regulation." Nature Reviews Neuroscience **5**(4): 317-328.
- Salvaterra, P. M. and T. Kitamoto (2001). "*Drosophila* cholinergic neurons and processes visualized with Gal4/UAS-GFP." Brain Res Gene Expr Patterns **1**(1): 73-82.
- Saman, S., W. Kim, M. Raya, Y. Visnick, S. Miro, S. Saman, B. Jackson, A. C. McKee, V. E. Alvarez and N. C. Lee (2012). "Exosome-associated tau is secreted in tauopathy models and is selectively phosphorylated in cerebrospinal fluid in early Alzheimer disease." Journal of biological chemistry **287**(6): 3842-3849.
- Saman, S., W. Kim, M. Raya, Y. Visnick, S. Miro, S. Saman, B. Jackson, A. C. McKee, V. E. Alvarez, N. C. Y. Lee and G. F. Hall (2012). "Exosome-associated tau is secreted in tauopathy models and is selectively phosphorylated in cerebrospinal fluid in early Alzheimer disease." The Journal of biological chemistry **287**(6): 3842-3849.
- Sanders, David W., Sarah K. Kaufman, Sarah L. DeVos, Apurwa M. Sharma, H. Mirbaha, A. Li, Scarlett J. Barker, Alex C. Foley, Julian R. Thorpe, Louise C. Serpell, Timothy M. Miller, Lea T. Grinberg, William W. Seeley and Marc I. Diamond (2014). "Distinct Tau Prion Strains Propagate in Cells and Mice and Define Different Tauopathies." Neuron **82**(6): 1271-1288.
- Santacruz, K., J. Lewis, T. Spires, J. Paulson, L. Kotilinek, M. Ingelsson, A. Guimaraes, M. DeTure, M. Ramsden, E. McGowan, C. Forster, M. Yue, J. Orne, C. Janus, A. Mariash, M. Kuskowski, B. Hyman, M. Hutton and K. H. Ashe (2005). "Tau suppression in a neurodegenerative mouse model improves memory function." Science (New York, N.Y.) **309**(5733): 476-481.
- Santiago, J. A. and J. A. Potashkin (2021). "The Impact of Disease Comorbidities in Alzheimer's Disease." Front Aging Neurosci **13**: 631770.
- Semmelhack, J., Wang, J. (2009) "Select *Drosophila* glomeruli mediate innate olfactory attraction and aversion". Nature **459**, 218–223
- Scheffer, L. K. and I. A. Meinertzhagen (2019). "The Fly Brain Atlas." Annual Review of Cell and Developmental Biology **35**(1): 637-653.
- Scheres, S. H., W. Zhang, B. Falcon and M. Goedert (2020). "Cryo-EM structures of tau filaments." Curr Opin Struct Biol **64**: 17-25.
- Schneider, A., M. Ruppert, O. Hendrich, T. Giang, M. Ogueta, S. Hampel, M. Vollbach, A. Büschges and H. Scholz (2012). "Neuronal basis of innate olfactory attraction to ethanol in *Drosophila*." PLoS One **7**(12): e52007.
- Schweers, O., E. Schonbrunn-Hanebeck, A. Marx and E. Mandelkow (1994). "Structural studies of

tau protein and Alzheimer paired helical filaments show no evidence for beta-structure." J Biol Chem **269**(39): 24290-24297.

Sealey, M. A., E. Vourkou, C. M. Cowan, T. Bossing, S. Quraishe, S. Grammenoudi, E. M. C. Skoulakis and A. Mudher (2017). "Distinct phenotypes of three-repeat and four-repeat human tau in a transgenic model of tauopathy." Neurobiology of Disease **105**: 74-83.

Selkoe, D. J. and J. Hardy (2016). "The amyloid hypothesis of Alzheimer's disease at 25 years." EMBO Mol Med **8**(6): 595-608.

Sen, A., C. Shetty, D. Jhaveri and V. Rodrigues (2005). "Distinct types of glial cells populate the *Drosophila* antenna." BMC Dev Biol **5**: 25.

Serenó, L., M. Coma, M. Rodríguez, P. Sánchez-Ferrer, M. B. Sánchez, I. Gich, J. M. Agulló, M. Pérez, J. Avila, C. Guardia-Laguarta, J. Clarimón, A. Lleó and T. Gómez-Isla (2009). "A novel GSK-3 β inhibitor reduces Alzheimer's pathology and rescues neuronal loss in vivo." Neurobiology of Disease **35**(3): 359-367.

Shaner, N. C., R. E. Campbell, P. A. Steinbach, B. N. G. Giepmans, A. E. Palmer and R. Y. Tsien (2004). "Improved monomeric red, orange and yellow fluorescent proteins derived from *Discosoma* sp. red fluorescent protein." Nature Biotechnology **22**(12): 1567-1572.

Shang, Y., A. Claridge-Chang, L. Sjulson, M. Pypaert and G. Miesenböck (2007). "Excitatory local circuits and their implications for olfactory processing in the fly antennal lobe." Cell **128**(3): 601-612.

Shen, J. and R. J. Kelleher, 3rd (2007). "The presenilin hypothesis of Alzheimer's disease: evidence for a loss-of-function pathogenic mechanism." Proc Natl Acad Sci U S A **104**(2): 403-409.

Shimada, H., S. Ataka, T. Tomiyama, H. Takechi, H. Mori and T. Miki (2011). "Clinical course of patients with familial early-onset Alzheimer's disease potentially lacking senile plaques bearing the E693 Δ mutation in amyloid precursor protein." Dementia and geriatric cognitive disorders **32**(1): 45-54.

Shimada, H., S. Minatani, J. Takeuchi, A. Takeda, J. Kawabe, Y. Wada, A. Mawatari, Y. Watanabe, H. Shimada, M. Higuchi, T. Suhara, T. Tomiyama and Y. Itoh (2020). "Heavy Tau Burden with Subtle Amyloid β Accumulation in the Cerebral Cortex and Cerebellum in a Case of Familial Alzheimer's Disease with APP Osaka Mutation." International Journal of Molecular Sciences **21**(12): 4443.

Simón, D., E. García-García, F. Royo, J. M. Falcón-Pérez and J. Avila (2012). "Proteostasis of tau. Tau overexpression results in its secretion via membrane vesicles." FEBS Letters **586**(1): 47-54.

Song, Z., K. McCall and H. Steller (1997). "DCP-1, a *Drosophila* cell death protease essential for development." Science **275**(5299): 536-540.

Spitzer, P., L.-M. Mulzer, T. J. Oberstein, L. E. Munoz, P. Lewczuk, J. Kornhuber, M. Herrmann and J. M. Maler (2019). "Microvesicles from cerebrospinal fluid of patients with Alzheimer's disease display reduced concentrations of tau and APP protein." Scientific Reports **9**(1): 7089.

Stathopoulos, P. B., G. A. Scholz, Y. M. Hwang, J. A. Rumfeldt, J. R. Lepock and E. M. Meiering (2004). "Sonication of proteins causes formation of aggregates that resemble amyloid." Protein Science **13**(11): 3017-3027.

Steinhilb, M. L., D. Dias-Santagata, T. A. Fulga, D. L. Felch and M. B. Feany (2007). "Tau phosphorylation sites work in concert to promote neurotoxicity in vivo." Mol Biol Cell **18**(12): 5060-5068.

Stork, T., D. Engelen, A. Krudewig, M. Silies, R. J. Bainton and C. Klämbt (2008). "Organization and

function of the blood-brain barrier in *Drosophila*." J Neurosci **28**(3): 587-597.

Sweeney, S. T., K. Broadie, J. Keane, H. Niemann and C. J. O'Kane (1995). "Targeted expression of tetanus toxin light chain in *Drosophila* specifically eliminates synaptic transmission and causes behavioral defects." Neuron **14**(2): 341-351.

Takeda, S., S. Wegmann, H. Cho, S. L. DeVos, C. Commins, A. D. Roe, S. B. Nicholls, G. A. Carlson, R. Pitstick, C. K. Nobuhara, I. Costantino, M. P. Frosch, D. J. Müller, D. Irimia and B. T. Hyman (2015). "Neuronal uptake and propagation of a rare phosphorylated high-molecular-weight tau derived from Alzheimer's disease brain." Nature Communications **6**(1): 8490.

Talay, M., E. B. Richman, N. J. Snell, G. G. Hartmann, J. D. Fisher, A. Sorkaç, J. F. Santoyo, C. Chou-Freed, N. Nair, M. Johnson, J. R. Szymanski and G. Barnea (2017). "Transsynaptic Mapping of Second-Order Taste Neurons in Flies by trans-Tango." Neuron **96**(4): 783-795.e784.

Tampi, R. R., B. P. Forester and M. Agronin (2021). "Aducanumab: evidence from clinical trial data and controversies." Drugs Context **10**.

Tanaka, N. K., E. Suzuki, L. Dye, A. Ejima and M. Stopfer (2012). "Dye fills reveal additional olfactory tracts in the protocerebrum of wild-type *Drosophila*." J Comp Neurol **520**(18): 4131-4140.

Task, D., C. C. Lin, A. Vulpe, A. Afify, S. Ballou, M. Brbic, P. Schlegel, J. Raji, G. Jefferis, H. Li, K. Menuz and C. J. Potter (2022). "Chemoreceptor co-expression in *Drosophila melanogaster* olfactory neurons." Elife **11**.

Terwel, D., R. Lasrado, J. Snauwaert, E. Vandeweert, C. Van Haesendonck, P. Borghgraef and F. Van Leuven (2005). "Changed conformation of mutant Tau-P301L underlies the moribund tauopathy, absent in progressive, nonlethal axonopathy of Tau-4R/2N transgenic mice." J Biol Chem **280**(5): 3963-3973.

Tharp, W. G. and I. N. Sarkar (2013). "Origins of amyloid- β ." BMC Genomics **14**(1): 290.

The Alzheimer's Association (2022). "2022 Alzheimer's disease facts and figures." Alzheimer's & Dementia **18**(4): 700-789.

Tomiyama, T., S. Matsuyama, H. Iso, T. Umeda, H. Takuma, K. Ohnishi, K. Ishibashi, R. Teraoka, N. Sakama and T. Yamashita (2010). "A mouse model of amyloid β oligomers: their contribution to synaptic alteration, abnormal tau phosphorylation, glial activation, and neuronal loss in vivo." Journal of Neuroscience **30**(14): 4845-4856.

Tomiyama, T., T. Nagata, H. Shimada, R. Teraoka, A. Fukushima, H. Kanemitsu, H. Takuma, R. Kuwano, M. Imagawa, S. Ataka, Y. Wada, E. Yoshioka, T. Nishizaki, Y. Watanabe and H. Mori (2008). "A new amyloid beta variant favoring oligomerization in Alzheimer's-type dementia." Ann Neurol **63**(3): 377-387.

Ugur, B., K. Chen and H. J. Bellen (2016). "*Drosophila* tools and assays for the study of human diseases." Disease Models & Mechanisms **9**(3): 235-244.

United Nations Department of Economic and Social Affairs, P. D. (2020). "World Population Ageing 2020 Highlights: Living arrangements of older persons

Usardi, A., A. M. Pooler, A. Seereeram, C. H. Reynolds, P. Derkinderen, B. Anderton, D. P. Hanger, W. Noble and R. Williamson (2011). "Tyrosine phosphorylation of tau regulates its interactions with Fyn SH2 domains, but not SH3 domains, altering the cellular localization of tau." The FEBS Journal **278**(16): 2927-2937.

- van Dyck, C. H., C. J. Swanson, P. Aisen, R. J. Bateman, C. Chen, M. Gee, M. Kanekiyo, D. Li, L. Reyderman, S. Cohen, L. Froelich, S. Katayama, M. Sabbagh, B. Vellas, D. Watson, S. Dhadda, M. Irizarry, L. D. Kramer and T. Iwatsubo (2022). "Lecanemab in Early Alzheimer's Disease." N Engl J Med. 2023 Jan 5;388(1):9-21. doi: 10.1056/NEJMoa2212948. Epub 2022 Nov 29. PMID: 36449413.
- Van Rossum, I. A., P. J. Visser, D. L. Knol, W. M. van der Flier, C. E. Teunissen, F. Barkhof, M. A. Blankenstein and P. Scheltens (2012). "Injury markers but not amyloid markers are associated with rapid progression from mild cognitive impairment to dementia in Alzheimer's disease." Journal of Alzheimer's Disease **29**(2): 319-327.
- Vogel, J. W., Y. Iturria-Medina, O. T. Strandberg, R. Smith, E. Levitis, A. C. Evans and O. Hansson (2020). "Spread of pathological tau proteins through communicating neurons in human Alzheimer's disease." Nat Commun **11**(1): 2612.
- Vogel, J. W., et al Alzheimer's Disease Neuroimaging and S. the Swedish BioFinder (2020). "Spread of pathological tau proteins through communicating neurons in human Alzheimer's disease." Nature Communications **11**(1): 2612.
- von Bergen, M., S. Barghorn, J. Biernat, E.-M. Mandelkow and E. Mandelkow (2005). "Tau aggregation is driven by a transition from random coil to beta sheet structure." Biochimica et Biophysica Acta (BBA) - Molecular Basis of Disease **1739**(2): 158-166.
- Vosshall, L. B., H. Amrein, P. S. Morozov, A. Rzhetsky and R. Axel (1999). "A spatial map of olfactory receptor expression in the *Drosophila* antenna." Cell **96**(5): 725-736.
- Vosshall, L. B. and R. F. Stocker (2007). "Molecular Architecture of Smell and Taste in *Drosophila*." Annual Review of Neuroscience **30**(1): 505-533.
- Walker, E. S., M. Martinez, A. L. Brunkan and A. Goate (2005). "Presenilin 2 familial Alzheimer's disease mutations result in partial loss of function and dramatic changes in Abeta 42/40 ratios." J Neurochem **92**(2): 294-301.
- Wang, C., L. Fan, R. R. Khawaja, B. Liu, L. Zhan, L. Kodama, M. Chin, Y. Li, D. Le, Y. Zhou, C. Condello, L. T. Grinberg, W. W. Seeley, B. L. Miller, S.-A. Mok, J. E. Gestwicki, A. M. Cuervo, W. Luo and L. Gan (2022). "Microglial NF-κB drives tau spreading and toxicity in a mouse model of tauopathy." Nature Communications **13**(1): 1969.
- Wang, Y., V. Balaji, S. Kaniyappan, L. Krüger, S. Irsen, K. Tepper, R. Chandupatla, W. Maetzler, A. Schneider and E. Mandelkow (2017). "The release and trans-synaptic transmission of Tau via exosomes." Molecular neurodegeneration **12**(1): 1-25.
- Wegmann, S., R. E. Bennett, L. Delorme, A. B. Robbins, M. Hu, D. MacKenzie, M. J. Kirk, J. Schiantarelli, N. Tunio, A. C. Amaral, Z. Fan, S. Nicholls, E. Hudry and B. T. Hyman (2019). "Experimental evidence for the age dependence of tau protein spread in the brain." Science Advances **5**(6):
- Westermarck, P., M. D. Benson, J. N. Buxbaum, A. S. Cohen, B. Frangione, S.-I. Ikeda, C. L. Masters, G. Merlini, M. J. Saraiva and J. D. Sipe (2007). "A primer of amyloid nomenclature." Amyloid **14**(3): 179-183.
- Williams, D. R. (2006). "Tauopathies: classification and clinical update on neurodegenerative diseases associated with microtubule-associated protein tau." Internal medicine journal **36**(10): 652-660.
- Williams, D. W., M. Tyrer and D. Shepherd (2000). "Tau and tau reporters disrupt central projections of sensory neurons in *Drosophila*." Journal of Comparative Neurology **428**(4): 630-640.

- Wittmann, C. W., M. F. Wszolek, J. M. Shulman, P. M. Salvaterra, J. Lewis, M. Hutton and M. B. Feany (2001). "Tauopathy in *Drosophila*: neurodegeneration without neurofibrillary tangles." Science **293**(5530): 711-714.
- Wu, J. W., M. Herman, L. Liu, S. Simoes, C. M. Acker, H. Figueroa, J. I. Steinberg, M. Margittai, R. Kaye, C. Zurzolo, G. Di Paolo and K. E. Duff (2013). "Small Misfolded Tau Species Are Internalized via Bulk Endocytosis and Anterogradely and Retrogradely Transported in Neurons." Journal of Biological Chemistry **288**(3): 1856-1870.
- Wu, J. W., S. A. Hussaini, I. M. Bastille, G. A. Rodriguez, A. Mrejeru, K. Rilett, D. W. Sanders, C. Cook, H. Fu and R. A. Boonen (2016). "Neuronal activity enhances tau propagation and tau pathology in vivo." Nature neuroscience **19**(8): 1085-1092.
- Wu, M., A. Nern, W. R. Williamson, M. M. Morimoto, M. B. Reiser, G. M. Card and G. M. Rubin (2016). "Visual projection neurons in the *Drosophila* lobula link feature detection to distinct behavioral programs." eLife **5**: e21022.
- Yamada, K., J. K. Holth, F. Liao, F. R. Stewart, T. E. Mahan, H. Jiang, J. R. Cirrito, T. K. Patel, K. Hochgräfe, E.-M. Mandelkow and D. M. Holtzman (2014). "Neuronal activity regulates extracellular tau in vivo." Journal of Experimental Medicine **211**(3): 387-393.
- Yan, M. and T. Zheng (2021). "Role of the endolysosomal pathway and exosome release in tau propagation." Neurochemistry International **145**: 104988.
- Yetman, M. J., S. Lillehaug, J. G. Bjaalie, T. B. Leergaard and J. L. Jankowsky (2016). "Transgene expression in the Nop-tTA driver line is not inherently restricted to the entorhinal cortex." Brain Struct Funct **221**(4): 2231-2249.
- Zhang, W., B. Falcon, A. G. Murzin, J. Fan, R. A. Crowther, M. Goedert and S. H. W. Scheres (2019). "Heparin-induced tau filaments are polymorphic and differ from those in Alzheimer's and Pick's diseases." eLife **8**: e43584.
- Zhang, W., A. Tarutani, K. L. Newell, A. G. Murzin, T. Matsubara, B. Falcon, R. Vidal, H. J. Garringer, Y. Shi, T. Ikeuchi, S. Murayama, B. Ghetti, M. Hasegawa, M. Goedert and S. H. W. Scheres (2020). "Novel tau filament fold in corticobasal degeneration." Nature **580**(7802): 283-287.
- Zheng, J., H.-L. Li, N. Tian, F. Liu, L. Wang, Y. Yin, L. Yue, L. Ma, Y. Wan and J.-Z. Wang (2020). "Interneuron accumulation of phosphorylated tau impairs adult hippocampal neurogenesis by suppressing GABAergic transmission." Cell Stem Cell **26**(3): 331-345. e336.
- Zheng, Z., J. S. Lauritzen, E. Perlman, C. G. Robinson, M. Nichols, D. Milkie, O. Torrens, J. Price, C. B. Fisher, N. Sharifi, S. A. Calle-Schuler, L. Kmecova, I. J. Ali, B. Karsh, E. T. Trautman, J. A. Bogovic, P. Hanslovsky, G. Jefferis, M. Kazhdan, K. Khairy, S. Saalfeld, R. D. Fetter and D. D. Bock (2018). "A Complete Electron Microscopy Volume of the Brain of Adult *Drosophila melanogaster*." Cell **174**(3): 730-743.e722.
- Zhou, L., McInnes, J., Wierda, K. *et al.* (2017) "Tau association with synaptic vesicles causes presynaptic dysfunction." Nat Commun **8**, 15295
- Ziehm, M., M. D. Piper and J. M. Thornton (2013). "Analysing variation in *Drosophila* aging across independent experimental studies: a meta-analysis of survival data." Aging Cell **12**(5): 917-922.